

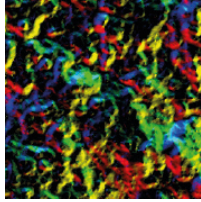
Magnetism 2018

9–10 April 2018

University of Manchester, Manchester, UK

Organised by the IOP Magnetism Group

<http://magnetism2018.iopconfs.org>



Magnetism 2018

Monday 9 April

Parallel Sessions

09:00 **Registration and refreshments**

Renold C8

Thin films and nanomagnets I

Renold C2

Chair: Stuart Cavill, University of York, UK

10:00 **Electrical transport signature of skyrmions in Pt/Co/Ir multilayer discs**

K Zeissler, University of Leeds, UK

10:15 **Exploring interfacial Dzyaloshinskii-Moriya interaction for in-plane thin film permalloy nanostructures using micromagnetic simulations and Lorentz microscopy**

K Fallon, University of Glasgow, UK

10:30 **Investigation of DMI Value for Chiral Domain Walls in Pt/Co/Ir/Ta Multilayers**

K Shahbazi, University of Leeds, UK

10:45 **Magnetism you can rely on: A materials-science based solution to stochastic domain wall pinning in magnetic nanowire devices**

T Broomhall, University of Sheffield, UK

11:00 **Topological magnetic writing: Defining specific magnetization states in nanostructures**

W Branford, Imperial College London, UK

11:15 **Exhibition and refreshments**

Renold C15

Spintronics I

Renold C9

Chair: Liam O'Brien, University of Liverpool, UK

(Distinguished Lecture) Spin conversion phenomena in spintronics

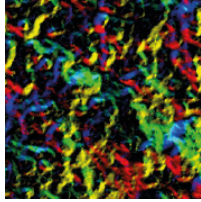
Y Otani, University of Tokyo, Japan

Spin injection and detection via the anomalous spin hall effect of a ferromagnetic metal

I Vera Marun, University of Manchester, UK

Spin pumping and spin transport in NbN/YIG structures

K Rogdakis, University College London, UK



Magnetism 2018

Special session: MMM – Magnificent Macro Magnets

Renold C2

Chair: Thomas Moore, University of Leeds, UK

- 11:45 **(Distinguished Lecture) Structural magnetostrictive alloys: From flexible sensors to energy harvesters and magnetically controlled auxetics**
A Flatau, University of Maryland, USA

12:00

12:15

- 12:30 **(Invited) Title: TBC**
A Walton University of Birmingham, UK

12:45

- 13:00 **Exhibition and lunch**
Renold C15

- 14:00 **IEEE UK Magnetism Group AGM**
Renold C2

Thin films and nanomagnets II

Renold C2

Chair: Katharina Zeissler, University of Leeds, UK

- 14:30 **Giant piezomagnetism in manganese antiperovskite nitrides**
L Cohen, Imperial College London, UK

Biomagnetism and nanoparticles

Renold C9

Chair: Matt Bryan, University of Exeter, UK

- (Invited) Novel magnetic nanoparticles beyond the bulk limits**
S Yang, University of Leicester, UK

- High frequency modes in ferromagnetic shells for microwave applications**
C McKeever, University of Exeter, UK

- Atomistic spin dynamics and finite size effects of magnetite nanocrystals**
D Meilak, University of York, UK

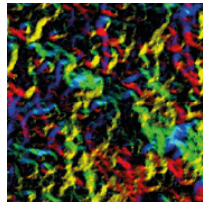
- Development of novel magnetic-elastic membranes for microfluidic applications**
E Martin, University of Exeter, UK

Theoretical and computational magnetism I

Renold C9

Chair: Julie Staunton, University of Warwick, UK

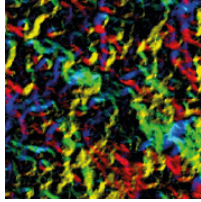
- (Invited) Merging the time and length scales in ultrafast spin dynamics**
T Ostler, Sheffield Hallam University, UK



Magnetism 2018

- 14:45 **Texture-Induced anisotropy in the magneto-electric coupling response of multiferroic composites**
T Mercer, University of Central Lancashire, UK
- 15:00 **Magnetic domain texture and Dzyaloshinskii-Moriya interaction in systems with perpendicular exchange bias**
R Khan, University of Leeds, UK
- 15:00 **The temperature dependence of magnetic anisotropy in ferrimagnets from first principles**
C Patrick, University of Warwick, UK
- 15:15 **Temperature dependence magnetic proximity effect in Pt/CoFeTaB/Pt trilayer**
O-O Inyang, Durham University, UK
- 15:15 **Temperature dependent domain wall width in ferrimagnets**
R Moreno Ortega, University of York, UK
- 15:30 **Temperature dependent magnetotransport in epitaxial RuO₂ films**
E Sharma, Imperial College London, UK
- 15:30 **Temperature dependence of magnetostriction: An ab initio theory**
G Marchant, University of Warwick, UK
- 15:45 **The thickness limit for sputter deposited ultra-thin Fe/Ni multilayers on epitaxial Cu/Si(001)**
A Frisk, Uppsala University, Sweden
- 15:45 **Comparing experimental and computational results for spin excitations**
M Lueders, STFC, UK
- 16:00 **Poster Session and Bierstube**
Renold C15

Chair: Tom Thomson, The University of Manchester, UK
- 17:30 **(Plenary) Topology and spin-orbit coupling in low dimensions lead to novel directions in spintronics**
A Fert, University of Paris-Sud, France
Renold C2
- 18:30 **Close**
- 19:30 **Conference Banquet**
The Midland Hotel
- 21:15 **After dinner talk: Spin-out, license or collaborate: the knowledge transfer dilemma**
Brian Tanner, Durham University, UK



Magnetism 2018

Tuesday 10 April

Parallel Sessions

08:30 **Registration**

Renold C8

Chair: Nicola Morley, University of Sheffield, UK

09:00 **(Wohlfarth Lecture) ATOMs - Atomistic to Micromagnetic modelling: from permanent magnets to magnetic hybrid materials**

G Hrkac, University of Exeter, UK

Renold C2

10:00 **Exhibition and refreshments**

Renold C15

High frequency spin dynamics

Renold C2

Chair: Tim Moorsom, University of Leeds, UK

10:30 **Picosecond reorientation of in-plane magnetisation within a nano-element by spin orbit torque**

P Keatley, University of Exeter, UK

10:45 **Femtosecond spin dynamics in molecular magnets**

O Johansson, University of Edinburgh, UK

11:00 **Magnon transport in multilayer magnetic system**

S Ruta, University of York, UK

11:15 **(Distinguished Lecture) Magnetic phase interference in artificial magnetic lattices: Functions and applications to optical, high-frequency, and spin wave devices**

M Inoue, Toyohashi University of Technology, Japan

11:30

Theoretical and computational magnetism II

Renold C9

Chair: Martin Lueders, STFC, UK

(Invited) Interplay of magnetism and microstructure in functional Heusler alloys: A first principles perspective

M Gruner, University of Duisburg-Essen, Germany

Temperature effects and inverse caloric responses in Mn-Antiperovskite carbide Mn₃GaC: Ab-initio theory

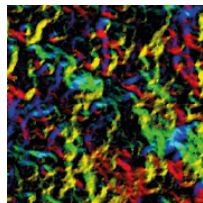
E Mendive Tapia, University of Warwick, UK

Non-uniform spin transfer torque switching dynamics in CoFeB/MgO magnetic tunnel junctions

A Meo, University of York, UK

Investigation into the origin of the athermal training effects in exchange bias multilayers

S Jenkins, University of York, UK



Magnetism 2018

11:45

Effect of aggregation on the radio-frequency heating of ferromagnetic manganite nanoparticles
J Cook, Queen's University Belfast, UK

Chair: Robert Hicken, University of Exeter, UK

12:00 **EPSRC Presentation**

Renold C2

12:15 **Poster Awards and IOP Group AGM**

Renold C2

12:45 **Lunch and Poster/Company Exhibitions**

Renold C15

Correlated electrons

Renold C2

Chair: Nina-Juliane Steinke, STFC, UK

14:00 **(Invited) Hunting majorana fermions in quantum spin-liquids**

J Knolle, Imperial College London, UK

14:15

14:30 **Multi-site exchange enhanced barocaloric response in Mn_3NiN**

D Boldrin, Imperial College London, UK

14:45 **Complex modulated magnetism in PrPtAl**

D Wermeille, XMaS - ESRF, UK

15:00 **Decomposing the Bragg glass and the peak effect in a Type-II superconductor**

C Larsen, University of Birmingham, UK

15:15 **Refreshments**

Renold C15

Spintronics II

Renold C9

Chair: Ivan Vera Marun, The University of Manchester, UK

Towards pure spin currents for oxide spintronic devices

C Cox, Loughborough University, UK

Magnetic oxides for spin injection: recent outcomes from the molecular spintronics

P Graziosi, CNR-ISMN, Italy

Multifunctional spintronic device based on spin dependent charge trapping

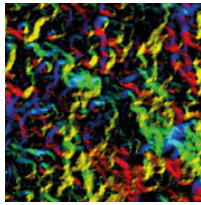
T Moorsom, University of Leeds, UK

Spintronics in high-quality graphene heterostructures via 1D contacts

V Guarochico-Moreira, University of Manchester, UK

Electrical and optical characterisation of Fe/n-GaAs non-local spin valve

J-Y Kim, University of York, UK



Magnetism 2018

Thin films and nanomagnets III

Renold C2

Chair: Shahid Hussain, Qinetiq, UK

15:45 **(Invited) Mapping three dimensional spin structures with X-ray magnetic tomography**

C Donnelly, ETH Zurich, Switzerland

16:00

16:15 **Two-photon lithography for 3D magnetic nanostructure fabrication**

M Hunt, Cardiff University, UK

16:30 **Spatial mapping of torques within a spin hall nano-oscillator**

T Spicer, University of Exeter, UK

16:45 **Macro-ferromagnetism in a novel artificial spin ice**

G Macauley, University of Glasgow, UK

17:00 Close of conference

Other topics in magnetism

Renold C9

Chair: Allan Walton, University of Birmingham, UK

Element-specific magnetic imaging with 20 nm spatial resolution using table-top high-harmonic source

S Zayko, Georg-August University, Germany

Chemical and structural analysis on magnetic tunnel junctions using a decelerated scanning electron beam

E Jackson, University of York, UK

Superconducting spintronics – active role of spin-orbit coupling and dynamics of triplet Josephson junctions

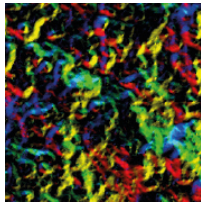
N Banerjee, Loughborough University, UK

The development of the hydrogen ductilisation process (HyDP) for NdFeB-type alloys

O Brooks, University of Birmingham, UK

Recycling of SmCo₅ magnets by HD process

A Eldosouky, Magneti, d.d., Slovenia



Magnetism 2018

Poster programme

P:01 Rapid fabrication of magnetic microstructures by laser direct writing (LDW)

Alaa Alasadi, University of Sheffield, UK

P:02 Effect of growth parameters on magnetostrictive amorphous thin films

Qayes Aldulaim, University of Sheffield, UK

P:03 Effect of post annealing on the magnetic properties of FeN with RF-sputtered amorphous carbon thin films

Shoug Alghamdi, University of Leeds, UK

P:04 Magnetic domains in Pt/CoFeB/Ir multilayers grown on piezoelectric substrates

Khulaif Alshammari, University of Leeds, UK

P:05 Improving the magnetic and dynamic properties of Yttrium Iron Garnet

Mohammed Alyami, University of Leeds, UK

P:06 Effect of growth conditions on the Soft Magnetostrictive properties of thin Fe-Co-Cr films

Saturi Baco, University of Sheffield, UK

P:07 On the use of electrostatic compensation of current carrying μ -coils for calibrated MFM

Craig Barton, National Physical Laboratory, UK

P:08 Investigation of sputtering conditions on the properties of Ta/CoFeB/MgO stacks

Charlotte Bull, The University of Manchester, UK

P:09 Strain control of the magnetic properties of FeRh thin-film heterostructures for data storage applications

Will Griggs, The University of Manchester, UK

P:10 Realization of ground state in artificial kagome spin ice via topological defect-driven magnetic writing

Jack Carter Gartside, Imperial College London, UK

P:11 Dynamic emergent behaviour of domain walls in interconnected nanoring arrays

Richard Dawidek, University of Sheffield, UK

P:12 Angular dependant FMR of rotational symmetry broken artificial kagome spin ice

Troy Dion, University College London, UK

P:13 Perpendicular Anisotropy in $\text{Co}_2\text{FeAl}_{0.5}\text{Si}_{0.5}$ for CPP-GMR devices

William Frost, University of York, UK

P:14 Atomistic modelling of granular exchange bias systems

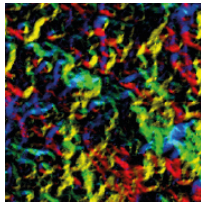
Sarah Jenkins, University of York, UK

P:15 Collective excitations of magnetic bubble domains in an antidot lattice

Angus Laurenson, University of Exeter, UK

P:16 Asymmetric relaxation of magnetic frustration observed in freestanding B2-ordered FeRh thin films

Jamie Massey, University of Leeds, UK



Magnetism 2018

P:17 Fabrication and characterisation of a three-dimensional magnetic nanowire lattice

Andrew May, Cardiff University, UK

P:18 Magnetic and structural influences of layer inversion in Pt/Co₃₂Fe₃₂Ta₂₀B₁₆/Ir trilayers

Ben Nicholson, Durham University, UK

P:19 Krypton doped polar ZnO films by Ion implantation gives enormous magnetisation

Ahmad Saeedi, University of Sheffield, UK

P:20 Investigation of magnetic properties for both cobalt and europium implanted ZnO films prepared by pulsed laser deposition

Ahmad Saeedi, University of Sheffield, UK

P:21 Implementation of VAMPIRE atomistic simulation on the synthetic ferrimagnet Ni₃Pt/Ir/Co

Jade Scott, Queen's University Belfast, UK

P:22 Atomistic magnetic modelling of FeRh finite-size systems

Mara Strungaru, University of York, UK

P:23 Magnetic imaging of phase domain development in laterally confined FeRh

Rowan Temple, University of Leeds, UK

P:24 Low temperature annealing of superconducting bismuth nickel bilayers

Matthew Vaughan, University of Leeds, UK

P:25 Strain mediated voltage control of layer switching order in synthetic antiferromagnets

Alexander Welbourne, University of Cambridge, UK

P:26 Magnetism in uranium thin films

Ming-Hung Wu, University of Bristol, UK

P:27 Preparation of Ca:YIG thin films by PLD

Aliaa M Zaki, University of Sheffield, UK

P:28 Spin-wave dynamics of honeycomb artificial spin ice in different microstates

Daan Arroo, Imperial College London, UK

P:29 Characterisation of iron-rich cobalt-iron-boron thin films using ferromagnetic resonance

Geet Awana, Loughborough University, UK

P:30 X-Ray detected ferromagnetic resonance (XFMR)

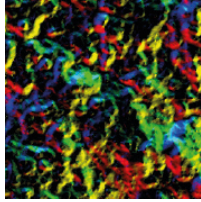
David Burn, Diamond Light Source, UK

P:31 Selective excitation of localised spin wave modes by optically pumped surface acoustic waves

T J Hayward, University of Sheffield, UK

P:32 Time-resolved x-ray detected ferromagnetic resonance measurements in a CoFe/NiO/Fe/NiFe multilayer structure

Takafumi Nakano, University of Exeter, UK



Magnetism 2018

P:33 Influence of interfacial structure and heavy metal thickness on spin mixing conductance for the enhancement of damping

Charles Swindells, Durham University, UK

P:34 Ferromagnetic resonant modes of synthetic antiferromagnetic structures

Harry Waring, The University of Manchester, UK

P:35 Theory of linear spin wave emission from a Bloch domain wall

Natalie Whitehead, University of Exeter, UK

P:36 Magnonic studies of ferromagnetic nanostructures I

Guru Venkat, Loughborough University, UK

P:37 Strain manipulation of the magnetoresistance in nickel and permalloy thin films

Mohammed Al-Qayoudhi, University of Nottingham, UK

P:38 Time resolved imaging of coupled nano-contact spin transfer vortex oscillators

Erick Burgos Parra, University of Exeter, UK

P:39 In-Situ PNR of the spin seebeck effect

Andrew Caruana, STFC, UK

P:40 Dynamic modelling of spin accumulation

Luke Elliott, University of York, UK

P:41 Manipulating the spin-dependent transport – thin films and β -Tungsten

Martin Gradhand, University of Bristol, UK

P:42 Simulation study of ballistic spin-MOSFET devices with ferromagnetic channels based on Heusler and oxide compounds

Patrizio Graziosi, CNR-ISMN, Italy

P:43 Exploration of new L1₀-ordered materials for their spintronic applications

Philip Thompson, The University of Manchester, UK

P:44 Finite size effects in antiferromagnetic materials

Sarah Jenkins, University of York, UK

P:45 Magneto-optical detection of spin accumulation under influence of mechanical rotation

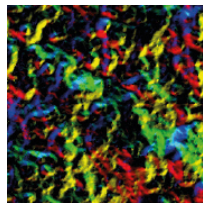
Jun-young Kim, University of York, UK

P:46 Proximity induced magnetization in Co₂FeAl ultrathin films: effects of the annealing temperature and the heavy metal material

Ariam Mora-Hernández, Durham University, UK

P:47 Towards a standard spin seebeck measurement

Kelly Morrison, Loughborough University, UK



Magnetism 2018

P:48 Investigating the role of Ga-substitution in Fe_{1-x}Ga_x (Galfenol) thin films

Syamashree Roy, University of Nottingham, UK

P:49 Theory of power combining of spin-torque nanooscillators

Ansar Safin, National Research University "Moscow Power Engineering Institute", Russia

P:50 Current-induced domain-wall motion in pinned magnetic wires

Marjan Samiepour, University of York, UK

P:51 Current biased splitting in the Peltier signal observed using lateral spin valves

Georgios Stefanou, University of Leeds, UK

P:52 XMCD studies of heavy-metal/ferromagnet heterostructures

Laura Stuffins, Loughborough University, UK

P:53 Paramagnetic spin Hall magnetoresistance

Amy Westerman, University of Leeds, UK

P:54 Multilayers for Skyrmion-based devices

Yuzhe Zang, The University of Manchester, UK

P:55 Muon measurements of magnetism in the frustrated spin-chain compound Sr₃NiIrO₆

Joel Barker, Paul Scherrer Institute, Switzerland

P:56 Towards control of uniaxial anisotropy in S = 1 magnetic systems

Sam Curley, University of Warwick, UK

P:57 Intermediate magnetic phase of charge-stripe ordered La₂NiO_{4.11} and the trigger for static magnetic ordering

Paul Freeman, University of Central Lancashire, UK

P:58 Magnetic properties of Sr_{3-x}Y_x(Fe_{1.25}Ni_{0.75})O_{7-δ}: a combined experimental and theoretical investigation

Samara Keshavarz, Uppsala University, Sweden

P:59 Theory of L-edge spectroscopy of strongly correlated systems

Johan Schödt, Uppsala University, Sweden

P:60 Local field distribution and orbital ordering in a multiferroic perovskite metal-organic framework

Zhengqiang Yang, Queen Mary University of London, UK

P:61 Emergent propagation modes of ferromagnetic swimmers in constrained geometries

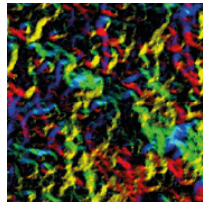
Matthew Bryan, University of Exeter, UK

P:62 Demagnetising factors of rectangular prisms packed with magnetic nanoparticles

Steven McCann, University of Central Lancashire, UK

P:63 The role of faceting and shape on the effective magnetic anisotropy of magnetite nanocrystals

Roberto Moreno Ortega, University of York, UK



Magnetism 2018

P:64 Multiwavelength magneto-optical characterization of magnetic nanoparticles for magnetic hyperthermia
Rémy Soucaille, Exeter University, UK

P:65 Dynamic simulation of a two-dimensional skyrmion lattice
Yu Li, The University of Manchester, UK

P:66 Magnetic nanowires of curved cross-section: A Micro-magnetic study
Arjen van den Berg, Cardiff University, UK

P:67 Implementing superconductivity into a green's function (KKR) method to explore the interactions between superconductivity and magnetism
Tom Saunderson, University of Bristol, UK

P:68 First-principles study of magnetisation of ZnO/Co and ZnCoO/Co systems
Fatma Gerriu, University of Sheffield, UK

P:69 Magnetic hyperthermia: Easy axis alignment of magnetic nanoparticles driven by Brownian rotation
Samuel Rannala, University of York, UK

P:70 3D FDTD-LLG modelling of magnetisation dynamics in thin film ferromagnetic structures
Feodor Ogrin, University of Exeter, UK

P:71 Mode analysis of the tree-like bio-inspired networks of vortex-based spintronic nanooscillators
Olga Katkova, National Research University "Moscow Power Engineering Institute", Russia

P:72 FP-LAPW calculations : Electronic and magnetic properties of Pr₂Fe₁₇ intermetallic compound
Karim Bakkari, Université de Tunis El Manar, Tunisia

P:73 3D-Printing polymer-based permanent magnets
Roger Domingo-Roca, University of Strathclyde, UK

P:74 The Structural and magnetic properties of GdCo₅-xNi_x
Amy Tedstone, University of Warwick, UK

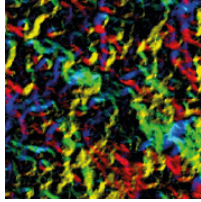
P:75 Atomistic calculations of magnetic properties of Sm(1-x)ZrxFe₁₂
Samuel Westmoreland, University of York, UK

P:76 Magnetic exchange disorder in low-dimensional quantum magnets
William Blackmore, University of Warwick, UK

P:77 Scanning probe microscopy at magnetic fields up to 34 T
Benjamin Bryant, Radboud University, The Netherlands

P:78 Magnetic properties of Bis-Lanthanoates
Kane Esien, Queen's University Belfast, UK

P:79 Ferromagnetic swimmers: Fabrication, controlled swimming, and applications
Joshua Hamilton, University of Exeter, UK



Magnetism 2018

P:80 Dynamics of the flux line lattice in high purity niobium studied with stroboscopic neutron scattering
Camilla Buhl Larsen, University of Birmingham, UK

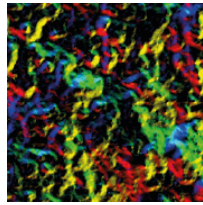
P:81 Probing proximity induced triplet states with point contact Andreev spectroscopy
Andy Moskalenko, Imperial College London, UK

P:82 Propagating spiral spin waves in magnetic nanostructures
David Osuna Ruiz, University of Exeter, UK

P:83 Remote magnetic monitoring of swelling in intermediate level waste canisters
Patrick Pan, University of Sheffield, UK

P:84 Magneto-optical imaging of dendritic flux avalanches in a superconducting MgB_2 tape
Thomas Qureshy, University of Oslo, Norway

P:85 Paramagnetic Meissner effect in metal-molecule hybrid systems
Matthew Rodgers, University of Leeds, UK



Magnetism 2018

Oral

Thin films and nanomagnets I

Electrical transport signature of skyrmions in Pt/Co/Ir multilayer discs

K Zeissler¹, S Finizio², K Shahbazi¹, J Massey¹, F A M'Mari^{1,3}, J Raabe², M Rosamond¹, E H Linfield¹, T A Moore¹, G Burnell¹ and C H Marrows¹

¹University of Leeds, UK, ²Paul Scherrer Institut, Switzerland, ³Sultan Qaboos University, Oman

Magnetic quasi-particles such as skyrmions are of importance for novel magnetic information storage designs. In ultrathin multilayer systems skyrmions are stabilised by the interfacial Dzyaloshinskii-Moriya interaction (1). This interaction occurs due to broken inversion symmetry at the interface between a ferromagnet and a heavy metal. Due to tunability and room temperature stability these multilayers have great scope for applications (2-5). Active focal areas are electrical skyrmion detection and manipulation. In the experiment outlined here a single skyrmion in a Ta (3.5 nm)/Pt (3.8 nm)/[Co (5.0 nm)/Ir (5.0 nm)/Pt (1.0 nm)]x10 Pt (3.2 nm) multilayer nanodisc was imaged using the PolLux scanning transmission X-ray microscopy as a function of out-of-plane magnetic field. The Hall resistance was measured *in situ* just before each image was taken. The circular polarized X-rays were tuned to L₃ cobalt edge and were transmitted perpendicular to the sample plane. The Hall resistance shows a clear difference between uniform magnetised states and a single skyrmion state. By directly correlating the measured Hall resistance to the magnetic state obtained from the imaging a magnetization independent resistance contribution to the Hall resistance was identified. This contribution was observed to be proportional to the number of skyrmions present in the disc. This work was funded by Horizon 2020 MagicSky.

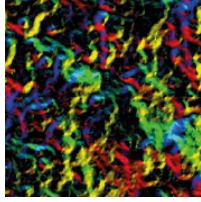
- [1] Fert, A. et al. *Nature Nanotechnology*. 2013, 8(3), pp.152-156.
- [2] Boulle, O. et al. *Nature Nanotechnology*. 2016, 11(5), pp.449-+.
- [3] Dupe, B. et al. *Nature Communications*. 2016, 7.
- [4] Jiang, W.J. et al. *Science*. 2015, 349(6245), pp.283-286.
- [5] Moreau-Luchaire, C. et al. (vol 11, pg 444, 2016). *Nature Nanotechnology*. 2016, 11(8), pp.731- 731.

Exploring interfacial Dzyaloshinskii-Moriya interaction for in-plane thin film permalloy nanostructures using micromagnetic simulations and Lorentz microscopy

K Fallon¹, S Azzawi², D Atkinson² and S McVitie¹

¹University of Glasgow, UK, ²Durham University, UK

Nanostructured soft ferromagnetic thin films readily form vortex structures with an out of plane singularity at the vortex core. Such a structure provides possibilities for interesting Dzyaloshinskii-Moriya (DMI) effects around the vortex core. To investigate this we have looked at the influence of interfacial DMI on vortex structures in thin (8nm) films of permalloy. Micromagnetic simulations were performed using MuMax³ and indicate that DMI causes twisting of the magnetisation around the vortex core - the magnetisation has a divergent component local to the vortex core and is no longer purely rotational (see fig1.). Furthermore, the simulations show that the sign and the strength of the divergent component relates to the sign and the strength of DMI. Hysteresis loops were calculated that show a relationship between the magnitude of DMI and the vortex expulsion field, with a smaller field required to expel vortices in systems with a larger



Magnetism 2018

magnitude of DMI. The vortex expulsion has been observed directly via in situ Lorentz transmission electron microscopy (TEM) experiments, using the Fresnel method to image domain walls. We note a reduction of the expulsion field for films with strong interfacial DMI compared to those with no expected DMI. We also report on using the quantitative method of differential phase contrast (DPC) to map the magnetic induction of the sample. Calculated images of the induction maps from micromagnetic simulations suggest the divergent component of the magnetisation provides a measurable signal from DPC. We will present details of these measurements.

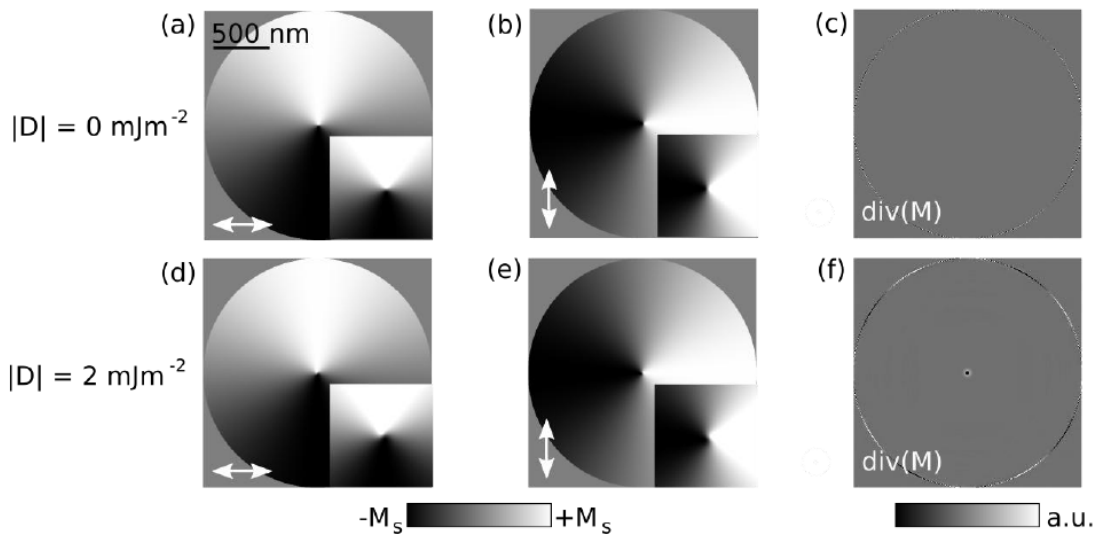


Figure 1: The results of MuMax³ simulations of permalloy disks (diameter 2 μm) with and without DMI are shown. Figures (a) and (b) show M_x and M_y of a vortex structure with no DMI. Image (c) shows the divergence of this magnetic state. Figures (d) and (e) show M_x and M_y of a vortex structure with DMI of 2 mJm^{-2} . Image (f) shows the divergence of this magnetic state. The insets show the core of the in-plane magnetisation components at a larger scale so that the twisting of the magnetisation is visible.

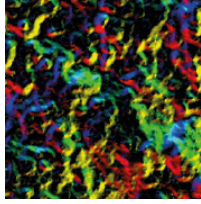
Investigation of DMI value for chiral domain walls in Pt/Co/Ir/Ta multilayers

K Shahbazi¹, J-V Kim², V Jeudy², T A Moore¹ and C H Marrows¹

¹University of Leeds, UK, ²Universites Paris-Sud et Paris-Saclay, France

Designing multilayer stacks with both high Dzyaloshinskii-Moriya interaction (DMI) and spin Hall effect (SHE) is of great current interest for spintronic devices exploiting chiral domain walls (DW) or skyrmions. But, up to date, correct estimation of DMI in different thin film structures was a struggle. The most used approach is asymmetric bubble expansion in presence of applied in-plane field, H_{ip} [1]. Nonetheless, it does not always show clean data as presented in Je's [1] and Hrabec's [2], in which you have one clear minimum point \sim (offset from zero) in graphs of DW velocity versus H_{ip} which accounts for DMI field. Our results here are in harmony with other recent reports of anomalies found when applying this method in the creep regime [3, 4], suggesting that more sophisticated models are needed.

In this work, we are investigating multilayers of Pt/Co/ β -Ta in which a thin layer of Ir is inserted between Co and top layer Ta. Changing the Ir thickness, we are investigating DMI variations using previously mentioned



Magnetism 2018

bubble expansion method [1, 2]. Whilst we have confirmed that all the data are in the creep regime, but there is nevertheless an unexpected restoration of DW velocity and the velocity symmetry especially for larger in-plane fields when bubble domain appear to grow symmetrically again (Figure 1). Not only does not the model above account this symmetrical expansion of bubbles at high in-plane fields, but also the offset field of does not always give the true DMI value for these experimental data [5]. As a result, we are proposing a model based on DW's elastic energy redefining the dependence of DW (elastic) energy on H_{ip} which can describe some aspects attributed to change of velocity asymmetry of chiral DWs and results in more realistic DMI value for such structures. We also compared the results with DMI calculated from Brillouin light scattering (BLS) measurements. All the results show that great care is needed when measuring DMI as different techniques on same samples do not necessarily show the same results.

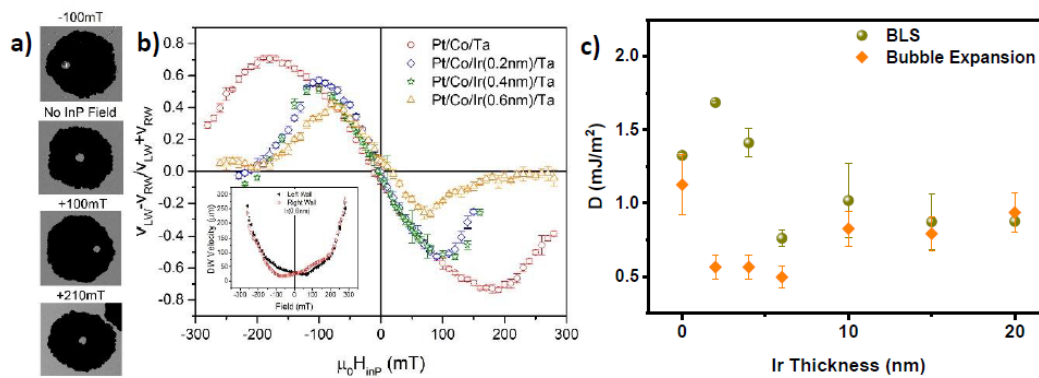


Figure. a) Images of bubble expansion in presence of applied in-plane field, H_{ip} , showing symmetrical propagation for H_{ip} . b) Velocity asymmetry with respect to H_{ip} for samples with different Ir thickness. The inset shows changes of DW velocity versus applied H_{ip} for both left side (black solid triangles) and right side (red open triangles) DWs. c) Comparison of D calculated from BLS and bubble expansion.

- [1] S.-G. Je, *et al.*, Physical Review B, 88, 214401, 2013.
- [2] A. Hrabec, *et al.*, Physical Review B, 90, 020402, 2014.
- [3] R. Lavrijsen, *et al.*, Physical Review B, 91, 104414, 2015.
- [4] M. Vanatka, *et al.*, Journal of Physics: Condensed Matter 27, 326002 (2015).
- [5] R. Soucaille, *et al.*, Physical Review B, 94, 104431, 2016.

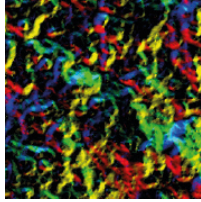
Magnetism you can rely on: A materials-science based solution to stochastic domain wall pinning in magnetic nanowire devices

T J Broomhall¹, P W Fry², M C Rosamond³, A W Rushforth⁴, D A Allwood¹ and T J Hayward¹

¹University of Sheffield, UK, ²University of Leeds, UK, ³University of Nottingham, UK

Proposed domain wall (DW) memory and logic devices rely upon the deterministic motion of domain walls through nanowires. However, their development has been hampered by the fact that DWs show exceptionally high levels of stochasticity in their pinning and depinning. Recent studies have shown that this stochasticity arises from Walker Breakdown phenomena, where DWs undergo periodic changes in their magnetisation structure at typical propagation fields, and thus that stochastic pinning is an intrinsic feature of DW behaviour¹.

In a previous theoretical work, we suggested that by doping small amounts of Rare earth elements into Ni₈₀Fe₂₀ to increase its Gilbert damping we can suppress Walker Breakdown², thus eliminating the root cause



Magnetism 2018

of stochastic pinning/depinning effects, and creating devices with inherently reliable behaviours. In this presentation we present the first experimental validation of this approach.

We perform focussed magneto-optic Kerr effect (FMOKE) measurements of domain wall pinning/depinning at artificial defect sites in $\text{Ni}_{80}\text{Fe}_{20}$ nanowires doped with 0-10 % Tb. For the undoped $\text{Ni}_{80}\text{Fe}_{20}$ nanowires DW depinning field distributions (DFDs) exhibit multiple modes with a wide range of depinning fields, consistent with previously characterised stochastic behaviours^{3,4} (Figure 1(a)). However, equivalent doped nanowires show much simpler behaviour, with some exhibiting quasi-deterministic, single mode DFDs (Figure 1(b)). We support these results with ferromagnetic resonance measurements of the doped-film's Gilbert damping constants, allowing us to estimate the DWs Walker breakdown fields in each device.

Our results illustrate the feasibility creating consistent, deterministic switching behaviour in nanowire devices through simple engineering of material properties.

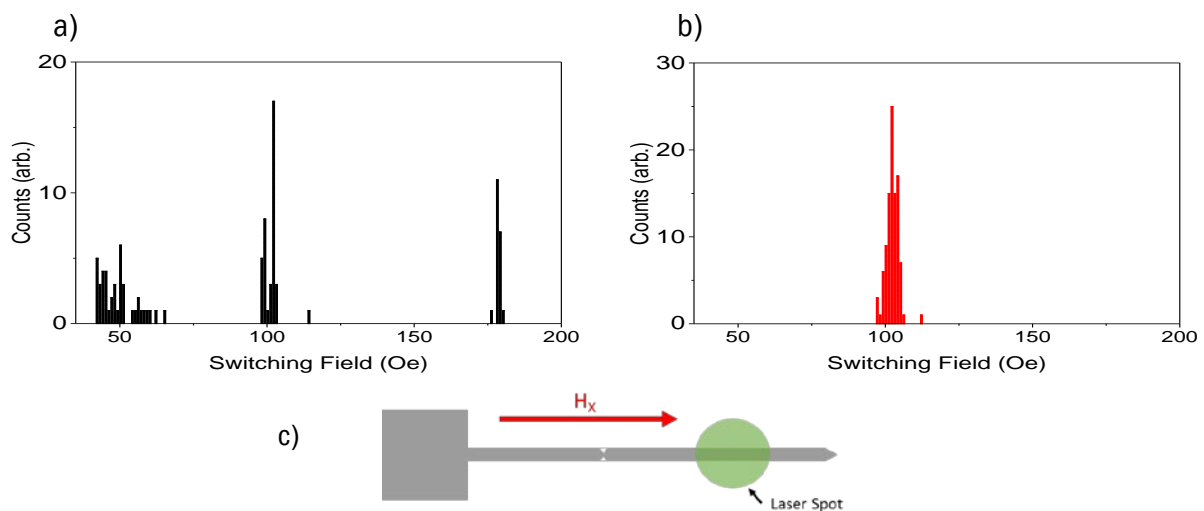
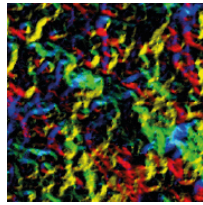


Figure 1. Depinning distributions found for a 50% double notch in an (a) Undoped $\text{Ni}_{80}\text{Fe}_{20}$ nanowire and (b) 5% Tb doped $\text{Ni}_{80}\text{Fe}_{20}$ nanowire. For an undoped nanowire, multiple depinning modes are seen with a large range of depinning fields. However in a doped sample, a single depinning mode is found, indicating a reduction in stochastic behaviour. (c) Schematic of nanowire design with laser spot indicating location of FMOKE measurement.

- [1] T. J. Hayward, *Sci. Rep.*, vol. 5, pp. 1–12, 2015.
- [2] T. J. Broomhall and T. J. Hayward, *Sci. Rep.*, vol. 7, no. 1, p. 17100, Dec. 2017.
- [3] K. A. Omari and T. J. Hayward, *Sci. Rep.*, vol. 7, no. 1, pp. 1–10, 2017.
- [4] M. Y. Im, L. Bocklage, P. Fischer, and G. Meier, *Phys. Rev. Lett.*, vol. 102, no. 14, pp. 1–4, 2009.



Magnetism 2018

Topological magnetic writing: Defining specific magnetization states in nanostructures

J C Gartside, D M Arroo, D M Burn, A Moskalenko, L F Cohen and W R Branford¹

Imperial College London, UK

Networks of magnetic nanostructures are of broad interest from novel data storage and computation to magnonic crystals. One family of nanomagnetic arrays, characterized by strong and frustrated magnetic interactions are the artificial spin ices (ASI). ASI structures have provided vast amounts of physical insight in recent years [1,2,3,4] in part due to their ability to model complex systems [5] and exhibit exotic phenomena such as ‘magnetic monopole’-like states [6]. The power of these networks stems from the extraordinary number of unique microstates, even in systems comprising relatively few nanostructures. However, magnetic nanoarrays in general, and ASI structures in particular, have yet to realise their full potential as the majority of microstates remain inaccessible due to the rudimentary state-writing tools currently available. An experimental means to prepare all potential microstates has huge implications, including realising ASI as a tunable-bandgap magnonic crystal [7] or reconfigurable neural-network [8]. We present a novel MFM-tip based state writing technique, building on our previously demonstrated domain-wall injection process [9]. It requires no global fields and is applicable to all nanostructure architectures, providing control over the spin-configuration and access to every possible microstate. We demonstrate our method via realisation of several exotic and thus-far unobserved states, unachievable via global field-protocols: ‘magnetic monopole-defect’ chains and the spin-crystal ground state [10] of kagome ASI.

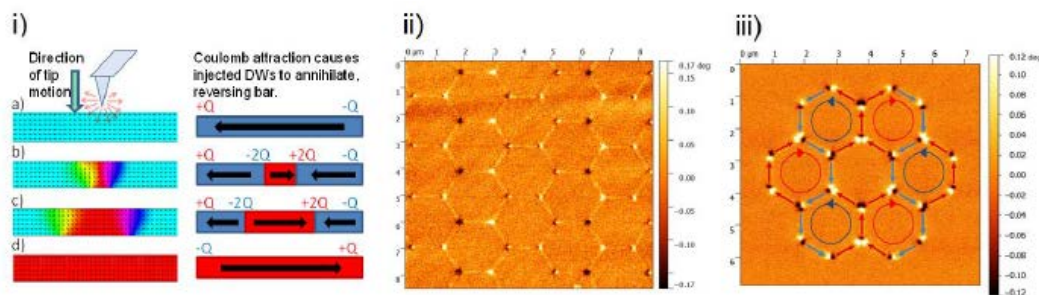
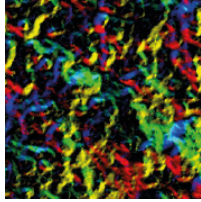


Figure 1: i) Micromagnetic simulation and accompanying schematic of writing process dynamics showing positions of magnetic charges ($\pm Q$). ii) MFM image of ‘ladder’ and ‘zigzag’ monopole- defect chain states written at RT on a NiFe ASI lattice. iii) MFM image of the spin-crystal chiral ground state of kagome ASI written at RT on a NiFe ASI rosette.

- [1] Wang, RF, et al. Nature 439.7074 (2006): 303-306.
- [2] Branford, W. R., et al. Science 335.6076 (2012): 1597-1600.
- [3] Zhang, Sheng, et al. Nature 500.7464 (2013): 553-557.
- [4] Perrin, Yann, Benjamin Canals, and Nicolas Rougemaille. Nature 540.7633 (2016): 410-413.
- [5] Qi, Yi, T. Brintlinger, and John Cumings. Phys. Rev. B 77.9 (2008): 094418.
- [6] Ladak, Sam, et al. Nature Physics 6.5 (2010): 359-363.
- [7] Heyderman, L. J., and R. L. Stamps. J. Phys.: Cond. Matt. 25.36 (2013): 363201.
- [8] Wang, Yong-Lei, et al. Science 352.6288 (2016): 962-966.
- [9] Gartside, J. C., et al. Scientific Reports 6 (2016)
- [10] Anghinolfi, L., et al. Nat. Comms. 6 (2015).



Magnetism 2018

Spintronics I

(Distinguished Lecture) Spin conversion phenomena in spintronics

Y C Otani

University of Tokyo, Japan

Since the discovery of giant magnetoresistance, spintronics research has been evolving and has reached a new phase in which the concept of spin currents, i.e., the flow of spin angular momenta, helps us understand various spintronics phenomena. These include all the recently discovered conversion phenomena, such as the direct and inverse spin Hall effects, spin Seebeck and Peltier effects, spin pumping, and the inverse Faraday effect. More recently, Rashba interfaces and the surface states of topological insulators were found to exhibit the so-called Edelstein effect, in which spin-momentum locking behavior brings about non-equilibrium spin accumulation.

These interface and surface effects thus provide an effective means of interconversion among spin, charge, and heat currents. Most of the above-mentioned spin conversion phenomena take place at simple nanoscale interfaces between two different types of materials (e.g., magnets, non-magnets, semiconductors, and insulators). These structures may enable us to advance spin-mediated interconversion among physical entities such as electricity, light, sound, vibration, and heat.

I will first give an introduction to the general spin-mediated spin-conversion processes and then will focus on magneto-electric spin conversion in conductive solids, including spin Hall effects and new conversion mechanisms: Edelstein effects arising at Rashba interfaces [1] and surface states of topological insulators [2], as discussed in a recently published progress article [3].

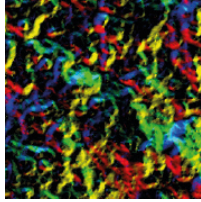
- [1] S. Karube, K. Kondou, and Y. Otani, "Experimental observation of spin-to-charge current conversion at non-magnetic metal/ Bi_2O_3 interfaces," *Appl. Phys. Exp.*, vol. 9, 033001, 2016.
- [2] K. Kondou et al., "Fermi-level-dependent charge-to-spin current conversion by Dirac surface states of topological insulators," *Nature Phys.*, vol. 12, pp. 1027-1031, 2016.
- [3] Y. Otani et al., "Spin Conversion on the nanoscale," *Nature Phys.*, vol. 13, pp. 829-832, 2017.

Spin injection and detection via the anomalous spin hall effect of a ferromagnetic metal

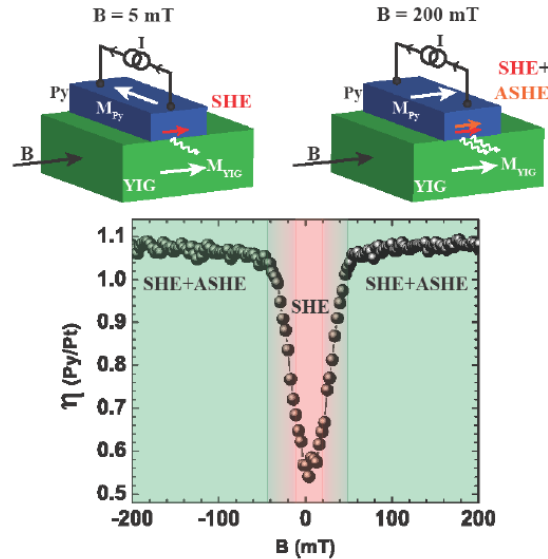
K S Das¹, W Y Schoemaker¹, B J van Wees¹ and I J Vera-Marun²

¹University of Groningen, The Netherlands, ²The University of Manchester, UK

Electrical injection of spin current via the spin Hall effect has a huge technological implication for spin transfer torque devices and in magnon spintronics. This effect generates a spin current perpendicular to a charge current but has so far relied on expensive heavy metals. We report a novel spin injection and detection mechanism via the anomalous Hall effect of a ferromagnetic metal [1]. The mechanism, which we name the anomalous spin Hall effect (ASHE) refers to the spin accumulation generated within a ferromagnet due to the anomalous Hall effect, along the direction of the ferromagnet's magnetization. We utilise the ASHE and its reciprocal effect to electrically inject and detect magnons in a magnetic insulator in a non-local geometry. Our experiments reveal that permalloy can have a higher spin injection and detection efficiency to that of platinum, owing to the ASHE. We also demonstrate the tunability of the ASHE via the orientation of the permalloy magnetization, thus creating new possibilities for spintronic applications.



Magnetism 2018



Top: Schematic diagram of the experimental geometry. A charge current (I) through the Py injector generates a transverse spin accumulation at the Py/YIG interface via the SHE (left) or via the combination of ASHE and SHE (right), which excites magnons in YIG by the transfer of angular momentum. The presence of ASHE is controlled by the orientation of the Py magnetization (M_{Py}). Bottom: The relative detection efficiency of Py over Pt [$\eta(\text{Py/Pt})$], as a function of applied magnetic field (B).

- [1] Das, K. S., Schoemaker, W. Y., van Wees, B. J. & Vera-Marun, I. J. *Phys. Rev. B* 96, 220408(R) (2017).

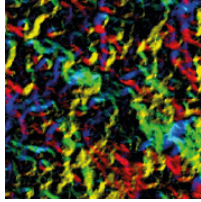
Spin pumping and spin transport in NbN/YIG structures

K Rogdakis¹, A Sud¹, M Amado², C M Lee², J W A Robinson², M G Blamire², L F Cohen³ and H Kurebayashi¹

¹University College London, UK, ²University of Cambridge, UK, ³Imperial College London, UK

Ferromagnetism and conventional singlet superconductivity can be regarded as competing ordering phenomena. However, a considerable body of theoretical work over recent years has predicted that at interfaces between the two systems competition or coupling between superconducting and magnetic phenomena are possible resulting in novel effects emergency such as triplet cooper pairs which can carry spin information, pi-phase Josephson Junctions etc [1]. In order to understand these emerging superconducting spintronics phenomena [2], it is important to quantify parameters of both magnetic dynamics and spin transport in structures including superconducting materials.

In this study, we present ferromagnetic resonance measurements (FMR) in NbN/YIG bi-layers by varying NbN thickness while keeping constant YIG thickness. In addition to FMR measurements, by attaching two side electrodes a charge voltage (V_{ISHE}) across the sample is simultaneously detected as a result of the inverse spin Hall Effect (Fig. 1) [3]. We have performed a number of systematic measurements on V_{ISHE} to extract key magnetic and spin-orbit parameters of both NbN and YIG layers. We will present the summary of this analysis, together with detailed discussions on the parameters extracted.



Magnetism 2018

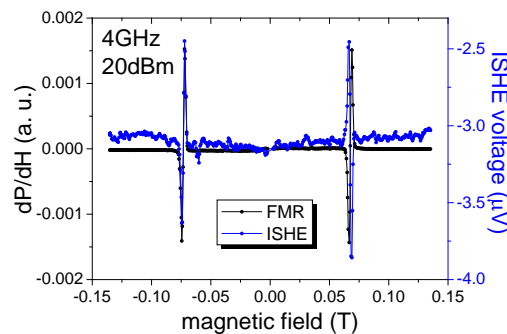


Figure1: Both FMR absorption spectrum and inverse spin-Hall voltage detected through NbN layer using a 20dBm microwave power excitation at 4GHz. Note that since we used ac magnetic field modulation technique, both peaks' shape corresponds to the derivative of a Lorentzian function.

- [1] M. Eschrig, Rep. Prog. Phys. 78,104501 (2015).
- [2] K. Roy, Phys. Rev. B 96, 174432 (2017).
- [3] K. Ando, S. Takahashi, K. Harii, K. Sasage, J. Ieda, S. Maekawa, and E. Saitoh, Phys. Rev. Lett. 101, 036601 (2008).

Special session: MMM – Magnificent Macro Magnets

(Distinguished Lecture) Structural magnetostrictive alloys: From flexible sensors to energy harvesters and magnetically controlled auxetics

A Flatau

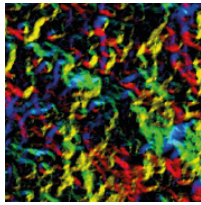
University of Maryland, USA

Novel sensors and energy harvesting transducers take advantage of the significantly expanded design space made possible by recent advances in structural magnetostrictive alloys. These alloys can be machined and welded, have high fracture toughness, and can actuate, sense, and carry load while subjected to tension, compression, and bending. The talk includes an introduction to magnetostrictive materials and on the use of low-cost rolling and annealing methods in lieu of more costly crystal growth methods for making bulk iron-gallium (Galfenol) and iron-aluminum (Alfenol) alloys. The process of using magnetostrictive materials to convert mechanical energy into magnetic energy and then into electrical energy is explained and demonstrated. Examples of magnetostrictive devices include prototypes ranging in size from nanowire-based pressure sensors to huge structures floating in the ocean that convert wave energy into electrical power for “community-scale” energy needs. The recent discovery of a particularly unique attribute of these alloys, their auxetic behavior, will also be discussed. In both Galfenol and Alfenol, both strain and magnetic fields can produce simultaneous increases in lateral and longitudinal dimensions, with measured values of the resulting Poisson ratio being not only negative, but also as low as -2 .

(Invited) Title and abstract unavailable

A Walton

University of Birmingham, UK



Magnetism 2018

Biomagnetism and nanoparticles

(Invited) High-moment magnetic nanoparticles formed in superfluid helium

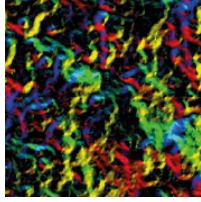
S Yang

University of Leicester, UK

Helium droplets are clusters of helium whose size can vary over a huge range, spanning a few dozen to in excess of 10^{11} helium atoms [2]. They possess some unique properties that are important for fabrication of nanomaterials [2], such as 1) a very low temperature (0.37 K), 2) superfluidity, 3) the ability to add materials sequentially, 4) the chemical inertness of helium.

This presentation will focus on novel magnetic nanoparticles formed using superfluid helium droplets as nano-reactors. Unlike other techniques, the very cold superfluid helium offers rapid continuous cooling, which instantly removes the thermal energy released during the growth of magnetic nanoparticles. As a result, the effect of exchange interactions is accentuated, leading to much enhanced magnetic moments. For antiferromagnetic chromium, we have obtained novel nanoparticles showing robust ferromagnetism, with a magnetic moment as high as $1.89 \mu_B/\text{atom}$ at 3 K [3]. For ferromagnetic elements, Ni/Au core-shell nanoparticles with a magnetic moment as high as $2.05 \mu_B/\text{atom}$ at room temperature and a magnetic moment approaching the atomic limit at 5 K have been formed. Theoretical modeling and high-resolution TEM imaging suggest that a *bcc* structure has been formed, rather than a *fcc* structure of bulk nickel.

- [1] S. Yang and A. M. Ellis, *Chem. Soc. Rev.* 42, 472-484 (2013).
- [2] E. Latimer, D. Spence, C. Feng, A. Boatwright, A. M. Ellis and S. Yang, *Nano Lett.* 14, 2902 (2014).
- [3] S. Yang, C. Feng, D. Spence, A. Al Hindawi, E. Latimer, A. M. Ellis, *et al.*, *Adv. Mater.* 29, 1604277 (2017).



Magnetism 2018

High frequency modes in ferromagnetic shells for microwave applications

C McKeever, M M Aziz and F Y Ogrin

University of Exeter, UK

The static and dynamic properties of curved geometrical structures such as hemispheres, nanotubes and spherical shells have undergone an explosion of interest in recent years, as part of a broader trend towards three-dimensional nanomagnetism [1] [2].

High frequency permeability in spherical particles is usually attributed to Aharoni exchange modes. However, experimental studies found large discrepancies between theory and experiment [3] [4] [5], which raised many questions. Here, the Aharoni theory is verified with extensive numerical simulations. It is shown that the higher-order modes with frequencies of practical interest are of the order of $10^2 - 10^3$ times smaller than the ferromagnetic resonance, and cannot explain the large microwave permeability observed in spherical particles. Deviations from the theory also emerge due to the 3D onion-state in shells, which breaks the degeneracy between the ferromagnetic resonance and the first exchange mode (see Fig. 1).

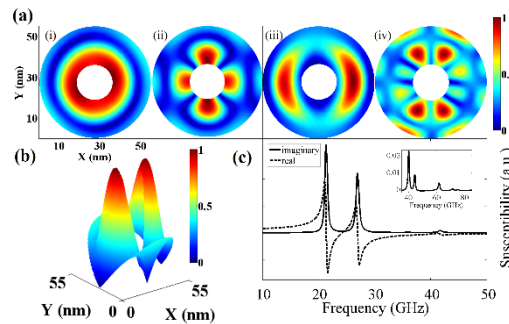


Figure 1: (a) Spatial Fourier transform of the hollow sphere for $R_2 = 27.5$ nm and $R_1/R_2 = 0.3$ in the presence of a 0.8 T biasing field applied in the z-direction corresponding to frequencies (i,ii) 63 GHz and (iii,iv) 98 GHz in the xy (i,iii) and (ii,iv) yz -plane. (b) Three-dimensional surface plot of the xy cross-section at 98 GHz corresponding to (a,iii). (c) Real and imaginary components of the dynamic susceptibility.

However, intensive resonance modes can be excited up to frequencies of 20-25 GHz within spherical particles which have been relaxed into the vortex state (see Fig. 2). Within this regime, the fundamental mode is not strictly the largest mode in the permeability, consistent with experimental observations. Moreover, the size dependence of the resonance modes is found to be significantly weaker than $1/R_2^2$, where R_2 is the outer radius.

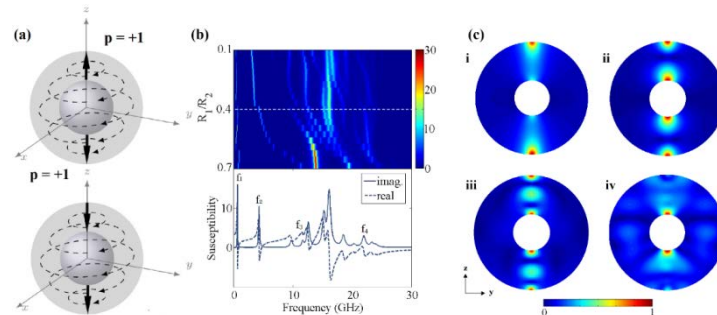
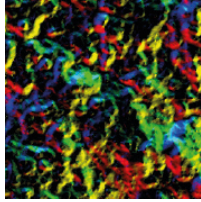


Figure 2: (a) Vortex domain structure for spherical shells with parallel and anti-parallel orientation of the vortex singularities. (b, top) The imaginary component of the susceptibility (colour-bar) for a spherical shell of outer radius 100 nm and varying shell thickness R_1/R_2 . The white dashed line corresponds to the plot of



Magnetism 2018

the susceptibility shown in (b, bottom). (c) Normalized spatial Fourier transform corresponding to the y-component of the magnetisation for a shell of outer radius 100 nm and ratio $R_1/R_2 = 0.3$. The modes (i)-(iv) correspond to $f_1 - f_4$ shown in (b, bottom).

- [1] Fernández-Pacheco A, Streubel R, Fruchart O, Hertel R, Fischer P and Cowbun R P 2017 Three-dimensional nanomagnetism *Nat. Commun.* 8 15756
- [2] Streubel R, Fischer P, Kronast F, Kravchuk V P, Sheka D D, Gaididei Y, Schmidt O G and Makarov D 2016 Magnetism in curved geometries *J. Phys. Appl. Phys.* 49 363001
- [3] Toneguzzo P, Viau G, Acher O, Fiévet-Vincent F and Fiévet F 1998 Monodisperse Ferromagnetic Particles for Microwave Applications *Adv. Mater.* 10 1032-5
- [4] Mercier D, Lévy J-C S, Viau G, Fiévet-Vincent F, Fiévet F, Toneguzzo P and Acher O 2000 Magnetic resonance in spherical Co-Ni and Fe-Co-Ni particles *Phys. Rev. B* 62 532-44
- [5] Viau G, Fiévet-Vincent F, Fiévet F, Toneguzzo P, Ravel F and Acher O 1997 Size dependence of microwave permeability of spherical ferromagnetic particles *J. Appl. Phys.* 81 2749-54.

Atomistic spin dynamics and finite size effects of magnetite nanocrystals

D Meilak, A Meo, S Majetich, V Lazarov and R Evans

University of York, UK

Magnetite nanoparticles are promising for a range of medical applications including magnetic hyperthermia, MRI contrast enhancement and targeted drug delivery. Due to the nanoscale nature of the particles, predicting the size dependent magnetic properties is challenging. We present finite size scaling (FSS) analysis for single crystal Fe₃O₄ nanoparticles using an atomistic spin model. In the model we explicitly model the sublattice ferrimagnetic magnetisation dynamics with an exact representation of the crystal structure and local ionic magnetic moments on the octahedrally and tetrahedrally coordinated Fe sites. We compare the effects of surface faceting on the finite size scaling for spherical and cubic particles and find different scaling behaviours depending on the surface Fe coordination. In particular, we find a strong dependence of the saturation magnetisation on the surface coordination for smaller particle sizes, as shown in Fig. 1. We also calculate the magnetic susceptibility in Fig. 2 which gives an additional determination of the Curie temperature. The susceptibility shows a strong size dependence in both the magnitude and position of the peak, and is significantly different for the different magnetic sublattices due to the antiferromagnetic coupling between sublattices.

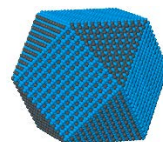
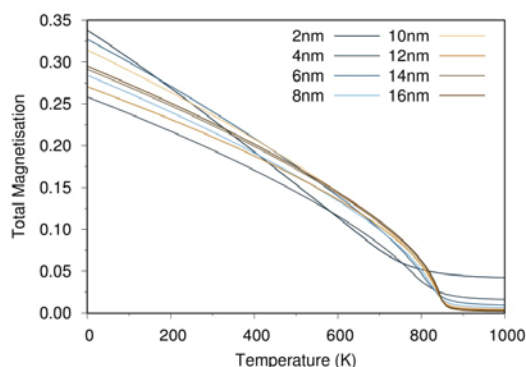
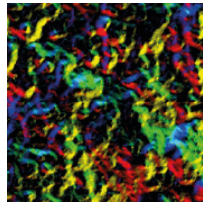


Figure 1: Plot of temperature dependent magnetisation for different magnetite particle sizes. The change in surface faceting leads to a large change in the saturation magnetisation arising from different numbers of



Magnetism 2018

atoms in each magnetic sublattice. A visualisation of a typical cubic particle with [100] and [111] terminating facets is shown inset.

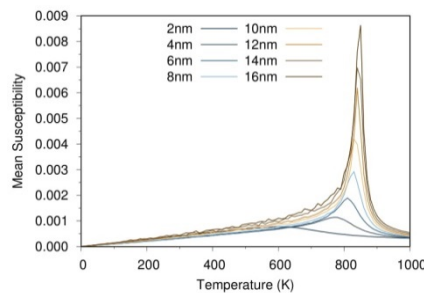


Figure 2: Temperature dependent magnetic susceptibility comparing different particle sizes. The susceptibility shows a strong size dependence in both the magnitude and position of the peak.

Development of novel magnetic-elastic membranes for microfluidic applications

E L Martin, M T Bryan and F Y Ogrin

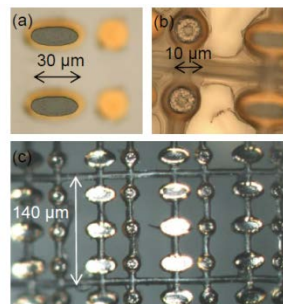
University of Exeter, UK

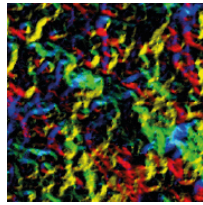
Microfluidic devices have potential to be used in portable point-of-care diagnostic devices. These diagnostic tests are performed by the transport of biological fluids around the devices onto a biosensor. These devices are required to be portable and of low power, which is still a challenge within the industry.

We propose a potential solution using magnetic-elastic membranes. These membranes comprise of an array of ferromagnetic elements, which are elastically linked via PDMS to create a network. This network spans an area of 12-50 mm² using photolithographic techniques.

One structure of interest has been a network based on an elastically linked group of magnetically actuated micromechanical motors[1-3], which operate in a low Reynolds regime and break time-reversible symmetry producing a net movement. This network contains two different types of ferromagnetic particles, electroplated CoNiP and Co particles, which have a different shape and anisotropy allowing the magnetic configuration of the particles to be controlled in an oscillating magnetic field.

Characterisation of the magnetic properties of the CoNiP and Co particles revealed that they had coercive fields of 400 Oe and 128 Oe, respectively. The difference in magnetisation, results in the particles responding differently in an external magnetic field, which can deform the network.





Magnetism 2018

Figure 1: (a) Ellipsoidal CoNiP particles and (b) Circular Co particles with PDMS links during the fabrication process. (c) The final product of the magneto-elastic membrane.

- [1] F. Y. Ogrin, P. G. Petrov, C. P. Winlove, *Phys. Rev. Lett.* 2008, *100*, 1.
- [2] A. D. Gilbert, F. Y. Ogrin, P. G. Petrov, C. P. Winlove, *Q. J. Mech. Appl. Math.* 2011, *64*, 239.
- [3] J. K. Hamilton, P. G. Petrov, C. P. Winlove, A. D. Gilbert, M. T. Bryan, F. Y. Ogrin, *Sci. Rep.* 2017, *7*, 44142.

Thin films and nanomagnets II

Giant piezomagnetism in manganese antiperovskite nitrides

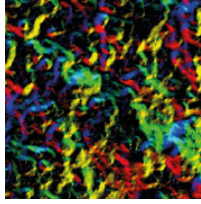
D Boldrin¹, A P Mihai¹, B Zou¹, J Zemen², P Petrov¹, W R Branford¹ and L F Cohen¹

¹Imperial College London, UK, ²Czech Technical University in Prague, Czech Republic

Development of new magnetic materials where the magnetism is highly responsive to small strains may lead to new device concepts for memory storage and energy harvesting. This presentation concerns the development of magnetic thin films of Mn₃AN (where A = Ni, Ga) that are indeed highly sensitive to local strain fields not as a result of magnetostriction, but due to a little studied effect called piezomagnetism. Both Mn₃NiN and Mn₃GaN have non-collinear antiferromagnetic ground states and relatively low spin-orbit coupling so the orientation and magnitude of the local magnetic moments is sensitive to the lattice distortions mostly due to frustrated exchange interactions rather than due to magnetocrystalline anisotropy varying with the underlying lattice (magnetostriction). Such properties were predicted in 2008 by Lukashev et al.¹ but experimental manifestation has not been explored to date.

In this presentation we will describe our experimental progress towards exploring the antiperovskite non-collinear antiferromagnetic Mn₃AN family. Films are deposited by pulse laser deposition and are measured structurally using X ray analysis and physically by vibrating sample magnetometry and magneto-transport measurement. We show that Mn₃NiN films can be deposited epitaxially on a variety of substrates with different values of lattice mismatch and that the induced magnetization and the Neel temperature depend linearly on the resulting biaxial strain experienced by the Mn-antiperovskite layer. We grow films on BaTiO₃ and make use of the induced strain at the structural phase transitions in this substrate to demonstrate in-situ strain control over the magnetism. Our experimental progress is preliminary but we have been able to provide definitive evidence for the piezomagnetic response in our films, consistent with theoretical prediction.^{2, 3} This is an exciting new topic which merits further fundamental study.

- [1] Lukashev, P., Sabirianov, R. F. & Belashchenko, K. Theory of the piezomagnetic effect in Mn- based antiperovskites. *Phys. Rev. B* *78*, 184414 (2008).
- [2] Zemen, J., Gercsi, Z. & Sandeman, K. G. Piezomagnetic effect as a counterpart of negative thermal expansion in magnetically frustrated Mn-based antiperovskite nitrides. *Phys. Rev. B* *24451*, 1– 8 (2017).
- [3] Zemen, J. *et al.* Frustrated magnetism and caloric effects in Mn-based antiperovskite nitrides: Ab initio theory. *Phys. Rev. B* *96*, 184438 (2017).



Magnetism 2018

Texture-induced anisotropy in the magneto-electric coupling response of multiferroic composites

T Mercer¹, S Bourn¹, P Bissell¹, S Lepadatu¹ and M Vopson²

¹University of Central Lancashire, UK, ²University of Portsmouth, UK

Multiferroic materials are an important area of interest that offer a wide range of potential applications [1]. Composites have a large Magneto-Electric (ME) response at room temperature and are considered here in the form of a NiFe₂O₄/PbZrTiO₃ (NFO/PZT) bi-layer. Crystallographic texture of the NFO layer leads to in-plane anisotropy in its magnetostriction and subsequent strain-mediated anisotropy in the electrical response of the PZT. For an NFO layer orientated parallel to the {100} plane, Fig.1 shows the maximum ME coupling observed at an optimum DC bias field as a function of sample orientation. From the strain response, we develop a theory to show the product of these two parameters describes magnetostriction for a given texture. This is illustrated in Fig.2, where a reasonable fit to the experimental data is observed along with the magnetic anisotropy axes determined experimentally [2]. As magnetostriction is greater along harder axes, the positions and types of these axes are consistent with the turning points and gives confidence in the theory. Results from {110} and {111} samples are also found to be dependent on the type and orientation of their in-plane anisotropy axes and thereby gives scope for designing device response by texture and applied field direction.

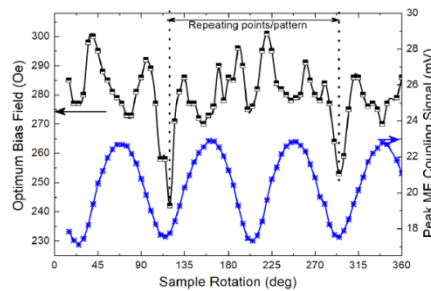


Figure 1. Optimum bias field and ME coupling signal of the {100} textured sample rotated relative to the bias field.

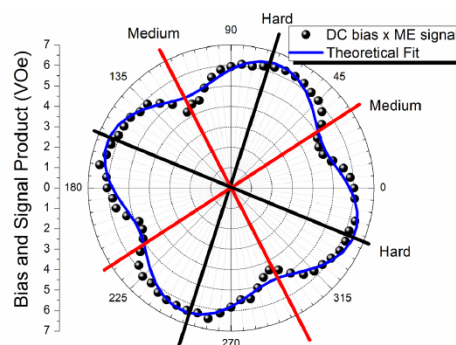
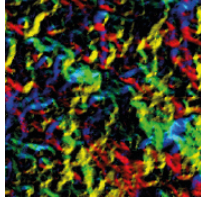


Figure 2. The product of bias field and ME signal (\propto magnetostriction), along with the magnetic anisotropy axes. The alignment of axes with the positions and types of turning points is consistent with their relative hardness.

- [1] H. Palneedi et al, Actuators, 5, 9 (2016).
- [2] S. Bourn et al, IEEE Trans. Magn., 51, 600604 (2015).



Magnetism 2018

Magnetic domain texture and Dzyaloshinskii-Moriya interaction in systems with perpendicular exchange bias

R A Khan¹, H T Nembach², M Ali¹, J M Shaw², C H Marrows¹ and T A Moore¹

¹University of Leeds, UK, ²National Institute of Standards and Technology, USA

In thin film systems with broken inversion symmetry, the Dzyaloshinskii-Moriya interaction (DMI) influences the field- or current-driven magnetic switching and domain wall (DW) motion by setting the chirality of magnetic textures [1-3]. Here, we sputter-deposited polycrystalline multilayers of Pt/Co/Ir₂₀Mn₈₀ and Pt/Co/Fe₅₀Mn₅₀ exhibiting perpendicular exchange bias (PEB). These multilayers are of interest because of the coincidence of the DMI with a vertical exchange field that could remove the need for an externally applied field to stabilise skyrmion bubbles.

We have measured the exchange bias in SiO₂/Ta(5)/Pt(2)/Co(t_{Co})/IrMn(t_{IrMn})/Pt(3) (Fig. 1) and SiO₂/Ta(5)/Pt(2)/Co(t_{Co})/FeMn(t_{FeMn})/Pt(3) stacks (thickness in nm) as a function of the layer thickness of Co (t_{Co} = 0.2-2 nm), IrMn (t_{IrMn} = 1-10 nm), and FeMn (t_{FeMn} = 1-8 nm) layers. The stacks were optimised to obtain a strong perpendicular anisotropy and large PEB in the as-grown state.

Interfacial interaction mechanisms were studied when crossing over the paramagnet to antiferromagnet (AFM) transition of the AFM layers. We found that the magnetic domain morphology of the ferromagnetic (FM) layer is influenced by the FM-AFM exchange coupling, and the anisotropy of these layers. The different phases of the AFM layer were confirmed by identifying the Néel temperatures (T_N) and the blocking temperatures (T_B) (Fig. 2).

We also investigated the DMI in these systems, particularly how it is affected by the AFM spin order. For this, the DMI was measured at three different phases: paramagnet phase, AFM phase without PEB, and AFM phase with PEB. We quantified the DMI by the Brillouin light scattering (BLS) spectroscopy technique [4-5], by taking advantage of the non-reciprocity of propagating spin waves.

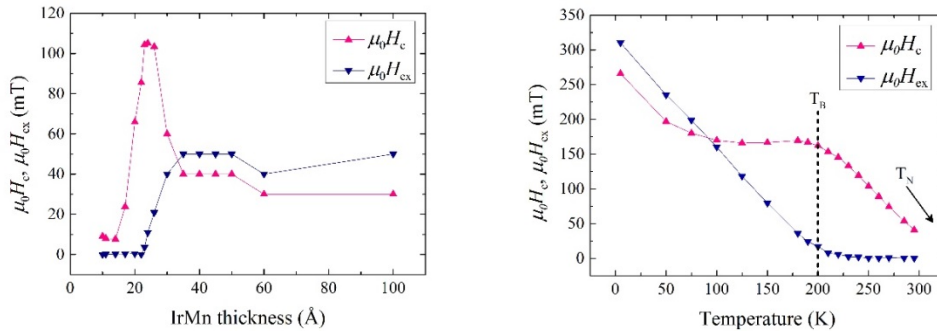
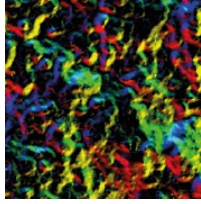


Figure 1: Coercivity H_c and exchange field H_{ex} in Pt(5 nm)/Co(1 nm)/IrMn(t_{IrMn}).

Figure 2: Coercivity H_c and exchange field H_{ex} in Pt(3 nm)/Co(1 nm)/IrMn(2 nm) as a function of temperature.

- [1] S Emori et al. *Nature Materials* 9, 611-616 (2013).
- [2] R Khan et al. *App. Phys. Lett.* B 109, 132404 (2016).
- [3] A Wells et al. *Phys. Rev. B* 95, 054428 (2017).
- [4] J-H Moon et al. *Phys. Rev. B* 88, 184404 (2013).
- [5] H Nembach et al. *Nat. Phys.* 11, 825 (2015).



Magnetism 2018

Temperature dependence magnetic proximity effect in Pt/CoFeTaB/Pt trilayer

O-O Inyang¹, L Bouchenoire², M Tokac¹, R Rowan-Robinson¹, B Nicholson¹, D Atkinson¹, C Kinane³ and A Hindmarch¹

¹Durham University, UK, ²XMaS beamline, France, ³ISIS Neutron Facility, UK

Spintronics application performance has recently been linked with the ability to generate and detect pure spin current, which further depends on the spin transport across interfaces. This is sensitive to the details of the interface structure; at an interface, the magnetic properties can also be significantly modified by magnetic degradation due to inter-diffusion and alloying at the interface [1, 2], or proximity polarization of the heavy metal [3]. Our focus in this work is to understand the temperature dependent evolution of magnetic properties at the interface between Pt in proximity with $\text{Co}_{28}\text{Fe}_{28}\text{Ta}_{30}\text{B}_{14}$ (CFTB).

The sample structure is sputter deposited Pt(30Å)/CFTB(100Å)/Pt(30Å) on Si/SiO₂ substrate which enables simultaneous probing of both interfaces. Temperature dependence measurements with SQUID magnetometry, polarized neutron reflectivity (PNR) and x-ray resonance magnetic reflectivity (XRMR) conducted at Pt L₃ absorption edge were performed on the same sample. The scattering length density (SLD) depth profiles were extracted by GenX simulation of PNR and XRMR data.

The SQUID magnetometry measurement (see Fig 1a) showed three transition temperature suggesting interfacial magnetic proximity effect (MPE) in the sample and possible Ta diffusion within the CFTB layer modifying the magnetic moment across the sample [3]. The PNR measurement (see Fig 1b) shows enhanced magnetic moment around the interfaces. The strong presence of strong MPE was verified with the XRMR measurements (see Fig 1c). The magnetic moment within the bulk of the CFTB layer at 50K, which turns-off at 100K, is consistent to T_{c3} on the SQUID measurement while T_{c2} is consistent with the temperature at which the magnetic moment near the top interface turns-off and T_{c1} is the ferromagnetic to paramagnetic phase transition near the lower interface. From the XRMR, the Pt polarization changes with temperature [4]. The Pt polarization from XRMR scales with the CFTB magnetic moment from PNR in a manner which is contrary to the anticipated temperature independent magnetic susceptibility for a Pauli paramagnet.

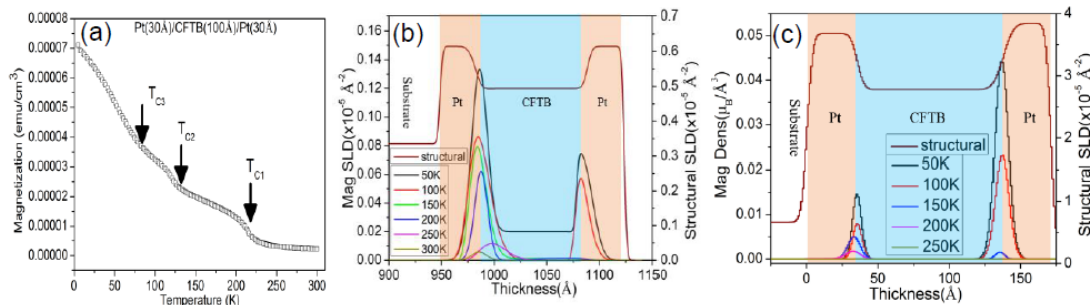
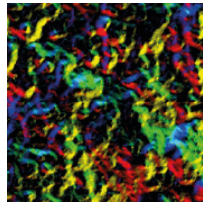


Figure 1(a) SQUID magnetometry measurement (b) PNR SLD profile (c) XRMR SLD profile

- [1] S. Singh et al, J. Appl. Phys. 107, 123903 (2010).
- [2] T. Zhu et al, Appl. Phys. Lett. 100, 202406 (2012).
- [3] M. Tokac et al, AIP Advances 7, 116022 (2017)
- [4] T. Hase et al, Phys. Rev. B 90, 104403 (2014).



Magnetism 2018

Temperature dependent magnetotransport in epitaxial RuO₂ films

E Sharma¹, K Stoerzinger², D Payne¹, L F Cohen¹ and W R Branford¹

¹Imperial College London, UK, ²Massachusetts Institute of Technology, USA

RuO₂ is a material which possesses a tetragonal structure, which is closely lattice matched with rutile oxide structures, for example IrO₂, CrO₂ and TiO₂, and its electronic properties have been studied extensively[1] for applications in ferroelectric random access memory (FRAM). IrO₂ has previously been considered a very promising material for spin detection[2] based on the Spin Hall Effect[3] exhibited by the material. However there is growing interest in RuO₂ as another candidate due to its high spin orbit coupling and similar structure to IrO₂. Both IrO₂ and RuO₂ have a complex Fermi surface and the Hall response of epitaxial thin films IrO₂ is very sensitive to the epitaxial growth direction.

Here we study how the magnetotransport varies with temperature in epitaxial thin films of RuO₂ oriented in the [100], [101] [110] and [111] directions. We measure both longitudinal and transverse resistivity for the 4 different crystallographic orientations over a range of temperatures from 290K to 2K. The transverse resistivity measurements were fitted to a single carrier model to extract the Hall coefficient and apparent carrier concentration. The sensitivity of the properties to the growth direction suggests that complex Fermi Surface plays a strong role in the magnetotransport properties.

- [1] Al-Shareef, H. N., Bellu, K. R., Kingon, A. I. & Auciello, O. Influence of platinum interlayers on the electrical properties of RuO₂/ Pb(Zr_{0.53}Ti_{0.47})O₃/RuO₂ capacitor heterostructures. *Appl. Phys. Lett.* 239, 2-5 (1995).
- [2] Fujiwara, K. *et al.* 5D Iridium Oxide As a Material for Spin-Current Detection. *Nat. Commun.* 4, 2893 (2013).
- [3] Onoda, S., Sugimoto, N. & Nagaosa, N. Quantum transport theory of anomalous electric, thermoelectric, and thermal Hall effects in ferromagnets. *Phys. Rev. B* 77, 165103 (2008).

The thickness limit for sputter deposited ultra-thin Fe/Ni multilayers on epitaxial Cu/Si(001)

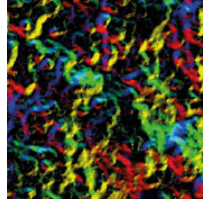
A Frisk^{1,2}, H Ali¹, P Svedlindh¹, K Leifer¹, G Andersson¹ and T Nyberg¹

¹Uppsala University, Sweden, ²Diamond Light Source Ltd, UK

FeNi L1₀ has in the recent years been investigated as possible rare earth free permanent magnet material, with high saturation magnetization and relatively large anisotropy [1]. Two groups has succeeded with thin film fabrication of this phase, [2-4]. Our approach using sputtering onto Cu buffered Si substrates, [5, 6], resulted in some chemical disorder which we believe is due to surface roughness.

To further investigate the Fe/Ni interfaces, using the same procedure as for L1₀ growth, we have fabricated thicker multilayers of (*n* Fe)/(*n* Ni), with individual thicknesses from *n* = 4 to *n* = 48 monolayers (ML). The microstructural evolution and magnetic properties versus *n* have been studied. The interface width composed of interface roughness as well as the interdiffusion between layers, was quantified although the relative contributions from these two sources could not be concluded by the techniques used. Transmission electron microscopy show elemental layering down to *n* = 4 ML layer thickness, and an intermixed region is found to be present. The measured elemental layering and X-ray reflectivity give an upper limit to the interface width which must be smaller than the thinnest layers, 4 ML.

A decreased total magnetic moment versus *n* was observed. This we explain by the variation in structure. X-ray diffraction showed that an epitaxial fcc (001) structure is maintained throughout the multilayers up to *n* ≤ 8 ML. While for larger *n* values there is relaxation, starting with Fe_{fcc}⁰⁰¹ layers changing into Fe_{bcc}¹¹⁰, then



Magnetism 2018

followed by Ni_{fcc}^{001} layers changing into (111) orientation along the growth direction. For the fully epitaxial multilayers the fcc Fe layers being partly antiferromagnetic can explain the decreased measured magnetic moments, whereas the relaxed multilayers exhibit the expected magnetic properties of (bcc Fe) + (fcc Ni).

- [1] Lewis et al., Magnet. Technol. Int. 8-11 (2012)
- [2] Shima et al., J. Magn. Magn. Mater. 310(2), 2213, (2007)
- [3] Kojima et al., J. Phys.: Condens. Matter 26, 064207, (2014)
- [4] Frisk et al., J. Phys.: Condens. Matter, 28, 406002, (2016)
- [5] Frisk et al., J. Phys. D: Appl. Phys., 50, 085009, (2017)
- [6] Frisk et al., Thin Solid Films, 646, 117, (2018)

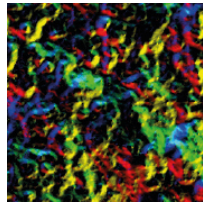
Theoretical and computational magnetism I

(Invited) Merging the time and length scales in ultrafast spin dynamics

E Iacocca^{1,2,3}, T Liu⁴, A H Reid⁴, P Granitzka⁴, A X Gray⁴, S Bonetti⁴, E Jal⁴, C Graves⁴, R Kukreja⁴, Z Chen⁴, D Higley⁴, T Chase⁴, L le Guyader⁴, K Hirsch⁴, H Ohldag⁴, W Schlotter⁴, G Dakovski⁴, G Cosolovich⁴, M Hoffmann⁴, S Carron⁴, A Tsukamoto⁵, M Savioni⁶, A Kirilyuk⁶, A V Kimel⁶, T Rasing⁶, J Stohr⁴, M A Hoefer¹, S Fu⁷, R Evans⁷, T Ostler⁷, R Chantrell⁷, T J Silva³, H A Dürr⁴, R Cuadrado⁸, L Szunyogh⁹, L Oroszlány⁹, G Hrkac¹⁰

¹University of Colorado, USA, ²National Institute of Standards and Technology, USA, ³Chalmers University of Technology, Sweden, ⁴SLAC National Accelerator Laboratory, USA, ⁵Nihon University, Japan, ⁶Radboud University Nijmegen, The Netherlands, ⁷Sheffield Hallam University, UK, ⁸Institut Catala de Nanociencia I Nanotecnologia, Spain, ⁹Budapest University of Technology and Economics, Hungary, ¹⁰The University of Exeter, UK

Magnetization processes occur across a huge range of time and length-scales, creating huge difficulties in constructing accurate and reliable models that capture the full range of dynamics. In the past 20 years the field of ultrafast spin dynamics has burgeoned into an exciting field of physics that is interesting from a purely scientific prospective, but also has the potential to realise new technological devices. Here, I will present two different multiscale approaches to describe the magnetic properties of complex systems. The first, based on a hierarchical method uses parameterised models to pass physical parameters from one length-scale to another. In layered systems, this is particularly powerful as one can capture the site-by-site properties, which are extremely tricky to measure experimentally, but has consequences for the resulting dynamics. The second involves passing information directly from one configuration to another. After laser excitation of a ferrimagnetic thin film we find that after the initial ultrafast demagnetization and all-optical magnetic switching, the magnetization evolves at picosecond timescales through the coalescence of magnons into transient solitons. Our results are directly compared with soft X-ray magnetic scattering measurements performed at the LCLS to probe the temporal and spatial evolution of the system.



Magnetism 2018

The temperature dependence of magnetic anisotropy in ferrimagnets from first principles

C E Patrick¹, S Kumar¹, G Balakrishnan¹, R S Edwards¹, M R Lees¹, L Petit² and J B Staunton¹

¹University of Warwick, UK, ²Daresbury Laboratory, UK

The magnetocrystalline anisotropy (MCA) of a ferromagnet is already a challenging quantity to calculate, requiring the solution of the relativistic quantum mechanical problem to a high numerical precision [1]. However, many important magnetic materials (particularly those based on rare-earths and transition metals, RE-TM) are in fact *ferrimagnets*, containing different magnetic sublattices which couple to external fields with different strengths. Crucially, this coupling can induce canting between these magnetic sublattices [2]. Here we consider the prototypical RE-TM ferrimagnet GdCo₅ and show that a “standard” calculation of the MCA which neglects this canting gives numbers that are in disagreement with experimentally-measured anisotropy constants. Instead we develop a “first-principles magnetisation vs field” (FPMvB) approach [3] which accounts for the canting, and mirrors the so-called Sucksmith-Thompson procedure [4] used to extract anisotropy energies experimentally. These new calculations agree well with experimental data measured on a single crystal of GdCo₅ recently grown by us [5].

The present work forms part of the PRETAMAG project, funded by the UK Engineering and Physical Sciences Research Council, Grant no. EP/M028941/1.

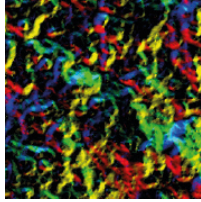
- [1] J. B. Staunton et al., Phys. Rev. B 74, 144411 (2006)
- [2] R Radwański et al., J. Magn. Magn. Mater. 104, 1321 (1992)
- [3] C. E. Patrick et al., submitted
- [4] W. Sucksmith and J. E. Thompson, Proc. Royal Soc. A 225, 362 (1954).
- [5] C. E. Patrick et al., Phys. Rev. Materials 1, 024411 (2017).

Temperature dependent domain wall width in ferrimagnets

R Moreno Ortega¹, S Khmelevskyi², R F L Evans¹ and O Chubykalo-Fesenko³

¹University of York, UK, ²Vienna University of Technology, Austria, ³Instituto de Ciencia de Materiales de Madrid, Spain

The study of the temperature dependence of the domain wall width is important for several reasons, e.g., it defines the domain wall velocity. For the specific case of ferrimagnetic materials, it has been shown that near the compensation point (T_M), the domain wall velocity sharply increases [1]. In our work, using atomistic spin dynamics simulations (Vampire code [2]), the temperature dependence of the domain wall width in ferrimagnets is studied. As a prototype, we use initially TbFe₂ in a Laves phase C15 atomic structure. Firstly, the long-range exchange parameters are obtained from ab-initio calculations. Secondly, because with this parametrisation we don't observe any compensation point, we varied the intersublattice exchange (J_{AFM}). In the ground state ($T=0K$), both analytical and numerical results show that the width of domain walls is the same in transition and rare earth metals for J_{AFM} values larger than 3% of the ab-initio value of J_{Fe-Fe} . Its value increases with J_{AFM} . Different domain widths in Fe and Tb are observed for small values of J_{AFM} . The domain wall width monotonically increases with temperature when the system does not present a compensation point. However, when T_M exists, an additional maximum is observed near the compensation point. The calculated domain wall width together with the temperature dependence of the macroscopic damping parameter allows us to analyse the domain wall velocity as a function of temperature in ferrimagnets.



Magnetism 2018

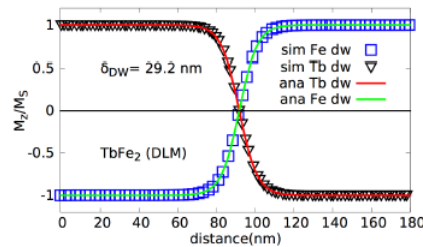


Figure 1: Sublattice resolved domain walls for TbFe₂. M_z/M_s is the sublattice resolved z component of the magnetisation divided by its corresponding saturation magnetisation M_s . Blue squares and black triangles represent the simulated domain walls for Fe and Tb respectively. Green and red lines represent the analytical domain wall profile.

- [1] Kim, K.-J. et al, Fast domain wall motion in the vicinity of the angular momentum compensation temperature of ferrimagnets, *Nat. Mat.* 16, 1187-1192 (2017).
- [2] Evans, R. F. L. et al. Atomistic spin model simulations of magnetic nanomaterials. *J. Phys. Condens. Matter* 26, 103202 (2014).

Temperature dependence of magnetostriction: An *ab initio* theory

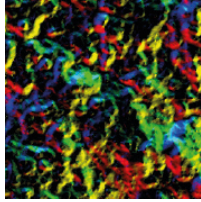
G A Marchant¹, C E Patrick¹, J B Staunton¹, M Laver³ and R Arnold³

¹University of Warwick, UK, ²University of Birmingham, UK

Through the use of the fully relativistic disordered local moment (DLM) theory [1], *ab initio* calculations of the magnetic torque have been performed on tetragonally distorted Fe and Fe-rich Fe_{1-x}Ga_x ($0 \leq x \leq 20$) (Galfenol) in order to devise the temperature-dependence of their magnetoelasticity. An overview of the intrinsic mechanisms of magnetostriction is given, as well as its relationship with magnetocrystalline anisotropy (MCA) and thus the torque method, in particular how it can be used alongside basic linear fitting procedures to calculate the magnetoelastic coupling coefficients B_1 and B_2 . It is thus shown how DLM theory, in conjunction with the torque method, allows for the calculation of finite temperature magnetoelasticity. To demonstrate application of the method and its accuracy, calculations of B_1 have been performed on bcc iron across its ferromagnetic temperature range. The method has also been used to calculate finite temperature magnetoelasticity in fully disordered Fe-rich Galfenol, a widely applied alloy due to its giant magnetostriction [2], the origins of which are still contested [3, 4, 5]. Our calculations show that the enhancement in magnetostriction with respect to Ga concentration cannot be a result of the fully disordered structure and that a local ordering model could be required.

The present work forms part of the PRETAMAG project, funded by the UK Engineering and Physical Sciences Research Council, Grant No. EP/M028941/1.

- [1] BL Gyorffy et al. "A first-principles theory of ferromagnetic phase transitions in metals". In: *Journal of Physics F: Metal Physics* 15.6 (1985), p. 1337.
- [2] Arthur E Clark et al. "Magnetostrictive properties of body-centered cubic Fe-Ga and Fe-Ga-Al alloys". In: *IEEE Transactions on Magnetics* 36.5 (2000), pp. 3238-3240.
- [3] Mark Laver et al. "Magnetostriction and magnetic heterogeneities in iron-gallium". In: *Physical review letters* 105.2 (2010), p. 027202.
- [4] JR Cullen et al. "Magnetoelasticity of Fe-Ga and Fe-Al alloys". In: *Journal of Magnetism and*



Magnetism 2018

Magnetic Materials 226 (2001), pp. 948-949.

- [5] AG Khachaturyan and D Viehland. "Structurally heterogeneous model of extrinsic magnetostriction for Fe-Ga and similar magnetic alloys: Part I. Decomposition and confined displacive transformation". In: *Metallurgical and Materials Transactions A* 38.13 (2007), pp. 2308-2316.

Comparing experimental and computational results for spin excitations

M Lueders¹, T Perring², A Buts² and H Mook³

¹STFC, Daresbury Laboratory, UK, ²STFC, Rutherford-Appleton Laboratory, UK, ³Oak Ridge National Laboratory, UK

In this presentation, we report on computational tools to simulate spin excitations spectra as measured by the ISIS neutron scattering facility. The tools are based on ab-initio electronic structure calculations, using methods like time-dependent density functional theory and beyond. We demonstrate that the computational results are robust by comparing calculations using different methods and computer codes, as well as comparing the results with experimental data. In particular the effects of the experimental resolution will be addressed.

(Plenary) Topology and spin-orbit coupling in low dimensions lead to novel directions in spintronics

A Fert

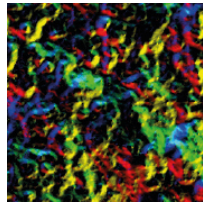
Université Paris-Sud, France

The appearance of new phenomena induced by spin-orbit coupling (SOC) and topology effects at surfaces, interfaces and low dimension materials has led to the emergence of novel directions in spintronics. I will describe some of these and their potential for spintronic devices [1].

The electron states at surfaces or interfaces of topological insulators, Rashba interfaces and some interfaces between oxides are characterized by a locking between the spin and momentum degrees of freedom. Thanks to the Edelstein and Inverse Edelstein Effects, this locking can be exploited for very efficient conversions between spin and charge currents (which, parenthetically, is the basic function in any spintronic device). Promising similar effects are obtained in 2D materials with large SOC as, for example, ultra-thin films of Transition Metal Dichalcogenides (TMD) or heterostructures associating 2D materials.

Second example, the chiral spin interactions (Dzyaloshinskii-Moriya interactions) induced by SOC at the interface of a magnetic film with a heavy metal can be used to create skyrmions, nanoscale spin whirls that are stabilized by their topology. The recent results in several groups on the electrical creation, manipulation and detection of skyrmions at room temperature in magnetic multilayers represent real advances on the route to applications.

- [1] Example of recent review: A. Soumyanarayanan, N. Reyren, A. Fert and C. Panagopoulos, *Nature* 539, 509 (2016).



Magnetism 2018

(After dinner talk) Spin-out, license or collaborate: the knowledge transfer dilemma

B Tanner

Durham University, UK

Spinning out a company is only one way of transferring the results of successful academic research into the commercial sector. In this after-dinner talk, which I will endeavour to keep at a level suitable to the occasion, I will look at three modes of knowledge transfer and try to identify when a spin-out company might be the right course of action. Drawing on my own experience of direct involvement in five spin-out companies (two successful, two indifferent and one failure), together with observation of many more, I will explore what it takes to spin-out successfully. The random walk of my own experiences will mirror the convivial effects of the dinner.

(Wohlfarth Lecture) ATOMs -Atomistic to Micromagnetic modelling: from permanent magnets to magnetic hybrid materials

G Hrkac

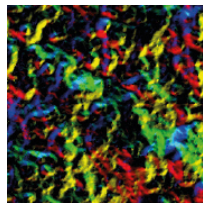
University of Exeter, UK

In our research we show that the combination of atomistic and micromagnetic simulations in connection with TEM and synchrotron measurements can give a better understanding of the morphological and chemical composition of magnetic and metallic hybrid materials [1,2]. The problem of interface and grain boundaries and its changes in intrinsic properties are rooted in structural defects of crystal structures and influence effects like intrinsic magnetic properties and interface phenomena like spin scattering. We discuss these effects and its influence on permanent magnets used in hybrid cars, over novel magnetic hybrid structures to artificial spin ice structures.

Anisotropic sintered NdFeB magnets consist of polyhedral grains, which have a distribution of size and shape, separated by a grain boundary phase with various compositions. Such magnets are sensitive to the crystallographic structure near grain boundaries and interfaces, and this considerably influences the magnetic properties that can be understood and quantified with solid-state molecular dynamics. It is shown that change in local properties can be linked to the strain/stress effects on the atomistic scale.

Such interface and coupling effects also play an important role in magnetic hybrid as well as in artificial spin ice structures. Where it was found that heterogeneous nanostructures of Co/Pd and permalloy multilayers exhibit mutual domain imprinting that support either a pure closure-domain pattern, a mixed Landau-maze domain state or a perpendicular exchange-spring magnetization structure and in artificial spin ice systems where geometrical manipulation of arrays can induce chirality. Control over such hybrid and spin ice structures could lead to the development of a wide range of technologies, from multilayer data storage media and radio-frequency nano-oscillators [3] to encryption applications[4].

- [1] G. Hrkac, T. Woodcock, et al, Applied Physics Letters 97, 2010, 232511
- [2] T. Woodcock, Y. Zhang, G. Hrkac et al. Scripta Materialia, Volume 67, Issue 6, 2012, Pages 536–541
- [3] P. Wohlfhütter, M. Bryan et.al. Nature Communications 6, 7836 (2015)
- [4] S. Gliga, G. Hrkac et al. Nature Materials 16, 1106–1111 (2017).



Magnetism 2018

High frequency spin dynamics

Picosecond reorientation of in-plane magnetisation within a nano-element by spin orbit torque

P S Keatley¹, R J Hicken², G Mihajlović², L Wan², Y S Choi² and J A Katine²

¹University of Exeter, UK, ²San Jose Research Center, USA

In-plane magnetised devices activated by spin-orbit torque (SOT) combine simplicity of design with energy efficient switching for future magnetic memory elements. SOT switching of in-plane magnetised CoFeB(2 nm) nanoscale ellipses fabricated at the centre of Pt Hall crosses has previously been investigated using a differential planar Hall effect technique.[1] Their planar nature allows complimentary optical techniques to probe switching speed and uniformity. Here, time-resolved scanning Kerr microscopy was used to probe picosecond magnetisation dynamics of a 400 nm×1000 nm ellipse in response to a current pulse passed through a Pt(6 nm) Hall cross parallel to the ellipse minor (hard) axis. The associated Oersted magnetic field (Oe-field), and the polarisation of spins traversing the Pt/CoFeB interface due to the spin Hall effect, were then parallel to the ellipse major (easy) axis. When magnetised along the easy axis, between remanence and the reversal switching field, asymmetry in the amplitude and relaxation of the dynamics was observed for opposite field history, *i.e.* magnetisation parallel or anti-parallel to the spin polarisation, indicating active SOTs on picosecond timescales. When magnetised away from the easy axis, a transient offset and temporary suppression of the dynamics was observed at the centre of the ellipse, while its ends revealed remarkably different dynamics. Time-resolved images indicate a precessional reorientation of the magnetisation that nucleates at one end of the ellipse and rapidly propagates along its major axis, before returning to the equilibrium state. Further measurements and modelling are required to disentangle the Oe-field and SOT contribution to the reorientation.

[1] G. Mihajlović, Appl. Phys. Lett., 109, 192404 (2016).

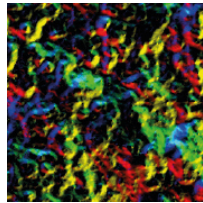
Femtosecond spin dynamics in molecular magnets

J O Johansson¹, J-W Kim², L Hedley¹, F Liedy¹, E Allwright¹, D M Rogers¹, N Robertson¹ and J-Y Bigot²

¹University of Edinburgh, UK, ²Université de Strasbourg, France

Despite the rapid expansion of femtomagnetism, molecular magnets have so far been under-explored using ultrafast techniques. These materials offer interesting possibilities because it is possible to systematically tune the nature of the magnetic interactions due to the vast library of structures available with synthetic chemistry, which is not as trivial in conventional magnets. We report the first ultrafast magneto-optical (MO) study of a molecule-based magnet [1]. We found a fast magnetic response on a femtosecond timescale, which was attributed to the super-exchange interaction between the metal ions.

Femtosecond pump-probe spectroscopy was used to measure the MO dynamics of thin films of the V-Cr Prussian blue analogue (PBA), which is a room-temperature molecule-based magnet. The MO measurements could detect a change in the super-exchange interaction taking place as a result of a spin flip occurring in less than 250 fs after the absorption of a pump photon. We have more recently explored the initially excited state by comparing femtosecond transient absorption spectroscopy with spectroelectrochemistry [2] and also developed coloured magnetic heterostructures [3]. These results demonstrate the powerful combination of transient absorption spectroscopy, magneto-optics, and spectroelectrochemistry in understanding photoinduced magnetisation dynamics in magnetic functional materials.



Magnetism 2018

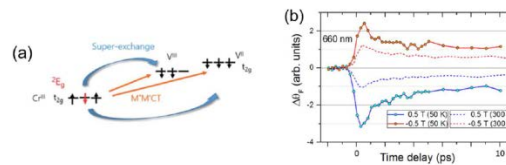


Figure 1: (a) The probe pulse is sensitive to the metal-to-metal charge transfer (MM'CT) transition, which is affected by the change in spin-configuration on the Cr ion after pumping at the ligand-to-metal charge-transfer transition. (b) Change in Faraday rotation $\Delta\theta_F$ at 660 nm as a function of pump-probe delay for two different temperatures and external magnetic field directions.

- [1] J. O. Johansson, J.-W. Kim, E. Allwright, D. M. Rogers, N. Robertson, and J.-Y. Bigot, Chem. Sci. 7, 7061 (2016).
- [2] L. Hedley, M. D. Horbury, F. Liedy, and J. O. Johansson, Chem. Phys. Lett. 687, 125 (2017).
- [3] L. Hedley, L. Porteous, D. Hutson, N. Robertson, and J. O. Johansson, J. Mater. Chem. C 6, 512 (2018).

Magnon transport in multilayer magnetic system

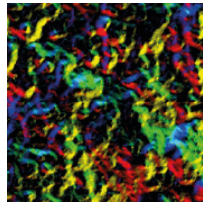
Z Fu², S Ruta¹, T Ostler³, A Kimel⁴, R Evans¹ and R Chantrell¹

¹University of York, UK, ²Tongji University, China, ³Sheffield Hallam University, UK, ⁴Radboud University Nijmegen, Netherlands

In the research community, the coupling of spins with a thermal bath has been widely studied for various applications[1], for example, in waste energy recovery by converting heat to electricity [3]. Non-homogeneous temperature profiles over a spin system, leads to a spin chemical potential that generates a transfer of spins between regions. In this work, we present numerical evidence for the existence of a energy transport via magnons on the sub-picosecond time-scale.

The simulations are done using an atomistic spin dynamics model. The variation of the spin temperature depends on a combination of factors such as bath coupling, exchange interaction, and material properties. Having a bilayer system, with different properties leads to a different effective spin temperature, thereby creating a spin chemical potential resulting in magnon transport between the two layer layers.

To investigate the energy transfer (magnon transport) between regions just due to the spin temperature difference between the layers, we construct a model system where the two layers are divided in two regions with low and high temperature, generated by the laser. The regions are first equilibrated at the corresponding temperature before coupling at the interface. The two regions will have magnons with different energies, leading to an temperature imbalance. To re-equilibrate there will be a net magnon (energy) transfer via the exchange interaction. The spins from the hot region have a higher angular momentum than the ones from the cold regions and, due to the exchange coupling, there is a net energy transfer. Thus high energy magnons from the hot regions will cross the interface and propagate into the cold region. The propagation can be visualised via the change in the net magnetisation normalised to a constant proportional to the noise in the system. This can be observed in figure 1, where the low magnetisation values develop at interface (Fig. 1 (a)) which then propagates into the cold region (Fig. 1 (b)). The speed of propagation is on the order of several km/s.



Magnetism 2018

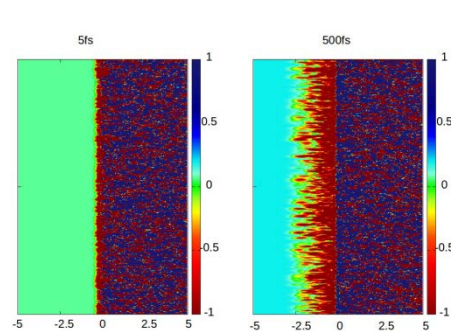


Figure 1: Magnetisation map of the bilayer system at (a) 5 fs and (b) 500 fs. The system is divided along the X-direction in two regions with the interface at $x=0$. The left side is equilibrated at 0 K and the right side at 100 K. The evolution of the Z-component of magnetisation is shown as a colour map, where green corresponds to the equilibrium value of each region individually, and red and blue correspond to increase and decrease of the magnetisation with respect to the equilibrium value.

- [1] G.-M. Choi, C.-H. Moon, B.-C. Min, K.-J. Lee, and D. G. Cahill, *Nature Physics* 11, 576 (2015).
- [2] K. Uchida, S. Takahashi, K. Harii, J. Ieda, W. Koshibae, K. Ando, S. Maekawa, and E. Saitoh, *Nature* 455, 778 (2008).
- [3] D. Hinzke and U. Nowak, *Physical Review Letters* 107, 027205 (2011).
- [4] G. E. W. Bauer, E. Saitoh, and B. J. van Wees, *Nature Materials* 11, 391 (2012).

(Distinguished Lecture) Magnetic phase interference in artificial magnetic lattices: Functions and applications to optical, high-frequency, and spin wave devices

M Inoue, H Uchida, Y Nakamura, P B Lim and T Goto

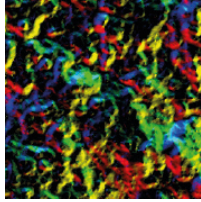
Toyohashi University of Technology, Japan

The introduction of artificial magnetic structures into magnetic materials can induce novel electromagnetic and spin-wave behavior. Nano- and submicrometer-scale artificial magnetic lattices (AMLs) can control optical (electromagnetic) waves in magnetophotonic microcavity structure [1], in which large enhancement of magneto-optical Faraday effect is obtained. volumetric magnetic holograms [2] and labyrinthian magnetic domain structures [3] are also considered to be such materials that contain magnetic domain patterns with optical phase information. This is also the case for spin waves travelling in magnonic crystals [4].

In this talk, the fundamental properties of such AMLs, mainly in magnetic garnet films and alloy thin films, are discussed, followed by demonstrations of their applications in optical and spin-wave micro-devices driven by magnetic phase interference: volumetric magneto-optic (MO) hologram data storage [2] and three-dimensional MO holographic displays [5] with magnetophotonic crystals; high-speed MO Q-switch micro-chip lasers with iron-garnet films with labyrinthian magnetic domain structures [3]; and highly sensitive magnetic sensors and spin-wave logic circuits with magnonic crystals [6]. The spin-wave devices with AMLs could open a new paradigm of magnonics (electron non-transport electronics), where spin waves play an important role as the information carrier.

At the conference, based on our research activities, followed by the concept and fundamental properties of artificial magnetic lattices, their use in MO hologram data storage and the relation to magnetoplasmonics will be mainly presented and discussed.

- [1] T. Goto et al., "Magnetophotonic crystal comprising electro-optical layer for controlling helicity of light," *J. Appl. Phys.*, vol. 111, 07A913, 2012.



Magnetism 2018

- [2] Y. Nakamura et al., "Error-free reconstruction of magnetic hologram via improvement of recording conditions in collinear optical system," *Optics Exp.*, vol. 25, pp. 15349-15357, 2017.
- [3] R. Morimoto et al., "Magnetic domains driving a Q-switched laser," *Sci. Rep.*, vol. 6, 38679, 2016.
- [4] N. Kanazawa et al., "Metal thickness dependence on spin wave propagation in magnonic crystal using yttrium iron garnet," *J. Appl. Phys.*, vol. 117, 17E510, 2015.
- [5] K. Nakamura et al., "Improvement of diffraction efficiency of three-dimensional magneto-optic spatial light modulator with magnetophotonic crystal," *Appl. Phys. Lett.*, vol. 108, 02240, 2016.
- [6] N. Kanazawa et al., "Demonstration of a robust magnonic spin wave interferometer," *Sci. Rep.*, vol. 6, 30268, 2016.

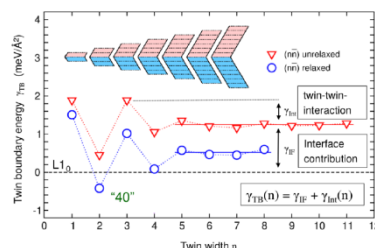
Theoretical and computational magnetism II

(Invited) Interplay of magnetism and microstructure in functional Heusler alloys: A first-principles perspective

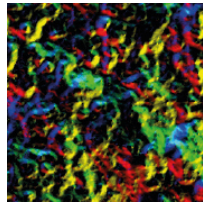
M E Gruner¹, P Entel¹ and S Fähler²

¹University of Duisburg-Essen, Germany, ²IFW Dresden, Germany

Depending on composition and chemical order, Ni-Mn-based Heusler alloys exhibit a variety of functional properties, such as half-metallicity, good magnetocaloric properties or a large magnetic shape memory effect, which render them useful for a manifold of potential applications. For the latter cases this is linked to the presence of hierarchically twinned modulated structures. These can be interpreted in terms of an adaptive, self-organized arrangement of [110]-aligned nanotwins consisting of tetragonal, non-modulated L1₀ building blocks. Total energy calculations in the framework of density functional theory reveal that the transformation path from cubic austenite to nanotwinned martensite is essentially downhill, due to a pronounced shear anomaly arising from a electronic band-Jahn-Teller-type reconstruction of the Fermi surface which in particular softens the [110] transversal acoustic phonons. The twin interface energy contains an interaction between two neighboring interfaces depending on the separation [1]. It can be attractive, leading to a competition between non-modulated tetragonal and adaptive martensites and favors the two-layer building blocks in the adaptive stacking sequence experimentally observed for the 14M martensite. We relate this behavior to the frustrated antiferromagnetic coupling between neighboring Mn atoms, which depends on their specific distance and spatial orientation, in particular in martensite. Further challenges and perspectives arise from disorder and segregation encountered in off-stoichiometric compounds [2-4].



Twin boundary energy γ_{TB} as a function of the twin width specified in lattice planes n of equilibrium non-modulated L1₀ martensite of Ni₂MnGa ($c/a = 1.25$).



Magnetism 2018

- [1] M. E. Gruner, R. Niemann, P. Entel, R. Pentcheva, U. K. Rössler, K. Nielsch, S. Fähler, arXiv:1701.01562
- [2] P. Neibecker, M. E. Gruner, X. Xu, R. Kainuma, W. Petry, R. Pentcheva, M. Leitner, Phys. Rev. B 96, 165131 (2017)
- [3] B. Schleicher *et al.*, J. Phys. D.: Appl. Phys. 50, 465005 (2017)
- [4] P. Entel *et al.*, Phys. Stat. Sol. B, DOI:10.1002/pssb.201700296

Temperature effects and inverse caloric responses in Mn-antiperovskite carbide Mn_3GaC : Ab-initio theory

E Mendive Tapia and J B Staunton

University of Warwick, UK

Magnetic refrigeration based on the magnetocaloric effect has become a widely investigated technology and promises to be an environmentally friendly and more efficient alternative to gas-compression based devices[1]. The diverse magnetism that originates in Mn-based antiperovskite structures can offer new pathways towards novel cooling cycles, as recently shown for the magnetically frustrated states in Mn_3GaN^2 . Moreover, the first order antiferromagnetic-ferromagnetic transition present in the carbide Mn_3GaC system has been subject of experimental studies in the recent decades due to the substantial inverse magnetocaloric effect measured experimentally[3-5]. Contrary to conventional caloric responses, the inverse magnetocaloric effect is based on cooling by adiabatic magnetization when an external magnetic field is applied, yielding a positive increment of the entropy at the transition. Here we present an *ab-initio* DFT-based Disordered Local Moment (DLM) theory[6-8] for the temperature effects and subsequent inverse caloric responses of ordered-to- ordered magnetic phase transitions in Mn_3GaC . Our calculations correctly predict the second order paramagnetic-ferromagnetic transition with a Curie temperature in agreement with experiment. In addition to the antiferromagnetic structure measured experimentally (Fig 1c), we predict that the ferromagnetic state is unstable to the formation of a new antiferromagnetic phase (Fig 1b) by lowering the temperature. We show that the stability competition between these two antiferromagnetic states strongly depends on the volume of the unit cell and present quantitative results of the different inverse caloric effects triggered by the transitions.

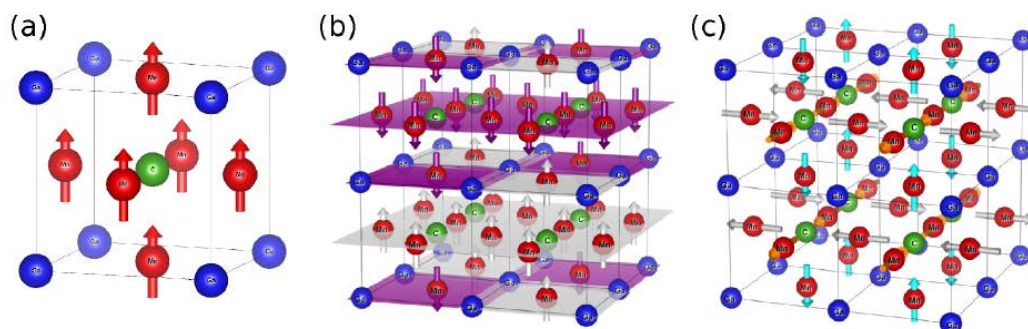
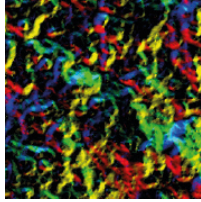


Figure 1: The figure shows the Mn-based antiperovskite structure of Mn_3GaC and the stable magnetic phases found by our *ab-initio* theory, (a) the high temperature ferromagnetic phase, (b) the new antiferromagnetic phase predicted, and (c) the antiferromagnetic phase measured experimentally.

- [1] A. M. Tishin and Y. I. Spichkin, *The Magnetocaloric Effect and its Applications*, vol. 6 (2003)
- [2] J. Zemen, *et al.*, Phys. Rev. B 95, 184438 (2017)
- [3] M.-H. Yu, *et al.*, J. Appl. Phys., 93, 10128 (2003)



Magnetism 2018

- [4] T. Tohei, *et al.*, J. Appl. Phys., 94, 1800 (2003)
- [5] O. Çakir, *et al.*, J. Appl. Phys. 115, 043913 (2014)
- [6] B. L. Gyorffy, *et al.*, J. Phys. F 15, 1337 (1985)
- [7] J. B. Staunton, *et al.*, Phys. Rev. B 74, 144411 (2006)
- [8] E. Mendive-Tapia and Julie B. Staunton, Phys. Rev. Lett. 118, 197202 (2017)

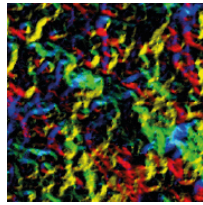
Non-uniform spin transfer torque switching dynamics in CoFeB/MgO magnetic tunnel junctions

A Meo¹, P Chureemart², S Wang³, R Chepulskyy³, D Apalkov³, P B Visscher⁴, R Chantrell¹ and R F L Evans¹

¹University of York, UK, ²Maharakham University, Thailand, ³Samsung Electronics, USA, ⁴University of Alabama, USA

Spin transfer torque magnetic random access memory (STT-MRAM) is a high-density non-volatile data storage device based on magnetised magnetic tunnel junctions (MTJs), trilayer stacks composed of two magnetic layers separated by a thin insulating layer. CoFeB/MgO-based MTJs represent a suitable candidate for STT-MRAM due to the high perpendicular magnetic anisotropy, low Gilbert damping and high TMR, required to obtain a high efficiency STT-MRAM device. The nature of the magnetisation reversal determines the switching properties of such devices and therefore, a deep understanding of the mechanism of the magnetisation reversal under the application of a spin-polarised current is of fundamental interest. Nonetheless, a model able to provide a complete description of this phenomenon has not emerged yet. Here we use an atomistic spin model to investigate the nature of the magnetisation reversal in STT-induced switching and its time-scale. The STT field is modelled based on Slonczewski's approach [1] as parametrised by Zhang *et al.* [2] and adapted to an atomistic level. Our results show a non-uniform switching of the magnetisation, with a reversed region forming near the edge and enlarging. It is not a domain in the usual sense of something bounded by slowly-moving walls - it rotates rapidly, on a precessional time scale, and can be thought of as an interference pattern between normal modes[3], whose orientation depends on the instantaneous relative phase of the modes. Since the rotation persists into the nonlinear region where the normal mode picture is invalid, we can define it as "soliton domain". The rotation continues as the mean magnetization passes the equator and switches, and occurs both at 0K and at finite temperature. Our results suggest a more complex switching dynamics than often assumed for STT devices and should lead to better understanding of the phenomenon.

- [1] Slonczewski J C 1996 J. Magn. Magn. Mater. 159 L1-7
- [2] S. Zhang, P.M. Levy, and A. Fert, Phys. Rev. Lett. 88, 236601 (2002)
- [3] K. Munira and P. B. Visscher, J. Appl. Phys. 117, 17B710 (2015).



Magnetism 2018

Investigation into the origin of the athermal training effect in exchange bias multilayers

S Jenkins, R W Chantrell and R F L Evans

University of York, UK

The exchange bias effect occurs when a ferromagnet is coupled to an antiferromagnet, causing a shift of the magnetic hysteresis loop. The shift is caused by pinned interfacial spins, causing a unidirectional field pinning the exchange coupling of atomic spins at the interface. The training effect causes a large drop in the measured exchange bias after the first measured hysteresis loop[1]. This has two main causes: thermal training and athermal training¹. Thermal training is due to well understood thermal instabilities in the AFM¹. The origin of athermal training however is still a widely disputed problem due to the difficulty in experimentally probing the rearrangement of AFM spins at the interface. It has been proposed to be due to the degree of order of the AFM at the interface. Here we investigate the origin of training in a CoFe/ γ -IrMn₃ ferromagnet/antiferromagnet (FM/AFM) bilayer using an atomistic spin model. To model the properties of the γ -IrMn₃/CoFe bilayer we have developed an atomistic spin model[2]. The properties of the disordered γ -IrMn₃ AFM are modelled using the Heisenberg form of the exchange interaction and the anisotropy is calculated using the Néel pair anisotropy model. These reproduce key experimental results including the Néel temperature and magnetic ground state.

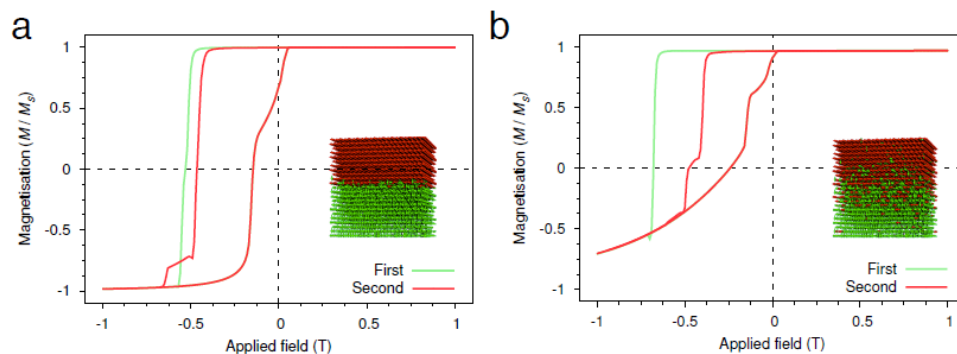
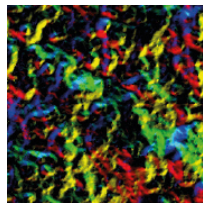


Figure1. Simulated hysteresis loops showing the athermal training effect for low (a) and high (b) intermixing (visualization of atomic structure inset).

It was found that for a single grain with an atomically flat interface that there is no training effect and the exchange biased loops are completely repeatable. As the width of the interface mixing is increased we see an increase in the a-thermal training effect, as shown in Fig. 1. The exchange bias was observed to increase with interface mixing for the initial hysteresis loop but the training effect causes a much larger reduction for subsequent hysteresis loops when the interface is mixed. We will present systematic calculations of the exchange bias and training effects as a function of interface mixing and further simulations of the temperature dependence of the exchange bias with thermal training and a statistical study of polygranular exchange biased systems.

This work used the ARCHER UK National Supercomputing Service (<http://www.archer.ac.uk>).

- [1] X. P. Qiu, D. Z. Yang, S. M. Zhou, R. Chantrell, K. O'Grady, U. Nowak, J. Du, X. J. Bai, and L. Sun. Rotation of the pinning direction in the exchange bias training effect in polycrystalline NiFe/FeMn bilayers. *Phys. Rev. Lett.*, 101: 147207, Oct 2008.
- [2] Evans R F L, Fan W J, Chureemart P, Ostler T A, Ellis M O A, and Chantrell R W. Atomistic spin model simulations of magnetic nanomaterials. *Journal of Physics:Condensed Matter*, 26, 2014.



Magnetism 2018

Effect of aggregation on the radio-frequency heating of ferromagnetic manganite nanoparticles

J Cook, K McBride, D Poulidi and L Stella

Queen's University Belfast, UK

Ferromagnetic manganite nanoparticles of high crystallinity are readily heated up using a radio-frequency magnetic field [1]. Thanks to their relative low (260-350K) Curie temperature are, they also possess a natural “switch- off” mechanism that prevents dangerous over-heating, e.g., in medical applications. In principle, the specific absorption rate of ferromagnetic manganite nanoparticles in solution can be inferred from a numerical simulation. In practise, magnetic colloids are complex systems which display competing magnetic response mechanism, e.g., domain, Brownian relaxation, and Néel relaxation.

In this work, we have model ferromagnetic manganite nanoparticles in solution including both the Brownian and Néel relaxation. The solvent- nanoparticle interaction is modelled implicitly using the stochastic Landau-Lifshitz-Gilbert (sLLG) equation. Dipole-dipole and soft sphere potentials have been used to simulate the many-body interaction. Our real time simulation give access to the linear response of manganite nanoparticles in solution.

The effect of temperature and viscosity of the solvent on relaxation times, along with the size of the particle, have been investigated. The influence of strong dipole-dipole interaction and the formation of nanoparticle chains is alsodiscussed.

- [1] K. McBride, S. Bennington-Gray, J. Cook, L. Stella, S. Felton, and D. Poulidi. “Improving the crystallinity and magnetocaloric effect of the perovskite $\text{La}_{0.65}\text{Sr}_{0.35}\text{MnO}_3$ using microwave irradiation”. In: *Crys- tEngComm* vol 19 (27, 2017), pp. 3776–3791. doi: 10.1039/C7CE00882A.

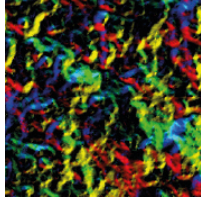
Correlated electrons

(Invited) Hunting majorana fermions in quantum spin--liquids

J Knolle

Imperial College London, UK

Theoretically, some quantum spin liquids (QSLs) – new topological phases which can occur when quantum fluctuations preclude a magnetically long range ordered state – are known to exhibit Majorana fermions as quasiparticles arising from fractionalization of spins. Alas, despite much searching, their experimental observation remains elusive. Here, I will give an overview of the dynamical response of the paradigmatic Kitaev honeycomb QSL and connections to recent experiments on RuCl_3 . I argue that inelastic neutron and light scattering experiments admit straightforward interpretations in terms of Majorana Fermion excitations.



Magnetism 2018

Multi-site exchange enhanced barocaloric response in Mn_3NiN

D Boldrin¹, E Mendive-Tapia², J Zemen^{1,3}, J B Staunton³, P Lloveras⁴, X Moya⁵ and L F Cohen¹

¹Imperial College London, UK, ²University of Warwick, UK, ³Czech Technical University in Prague, Czech Republic, ⁴Universitat Politècnica de Catalunya, Barcelona, ⁵University of Cambridge, UK

Caloric materials offer opportunities for more energy-efficient and less environmentally harmful refrigeration. Whilst magnetocalorics initially drove research into this field, mechanocalorics (baro- and elastocalorics) have gained relatively little attention yet may offer several advantages [1,2]. Here we have studied the barocaloric effect (BCE), by means of magnetometry and calorimetry under hydrostatic pressure, in a select number of materials belonging to the Mn_3AN antiperovskite family, which are geometrically frustrated antiferromagnets. In Mn_3NiN , the triangular spin arrangement of the compensated antiferromagnetic state is thought to be responsible for the relative insensitivity of T_N to pressure, $dT_N/dp = -14 \text{ K GPa}^{-1}$ (Fig 1a), in spite of large magnetovolume coupling. This leads to a larger barocaloric entropy change, $\Delta S = 35 \text{ J K}^{-1} \text{ kg}^{-1}$ (Fig 1b), than in the recently discovered giant BCE of the isostructural Mn_3GaN [2,3]. We compare the BCE in both Mn_3NiN and Mn_3GaN using a Landau free-energy expansion and find that, despite the lower magnetovolume coupling in Mn_3NiN , the enhanced barocaloric entropy change and 1st-order character of the magnetic transition originate from multi-site exchange interactions amongst the local Mn magnetic moments and their coupling with itinerant electron spins (Fig 1c). Using this framework, we have begun to explore routes to maximize the BCE beyond Mn_3NiN in the broad and chemically flexible Mn_3AN family.

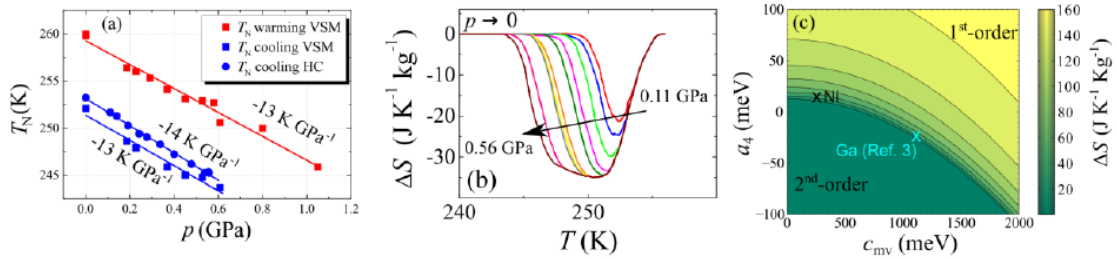
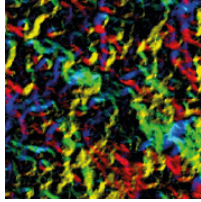


Figure 1: (a) Pressure dependence of the Néel temperature measured using magnetometry and calorimetry. Solid lines are linear fits to the data. (b) Isothermal entropy changes determined from temperature dependent heat flow measurements performed under pressure. (c) The dependence of ΔS as a function of a_4 which describes the multi-site interactions amongst the local Mn magnetic moments.

- [1] L. Mañosa and A. Planes, Adv. Mater. 29, 1603607 (2017).
- [2] P. Lloveras, E. Stern-Taulats, et al., Nat. Commun. 6, 8801 (2015)..
- [3] D. Matsunami, A. Fujita, K. Takenaka, and M. Kano, Nat. Mater. 14, 73 (2014).



Magnetism 2018

Complex modulated magnetism in PrPtAl

G Abdul-Jabbar¹, D A Sokolov¹, C D O'Neill¹, C Stock¹, D Wermeille^{2,3}, F Demmel⁴, F Krüger^{4,5}, A G Green⁵, F Lévy-Bertrand⁶, B Grenier⁷ and A Huxley¹

¹University of Edinburgh, UK, ²XMaS, The UK-CRG, France, ³University of Liverpool, UK, ⁴ISIS, STFC, UK,

⁵University College London, UK, ⁶CNRS, France, ⁷UGA & CEA, France

The transition between ferromagnetism and paramagnetism is one of the simplest examples of a continuous phase transition. Interesting behaviour is expected when the transition temperature becomes small because incoherent fluctuations above the transition temperature then exist to low temperatures. Ultimately, for lower transition temperatures, either the transition must become first order or new forms of order must appear to satisfy the third law of thermodynamics. A new theory known as “order-by-disorder” [1] clarifies how the fluctuations associated with different competing ground states may stabilise new forms of order under these circumstances. Our findings on PrPtAl provide the first concrete vindication of one of the predictions of this approach: the formation of modulated magnetic structures [2].

Our X-ray diffraction study at XMaS has allowed us to characterise complex magnetic states discovered in PrPtAl at the boundary between ferromagnetism and paramagnetism. Much of the observed behaviour is consistent with the predictions of the order-by-disorder theory, including a change from ferromagnetism to a modulated state whose modulation vector increases with temperature. Surprisingly, the phase diagram is also more complex. Rather than this modulated state changing directly into the paramagnetic state as the temperature is further increased, it changes to a doubly modulated state before paramagnetism is finally attained. This second modulated state is very unusual, having two simultaneous collinear incommensurate ordering vectors (Figure 1).

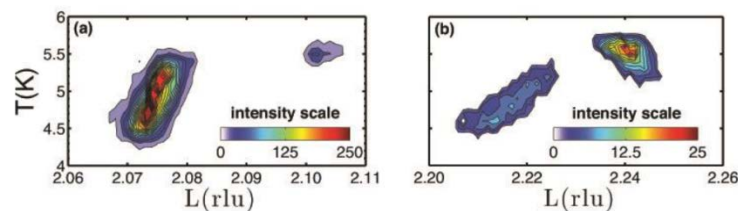
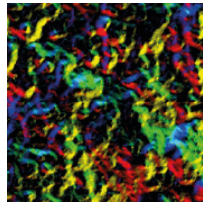


Figure 1: The figure shows intensity maps around satellites at (00L) close to the (002) Bragg peak as a function of temperature for PrPtAl measured at the Pr LII edge. At lower temperature a single modulation wavevector $q \approx 0.07$ (rlu) (a) and a third harmonic (b) are seen. The change of wavevector with temperature and the strong third harmonic are well explained by the “order-by-disorder” theory. Just before 6 K, two new vectors appear at $q \approx 0.1$ (rlu) (a) and 0.24 (rlu) (b).

[1] G.J. Conduit *et al.*, Phys. Rev. Lett. 103, 207201 (2009).

[2] G. Abdul-Jabbar *et al.*, Nat. Phys. 11, 321–327 (2015).



Magnetism 2018

Decomposing the Bragg glass and the peak effect in a Type-II superconductor

R Toft-Petersen^{1,2}, A B Abrahamsen¹, S Balog³, L Porcar⁴, M Laver⁵ and C Larsen⁵

¹Technical University of Denmark (DTU), Denmark, ²Helmholtz-Zentrum Berlin für Materialien und Energie, Germany, ³University of Fribourg, Switzerland, ⁴Institut Laue-Langevin, France, ⁵University of Birmingham, UK

In Type-II superconductors, disorder generally works to pin vortices, giving zero resistivity below a critical current j_c . However, peaks have been observed in the temperature and field dependences of j_c . This peak effect is difficult to explain in terms of an ordered Abrikosov vortex lattice. Here we test the widespread paradigm that an order-disorder transition of the vortex ensemble drives the peak effect.

We use small-angle neutron scattering (SANS) to probe the vortex order in superconducting vanadium. The SANS technique provided the first experimental evidence for a quasi-long-range-ordered phase stabilised in the presence of weak disorder, known as the Bragg glass [1]. We find evidence from the field dependence of SANS for a Bragg glass picture at intermediate fields. We further demonstrate the presence of a Bragg glass regime by characterising the shape of the diffraction peak in a high-resolution experimental set-up and using reverse Monte Carlo refinement to extract correlation functions from our data [2]. Our SANS experiments allow the order-disorder transition $B_{dis}(T)$ to be located. Comparing this line with the critical current density j_c determined by magnetometry, we discern no jump in j_c around B_{dis} in our sample. Instead, we observe a nascent peak effect at fields and temperatures close to $B_{c2}(T)$, in a region where thermal fluctuations of individual vortices become significant [3].

- [1] Klein, T. *et al.* A Bragg glass phase in the vortex lattice of a type II superconductor. *Nature* 413, 404–406 (2001).
- [2] Laver, M. *et al.* Uncovering flux line correlations in superconductors by reverse Monte Carlo refinement of neutron scattering data. *Phys. Rev. Lett.* 100, 107001 (2008).
- [3] Toft-Petersen, R. *et al.* Decomposing the Bragg glass and the peak effect in a Type-II superconductor. *Nat. Commun.* (accepted; in press).

Spintronics II

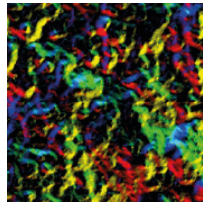
Towards pure spin currents for oxide spintronic devices

C Cox¹, A Caruana^{1,2}, B Nicholson³, A Mora-Hernandez³, A Hindmarch³, C Kinane², T Charlton⁴ and K Morrison¹

¹Loughborough University, UK, ²STFC Rutherford Appleton Laboratory, UK, ³Durham University, UK, ⁴Oak Ridge National Lab, USA

The advent of commercial spintronics is ever approaching and the realization of such devices is contingent upon calculable manipulation of spin currents across material interfaces. Magnetic proximity effects (MPE) (resulting in the polarization of spins in non-magnetic materials such as Pt due to adjacent magnetic material), have the potential to contaminate and even annihilate spin current injection/production in such devices and render them unreliable. Of particular interest is the use of ferrites, e.g. Fe_3O_4 , as the magnetic material. We present the characterisation and investigation of high quality $\text{Fe}_3\text{O}_4/\text{Pt}$ bilayers grown by pulsed laser deposition [1]. In Fe_3O_4 , the thoroughly characterized metal-insulator (Verwey) transition, T_v , provides the opportunity to investigate if the origin of the MPE exists in the two states[2].

Synchrotron techniques, such as X-ray Resonant Magnetic Reflectivity (XRMR)[3], have the ability to tune to the L_3 -edge of Pt providing element specific magnetic contrast in addition to the structural contrast of



Magnetism 2018

standard x-ray reflectivity (XRR), as shown in Figure 1a. Utilising XRMR, the magnitude and coherence length of the induced magnetic moment in the adjacent Pt has been evaluated (asymmetry scan and fits shown in Figures 1b and c). Initial results hint at the presence of a 1-2 nm region of magnetized Pt ($0.1\mu_B/\text{Pt atom}$) at temperatures above the T_v . Whilst at low temperatures, below the T_v , XRMR suggests the magnetisation in Pt is reduced but not eradicated, leading to the conclusion that the metallic state is correlated to, but not a determining factor for, the MPE.

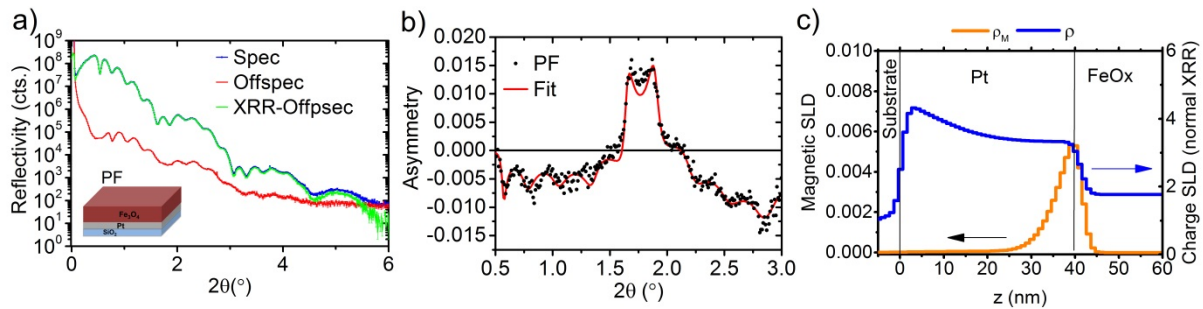


Figure 1 (a) XRR – specular and off-specular scattering of Pt/Fe₃O₄ bilayers, (b) Asymmetry of the XRMR curves and (c) SLD fit profiles of XRMR data.

- [1] A. J. Caruana *et al.*, *Phys. status solidi - Rapid Res. Lett.*, 10 (8) 613-617, 2016
- [2] M. Collet *et al.*, *Appl. Phys. Lett.*, 111 (20) 202401, 2017.
- [3] P. Bougiatioti *et al.*, *Phys. Rev. Lett.*, 119 (22) 227205, 2017.

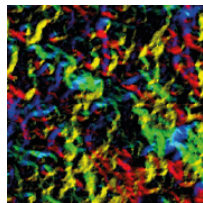
Magnetic oxides for spin injection: recent outcomes from the molecular spintronics

P Graziosi¹, L Poggini², G Cucinotta², R Sessoli², M Mannini², S Picozzi¹, I Bergenti¹ and V A Dediu¹

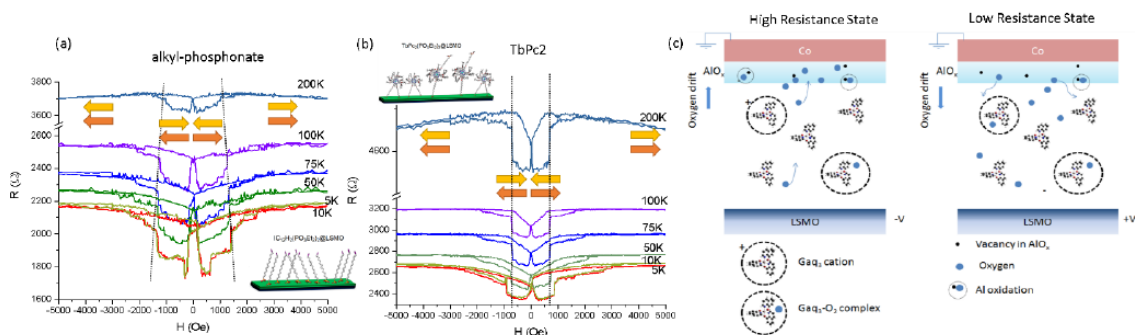
¹CNR-ISMN, Italy, ²Università degli Studi di Firenze, Italy

Spintronics has fostered an impressive modernization of our day-life starting from '90s and is currently in the forefront of the exploration of new functionalities in communication, information storage, advanced computing (e.g. quantum computing and “computing-in-memory”). Magnetic oxides and related compounds (nitrides, sulfides, as well as bilayers like Co/Al₂O₃) stand out in the materials science playground for their unique functional properties and versatilities. Moreover, the use of magnetic oxides in organic spintronics is expected to endorse conceptually new applications, including the device downscaling until its ultimate functional limits confined in the interface. [1]

We present the most recent achievements in molecular spintronics involving magnetic oxide electrodes at the spin injecting interface level. We report on the functionalization of the so-called spinterface by chemisorbing a monolayer of molecular radicals [2] and single molecule magnets (SMM), [3] that results in the tuning of the device performances. We describe finally a model based on the combined analysis of magnetotransport and spectroscopic results and explaining why the presence of at least one oxide electrode is so relevant in the performance of molecular devices, for both spintronic and memristive effects. [4]



Magnetism 2018



Magnetoresistances of the same device structure but with different spinterface functionalization: inert (a) and SMM (b) monolayers. [3] It is remarkable the different temperature trend of the switching fields associated with the functionalized electrode. Sketch (c) of the conceptual model for the electrical bistability driven by oxygen motion in the molecular layer.

[1] M. Cinchetti, L. Hueso, V. A. Dediu, Nat

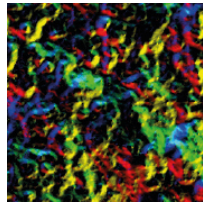
Multifunctional spintronic device based on spin dependent charge trapping

T Moorsom¹, M Rogers¹, I Scivetti², S Bandaru³, G Teobaldi^{2,3}, M Valvidares⁴, M Flokstra⁵, S Lee⁵, R Stewart⁵, T Prokscha⁶, P Gargiani⁴, G Stefanou¹, M Ali¹, F Al Ma 'Mari^{1,7}, G Burnell¹, B J Hickey¹ and O Cespedes¹

¹University of Leeds, UK, ²University of Liverpool, UK, ³Beijing Computational Science Research Centre, China, ⁴ALBA Synchrotron, Spain, ⁵University of St Andrews, UK, ⁶Paul Scherrer Institute, Switzerland, ⁷Sultan Qaboos University, Oman

Molecular spintronics has the potential to revolutionise spintronic architecture because of the multifunctionality possible in molecular devices.[1] Key to achieving this are the complex magnetic interface effects which emerge between molecules and other materials.[2] These 'spinterface' effects have been linked to emergent magnetism, interface magnetoresistance and active control of magnetic semiconductors and topological spin textures.[3-6] There is now a growing effort to create devices utilising these unique effects.[7]

Here, we present a multifunctional molecular spintronic device based on a $\text{MnO}_2/\text{C}_{60}$ interface, exhibiting spin filtering, photovoltaic and memristor effects. Half metallic surface states are induced in the manganate through hybridisation with C_{60} . In addition, the $\text{C}_{60}\text{-O}$ ion pair forms a polar layer, creating an interfacial well which traps charge.[8] Accumulated charge decays with a spin dependent lifetime due to the spin filtering interface, allowing capacitance to be tuned by external fields. This effect can be observed in XAS, transport and is predicted by DFT, figure 1. This research has implications for organic devices using LSMO electrodes as well as presenting a path to a molecular spin capacitor. Furthermore, the vital role of oxygen in this spin trapping effect posits a new route to active control of spinterface effects: redox activity. Devices based on $\text{MnO}_2/\text{C}_{60}$ interfaces can be made to switch between different resistance states by applying a sufficiently large programming voltage which affects the interfacial potential and, by extension, spinterface properties in a reversible manner.



Magnetism 2018

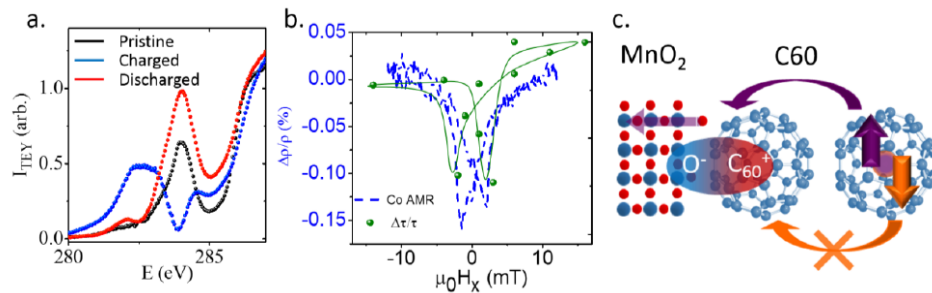


Figure 1. a. XAS measured in a $\text{MnO}_2/\text{C}_{60}/\text{Co}$ junction showing modification of the molecular orbitals due to charge accumulation. b. Decay time constant for the open circuit voltage measured in the same structure (green points, line is a guide to the eye), and AMR (blue) of the Co electrode. c. Schematic of the charge trapping. Charge accumulates in the potential well created by the interfacial polar layer. Spin up charges can decay across the spin filtering interface. The quantisation axis is set by external fields or magnetic electrodes.

- [1] S. Sanvito, Chem. Soc. Rev. 40, 3336 (2011).
- [2] S. Sanvito, Nat. Phys. 6, 563 (2010).
- [3] F. A. Ma'Mari, et al., Nature 524, 69 (2015).
- [4] K. V. Raman, et al., Nature 493, 509 (2013).
- [5] X. Wang, et al., Adv. Mat. 27, 8043 (2015).
- [6] S. Jakobs, et al., Nano Lett. 15, 6. 6022 (2015).
- [7] M. Cinchetti, V. A. Dediu, and L. E. Hueso, Nat. Mat. 16, 507 (2017).
- [8] L. Shulz, et al., Nat. Mat. 10, 39 (2010).

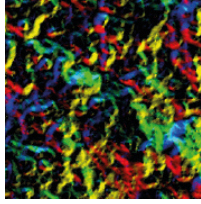
Spintronics in high-quality graphene heterostructures via 1D contacts.

V H Guarochico-Moreira^{1,2}, J L Sambricio¹, I Grigorieva¹ and I J Vera-Marun¹

¹The University of Manchester, UK, ²Departamento de Física, Escuela Superior Politécnica del Litoral, Ecuador

We report the first observation of nonlocal pure spin currents in high-quality graphene channels that are fully encapsulated by hexagonal boron nitride (hBN) layers. Our heterostructure devices prevent residual contamination from the fabrication process, routinely allowing high-quality channels¹. This architecture is enabled by creating spin injectors based on edge one-dimensional (1D) contacts², which avoid any significant charge doping from the contacts in the centre of the channel. We present evidence for spin transport and precession both at room and low temperatures. Our approach avoids extrinsic factors of spin relaxation which have been reported so far, like inhomogeneity in the channel, quality of tunnelling contact and lithographic impurities. We believe this is a step forward in the quest to understand and directly measure the intrinsic spin transport in graphene.

- [1] Kretinin, A. V., et al. "Electronic properties of graphene encapsulated with different two-dimensional atomic crystals." *Nano letters* 14.6 (2014): 3270-3276.
- [2] Wang, L., et al. "One-dimensional electrical contact to a two-dimensional material." *Science* 342.6158 (2013): 614-617.



Magnetism 2018

Electrical and optical characterization of Fe/*n*-GaAs non-local spin valve

J-y Kim¹, M Samiepour¹, J Ryu², D Iizasa², T Saito², M Kohda², J Nitta², H E Beere³, D A Ritchie³ and A Hirohata¹

¹University of York, UK, ²Tohoku University, Japan, ³University of Cambridge, UK

The spin field-effect transistor (FET) [1, 2] is a critical vehicle to study injection, manipulation and detection of spin-polarised carriers in a semiconductor. In this study, we fabricated Fe/*n*-GaAs non-local spin valves and investigated spin transport using electrical and optical methods.

Electrical properties of the devices were measured in a vector-magnet He cryostat. As seen in Fig.1(a), 3- and 4-terminal Hanle-like peaks were obtained with half-width at half-maximum field values of around 440 mT. According to the formula used in Nam *et al.* [3], the spin dephasing time was calculated to be around 60 ps. Our spin dephasing time was about 200-times smaller than previous reports. The large (~ 1 T) field required to saturate the both 3T and 4T signals indicated possible magnetisation rotation of the Fe injector and detector bars as a possible source of the resistance changes. This was confirmed by pump-probe time-resolved Kerr rotation measurements on *n*-GaAs channel. As seen in Fig. 1(b), the strongest Kerr modulation was observed at the excitation wavelength of 821 nm (1.51 eV) at 30 K. From this oscillation, a spin dephasing time of 2.9 ns and an electron g -factor of -0.43 were estimated. Further optimisation of the Fe/*n*-GaAs interface has been achieved using non-destructive junction imaging [4].

This work has partially been supported by UK-EPSC (EP/M02458X/1).

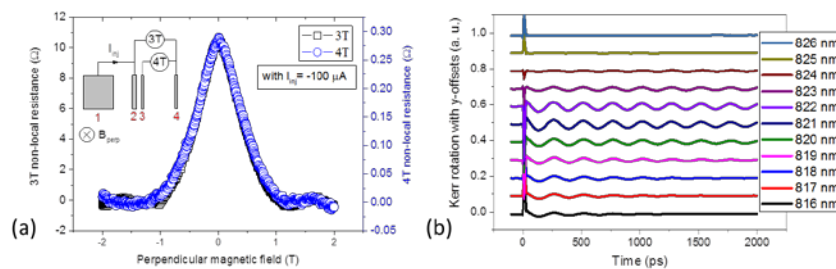
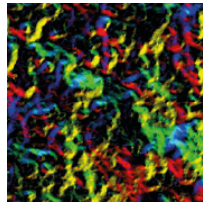


Fig. 1 (a) Three- and four-terminal non-local resistance at 4 K with a perpendicular magnetic field at -100 μ A injection current. (b) Wavelength dependence of the time-resolved Kerr rotation results on the *n*-GaAs channel at 30 K with an applied in-plane field of 0.65 T.

- [1] S. Datta and B. Das, *Appl. Phys. Lett.* 56, 665 (1990).
- [2] X. Lou *et al.*, *Nature Phys.* 3, 197 (2007).
- [3] S. H. Nam *et al.*, *Appl. Phys. Lett.* 109, 122409 (2016).
- [4] A. Hirohata *et al.*, *Nature Commun.* 7, 12701 (2016).



Magnetism 2018

Thin films and nanomagnets III

Mapping three dimensional spin structures with X-ray magnetic tomography

C Donnelly

ETH Zurich, Switzerland

Three dimensional magnetic systems are of growing interest due to the possibilities for complex spin textures and new functionalities such as curvature-induced magnetochirality effects. For the experimental realisation of these new systems, however, suitable characterisation techniques are required. We have developed hard X-ray magnetic nanotomography [1], a new technique to visualise three-dimensional magnetisation configurations at the nanoscale within micrometre-sized samples. We combine hard X-ray magnetic imaging with a dual axis tomographic setup, and a new reconstruction algorithm that requires no prior knowledge of the magnetic properties of the sample and, in a first demonstration of the technique, we have determined the three-dimensional magnetic structure within the bulk of a micrometre-sized GdCo₂ pillar to a spatial resolution of 100 nm. The internal magnetic configuration is complex, and includes a number of structures such as vortices, anti-vortices and domain walls. At the intersections of these structures, magnetisation singularities – Bloch points – occur, and we are able to identify different types of Bloch points – a circulating Bloch point and an anti-Bloch point. With its high penetration depth, hard X-ray magnetic tomography will allow for the determination of three-dimensional magnetic configurations within a wide range of systems.

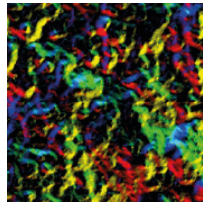
[1] Donnelly et al., *Nature* 547, 328 (2017).

Two-photon lithography for 3D magnetic nanostructure fabrication

G Williams¹, M Hunt¹, B Boehm², A May¹, M Taverne³, D Ho³, S Giblin¹, D Read¹, J Rarity³, R Allenspach² and S Ladak¹

¹Cardiff University, UK, ²IBM Research – Zurich, Switzerland, ³University of Bristol, UK

UK Three-dimensional magnetic nanostructures are gaining intense interest recently due to their potential in realising next generation storage architectures as well as their capacity to realise artificial crystals that mimic bulk frustrated materials. Two-photon lithography (TPL) is a relatively new technique that has largely been exploited within the metamaterials and microfluidic communities to fabricate complex 3D nanostructured materials. In order to demonstrate the versatility of this technique in fabricating 3D magnetic nanostructures, we have used TPL to fabricate arrays of complex 3D tetrapod structures [1]. A single tetrapod structure is shown in figure 1(a). The structures were subsequently probed using spin- polarised scanning electron microscopy (Spin-SEM) and magneto-optical Kerr effect (MOKE) magnetometry within both polar and longitudinal geometries. Figure 1(b) shows the longitudinal MOKE loop that is obtained upon the tetrapod array when the magnetic field is parallel to the projection of the lower wire long-axes. In this talk we will discuss the magnetometry results obtained with reference to spin-SEM measurements and micro- magnetic simulations. Finally, we will discuss our most recent attempts at realising single domain 3D magnetic nanowires.



Magnetism 2018

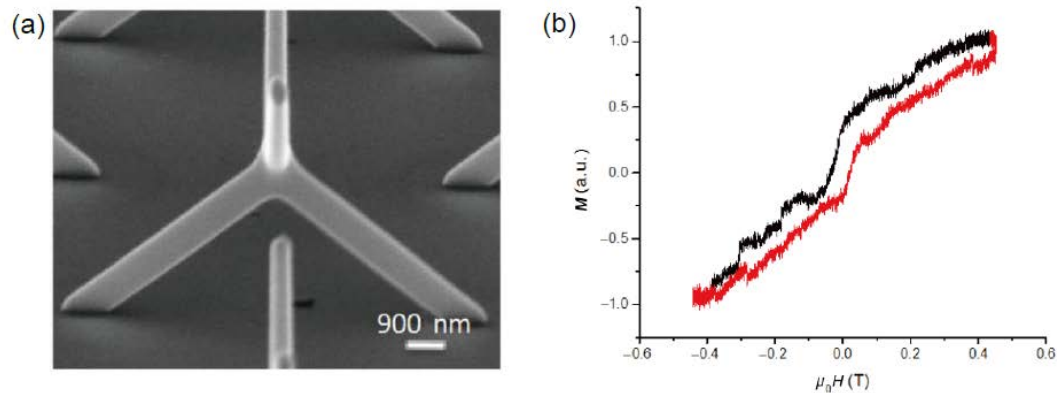


Figure 1: (a) Co Tetrapod structure fabricated using TPL and electrodeposition, (b) Longitudinal geometry MOKE hysteresis loop.

- [1] Williams, G., Hunt, M., Boehm, B. et al. Nano Res. (2018) 11: 845.
<https://doi.org/10.1007/s12274-017-1694-0>

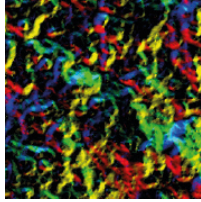
Spatial mapping of torques within a spin hall nano-oscillator

T M Spicer¹, P S Keatley¹, M Dvornik², A A Awad², P Dürrenfeld², A Houshang², M Ranjbar², R K Dumas², J Åkerman^{2,3,4}, V V Kruglyak¹ and R J Hicken¹

¹University of Exeter, UK, ²University of Gothenburg, Sweden, ³KTH Royal Institute of Technology, Sweden,

⁴NanOsc AB, Sweden

Time-resolved scanning Kerr microscopy (TRSKM) was used to study the precessional magnetization dynamics induced by a microwave current within a (Al₂O₃/Py(5 nm)/Pt(6 nm)/Au(150 nm)) spin Hall nano-oscillator structure[1]. The Au layer was patterned so as to form two needle-shaped electrical contacts that concentrated the current within the centre of a Py/Pt mesa of 4 micron diameter. Due to the Spin Hall Effect, the current passing through the Pt layer generates a spin current that propagates into the Py layer, exerting a spin transfer torque (STT) [2]. By injecting an RF current, and exploiting the phase-sensitivity of TRSKM and the symmetry of the device structure, the STT and the torques due to the in-plane and out-of-plane components of the Oersted field have been separated and spatially mapped. The STT and the torque due to the in-plane Oersted field are found to be significantly reduced at the centre of the device, most likely due to a reduction of the local current density, and perhaps the saturation magnetization, due to heating effects. Knowledge of the local torques is essential for understanding the conditions under which auto-oscillations can be induced.



Magnetism 2018

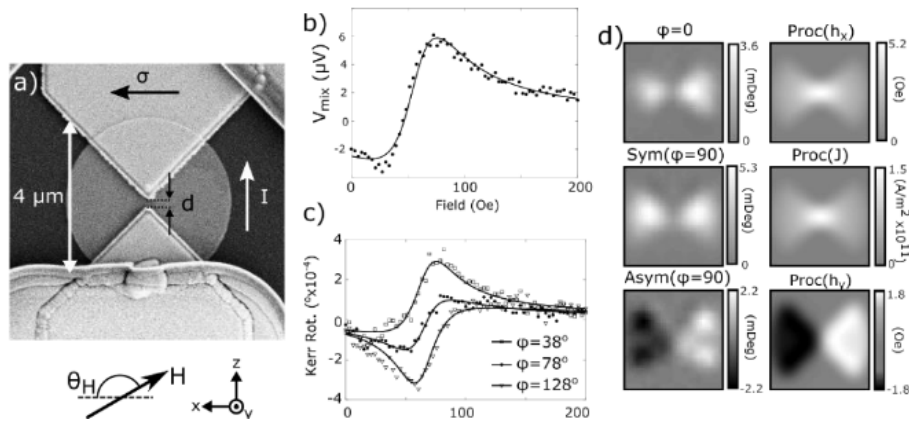


Figure 1 (a) SEM image of an SHNO showing the electrode separation d , directions of the net charge current, with magnitude I , average polarization σ of the spin current injected into the Py layer, and field H orientated at angle θ_H relative to the x axis. (b) Dependence of mixing voltage V_{mix} upon applied field H_{ext} applied at $\theta_H = 150^\circ$. The continuous curve is a fit to an analytical expression [3]. (c) Polar Kerr rotation curves recorded with the optical spot positioned between the tips of the NC for three values of the microwave phase ϕ . Continuous lines are fits to a derived equation for optical response. (d) Polar Kerr image images acquired for $\phi = 0^\circ$, $\theta_H = 90^\circ$ and $H_{\text{ext}} = 75$ Oe are presented next to the calculated distribution of in-plane Oersted field. Symmetric and antisymmetric parts of the polar Kerr data acquired at $\phi = 90^\circ$, are presented next to the vertical component of the current density J_z and the out of plane Oersted field. The calculated images were masked by the shape of the NCs and then convolved with a Gaussian spot of 880 nm half maximum radius.

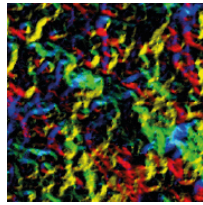
- [1] V. E. Demidov, et al, Nature communications 5, 3179 (2014)
- [2] L. Liu, T. Moriyama, et al, Physical Review Letters 106, 036601 (2011)
- [3] A. A. Tulapurkar, et al, Nature 438, 339 (2005).

Macro-ferromagnetism in a novel artificial spin ice

G M Macauley¹, R Macêdo¹, Y Li¹, F S Nascimento², S McVitie^{1,3} and R L Stamps^{1,3}

¹University of Glasgow, UK, ²Universidade Federal de Viçosa, Brazil, ³University of Manitoba, Canada

Artificial Spin Ices (ASIs) are arrays of strongly correlated nano-scale magnetic islands. While initially envisaged as a two-dimensional analogue of bulk frustrated pyrochlores[1], they are now seen as a possible avenue for designing functional materials. Recently, a new tiling pattern of artificial spin ice has gained attention for its unusual ordering processes[2]. This patterning, called the *pinwheel*, is a variation on the canonical square ice, and is formed by rotating each island through 45° about its centre. Here, we investigate this pinwheel spin ice. Using micromagnetic simulations and Monte Carlo techniques, we examine the effect that this rotation has on the ground state and hysteresis behaviour of pinwheel arrays. By weakening the nearest-neighbour coupling, this rotation leads to a system dominated by long range interactions. A phase transition of the type envisaged by Landau and Binder is observed[3]. Unlike square ASI which possesses an antiferromagnetic ground state, pinwheel spin ice appears to behave as a ferromagnet. The base unit for this macro-ferromagnetism is the net moment of each pinwheel vertex. Structures reminiscent of domains and domain walls in continuous media are seen[4]. Indeed, ground states similar to Landau flux closure patterns are shown to be energetically favourable as they minimise stray fields. This apparent ferromagnetism is confirmed by our preliminary thermal and field-driven results from Lorentz transmission electron microscopy (LTEM).



Magnetism 2018

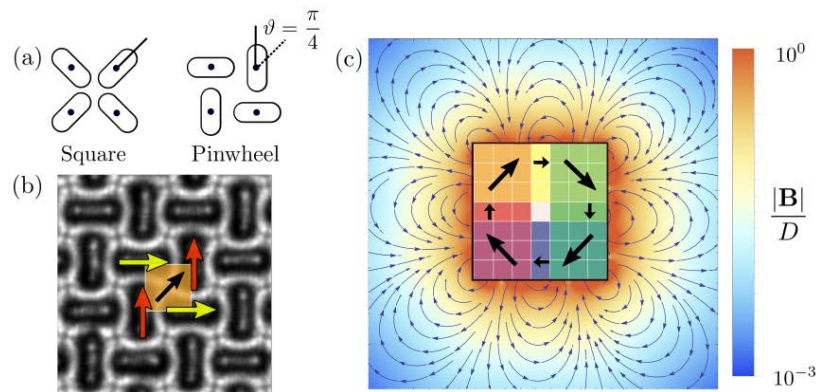


Figure 1. Pinwheel spin ice as a macro-ferromagnet. The pinwheel is obtained from square spin ice by rotating each nano-magnet through 45° as in part (a). Fresnel imaging in LTEM can be used to identify the orientation of magnetisation within individual islands. For example, in (b), we show the island moments for a single pinwheel taken from recent experimental results. The direction of the net vertex moment is indicated by the black arrow. In part (c), we show the predicted ground state of a pinwheel array using a Monte Carlo approach. As in part (b), each coloured square represents a single pinwheel unit, with an associated net moment. The streamlines and colour map (in units of $D = \mu_0 M_s V / (4\pi a^3)$) give the direction and magnitude of the stray field. The system has formed ‘mesoscopic’ domains, similar to a Landau flux closure pattern. The closure structure is stabilised by the flower-like shape of the stray field lines.

- [1] R F Wang et al., *Nature* 439, 303-306 (2006).
- [2] S Gliga et al., *Nature Materials* 16, 1106 (2017).
- [3] D P Landau and K Binder, *Phys. Rev. B* 31, 5946 (1985)
- [4] S McVitie and J Chapman, *MRS Bulletin* 20 (10), 55-58 (1995).

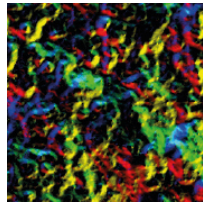
Other topics in magnetism

Element-specific magnetic imaging with 20 nm spatial resolution using table-top high-harmonic source

S Zayko¹, O Kfir¹, M Heigl², M Sivi¹, M Albrecht², and C Ropers¹

¹University of Göttingen, Germany, ²University of Augsburg, Germany

Studying the behavior of microscopic magnetic arrangements, such as skyrmions or domain patterns, requires techniques capable of nanoscale magnetic imaging combined with a possibility to access ultrafast magnetization dynamics [1]. Compact sources based on high-harmonic generation (HHG) are very appealing for such studies due to their extreme-UV to soft-x-ray spectral range and a femtosecond pulse duration [2,3]. Here, we demonstrate the first magnetic imaging using high-harmonic radiation [2]. In this implementation, we illuminate a Co/Pd multilayer structure with femtosecond pulses of circularly polarized harmonics, and retrieve the magnetization domain pattern with lensless imaging techniques reaching a spatial resolution of 20 nm. Due to excellent coherence properties high-harmonic beams, the resolution of this full-field imaging scheme is diffraction-limited and competes with large scale facilities, such as synchrotrons and free-electron lasers, even at a larger field-of-view [2,4,5]. This work allows for in-house magneto-optical microscopy with very high spatial resolution, and paves the way towards spatially-resolved and element-specific femtosecond movies of ultrafast motion of the magnetization.



Magnetism 2018

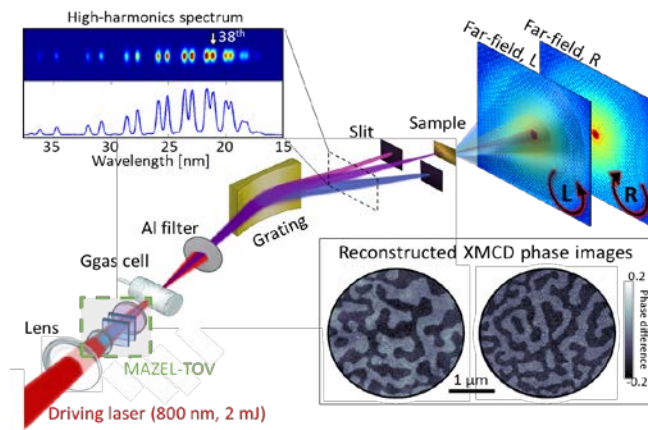


Figure 1. Schematic of the experimental setup. A bi-chromatic counter-rotating beam, tailored by a MAZEL-TOV device [6], generates circularly polarized high harmonics in a He-filled cell. Using a toroidal grating and a slit, the 38th harmonic order (photon energy, 59 eV; wavelength, 21 nm) is selected and focused onto the sample. The scattered radiation is collected with a CCD camera for left- and right-handed circularly polarized illumination and the recorded diffraction patterns are reconstructed using an iterative phase retrieval algorithm. The bottom right corner shows the reconstructed quantitative magneto-optical phase maps of Co/Pd multilayer structures.

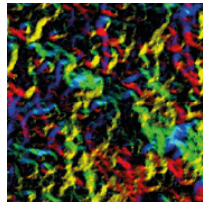
- [1] F. Büttner *et al.*, *Nat. Nanotechnology* 12, 1040–1044 (2017).
- [2] O. Kfir, S. Zayko *et al.*, *Science Advances* 3, EAA04641 (2017).
- [3] S. Mathias *et al.*, *J. Electron Spectrosc. Relat. Phenom.* 189, 164–170 (2013).
- [4] S. Zayko *et al.*, *Opt. Express* 23, 19911 (2015).
- [5] P. Fischer, *J. Phys. D: Appl. Phys.* 50, 313002 (2017).
- [6] O. Kfir, *et al.*, *App. Phys. Lett.* 108, 211106 (2016).

Chemical and structural analysis on magnetic tunnel junctions using a decelerated scanning electron beam

E Jackson¹, M Sun², T Kubota², K Takanashi² and A Hirohata¹

¹University of York, UK, ²Tohoku University, Japan

A series of magnetic tunnel junctions (MTJs), shown in fig. 1a, were produced on a single wafer. These MTJs could be split into two distinctive groups, High or low tunnelling magnetoresistance (TMR). This corresponds with the effective yield of the process. To improve the total yield the devices were investigated using a recently developed imaging technique [1]. This technique utilises CASINO [2], an electron scattering in solids simulator, to find a controlled voltage which will penetrate the sample down to a chosen interface. The impact voltages chosen were 10, 10.5 and 11 keV allowing the CoFe, MgO and CFMS interfaces to be analysed using the back scattered electrons produced. These images were taken using the JEOL JSM 7800F Prime. The technique found the main difference between the two groups was a build-up of material around the low TMR MTJs, an example is shown in fig. 1b. Energy-dispersive X-ray spectroscopy was utilised to identify the material around the pillar, with both spectra and chemical maps obtained. These two techniques led to the conclusion that the material was most likely to be an aluminium carbide, such as Al₄C₃, formed during the deposition of the insulator, AlO, and carbon from the resist used during the etching stage.



Magnetism 2018

This new technique, in combination with previously established techniques, has shown to be effective in identifying the origin of faults that arise during the production of batches of MTJ nanopillars. This information has been utilised to further optimise this production process, showing great potential for it to provide quality assurance in a device production line.

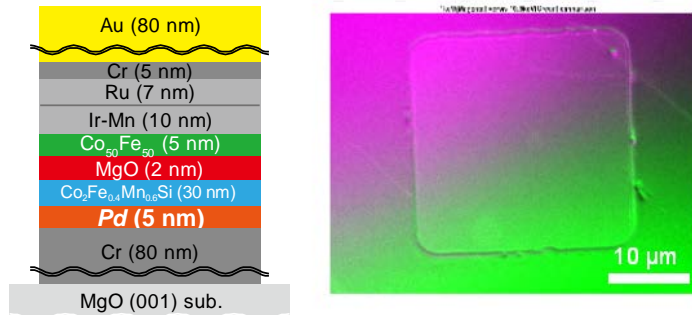


Figure 1: (a) The general structure of the pillar (b) A subtraction image highlighting the edge defects found using [1].

We thank JEOL UK for their support and acknowledge the funded provided through EPSRC EP/M02458X/1 and the JSPS Core-to-Core grant.

- [1] A. Hirohata et al., Nat. Commun. 7, 12701 (2016)
- [2] D. Drouin, et al., Scanning, 29, 92-101 (2007).

Superconducting spintronics – active role of spin-orbit coupling and dynamics of triplet Josephson junctions

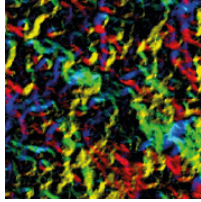
N Banerjee

Loughborough University, UK

The existence of unconventional triplet superconductivity in artificial superconductor/ferromagnet interfaces has been demonstrated recently in a number of experiments [1]. These equal-spin triplet Cooper pairs are immune to the pair breaking exchange field in a ferromagnet and can propagate over length scales which are significantly longer than the singlet pair coherence lengths. These dissipationless triplet currents carry a net spin creating a bridge between superconductivity and conventional spintronics.

Recently, we discovered an entirely new connection between triplet superconductivity and spin-orbit coupling [2]. In this talk, I will summarise our results where we observe non-monotonic dependence of the superconducting transition temperature with applied magnetic fields in heterostructures of Pt/Co/Pt proximity coupled to a conventional spin-singlet superconductor (Nb). The results are explained on the basis of spin-orbit coupling actively controlling the generation of triplet Cooper pairs in the system. We will also discuss some recent results on the electrodynamics of triplet Josephson junctions.

- [1] J. Linder and J. W. A. Robinson, *Nature Physics* 11, 307-315 (2015).
- [2] N. Banerjee *et al.* (arXiv:1709.03504, 2017).



Magnetism 2018

The development of the hydrogen ductilisation process (HyDP) for NdFeB-type alloys

O P Brooks, A Walton, W Zhou and I R Harris

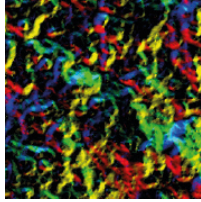
University of Birmingham, UK

In the past two decades the use of neodymium-iron-boron permanent magnets has increased substantially due to their application in emerging green technologies, such as electric vehicles, wind turbine generators, and in computer hard disc drives [1].

Generally, the magnets used in these applications are produced through powder metallurgy processing routes which require multiple complicated and costly steps [3]. Due to the brittle nature of the NdFeB alloy a final machining step is required to produce the final shape, this is energy intensive, time consuming and produces significant quantities of waste material which are not readily recycled.

The work outlined here demonstrates a new, exciting processing technique, which employs a high temperature solid hydrogenation disproportionation reaction[5]. This transforms the brittle $\text{Nd}_2\text{Fe}_{14}\text{B}$ intermetallic matrix phase into a ductile mixture of αFe , Fe_2B and NdH_2 . In this condition the material can be readily shaped, with little to no material loss, and the hydrogen can subsequently be removed, recombining the mixture to form a now submicron grain sized $\text{Nd}_2\text{Fe}_{14}\text{B}$ phase. Furthermore, it can be shown that under appropriate conditions it is possible to produce a useful degree of anisotropy in the recombined material.

- [1] O. Gutfleisch, M. A. Willard, E. Brück, C. H. Chen, S. G. Sankar and J. P. Liu, "Magnetic Materials and Devices for the 21st Century: Stronger, Lighter, and More Energy Efficient," *Journal of Advanced Materials*, vol. 23, no. 7, pp. 821-842, 2011.
- [2] Y. Yang, A. Walton, R. Sheridan, K. Güth, R. Gauß, O. Gutfleisch, M. Buchert, B.-M. Steenari, T. Van Gerven, P. T. Jones and K. Binnemans, "REE Recovery from End-of-Life NdFeB Permanent Magnet Scrap: A Critical Review," *Journal of Sustainable Metallurgy*, vol. 3, pp. 122-149, 2017.
- [3] I. Harris, C. Noble and T. Bailey, "The hydrogen decrepitation of an Nd₁₅Fe₇₇B₈ magnetic alloy," *Journal of the Less Common Metals*, vol. 106, no. 1, pp. 1-4, 1985.
- [4] I. Harris and P. McGuiness, "Hydrogen: its use in the processing of NdFeB-type magnets," *Journal of the Less Common Metals*, vol. 172, no. 0022-5088, pp. 1273 - 1284, 1991.
- [5] O. Gutfleisch and I. R. Harris, "In-situ electrical resistivity measurements: study of magnetic and phase transitions and solid-HDDR processes in Nd-Fe-B-type alloys," *Journal of material science*, vol. 30, pp. 1397-1404, 1995.



Magnetism 2018

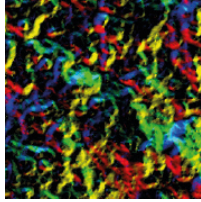
Recycling of SmCo_5 magnets by HD process

A Eldosouky and I Škulj

Magneti, d.d, Slovenia

Hydrogen decrepitation (HD) is a size reduction technique, where the material reacts with hydrogen gas and disintegrates to lower particle sizes. The process is well known for the preparation and recycling of $\text{NdFeB}^{1,2}$. In this study, HD is applied for the recycling of SmCo_5 sintered magnets at low hydrogen pressure, lower than 9.5 bar. The magnets for recycling were collected out of production lines as they do not meet the shape specifications. The magnets were decrepitated in a rotating instrument. After decrepitation, the powder was milled in a jet mill with nitrogen atmosphere to a particles size lower than 20 μm . Sintered recycled magnets were prepared from the milled powder using the isostatic pressing route. The magnetic properties of the recycled magnets sowed to be higher than the original magnet. It was shown that the remanence and maximum energy product of the recycled magnet are 0.94 T and 171.1 kJ/m^3 , respectively, in comparison to 0.91 T and 156.8 kJ/m^3 , respectively for the original magnet before recycling. The microstructure and the XRD of the original magnet, the decrepitated powder and the recycled magnet were studied in order understand the reason for the increase in the magnetic properties after recycling.

- [1] McGuinness, P. The Study of NdFeB hydrides and their application to the production of permanent magnets. *University of Birmingham*, (1989).
- [2] Walton, A., Han Yi, Rowson, N. A., Speight, J. D., Mann, V. S. J., Sheriden, R. S., Bradshaw, A., Harris, I. R. & Williams, A. J. The Use of Hydrogen to Separate and Recycle Neodymium-Iron-Boron-type Magnets from Electronic Waste. *J. Clean. Prod.* 104, 236-241 (2015).



Magnetism 2018

Posters

P:01 Rapid fabrication of magnetic microstructures by laser direct writing (LDW)

A Alasadi, F Claeysens and D A Allwood

University of Sheffield, UK

1-D and 2-D magnetic microstructures have been fabricated from thin films using laser direct writing (LDW) in a single step and without any chemical processing.

90nm thick films of permalloy ($\text{Ni}_{81}\text{Fe}_{19}$) were patterned by laser ablation using a pulsed laser of 532 nm wavelength and 800 ps pulse length focused to a $1.85\mu\text{m}$ diameter spot to achieve a fluence of 350 mJ.cm^{-2} . A sample scan-speed of 7.5mm/s and laser pulse repetition rate of 6kHz created 30% overlap between successive laser pulses on the sample.

Magnetic wires with widths 650 nm - $6.7 \mu\text{m}$ were patterned using single-axis sample scans and showed coercivity reducing across this range from 47 Oe to 10 Oe. Attempts to fabricate narrower wires (to 150 nm width) resulted in discontinuities in the wires and a decrease in coercivity. Arrays of squares, rectangles and parallelograms were produced using sample scans along two axes and showed geometry and size-dependent hysteresis properties.

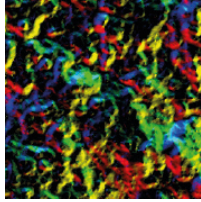
The time for LDW fabrication is increased by scan direction reversal between successive exposure times but is still extremely rapid. For example, the exposure parameters above allowed 75 magnetic wires of 4.0mm length to be fabricated in 85s at an effective fabrication rate of 3.5 mm.s^{-1} .

P:02 Effect of growth parameters on Magnetostrictive Amorphous thin films

Q Aldulaim^{1,2}, N A Morley¹, T Hayward¹ and T Thomson³

¹University of Sheffield, UK, ²University of Anbar, Iraq, ³The University of Manchester, UK

Magnetostrictive amorphous thin films are being developed for a wide range of MEMS applications, including strain sensors and magnetostrictive actuators [1]. To achieve the sensitivities required for these applications the magnetic films used have to possess a large magnetostriction constant ($>50\text{ppm}$) and a small anisotropy field ($<10\text{kA/m}$). The work presented here investigates magnetostrictive amorphous thin films, including FeSiB and FeGaSiB films, to achieve these required parameters. A co-sputtering – evaporation deposition technique [2] was used to fabricate the films, which allows control of the Ga percentage within the films. The films were grown on the silicon (100) substrates. The effect of changing the growth parameters including the sputtering power, the chamber pressure and the Ga evaporation rate were studied to determine their influence on the structural, magnetic and magnetostriction properties of these amorphous films. While the magnetic properties (coercive and anisotropy field and magnetostriction constant) were measured on a Magneto-optical Kerr effect (MOKE) magnetometer. A VSM was used to measure the magnetisation of films. A bending tool was used to strain the films via the Villari Effect [3], and thus the magnetostriction constant, λ_s was determined. The magnetostriction result showed that increasing the sputtering power from 20W to 60W increased the magnetostriction constant for FeSiB films from 4 ppm to 20 ppm and decreased it for FeGaSiB film from 14 ppm to 5ppm. While increasing the power, changed the magnetisation of FeGaSiB film from 850 kA/m to 1200 kA/m. The magnetostriction constant decreased from 17.5 ppm to 10 ppm with increasing Ga rate (Ga concentration in the FeGa films) and decreased from 11.4 ppm to 4.9 ppm for increasing the chamber pressure. Thus it was possible to determine the optimum fabrication parameters for FeGaSiB films to achieve the required soft magnetic properties.



Magnetism 2018

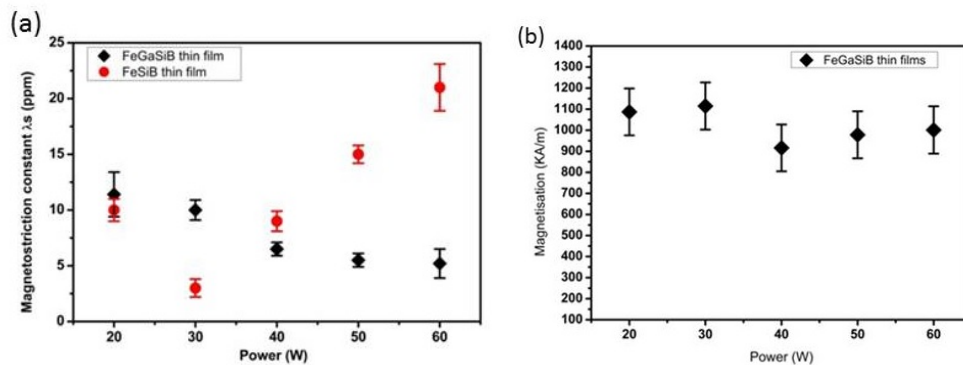


Figure (a) Magnetostriction constant of FeSiB and FeGaSiB films (b) Magnetisation of FeGaSiB via sputtering power.

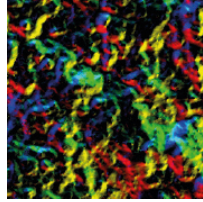
- [1] M.R.J. Gibbs, R. Watts, W.J. Karl, A.L. Powell, and R.B. Yates, *Sensors Actuators A*, 59, 229, 1997.
- [2] N. A. Morley, S. L. Yeh, S. Rigby, A. Javed, and M. R.J. Gibbs, *Journal of Vacuum Science and Technology A*, 26, 581, 2008.
- [3] N. A. Morley, A. Javed, M. R.J. Gibbs, *Journal of Applied Physics*, 105, 07A912, 2009.

P:03 Effect of post annealing on the magnetic properties of FeN with RF-sputtered amorphous carbon thin films

S Alghamdi, F AL-Mamari, T Moorsom, M Ali, B Hickey and O Céspedes

University of Leeds, UK

Recent theoretical and experimental developments in the interaction between carbon-based molecules and ferromagnetic metals have led to novel studies that are significant for carbon-based spintronics [1] [2]. Interdiffusion between two materials after heat treatment has attracted attention due to its influence on tuning the magnetic properties [3]. The diffusion between iron nitride (FeN) and RF sputtered amorphous carbon (a-C) have been extensively investigated in this work. FeN shows a variety of phases of crystal structures due to different N_2 contents [4]. We are interested in the structural properties of FeN / a-C where small changes at the interface due to different FeN phases could have significant effect on the magnetic properties of FeN/a-C before and after annealing. We have made progress in manipulating this interfacial coupling and tuning the anisotropy and coercivity (H_c) so that magnetic hardening is possible after annealing. The studied samples are films of FeN grown at different thickness and kept in contact with RF sputtered amorphous carbon (a-C). The FeN layers were grown with different percentage of N_2 (10% and 15%) but Ar flow was fixed at a constant flow. The possibility of tuning the magnetisation (M_s) and H_c at different Ar/ N_2 gas flow has been explored at these percentage of N_2 flow. The saturation magnetisation (M_s) has shown dependence on the FeN film thicknesses. The thickness dependence shows different behaviour as the N_2 fraction in a mixture of N_2 / Ar gas flow has also varied. M_s of about 1600 emu/cc and 1000 emu/cc were obtained for 10% and 15% of N_2 , respectively (Fig1.a,c). This value is slightly lower than that of pure Fe thin film (1700 emu/cc). This changes in both M_s and H_c behaviour could be due to hybridisation which can generate interfacial spin polarisation and change the magnetic properties of FeN/a-C. The effect of hybridisation could vary with the nitrogen content in the films which forms different phases of FeN hence different interfaces as observed at 10% of N_2 interface. However, annealing the films up to 500 °C give rise to rapid increase in the hardness H_c and M_s by a factor 5 in the FeN thickness range 2 and 11 nm (Fig1.b). The same effect is still observed with further annealing to 550 °C. This rapid increase in the hardness could be due to the formation of iron carbide by diffusion of carbon in iron grain boundaries as proved by TEM and XRR techniques. Samples grown at



Magnetism 2018

15% of the nitrogen are examined after annealing and the results exhibited smaller H_c dependence (~ 3 times) than that of 10% of N_2 (Fig1.d). The findings highlight the influence of annealing on the formation iron carbide by interdiffusion and chemical mixing of carbon and its effect in manipulating the hardness of the carbon base materials.

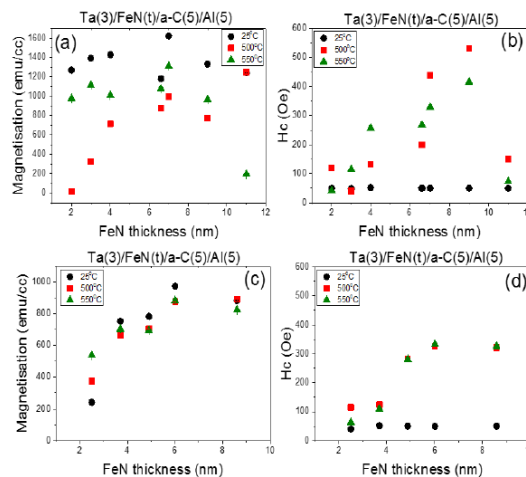


Figure 1: Ms and HC as a function of FeN thickness measured at 300 K For un-annealed and annealed films grown at (a,b) 10% (c,d) 15% of N_2 fraction.

- [1] Moorsom, T. et al. Spin-polarized electron transfer in ferromagnet/C60 interfaces. *Physics review B*. 2014, 90, pp. 125311(1-6).
- [2] Dediu, V. A. et al. Spin routes in organic semiconductors. *Nature materials*. 2009, 8, pp. 707-716.
- [3] Zotov, N. et al. Interdiffusion in Fe-Pt multilayers. *Journal of applied physics*. 2006, 100, p.073517.
- [4] Naganuma, H. et al. Magnetic and electrical properties of iron nitride films containing both amorphous matrices and nanocrystalline grains. *Science and Technology of Advanced Materials*. 2004, 5, pp.101-106.

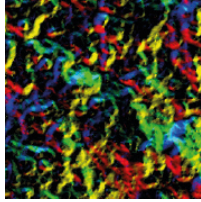
P:04 Magnetic domains in Pt/CoFeB/Ir multilayers grown on piezoelectric substrates

K Alshammari, P M Shepley and T A Moore

University of Leeds, UK

At the interface of a 5d metal and a thin film 3d ferromagnet such as Pt/Co, the interfacial Dzyaloshinskii-Moriya interaction (DMI) leads to domain walls with a defined chirality and skyrmion-like domains in the ferromagnet that are promising for low power magnetic memory devices [1]. Furthermore, the strain control of thin film magnetism promises power-reduction in nanomagnetic devices [2]. Recently, skyrmion bubbles have been imaged and their magnetotransport signature recorded in a Pt/Co/Ir multilayer dot [3,4], and we have measured the effect of out-of-plane strain on domain walls in Pt/Co thin films [5,6]. In this work we seek to enhance the sensitivity of magnetic properties to strain by depositing Pt/CoFeB/Ir thin films directly onto piezoelectric substrates.

Ta(5)/[Pt(2.3)/Co₆₈Fe₂₂B₁₀(0.7)/Ir(0.5)]_n/Pt(2.3) multilayers (thickness in nm) were deposited by dc magnetron sputtering onto polished PMN-PT(001) substrates. Before deposition, the substrates are poled in 1 kV and rms roughness on the order of 2 nm was measured by atomic force microscopy. The difference in surface roughness between PMN-PT and standard oxidised Si substrates is apparent in the magnetic



Magnetism 2018

properties of the multilayers on top, measured by magneto-optic Kerr effect hysteresis loops (Fig. 1). While both samples exhibit a dominant perpendicular magnetic anisotropy, the coercive field of the multilayer on PMN-PT is about ten times larger than the identical film on Si. Together with the more gradual approach to saturation, this suggests that domain wall pinning plays a greater role in the film on PMN-PT and that the anisotropy distribution is broader. In magnetic images captured by wide field Kerr microscopy, while the film on Si exhibits large 100 μm -scale domains whose walls meet to create an extended network of 360° walls that are stable because of their homochirality, the film on PMN-PT has smaller domains, width $<5 \mu\text{m}$, that grow dendritically. Determination of the DMI has been shown to be possible by modelling such domain patterns [7,8].

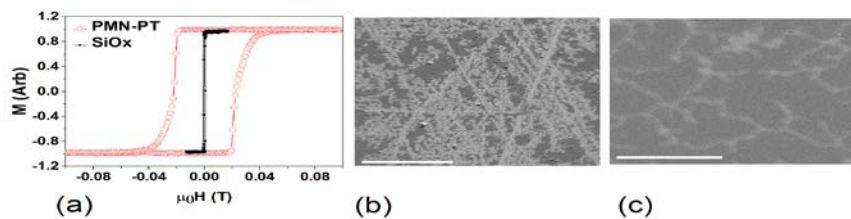


Figure 1. (a) Hysteresis loops of Ta(5)/Pt(2.3)/CoFeB(0.7)/Ir(0.5)/Pt(2.3) film grown on Si (inner) and on PMN-PT(001) (outer). Kerr microscope image of magnetic domains in the film grown on PMN-PT(001) (b) and on Si (c). Scale bar: 100 μm .

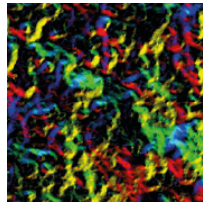
- [1] A. Fert et al., *Nat. Nanotechnol.* 8, 15(2013).
- [2] K. L. Wang et al., *IEEE Proc.* 104, 1974 (2016).
- [3] K. Zeissler et al., *Sci. Rep.* 7, 15125 (2017).
- [4] K. Zeissler et al., arXiv:1706.06024.
- [5] P.M. Shepley et al., *Sci. Rep.* 5, 7921 (2015).
- [6] P.M. Shepley et al., arXiv:1703.05749.
- [7] M.J. Benitez et al., *Nat. Commun.* 6, 8957 (2015).
- [8] I. Lemesh et al., *Phys. Rev. B* 95, 174423 (2017).

P:05 Improving the magnetic and dynamic properties of Yttrium Iron Garnet

M Alyami, E Darwin, M Ali, O Cespedes and B J Hickey

University of Leeds, UK

We want to explore potential improvements in the growth of Yttrium Iron Garnet (YIG). YIG thin films are deposited by radio frequency (RF) magnetron sputtering and open air annealing at 850 $^\circ\text{C}$. We have recently shown [1] that YIG grown on Gadolinium Gallium Garnet (GGG), the favoured substrate for most, suffers from the problem of Gd – Y co-diffusion as part of the annealing process. From chemical analyses of cross-sectional TEM measurements, we have shown that this behavior is vacancy driven and we suspect that this could be due to oxygen deficiency. We have varied the oxygen pressure during sputtering to study the possible effects of reducing vacancies. At room temperature, the inter-diffused layer is non-magnetic i.e. a dead layer, as temperature is reduced, the Gd-based layer becomes magnetic and orders anti-parallel to the YIG – these effects are detected by SQUID magnetometry as a function of temperature. Thin films were grown on two different substrates: and Yttrium Aluminum Garnet (YAG) and GGG and subjected to an annealing process. Figure 1 shows that we have grown high quality thin films of YIG by reducing the vacancies. Figure 2 shows that the temperature dependence of the saturation magnetisation for different percentages of oxygen. This figure demonstrates that the thickness of the inter-diffused layer can be changed with changing the O/Ar %, therefore greatly improving the magnetic properties of thin film RF sputtering YIG.



Magnetism 2018

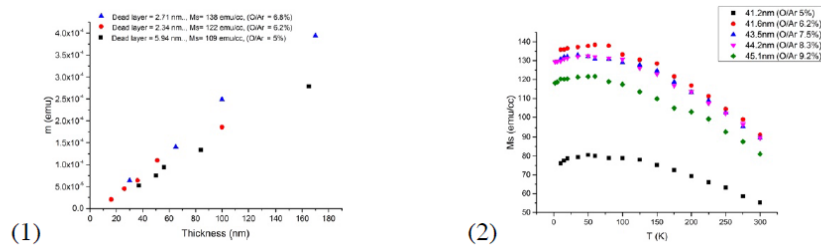


(Figure 1) The magnetic moment as a function of thickness at room temperature.

(Figure 2) SQUID magnetometry measurement of YIG magnetisation at different temperatures.

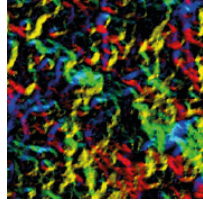
- [1] Mitra, A., Cespedes, O., Ramasse, Q., Ali, M., Marmion, S., Ward, M., Brydson, R.M.D., Kinane, C.J., Cooper, J.F.K., Langridge, S. and Hickey, B.J., 2017. Interfacial Origin of the Magnetisation Suppression of Thin Film Yttrium Iron Garnet. *Scientific reports*, 7(1), p.11774.

P:06 Effect of growth conditions on the soft magnetostrictive properties of thin Fe-Co-Cr films

S Baco¹, Q A Abbas¹, Z Leong¹, T J Hayward¹, N A Morley¹ and T Thomson²

¹University of Sheffield, UK, ²The University of Manchester, UK

Soft magnetic materials which have low anisotropy and coercive fields, large magnetostriction constant and saturation magnetisation are required in microelectromechanical systems (MEMs) for sensor and actuator devices. One material example with these properties is FeCo, however this material can also have a large coercive ($H_c > 10 \text{ kA/m}$) in particular for as deposited films. Therefore in this paper we present the magnetostrictive properties of FeCo films alloyed with Cr which show reduction in the coercive and anisotropy fields. Since the magnetic properties are also influenced by microstructure and the growth parameters, we investigate the magnetostrictive properties of FeCoCr film as a function of film thickness (56 nm to 165 nm) and sputtering power (75 W to 150 W) deposited by RF Sputtering. The composition, microstructure and magnetic properties were investigated by Scanning Electron Microscope (SEM-EDX), Atomic Force Microscopy (AFM), X-Ray Diffraction (XRD) and High-Field MOKE magnetometry respectively, while the Villari technique was used for the magnetostriction measurement. XRD measurement determined that the thinnest film (56 nm) had an amorphous structure, while the XRD peaks intensity improved as the thickness increased. For the films grown at higher powers (125 W to 150 W), the structure changed to polycrystalline with two sharp peaks observed corresponding to FeCoCr bcc (110) and bcc (211). MOKE measurement showed all FeCoCr films thicknesses exhibited weak uniaxial anisotropy. It was found that soft magnetic properties had been achieved by the addition of Cr, with the coercive fields being reduced by factor 6 compared to a 100 nm FeCo film grown with the same sputtering parameter (Fig. 1c). For the 100 nm films grown at various power the grain size, anisotropy and coercive fields increased rapidly at higher power, 150 W (Fig. 1b). The effective magnetostriction constants, λ_{eff} of FeCoCr films as a function of thickness did not significantly change with thickness. However magnetostriction constant with respect to sputtering power showed the films grown at the lowest power (75 W) had $\lambda_{\text{eff}} \sim 28 \text{ ppm}$ which was nearly five times higher than the film grown at the highest power 150 W. The soft magnetic properties have been achieved by Cr addition into FeCo with low coercive ($< 2 \text{ kA/m}$) and anisotropy fields (12 kA/m), while maintaining high magnetostriction constant for films grown for thicknesses between 100 and 125 nm and at a 75 W power.



Magnetism 2018

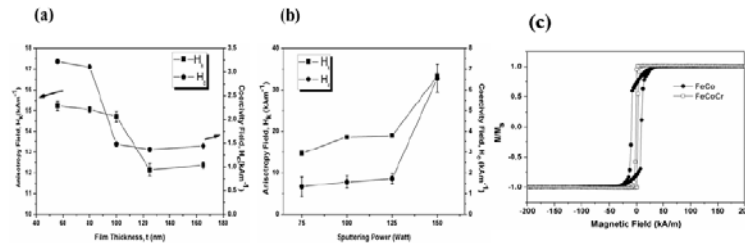


Figure 1: (a) Coercive and anisotropy fields at various film thickness and (b) coercive and anisotropy fields as a function of sputtering power (c) normalised magnetisation loops of FeCo and FeCoCr.

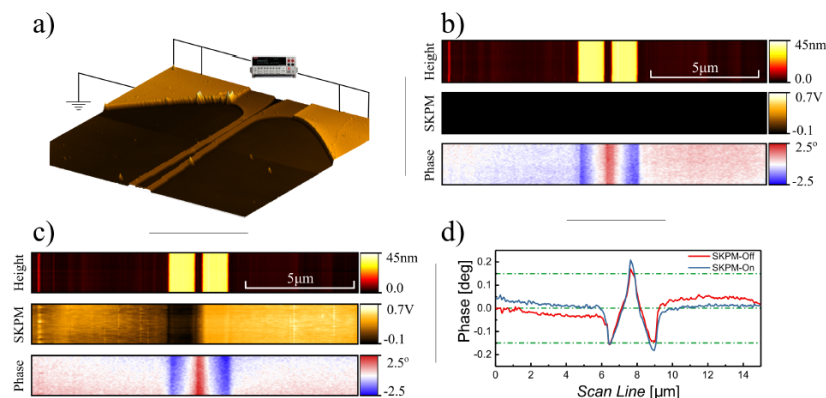
P:07 Calibrated MFM: electrostatic compensation of μ -coils.

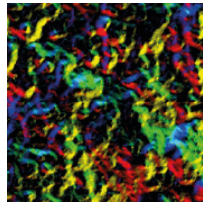
C Barton¹, R Puttock^{1,2}, H Corte-León¹, M Gerken³, A Manzin⁴, V Neu⁵, H W Schumacher² and O Kazakova¹

¹National Physical Laboratory, UK, ²Royal Holloway University of London, UK, ³Physikalisch-Technische Bundesanstalt, Germany, ⁴Istituto Nazionale di Ricerca Metrologica, Italy, ⁵Leibniz-Institut für Festkörper, Germany

Magnetic force microscopy (MFM) is used to detect and visualise the stray magnetic fields that emanate from the surface of magnetic materials [1]. Typically, MFM is used qualitatively to gain physical insight into the morphology of magnetic domains. However, there are established methods that can be employed to make quantitative measurements. Calibration can be obtained by using current carrying microstructures, which are used to generate a well-defined field profile [2,3].

In this work we explore the use of current-carrying coils of micrometric dimension Fig a). In particular, we focus on the role of electrostatic compensation on the measured values of the dipole contribution to the magnetic probe, Fig b-c). The electrical compensation is achieved by applying an a.c. signal between the probe and sample. A lock-in technique is used to measure resulting side bands and a feedback loop is employed to keep the magnitude of the side bands to zero via a d.c. voltage. This d.c. signal is then applied during the lift pass, where the MFM response is recorded, in order to reduce electrostatic force gradients acting on the tip, Fig d). Least-squares optimisation is the used to compare the electrostatic compensation on the extracted magnetic dipole moment.





Magnetism 2018

Figure 1: Calibrated MFM: a) μ -coil topography with the contact pads and electrical configuration including the grounding scheme used in this work (scan-size $50\mu\text{m}$); b) MFM scan (bottom) without electrostatic compensation; c) MFM scan (bottom) with electrostatic compensation demonstrating reduced contrast in the region of the the coil and also the charged substrate around the coil. The sub figures in (b-c) are topography, SKPM and phase signals respectively; d) an example of the extracted average line profiles taken from the MFM data with/without any electrostatic compensation.

- [1] E. Meyer, *et al.*, *Scanning probe microscopy (Springer)*, 97 (2004).
- [2] J. Lahou, *et al.*, *J. Appl. Phys.*, 86, 3410 (1999).
- [3] Th. Kebe and A. Carl, *J. Appl. Phys.*, 95, 775 (2004).

P:08 Investigation of sputtering conditions on the properties of Ta/CoFeB/MgO stacks

C Bull, P Nutter and T Thomson

The University of Manchester, UK

Spin-transfer-torque magnetoresistive random access memory (STT-MRAM) is a non-volatile technology with excellent scalability and fast read/write speed. However, STT-MRAM faces challenges for future development such as reducing the critical switching current whilst maintaining thermal stability [1]. The use of graded anisotropy films, based on the concept of exchange spring media [2], has been shown to switch at a reduced field whilst remaining thermally stable [3]. We plan to investigate the benefit of including a graded free layer in the magnetic tunnel junction (MTJ) with a view to reducing the required STT switching current of the structure. To fabricate structures, optimisation of individual layers is essential. High quality tunnel barriers are critical to achieving large tunnelling magnetoresistance ratios (TMR) [4], therefore initial work has focussed on precisely tailoring the growth parameters of thin MgO layers created by sputtering. Here, we have investigated the effects of deposition power and annealing temperature of MgO on the properties of Ta(3nm)/Co₂₀Fe₆₀B₂₀(5nm)/MgO(t) stacks (Fig. 1) where the MgO thickness (t) was varied from 1.0-3.0nm. As a smooth MgO/CoFeB interface is essential for large effective anisotropy energy [5], the surface roughness of the MgO layer was investigated. We have used Kelvin Probe Force Microscopy (KPFM) to characterise electron transport and pinhole density as a function of thickness. Following optimisation of the MgO layer, the fabrication of bottom-electrode/Ta(3nm)/Co₂₀Fe₆₀B₂₀(5nm)/MgO(t)/Co₂₀Fe₆₀B₂₀(5nm)/top-electrode MTJs will allow the study of TMR dependence on MgO sputtering conditions. This work will enable the later fabrication of MTJs with a graded anisotropy free layer.

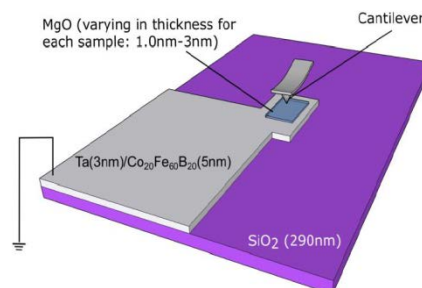
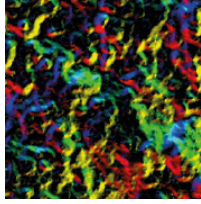


Figure 1: Ta(3nm)/Co₂₀Fe₆₀B₂₀(5nm)/MgO(t) stacks for KPFM measurements. Stacks were fabricated using optical lithography and RF magnetron sputtering.

- [1] D. Apalkov *et al.* *Proc. IEEE* 104 1796-1830 (2016).
- [2] D. Suess, *Appl. Phys. Lett.* 89 113105 (2006).



Magnetism 2018

- [3] C. Zha *et al. Appl. Phys. Lett.* 97 182504 (2010).
- [4] S. Ikeda *et al. Appl. Phys. Lett.* 93 082508 (2008).
- [5] A. Kaidatzis *et al. J. Phys.: Conf. Ser.* 903 012019 (2017).

P:09 Strain control of the magnetic properties of FeRh thin-film heterostructures for data storage applications

C Bull¹, C Barton¹, W J Griggs¹, A Caruana², C J Kinane², P W Nutter¹ and T Thomson¹

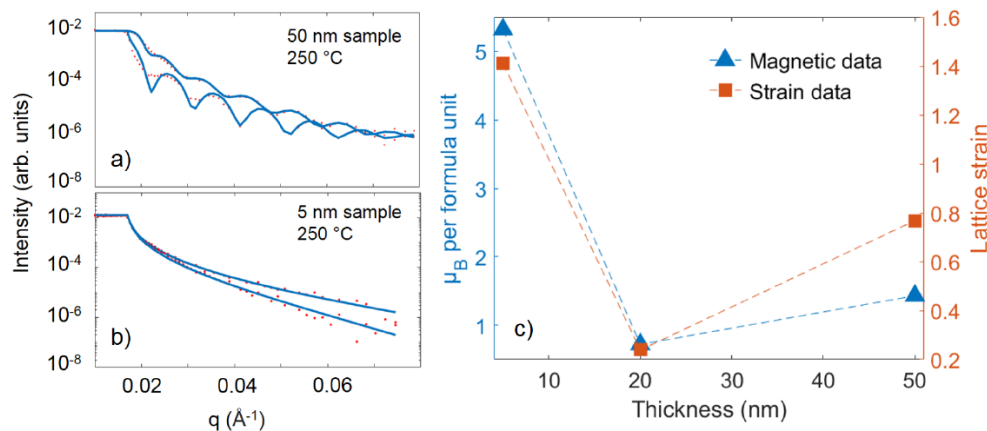
¹The University of Manchester, UK, ²Rutherford Appleton Laboratory, UK

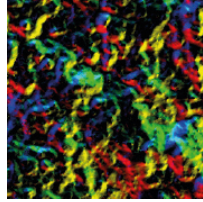
Equiatomic FeRh in thin-film form has attracted increasing research interest over the last few years, owing to the fact that it undergoes a first-order phase transition from an antiferromagnetic (AF) to a ferromagnetic (FM) ordering at $\sim 350\text{K}$. Such magnetic switchability at modestly elevated temperature underpins its candidacy as a material for several novel applications, such as heat assisted magnetic recording and antiferromagnetic memories.

The change in magnetic order at the FeRh phase transition is accompanied by a $\sim 1\%$ increase in the unit cell volume, and previous work has shown that the onset and width of the transition are highly dependent on lattice strain [1,2]. Thus, control of stress fields in FeRh provides a means by which the transition may be tuned. Hence, in order for viable implementations of strain-induced switching of FeRh thin films to be realised, a comprehensive understanding of the various mechanisms through which strain may be induced is essential. One such mechanism is epitaxial strain from the substrate.

Here we report polarised neutron reflectivity (PNR) measurements performed on FeRh films of varying thicknesses (5nm, 20nm, 50nm). These data have allowed us to develop a model that identifies the role of island formation, an important means by which strain may be mediated, on the magnetism in FeRh with depth-resolution.

In fitting scattering-length-density (SLD) profiles to the PNR datasets (as shown in Figures 1(a) and 1(b), for example), comparisons may be drawn between the magnetic properties of each sample and the FeRh lattice strain (see Figure 1(c)). Strain values were obtained from x-ray diffraction (XRD) measurements. The experimental findings are discussed in the context of each sample's surface topography, which was measured via atomic force microscopy.





Magnetism 2018

Figure 1: (a) and (b) show fitted PNR data from the 5 nm and 50 nm samples respectively, while in (c) the variation in magnetisation (expressed in Bohr magnetons per FeRh formula unit) and lattice strain with film thickness is shown.

[1] C. W. Barton *et al.*, Sci. Rep., 7, 44397, 2016.

[2] T. A. Ostler *et al.*, Phys. Rev. B, 95, 064415, 2017.

P:10 Realization of ground state in artificial kagome spin ice via topological defect-driven magnetic writing

J C Gartside¹, D M Arroo¹, D M Burn², A V Moskalenko¹, V L Bemmer¹, L F Cohen¹ and W R Branford¹

¹Imperial College London, UK, ²Diamond Light Source, UK

Arrays of non-interacting nanomagnets are widespread in data storage and processing. As current technologies approach fundamental limits on size and thermal stability, enhancing functionality through embracing the strong interactions present at high array densities becomes attractive.

In this respect, artificial spin ices¹⁻⁴ are geometrically frustrated magnetic metamaterials that offer vast untapped potential due to their unique microstate landscapes, with intriguing prospects in applications from reconfigurable logic to magnonic devices⁶ or hardware neural networks⁷.

However, progress in such systems is impeded by the inability to access more than a fraction of the total microstate space. To address this, we have developed a novel scanning probe technique, Topological Defect-Driven Magnetic Writing (TMW)⁵, which provides full access to all possible microstates in artificial spin ices and related arrays of nanomagnets.

We employ TMW to create previously elusive magnetic configurations such as the spin-crystal ground state⁸ of artificial kagome dipolar spin ices and high-energy, low-entropy ‘monopole-chain’ states that exhibit negative effective temperatures.

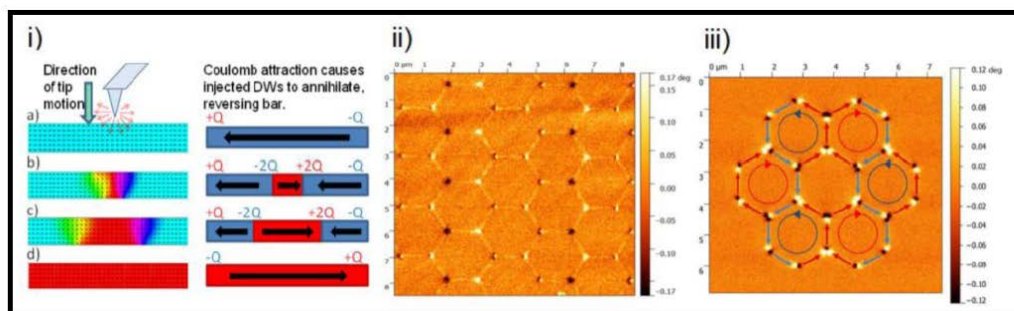


Figure 1:

i) Micromagnetic simulation and accompanying schematic of writing process dynamics showing positions of magnetic charges ($\pm Q$).

ii) MFM image of ‘ladder’ and ‘zigzag’ monopole-defect chain states written at RT on a NiFe ASI lattice.

iii) MFM image of the spin-crystal chiral ground state of kagome ASI written at RT on a NiFe ASI rosette.

[1] Wang, RF, et al. *Nature* 439.7074 (2006): 303-306.

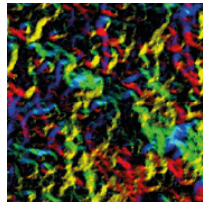
[2] Branford, W. R., et al. *Science* 335.6076 (2012): 1597-1600.

[3] Zhang, Sheng, et al. *Nature* 500.7464 (2013): 553-557.

[4] Perrin, Yann, et al. *Nature* 540.7633 (2016): 410-413.

[5] Gartside, J. C., et al. *Nature Nanotechnology* 13 (2017): 53-58.

[6] Heyderman, L. J., and R. L. Stamps. *J. Phys.: Cond. Matt.* 25.36 (2013): 363201.



Magnetism 2018

- [7] Wang, Yong-Lei, et al. *Science* 352.6288 (2016): 962-966.
- [8] Anghinolfi, L., et al. *Nat. Comms.* 6 (2015).

P:11 Dynamic emergent behaviour of domain walls in interconnected nanoring arrays

R W S Dawidek¹, T J Hayward¹, T J Broomhall¹, M Negoita¹, M Mamoori¹, P W Fry¹, J Cooper², N-J Steinke², M Y Im³ and D A Allwood¹

¹University of Sheffield, UK, ²Large Scale Structures, UK, ³Lawrence Berkeley National Lab, USA

Emergence in artificial nanomagnetic structures is well explored in artificial spin ice systems. The emergent magnetic configurations of these systems are usually achieved following annealing or change of geometry^{1,2}, and thus are relatively static. We show here how the domain wall (DW) population of an array of interconnected ferromagnetic nanorings shows emergent properties and can be dynamically tuned with external magnetic field.

We have studied 2×2 cm patterns of interconnected Ni₈₀Fe₂₀ rings of 400 nm wire width, 20 nm thickness and 4 μm outer-ring diameter, each overlapping its closest neighbours in a square array by 200 nm.

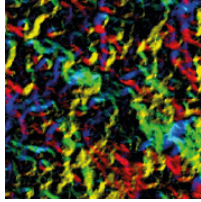
The most-preferred magnetic configurations of ferromagnetic nanorings are continuous ‘vortex’ states, with no DWs, and bi-domain ‘onion’ states, with two DWs. An in-plane rotating field can move DWs around a ring and, in the interconnected ring array, into junctions where they will encounter a pinning potential. Under sufficiently high field strengths DWs pass through junctions and continue to move through the rings while under sufficiently low field strengths no walls in the ensemble are able to enter junctions. At intermediate field strengths DW passage through junctions is probabilistic and field-dependent, as we observe through magnetic transmission X-ray microscopy (M-TXM) measurements of separate single-junction structures.

Our micromagnetic modelling has showed that if a DW passing around a ring encounters the other DW from the ring due to this being pinned, the DWs annihilate and the DW population of the ensemble will decrease. Modelling also showed that a DW propagating through a junction with an adjacent ‘vortex’ ring will create two new DWs in the empty ring, increasing the DW population. Analytical modelling of DW population of ring arrays reveals an equilibrium DW population that varies non-monotonically with DW pinning probability, between no DWs and a fully saturated onion state array, and that depends upon the ring array size and configuration.

Polarised Neutron Reflectometry (PNR) and MOKE measurements were performed on the large nanoring arrays either following (PNR) or during (MOKE) application of in-plane rotating magnetic fields to equilibrate the DW population. These approaches showed good agreement with the behaviour predicted by the analytical model. Magnetic force microscopy (MFM) of these arrays allowed DW configurations to be observed directly. This confirmed the saturation state of two DWs per ring and of DW loss following application of intermediate rotating field strength.

Dynamic tuneability of emergent behaviour, as offered by interconnected nanoring arrays, could see applications in computing architectures that don’t conform to traditional Von Neumann models such as reservoir computing³.

- [1] Wang, R. F. *et al. Nature* 439, 303-306 (2006)
- [2] Gilbert, I. *et al. Nature Physics* 10, 670-675 (2014).
- [3] Soures, N. *et al IEEE Consumer Electronics Magazine* 67-73 (2017).



Magnetism 2018

P:12 Angular dependant FMR of rotational symmetry broken Artificial Kagome Spin Ice

T Dion¹, D M Arroo², K Yamanoi³, T Kiumura³, L F Cohen², H Kurebayashi¹ and W R Branford²

¹University College London, UK, ²Imperial College London, UK, ³Kyushu University, Japan

Artificial spin ice (ASI) is an arrangement of single domain nano-bars each with Ising-like behaviour. In Kagome ASI the bars form a honeycomb lattice and at each vertex a pseudo ice rule is apparent where two spins point into the vertex and one out or one spin points in and two out. It has a highly degenerate ground state which results in frustrated magnetic ordering because the ice rules cannot be simultaneously satisfied long range [1]. They have also attracted attention in the field of magnonics due to their periodicity as a potential reconfigurable magnonic crystal. Few studies [2,3] have investigated symmetry broken artificial spin ice like elements. Here we present Kagome artificial spin ice with unequal bar sizes resulting in broken rotational symmetry. Magnetic force microscopy reveal ice rules are still present in this system, but the degeneracy will be lifted because of inhomogeneous bar size, however, the focus in this case is dynamic. Micromagnetic simulations [4] predict a ferromagnetic resonance (FMR) response that is a hybridization of three ideal ASI systems which is confirmed experimentally. Soft FMR modes dependant on switching distribution [5] can be changed by applying initialisation field protocols and are also affected by the broken symmetry. ASI has been studied for its interesting thermodynamics and static properties that require homogenous bars. This study demonstrates that dynamic properties of these systems can be further tuned providing more flexibility for spintronics or open up the possibility for interesting physics.

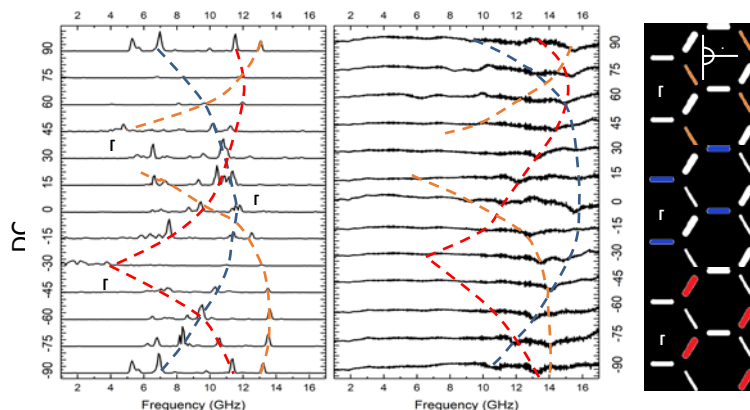
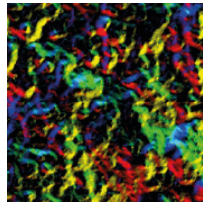


Figure 1. Angular dependent FMR. a) Micromagnetic simulation b) Experimental results. Dashed lines are modes that arising from excitation of a different bar orientation as shown in c). Maximum frequency occurs when the DC field is aligned with the long edge of the bar. The response of each of these modes is almost equivalent to a homogenous ASI of the corresponding bar size.

- [1] J. P. Morgan et. al., Nature Physics volume 7, pages 75–79 (2011)
- [2] W. Bang et. al., AIP Advances 8, 056020 (2018)
- [3] F. Montoncello et. al., Phys. Rev. B 97, 014421 (2018)
- [4] A. Vansteenkiste et. al., AIP Advances 4, 107133 (2014)
- [5] M. B. Jungfleisch et. al., Phys. Rev. B 93, 100401(R) (2016) RAPID.



Magnetism 2018

P:13 Perpendicular Anisotropy in $\text{Co}_2\text{FeAl}_{0.5}\text{Si}_{0.5}$ for CPP-GMR devices

W Frost, M Samiepour and A Hirohata

University of York, UK

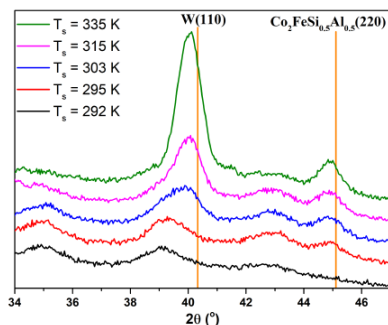
Previous work has shown that perpendicular anisotropy can be induced in Heusler alloys using a tungsten seed layer deposited at 400 °C [1]. In this work modest substrate temperatures $T_S < 75$ °C have been used prior to deposition. Samples with the structure Si/ W (10nm)/ $\text{Co}_2\text{FeAl}_{0.5}\text{Si}_{0.5}$ (12.5nm)/ W (1.2nm)/ $\text{Co}_2\text{FeAl}_{0.5}\text{Si}_{0.5}$ (2.5nm)/Ru (3nm) were used as a basic spin valve structure.

As shown in fig. 1(a) even the modest values of $T_S > 45$ °C lead to a partially crystallised tungsten seed layer, with a weakly crystallised $\text{Co}_2\text{FeAl}_{0.5}\text{Si}_{0.5}$ layer. These samples had a significant coercivity out-of-plane up to 500 Oe. The crystallisation was enhanced by T_S of 60 °C. With increasing crystallisation the tungsten reflection also relaxes towards the bulk position. The increasing crystallisation is matched by an increase in the coercivity up to 1 kOe caused by the increase in the grain size of the films from 3.5 nm to 8 nm.

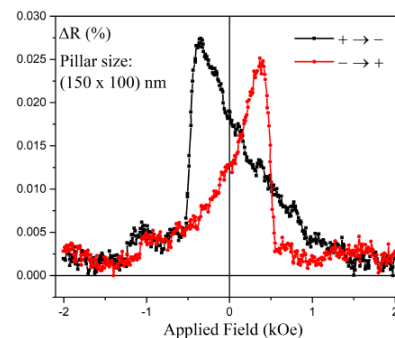
In order to improve the spin valve properties of the film a silver barrier layer was used with a 5 nm $\text{Co}_2\text{FeAl}_{0.5}\text{Si}_{0.5}$ layer giving the structure Si/ W(10nm)/ $\text{Co}_2\text{FeAl}_{0.5}\text{Si}_{0.5}$ (12.5nm)/ Ag (3nm)/ $\text{Co}_2\text{FeAl}_{0.5}\text{Si}_{0.5}$ (5nm)/ Ru (3nm) deposited at 70 °C. Figure 1(b) shows an example of a CPP-GMR measurement of a pillar with dimensions (150 x 100) nm. The observed ΔR is low at 0.03% but is sharp and distinct. The GMR ratio will be improved by further optimising layer thickness and deposition temperatures.

In this work we have shown that perpendicular anisotropy can be induced in $\text{Co}_2\text{FeAl}_{0.5}\text{Si}_{0.5}$ with modest substrate temperatures. Furthermore we have shown that the anisotropy is strongly dependent upon the crystallisation of a tungsten seed layer and the grain size. Finally, these Heusler alloys layers can be incorporated into CPP-GMR devices operated out of plane, with a small but distinct GMR.

The authors would like to acknowledge Kevin O'Grady, University of York for fruitful discussion and Seagate Technology, Derry for their support.

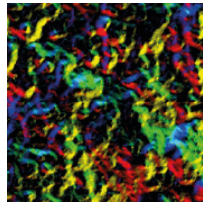


(a) $\theta/2\theta$ scans of Heusler alloy films with increasing substrate temperature.



(b) Out-of-plane GMR measurement on a (150 x 100) nm pillar based on $\text{Co}_2\text{FeAl}_{0.5}\text{Si}_{0.5}$.

- [1] W. Frost and A. Hirohata, *J. Magn. Magn. Mater.*, in press (2018).



Magnetism 2018

P:14 Atomistic modelling of granular exchange bias systems

S Jenkins, R W Chantrell and R F L Evans

University of York, UK

Exchange bias is a physical property of a magnetic material which is utilised in the read head of a hard drive. Further improvements to the read head are limited by our understanding of exchange bias and its scaling to nanoscale dimensions. The exchange bias effect occurs when a ferromagnet is coupled to an antiferromagnet (AFM), causing a shift of the magnetic hysteresis loop. The shift is caused by pinned interfacial spins from the AFM, these cause a unidirectional field pinning the exchange coupling of the FM spins at the interface[1]. The complexity of antiferromagnetic materials and their interfaces limits the applicability of simple approaches such as two sublattice antiferromagnets or micromagnetic models. To study the exchange bias effect we have developed an atomistic spin model of the antiferromagnet IrMn, considering localised atomic spin moments coupled with Heisenberg exchange reproducing key experimental results including the Néel temperature and magnetic ground state[1,2]. Here we investigate the grain size distribution and how set/unset grains effects the exchange bias in a IrMn/CoFe ferromagnet/antiferromagnet (FM/AFM) bilayer using an atomistic spin model[2].

Atomistic models are computationally expensive, therefore previously exchange bias has only been investigated in single grain structures¹. Real devices are comprised of hundreds of grains, which means the simulation must model millions of atoms. Using the parallel capability of the VAMPIRE software package it is possible to models million atom systems for nanosecond timescales. For a 50nm × 50nm × 8nm structure comprised of 6 nm grains, after field cooling and equilibration, a simulated hysteresis loop gave a large exchange bias field of 0.2T as shown in Fig. 1. We will present calculations of nanoscale exchange biased thin films including temperature effects and the role of the grain size distribution on the total exchange bias.

The effects of interfacial mixing and grain size distribution and the effective interface coupling.

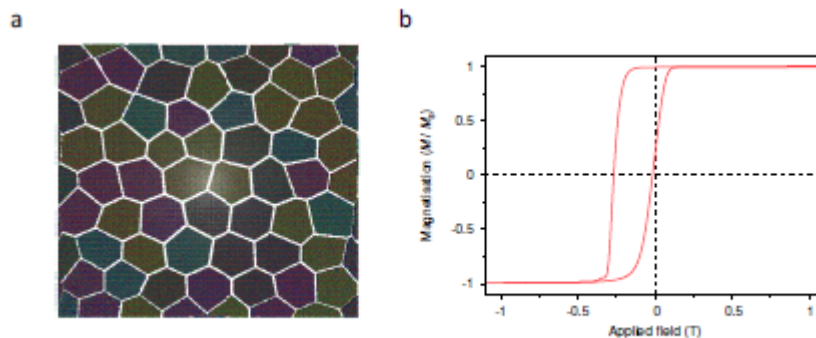
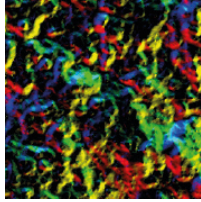


Figure 1. Multigrain structure of the IrMn layer and simulated hysteresis loop showing exchange bias.

This work used the ARCHER UK National Supercomputing Service (<http://www.archer.ac.uk>).

- [1] S. Jenkins, W. J. Fan, R. Gaina, R. Chantrell, T. Klemmer, and R.F.L. Evans. Uncovering the mystery of delocalised pinned interface spins responsible for exchange bias. URL arXiv:1610.08236.
- [2] Evans R F L, Fan W J, Chureemart P, Ostler T A, Ellis M O A, and Chantrell R W. Atomistic spin model simulations of magnetic nanomaterials. *Journal of Physics:Condensed Matter*, 26, 2014.



Magnetism 2018

P:15 Collective excitations of magnetic bubble domains in an antidot lattice

A S Laurenson¹, A I Marchenko², V N Krivoruchko², J Bertolotti¹ and V V Kruglyak¹

¹University of Exeter, UK, ²The National Academy of Sciences of Ukraine, Ukraine

Collective excitations in periodic magnetic media (magnonic crystals) are widely explored as constituents of future magnonic technologies. Their spectrum is characterised by presence of magnonic bands and band gaps, with some of the bands formed as a result of splitting of oscillatory eigenmodes of such magnetic textures as domain walls, vortices, skyrmions etc. The use of the collective excitations as information carriers may be especially promising because their dispersion depends on the static magnetic configuration and could in principle be reconfigured by changing the magnetic state of the device.

We use micromagnetic simulations to calculate the spectrum of collective excitations of magnetic bubble domains that form a honeycomb lattice within a hexagonal lattice of magnetic antidots (Fig. 1). We observe that the width of bands formed from different modes of an isolated bubble domain decreases dramatically as the mode number increases, with only the band associated with the $m=0$ “breathing” mode showing a significant group velocity. A theory based on the magneto-dipole coupling between the excited nearest neighbour bubble domains agrees qualitatively with the simulation results, suggesting the coupling as the principal mechanism of the collective mode formation at low frequencies.

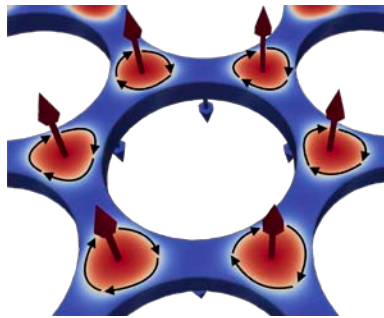
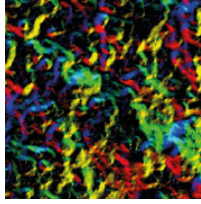


Figure 1. The bubble domain lattice. The red and blue colour intensities scale with the out-of-plane component of the magnetisation. The arrows show the magnetisation's orientations and circulation directions within domains and domain walls, respectively.

- [1] V. Kruglyak, S. O. Demokritov, and D. Grundler, "Magnonics", J. Phys. D – Appl. Phys. 43, 264001 (2010).
- [2] M. Mruczkiewicz, et al., "Collective dynamical skyrmion excitations in a magnonic crystal", Phys. Rev. B 93, 174429 (2016).
- [3] K. Wagner, et al., "Magnetic domain walls as reconfigurable spin-wave nanochannels", Nature Nanotechn. 11, 432 (2016).



Magnetism 2018

P:16 Asymmetric relaxation of magnetic frustration observed in freestanding B2-ordered FeRh thin films

J R Massey¹, R C Temple¹, T P Almeida², N A Peters¹, R Campion³, D McGrouther², S McVitie² and C H Marrows¹

¹University of Leeds, UK, ²University of Glasgow, UK, ³University of Nottingham, UK

B2-ordered FeRh undergoes a first order phase transition from an antiferromagnet to a ferromagnet upon heating through the transition temperature ~ 380 K [1]. The transition is accompanied by a change in entropy, and volume, as well as a large change in resistivity [2]. The transition temperature is known to be sensitive to the application of magnetic fields, composition, the use of dopants and application of strain [2]. The versatility and malleability of the transition, along with the easily achievable transition temperature makes FeRh an ideal candidate for use in magnetic memory devices. The coexistence of the two magnetic phases will lead to magnetic frustration in the institial region between adjacent domains, the relaxation of which could effect on the long term stability of any possible devices. Here we present magnetic relaxation measurements of freestanding B2-ordered FeRh thin films at various points within the transition. These relaxation measurements are fitted with a stretched exponential function, the results of which show changing values of the stretching exponent, b , and the relaxation times throughout the transition. The contrasting branches have distinctly different values (heating $b_{Max} \approx 0.6$ and cooling $b_{Max} \approx 2$), which suggest different regimes of relaxation dynamics as a consequence of the asymmetry in the nucleation kinetics of the domains of the minor phase on each branch.

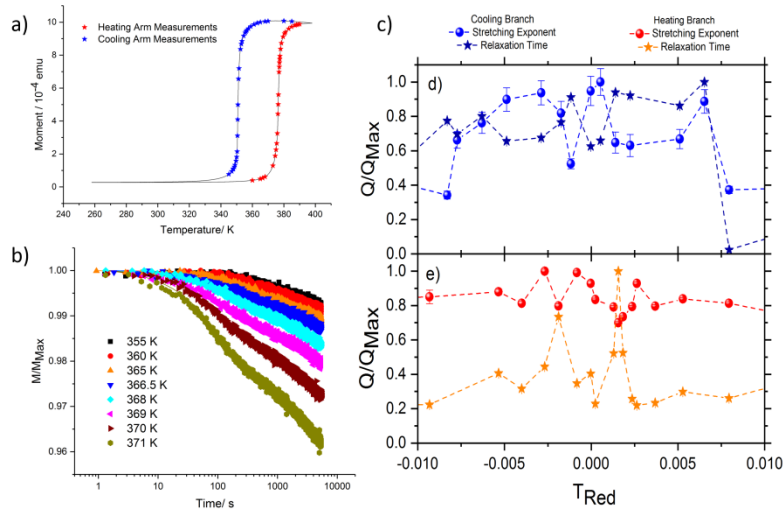
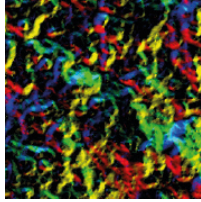


Figure 1: Panel a) shows the magnetization as a function of temperature (solid black line) alongside the positions of the relaxation measurements (red stars for the heating branch, blue stars for the cooling branch). Panel b) gives examples of the relaxation measurements including the fitted profile for temperatures on the heating branch. Panel c) shows the behaviour of normalized stretching exponent and relaxation times for the cooling (top) and heating (bottom) branches plotted against the reduced temperature.

- [1] G. Shirane et al, Phys. Rev. 134, 1964.
- [2] C. H. Marrows et al., J. Phys. D. 49, 2016.



Magnetism 2018

P:17 Fabrication and characterisation of a three-dimensional magnetic nanowire lattice

A May, M Hunt, A Van Den Berg and S Ladak

Cardiff University, UK

A key challenge today is the nanostructuring of magnetic materials into arbitrary 3D geometries. Such work would allow the realisation of next generation information technologies such as racetrack memory, the probing of novel curvature induced energy terms and 3D magnetic metamaterials with tuned properties. Here we show Ni₈₁Fe₁₉ nanowires of novel curved cross-section can be placed into complex 3D lattices by using a combination of two-photon lithography and line-of-sight deposition. In this study, the focus is upon samples where the nanowires map onto the bonds of a diamond lattice. Optical magnetometry has successfully been utilized in order to measure the switching within the array, in both longitudinal and polar geometries. Longitudinal loops exhibit an abrupt transition with an enhanced coercive field when compared to the sheet film, as well as a series of plateaus before reaching saturation. Polar loops exhibit a coercive field comparable to the sheet film with a more gradual approach to saturation. The loops will be discussed by comparison to magnetic force microscopy images, which have been obtained after saturation along principle directions.

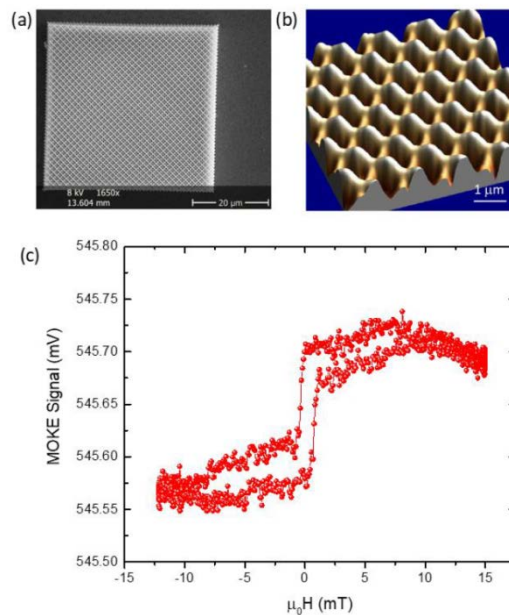
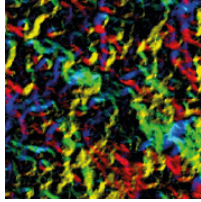


Figure 1: (a) Scanning electron microscope image of a 3D magnetic nanowire lattice. (b) Atomic force microscopy image of the nanowire lattice surface. (c) Longitudinal MOKE loop taken with field applied in substrate plane and perpendicular to upper wires long axes.



Magnetism 2018

P:18 Magnetic and structural influences of layer inversion in Pt/Co₃₂Fe₃₂Ta₂₀B₁₆/Ir trilayers

B Nicholson¹, C Kinane², A Caruana², A Mora-Hernandez¹, D Atkinson¹ and A T Hindmarch¹

¹Durham University, UK, ²Rutherford Appleton Laboratory, UK

The spin Hall effect is present in heavy metals (HM) with strong spin orbit coupling, for example Platinum, and can generate spin currents transverse to an applied charge current [1]. When injected into an adjacent ferromagnetic (FM) layer, this spin current exerts two torques on the magnetisation, a field like and a damping like torque. The efficiency of spin propagation across the HM/FM interface is characterised by the effective spin mixing conductance, which can vary beyond orders of magnitude by, but not necessarily limited to, material choice, crystal structure [2], intermixing and magnetic dead layers [3]. Asymmetric trilayer structures (HM₁/FM/HM₂) can produce spin currents at both the top and bottom FM interface which sum to produce a greater net spin Hall effect than bilayers alone.

Here we show that two trilayer thin films, Pt(3)/Co₃₂Fe₃₂Ta₂₀B₁₆(10)/Ir(3) (thickness in nanometres) and its structural inverse can display a significant difference in magnetic and structural properties. Samples were grown by magnetron sputtering and both as deposited and annealed structures were investigated. X-Ray reflectivity, grazing incidence X-ray diffraction, polarised neutron reflectivity and temperature dependent Kerr effect studies were performed and the results compared to iridium doped (Co₃₀Fe₃₀Ta₂₅B₁₅)_(1-x)Ir_x(10)/Al(3) structures. The X-ray results show a notable difference in structure which could explain the difference in magnetic properties observed, including a change in magnitude of polarised neutron reflectivity asymmetry (fig. 1) and a suppression of the Curie temperature of Ir/Co₃₂Fe₃₂Ta₂₀B₁₆/Pt by greater than 10% compared to Pt/Co₃₂Fe₃₂Ta₂₀B₁₆/Ir (fig. 2).

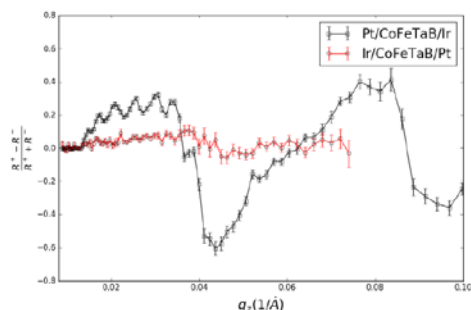


Figure 1. The difference in polarised neutron reflectivity asymmetry data for both trilayer structures.

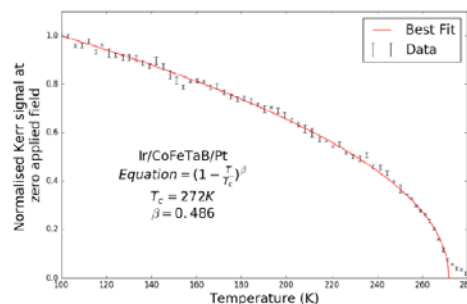
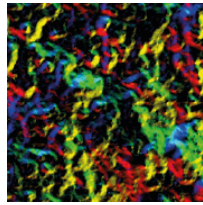


Figure 2. The temperature dependence on the magnetisation of Ir/Co₃₂Fe₃₂Ta₂₀B₁₆/Pt as measured by the magneto-optical Kerr effect.

- [1] MH. Nguyen et al, Physical Review Letters, 116(12), 2016.
- [2] M. Tokaç et al, Physical Review Letters, 115(5), 2015.
- [3] M. Tokaç et al, AIP Advances, 7(11), 2017.



Magnetism 2018

P:19 Krypton doped polar ZnO films by ion implantation gives enormous magnetisation

A Saeedi¹, M Ying², T Duan², M Yuan², S Heald³, M Fox¹ and G Gehring¹

¹University of Sheffield, UK, ²Beijing Normal University, China, ³Argonne National Laboratory, USA

We have reported on a series of experiments of ZnO films which have been implanted with ions of an inert gas. This means that the dopant will not combine electronically with the ZnO and the observed magnetism is due to the crystalline damage caused as the implanted ions lose energy and by strain after the ion comes to rest in the lattice.

ZnO is a polar material and so may be grown with an O-polar or a Zn-polar surface. Previous studies of ZnO with As showed similar dependence on polarity of ZnO. These also gave large M_s which was predominately on due to the radiation damage [1,2].

Two types of sample were used: a 300nm thick film of ZnO that had been deposited on a sapphire substrate (0.5mm thick) by MBE and a single crystal of ZnO with thickness 0.5mm which was also prepared with O-polar and Zn-polar surfaces and implanted by either Kr or Ar in different concentration.

We found an extremely large magnetisation temperature independent magnetisation, $\sim 186 \text{ emu/cm}^3$ is obtained for the highest doped of Kr ions implanted into O-polar surfaces as shown in Figure 1, but Krypton on Zn Polar has a small magnetisation. In contrast the magnetisation is very much smaller for implanted Ar ions. This is due to the lower energy used for the implantation and the fact that the Ar ions are much lighter than Kr. We conclude that the dominant cause of the magnetism is due to Zn ions being knocked into interstitial sites leaving Zn vacancies.

We deduced that V_{Zn} produced in larger numbers by implanted Kr are responsible for the magnetisation. A number of measurements have done so far including magnetisation measurements and the position of Kr and Ar in the lattice using EXAFS. Future measurements include MCD studies.

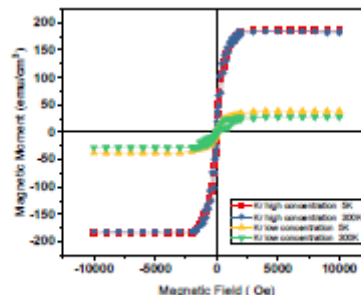
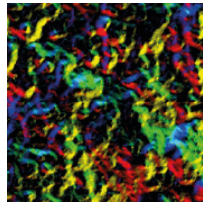


Figure 1. Magnetization data, which were found after subtracting the magnetisation signal measured for undoped O polar ZnO.

- [1] M.J. Ying et al Mater. Lett. 144 (2015)12-14
- [2] M.J. Ying et al Mater. Lett. 171 (2016)121-124.



Magnetism 2018

P:20 Investigation of magnetic properties for both cobalt and europium implanted ZnO films prepared by pulsed laser deposition

A Saeedi¹, N Peng², M Alshammari³, S Heald⁴, A M Fox¹ and G A Gehring¹

¹University of Sheffield, UK, ²Surrey University, UK, ³The National Center for Nanotechnology, KACST, Saudi Arabia, ⁴Argonne National Laboratory, IL, USA

One of the most critical characteristics of any magnet is the hysteresis loop measured at room temperature. A large coercive field is vital for information storage. Most of the literature reviews report that the coercive field of doped oxides is tiny and in the range $\leq 1000\text{e}$ at room temperature[1,2].

A recent study showed that a significant coercive field of 12000e at room temperature could be made by doping ZnO with both a transition metal Co and a rare earth element Eu. This film was doped by ion implantation[3].

Our aims are first to reproduce the result of Lee et al[3] using ion implantation and secondly to investigate ways to reproduce it using pulsed laser deposition (PLD). The results described here were all taken on films made by ion implantation.

Structural magnetic and optical properties are used to investigate films, with and without annealing after implantation, without annealing after implantation, using XRD, EXAFS, SQUID magnetometry, and magnetic circular dichroism MCD.

- [1] M. J. Ying, H. J. Blythe, W. Dizayee, S. M. Heald, F. M. Gerriu, A. M. Fox, and G. A. Gehring, Applied Physics Letters 109, 5, 072403 (2016).
- [2] C. Liu, F. Yun, and H. Morkoc, Journal of Materials Science-Materials in Electronics 16, 555 (2005).
- [3] J. J. Lee, G. Z. Xing, J. B. Yi, T. Chen, M. Ionescu, and S. Li, Applied Physics Letters 104, 012405 (2014).

P:21 Implementation of VAMPIRE atomistic simulation on the synthetic ferrimagnet $\text{Ni}_3\text{Pt}/\text{Ir}/\text{Co}$

J N Scott¹, W R Hendren¹, R M Bowman¹, R W Chantrell² and R F Evans²

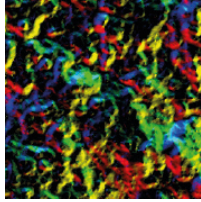
¹Queen's University Belfast, UK, ²University of York, UK

There has been limited exploration and validation of atomistic models using data arising from multilayered magnetic structures. We have successfully corroborated, in simulation and experiment, unexpectedly novel, magnetic response of a simple perpendicular synthetic ferrimagnet $\text{Ni}_3\text{Pt}/\text{Ir}/\text{Co}$ fabricated via UHV sputtering using the atomistic simulation package, VAMPIRE.

We describe the parametrisation of VAMPIRE from experimental data to generate simulations of the constituent magnetic layers (Ni_3Pt & Co). Figure 1 shows the VAMPIRE simulation of a Ni_3Pt (100\AA)/ Ir (5\AA)/ Co (10\AA) perpendicular synthetic ferrimagnet.

The setup for the VAMPIRE simulation comprised $\sim 106,000$ spins, parameterised from experimental data and with the exchange parameter J , derived from a hysteresis loop taken at 10K for the multilayer. A suitable roughness at the interface of the magnetic layers is also included. The experimental SQUID derived $M_R(T)$ data on Figure 1 agree with the simulation.

We observe that the overall simulated $M_R(T)$ does not show a single 'compensation' point, rather a magnetic reversal region between two temperatures where there is a magnetic compensation. This is confirmed by the SQUID data that shows negative remanence between these temperatures. In, addition, the experiment shows clear negative reversal switching in that region (inset, Figure 1) and will be discussed.



Magnetism 2018

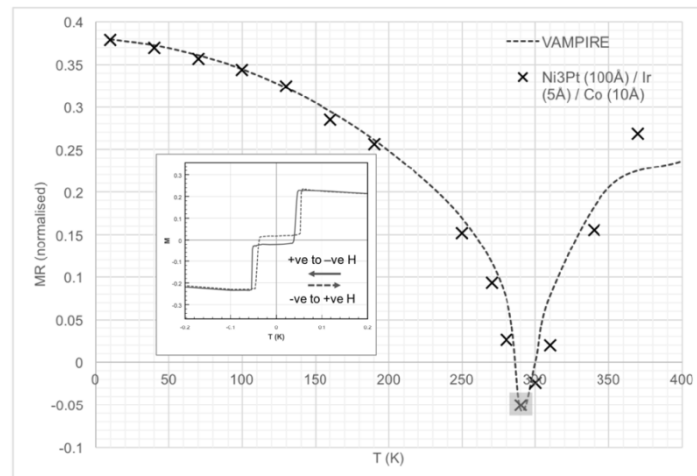


Figure 1. $M_R(T)$ VAMPIRE simulation compared to experimental SQUID measurements of Ni_3Pt (100Å) / Ir (5Å) / Co (10Å) multilayer. Hysteresis loop recorded at 290K showing negative reversal is shown inset.

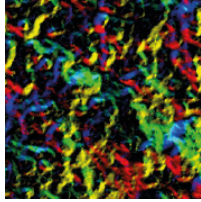
P:22 Atomistic magnetic modelling of FeRh finite-size systems

M S Strungaru, R F L Evans and R W Chantrell

University of York, UK

FeRh is an intensively studied material due to the fact that it exhibits a metamagnetic transition from antiferromagnetic (AFM) to ferromagnetic (FM) state at around 370K. The metamagnetic transformation of FeRh makes it suitable for a wide scope of applications, such as heat-assisted magnetic recording, where FePt/FeRh systems have potential for a high density of stored information, the soft ferromagnetic phase of FeRh allowing a lower coercivity of the system via the exchange spring mechanism [1].

Barker and Chantrell [2] have shown that different temperature scalings of terms in exchange interaction can lead to a first-order phase transition in FeRh systems. Their model assumes the presence of a higher-order exchange term in the form of four-spin exchange mediated by the Rh atoms, that is responsible for the AFM phase at small temperatures. In this work, the first-order phase transition of FeRh is systematically studied via the four-spin parametric model. As nanoscale applications of the FeRh systems are more likely due to the high cost of Rh, the finite size effects on the transition temperature are systematically investigated for FeRh thin films (Fig. 1) and grains. Additionally, the properties of FePt/FeRh bilayers have been explored, as this system is of particular interest for recording media applications.



Magnetism 2018

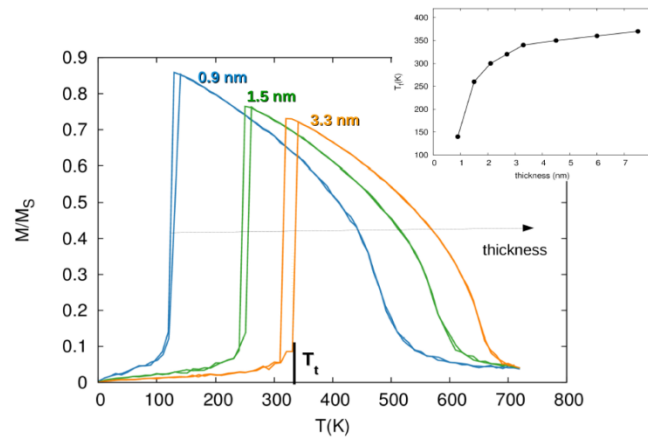


Fig. 1- Temperature dependence of the magnetisation for different thicknesses (in nm) of FeRh thin films during heating and cooling process. The transition temperature (T_t) corresponding to the heating branch is larger than in the case of the cooling, leading to a thermal hysteresis associated with the first-order phase transition. The system is simulated via the four-spin parametric model. (inset) Thickness dependence of the transition temperature in thin FeRh films. The transition temperature saturates at around 350 K for film thicknesses of about 7.5 nm.

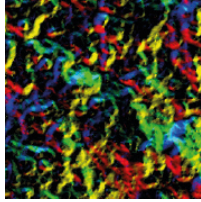
- [1] Thiele, J.U., Maat, S., & Fullerton, E.E. (2003), Applied Physics Letters, 82(17), 2859-2861
- [2] Barker, J. & Chantrell, R.W. (2015), Physical Review B, 92(9), 094402.

P:23 Magnetic imaging of phase domain development in laterally confined FeRh

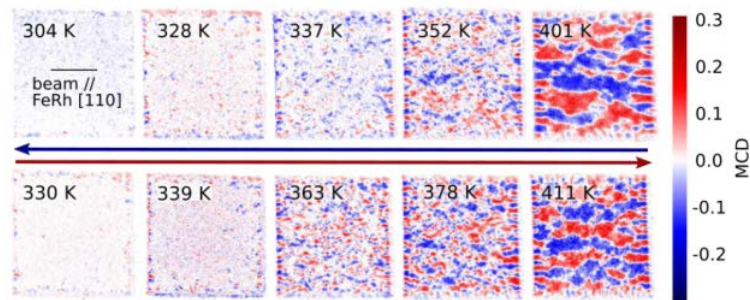
R C Temple¹, T P Almeida², J Massey¹, K Fallon², R Lamb², S Morley¹, S McVitie², T A Moore¹ and C H Marrows¹

¹University of Leeds, UK, ²University of Glasgow, UK

The antiferromagnetic (AF) to ferromagnetic (FM) phase transition in FeRh is imaged in laterally confined nanopatterned islands using x-ray photoemission electron microscopy. This unusual first order magnetic transition has unique possibilities for magnetic memory applications but the effects of lateral confinement on the structure are not well studied. Here we image the FM phase domains during heating and cooling through the transition in square islands of FeRh material ranging from 5 μm to 500 nm in width, above and below the typical final domain size. In the 5 μm structures this domain development during heating is shown to proceed in three distinct modes: nucleation, growth, and coarsening, each with subsequently greater energy costs. In the 500 nm structures the transition temperature was found to 30 K lower than the larger island. The magnetic transition is highly sensitive to small rearrangement of the crystalline order and the modification to the transition temperature is found to be caused by side wall damage during the mask transfer process. This common problem in nanofabrication will need to be overcome in order to advance towards patterned devices.



Magnetism 2018



Magnetic dichroism images of an island of side 5 μm shown as a function of temperature during the cooling process (upper) and the heating process (lower). The beam direction and magnetic sensitivity are shown in the top left image. Red and blue show magnetisation parallel and anti-parallel to the beam.

P:24 Low temperature annealing of superconducting bismuth nickel bilayers

M Vaughan and G Burnell

University of Leeds, UK

Bismuth nickel interfaces are of recent interest as there is speculation of unique states of superconductivity such as p-wave or topological superconductivity ([1, 2]). This work shows bismuth nickel bilayers will anneal at room temperature over a period of several days, increasing the T_c of the samples until it has saturated to 3.8k. The annealing creates a $NiBi_3$ alloy at the interface as indicated by a XRD $NiBi_3$ peak which is an already known superconductor with a similar T_c of 4.1k. The activation energy measured from the change in the onset of the meissner effect after annealing is $(0.86 \pm 0.06)\text{eV}$. The out-of-plane and in-plane critical fields are close fits for a 2D superconductor (2.a), but a similar linear dependence has also been seen in bulk NiB_3 ([3]). This aging process poses a challenge to studying distinct Bi/Ni interfaces as any slight heating will degrade the interface.

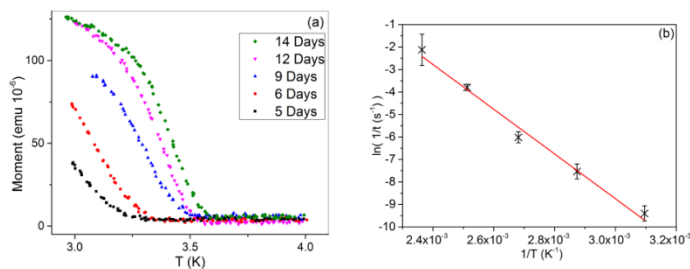
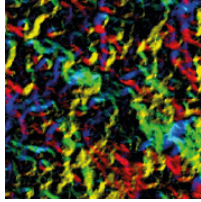


Figure 1: (a) Clear aging of the a sample at approx. 21 mT over a period of 2 weeks, out-of-plane moments from trapped flux are inverted when measured in-plane. (b) Arrhenius plot of Bi/Ni bilayers annealed between 50 $^{\circ}\text{C}$ and 150 $^{\circ}\text{C}$ with an activation energy of $(0.86 \pm 0.06)\text{eV}$.



Magnetism 2018

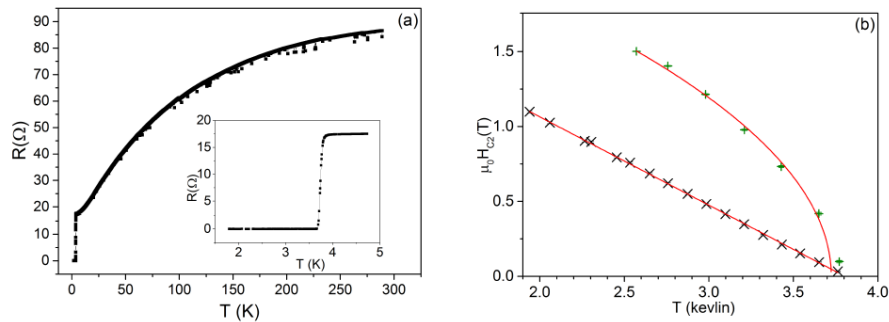


Figure 2: (a) $R(T)$ of Bi/Ni bilayers with inset of superconducting transition at 3.8K. (b) The out-of-plane (Black) and in-plane (Green) H_{c2} data fits well with for a Ginzburg-Landau model $\mathcal{C}2$ 2D superconductor. The critical field values are $H_{c2}^{\perp} = 2.244T$ and $H_{c2}^{\parallel} = 2.70T$.

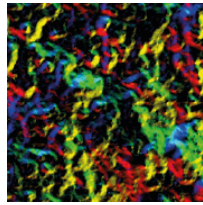
- [1] Z. He-Xin G. Xin-Xin. Possible p-wave superconductivity in epitaxial bi/ni bilayers. *Chinese Physics Letters*, 32(6):067402, 2015.
- [2] K. Mehdi G. Xin-xin. Time-reversal symmetry-breaking superconductivity in epitaxial bis-muth/nickel bilayers. *Science Advances*, 3(3), 2017.
- [3] B. Herrera E. Pineiro. Possible coexistence of superconductivity and magnetism in inter- metallic nibi3. *Solid State Communications*, 151(6):425 – 429, 2011.

P:25 Strain mediated voltage control of layer switching order in synthetic antiferromagnets

A Welbourne¹, W Lim², J-W Liao¹ and A Fernández-Pacheco¹

¹University of Cambridge, UK, ²Université Grenoble Alpes, France

Strain-mediated voltage control of magnetism is expected to play a crucial role in the next generation of magnetic devices [1]. Until now, most work in this field has focused on single layer magnetic systems [2,3]. Here, we investigate the effect of strain in synthetic antiferromagnets (SAFs) under external magnetic fields. The SAFs investigated are formed by two CoFeB layers, antiferromagnetically coupled by a Ru interlayer via RKKY interactions. By applying in-plane compressive or tensile uniaxial strain, with a total magnitude of 0.1%, we are able to control the reversal mechanism of these systems: moving between spin flip and spin flop regimes, an effect driven by the effective anisotropy of the two layers [4]. Moreover, we will show how for specific coupling strengths, the application of particular values of strain allows us to change the switching order of the layers under in-plane external fields, leading to remarkably different hysteresis loops depending on the magnitude of the voltage applied (Figure 1). Magneto-optical Kerr effect experimental measurements will be compared with macrospin simulations in order to understand the origin of this effect. This work shows how strain is a powerful method for controlling the magnetic state of antiferromagnetically coupled multilayered magnetic systems.



Magnetism 2018

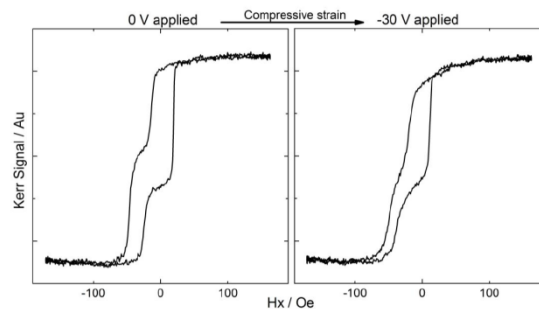


Figure 1: Change in switching order of CoFeB layers under application of compressive strain. A 35 Oe offset field is applied in H_y .

- [1] J. Hu, L. Chen, C. Nan, Multiferroic Heterostructures Integrating Ferroelectric and Magnetic Materials. *Adv. Mater.* 28, 15–39 (2015).
- [2] T. Wu *et al.*, Electrical control of reversible and permanent magnetization reorientation for magnetoelectric memory devices. *Appl. Phys. Lett.* 98, 262504 (2011).
- [3] D. E. Parkes *et al.*, Non-volatile voltage control of magnetization and magnetic domain walls in magnetostrictive epitaxial thin films. *Appl. Phys. Lett.* 101, 72402 (2012).
- [4] R. W. Wang, D. L. Mills, E. E. Fullerton, J. E. Mattson, S. D. Bader, Surface spin-flop transition in Fe/Cr(211) superlattices: Experiment and theory. *Phys. Rev. Lett.* 72, 920–923 (1994).

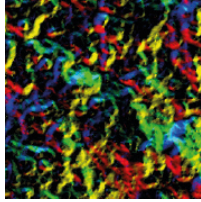
P:26 Magnetism in uranium thin films

M-H Wu and M Gradhand

University of Bristol, UK

Uranium, a light actinide metal that has itinerant electrons in the 5f band, has been investigated in past decades for its complex properties [1]. It shows a large variety of different crystal structures such as α (orthorhombic), β (bct), γ (bcc) and hcp phase and its strong spin-orbital coupling makes Uranium a promising material for spintronics applications [2]. Especially in magnetic multilayer systems the proximity between a heavy, large spin-orbit coupling, material and a ferromagnetic material promises interesting new behavior. For this reason Uranium has been investigated in multilayer systems for 3d-5f hybridization with ferromagnet metals such as Fe, Co and Ni [3–5]. However, in order to understand the complex physics in multilayer systems, we first focus on the properties of the Uranium surface. From our ab initio calculations we predict magnetic moments on the surface of α , γ and hcp phases in stark contrast to their corresponding bulk phases. For bcc in (100) and (111) termination, the magnetic moments are almost entirely induced in the outermost layer and decrease dramatically going deeper into the thin film. In contrast, for hcp Uranium the magnetic moment persists only in the thinnest films, but vanishes in thicker systems, even for its surface layer. Ultra-thin α uranium becomes magnetic as well, which is in agreement with a published theoretical work [6].

- [1] S. Adak, H. Nakotte, P. de Chatel, B. Kiefer, *Phys. B* 406, 3342 (2011).
- [2] Kevin T. Moore and Gerrit van der Laan, *Rev. Mod. Phys.* 81, 235 (2009).
- [3] F. Wilhelm, N. Jaouen, A. Rogalev, W. G. Stirling, R. Springell, S. W. Zochowski, A. M. Beesley, S. D. Brown, M. F. Thomas, G. H. Lander, S. Langridge, R. C. C. Ward, and M. R. Wells, *Phys. Rev. B* 76, 024425 (2007).
- [4] R. Springell, F. Wilhelm, A. Rogalev, W. G. Stirling, R. C. C. Ward, M. R. Wells, S. Langridge, S. W. Zochowski, and G. H. Lander, *Phys. Rev. B* 77, 064423 (2008).



Magnetism 2018

- [5] A. Laref, E. Saşioğlu, L. M. Sandratskii, J. Phys.: Condens. Matter 18, 4177 (2006).
- [6] N. Stojić, J. W. Davenport, M. Komelj, and J. Glimm, Phys. Rev. B 68, 094407 (2003).

P:27 Preparation of Ca:YIG thin films by PLD

A M Zaki¹, S M Heald², H J Blythe¹, A M Fox¹ and G A Gehring¹

¹University of Sheffield, UK, ²Argonne National Laboratory, USA

Magnetic thin films of yttrium iron garnet (YIG) and calcium doped YIG were prepared using pulsed laser deposition technique (PLD) on gadolinium gallium garnet (GGG) and yttrium aluminium garnet (YAG) substrates. The Ca concentrations $x = 0.05, 0.1, 0.2$ and 0.3 . The oxygen pressure in the chamber was increased from a base pressure of 3×10^{-2} mTorr to 400 mTorr and the substrate temperature was 500°C during the ablation. This was followed by an annealing step in air at 1000°C . This procedure gives good films of YIG [1].

The films thicknesses were between 100-120 nm and the X-ray diffraction (XRD) and Extended X-ray absorption fine structure (EXAFS) analysis showed that the Ca occupied the Y sites with decreasing in intensity when the Ca concentration increased. While the superconducting quantum interference device (SQUID) showed that the saturation magnetization (M_s) reduced with increasing Ca concentration in YIG/GGG film from 143 emu/cm^3 for the pure YIG thin film [2]. However, there were no reproducible loops for Ca:YIG/YAG due to the strains arising from the lattice mismatch between the YIG and YAG. The magnetic circular dichroism (MCD) showed paramagnetic peaks at 2.7 and 3 eV [3]. The pure YIG thin film is an insulator material with high resistivity about $2 \times 10^{22} \Omega \text{ cm}$. Hall effect measurements for Ca:YIG thin films showed a drop in the resistivity with increasing Ca concentration. This information can be valuable for the fabrication of p-type semiconductors with suitable magnetic properties.

- [1] Aliaa M. Zaki, Harry J. Blythe, Steve M. Heald, A. Mark Fox, Gillian A. Gehring. Journal of magnetism and magnetic materials (in press)
- [2] Song, Yong Jin, et al. Journal of magnetism and magnetic materials 154.1 (1996): 37-53.
- [3] Kučera, M., et al. Journal of magnetism and magnetic materials 157 (1996): 323-325.

P:28 Spin-wave dynamics of honeycomb artificial spin ice in different microstates

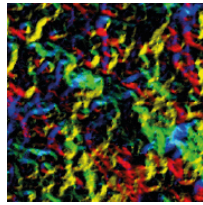
D M Arroo, J C Gartside, L F Cohen and W R Branford

Imperial College London, UK

The exponentially large microstate space available to artificial spin ice (ASI) systems has led to it being identified as a promising candidate for applications as a reprogrammable magnonic crystal [1,2]. In such applications, different microstates would have different spin-wave eigenmodes, while inter-island coupling and the periodicity already present in most ASI geometries would lead to the formation of a band structure through Bragg reflection.

It has recently been demonstrated that ASI systems may be prepared in specific microstates by locally reversing the magnetization of individual islands using the stray field of a magnetic-force microscopy tip³, bringing devices based on moving between selected microstates within reach.

In this work, the spin-wave dynamics of honeycomb ASI systems were probed in a subset of the microstate space via micromagnetic simulations⁴. It was found that altering the microstate of honeycomb ASI allows significant control over spin-wave eigenspectrum including the ability to shift resonant frequencies and tune



Magnetism 2018

the magnonic bandgap. ASI systems thus offer good prospects as components of reprogrammable magnonic device and microwave filters.

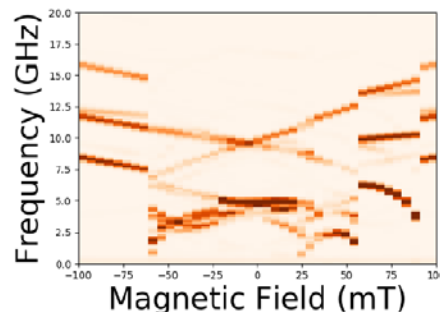


Figure 1: The spin-wave eigenmode spectrum of a honeycomb ASI system initialized in the maximum energy microstate and subjected to an external magnetic field. As the external field drives the system through different microstates, eigenmodes are shifted to different frequencies, offering a means of tunability for applications in microwave devices.

- [1] Heyderman, L. J. & Stamps, R. L. Artificial ferroic systems: novel functionality from structure, interactions and dynamics. *J. Phys. Condens. Matter* 25, 363201 (2013).
- [2] Krawczyk, M. & Grundler, D. Review and prospects of magnonic crystals and devices with reprogrammable band structure. *J. Phys. Condens. Matter* 26, 123202 (2014).
- [3] Gartside, J. C. *et al.* Realization of ground state in artificial kagome spin ice via topological defect-driven magnetic writing. *Nat. Nanotechnology*. 13, 53–58 (2018).
- [4] Vansteenkiste, A. *et al.* The design and verification of MuMax3. *AIP Adv.* 4, 107133 (2014).

P:29 Characterisation of iron-rich cobalt-iron-boron thin films using ferromagnetic resonance

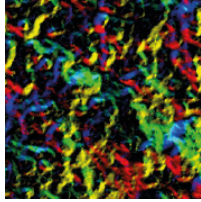
G Awana and D Backes

Loughborough University, UK

Magnetic thin films tend to align their magnetisation in the film plane. This is due to the strong demagnetising field in such layers, given by the saturation magnetisation M_s . Magnetic multilayers such as $[\text{Co/Ni}]_x$ and Fe-rich cobalt-iron-boron single layers are known for their large perpendicular magnetic anisotropy (PMA), potentially exceeding the demagnetising field. This can result in an overall out-of-plane anisotropy, where the magnetisation is aligned perpendicular to the plane.

We deposited thin films of $\text{Co}_{20}\text{Fe}_{60}\text{B}_{20}$ using pulsed laser deposition (PLD) on Ta seed layers in ultrahigh vacuum. The thickness range was varied between 2.5 and 5 nm. We characterised the perpendicular magnetic anisotropy (PMA) of these layers using a newly built network analyser-based ferromagnetic resonance (FMR) setup [1]. We find that with decreasing thickness the PMA becomes stronger, resulting in a downwards shift of the dispersion curve (see Fig. 1). This confirms that we can flexibly tune the magnetisation direction from in-plane to out-of-plane by decreasing the thickness even further. We do not observe any change of the damping parameter in the thickness range studied.

The ability to tune the anisotropy of magnetic adlayers will inform new spintronic devices based on topological materials, where contacts made of $\text{Co}_{20}\text{Fe}_{60}\text{B}_{20}$ could act as probes for the spin-orientation of Dirac surface states [2, 3].



Magnetism 2018

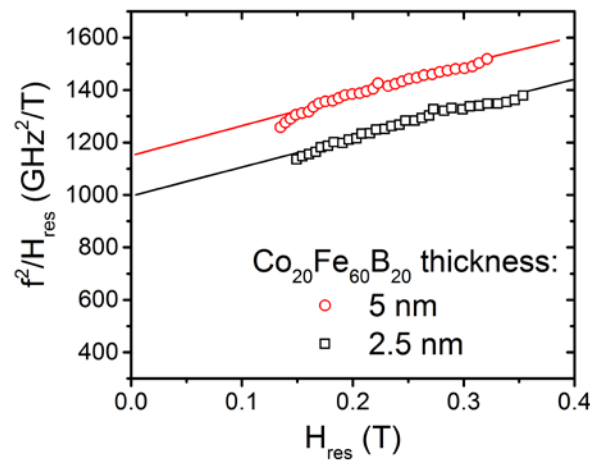


Figure 1 FMR dispersion curves for two different $\text{Co}_{20}\text{Fe}_{60}\text{B}_{20}$ thicknesses

- [1] D. Backes et al., J. Appl. Phys. 111, 07C721 (2012)
- [2] Z. Hasan and C.L. Kane, Rev. Mod. Phys. 82, 3045 (2010)
- [3] Y. Fan and K. L. Wang, SPIN 6, 164001 (2016).

P:30 X-Ray detected ferromagnetic resonance (XFMR)

D M Burn and G Van der Laan

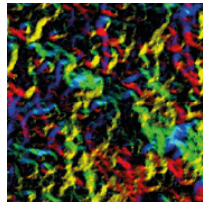
MSG group, Diamond Light Source, UK

Ferromagnetic resonance (FMR) is a standard technique for measuring magnetisation dynamics in thin film, multi-layered and single crystal systems. The absorption of a RF magnetic signal supplied from a co-planar waveguide reveals the field and frequency dependence to the magnetic resonance in the sample. However, this technique comes with limitations, for example it is not possible to determine the origin of resonance modes in complex multi-layered structures typically used in magnetism research today.

By combining FMR measurements with x-ray magnetic circular dichroism (XMCD) it is possible to overcome this limitation by exploiting the element selectivity available with x-ray absorption measurements. X-ray detected ferromagnetic resonance (XFMR) works by synchronising RF excitation of the sample with pulsed x-rays available at a synchrotron we stroboscopically probe the absorption as a function of pump-probe delay revealing the element specific magnetodynamics at picoseconds timescales [1,2].

We present a selection of recent XFMR results, including spin pumping across spin valves and spin transfer across a topological insulators [3-6], outlining the operating principles of the technique and the valuable insights it offers.

- [1] A.I. Figueroa, et. al., J. Magn. Magn. Mater. 400, 178 (2015).
- [2] M.K. Marcham et.al., J. Appl. Phys. 109, 07D353 (2011).
- [3] G.B.G. Stenning et. al., New. J. Phys. 17, 013019 (2015)
- [4] M.K. Marcham et. al., Phys. Rev. B 87, 180403 (2013).
- [5] A.A. Baker, et. al., Sci. Rep. 5, 7907 (2015).
- [6] A.A. Baker et. al., Sci. Rep. 6, 35582 (2016).



Magnetism 2018

P:31 Selective excitation of localised spin wave modes by optically pumped surface acoustic waves

C L Chang¹, R R Tamming¹, J Janusonis¹, P W Fry², R I Tobey¹ and T J Hayward²

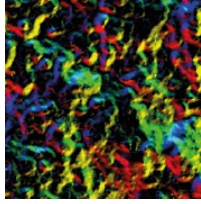
¹University of Groningen, The Netherlands, ²University of Sheffield, UK

With CMOS technology reaching the end of its scaling potential there is great interest in developing novel technologies that will allow further growth in the power and efficiency of computational hardware. Magnonic devices [1], in which information is transported and processed via the propagation and interaction of spin waves, are attractive candidates amongst these, since they can hypothetically perform computations without transporting electrical charge, thus increasing energy efficiency. Unfortunately, while propagating spin waves does not require current flow, their excitation, which is typically achieved using microwave striplines or spin torque effects, do.

To address these limitations, methods of exciting spin waves using applied voltages, rather than electric currents must be developed. One possible method of achieving this is to use magneto-elastic effects to couple spin waves to surface acoustic waves (SAWs). SAWs have similar frequencies to spin waves at the micro- and nano-scale, and can be excited by applying high frequency voltages to interdigitated transducers mounted to the surface of piezoelectric substrates. However, while previous studies have shown the feasibility of using SAWs to excite ferromagnetic resonance in continuous thin films [2], the coupling of SAWs to the more complex localized spin wave spectra of magnetic nanostructures has not been demonstrated.

Here, we use time-resolved, pump-probed optical magnetometry to demonstrate the selective excitation of localised spin wave modes by SAWs in an array of 250 nm wide Nickel nanowires. A 100 fs laser pulse is used to optically excite a standing SAW, with frequency ~ 6 GHz, via the array's spatially inhomogeneous optical absorption. Time-resolved probe measurements show that peaks in the amplitude of the array's magnetisation response occur when the applied magnetic field is of the correct magnitude to push either of the array's two primary spin wave modes into resonance with the SAW. Micromagnetic simulations, performed using the mumax³ software package, show these two modes to be spatially localised in the body and edges of the nanowires respectively, thus verifying that the SAW is resonantly exciting spatially non-uniform spin waves. We suggest that similar couplings of SAWs to the spin wave modes of a nanowire end domains could be used to create coherent sources of spin waves in future magnetic logic devices [3].

- [1] V.V. Kruglyak, S.O. Demokritov and D. Grundler, J. Phys. D: Applied Physics, 43, 264001 (2010).
- [2] M. Weiler, L. Dreher, C. Heeg, H. Huebl, R. Gross, M.S. Brandt and S.T.B. Goennenwein, Phys. Rev. Let. 106, 117601 (2011).
- [3] F.B. Mushenok, R. Dost, C.S. Davies, D.A. Allwood, B.J. Inkson, G. Hrkac and V.V. Kruglyak, Appl. Phys. Let. 111, 042404 (2017).



Magnetism 2018

P:32 Time-resolved x-ray detected ferromagnetic resonance measurements in a CoFe/NiO/Fe/NiFe multilayer structure

T Nakano¹, M Dabrowski¹, Q Li², M. Yang², C Klewe³, D. Burn⁴, P Shafer³, G van der Laan⁴, Z Q Qiu², E Arenholz³, and R J Hicken¹

¹University of Exeter, UK, ²University of California Berkeley, USA, ³Advanced Light Source, USA, ⁴Diamond Light Source, UK

Antiferromagnetic NiO films have been studied as media for the effective propagation of spin currents [1]. In order to detect the ac spin current propagating through a NiO film, which has not been reported so far, we performed element-specific x-ray detected ferromagnetic resonance (XFMR) measurements [2] on a CoFe/NiO/Fe/NiFe multilayer.

Figure 1(a) shows the XFMR delay scans acquired at the Co and Ni L_3 edges in the CoFe and NiFe layers respectively. The amplitudes and phases were extracted by fitting sine curves to the data acquired at different static magnetic fields, as shown in Figure 1(b) and (c). The FMR magnetic field was close to 60 Oe for both the CoFe and NiFe layers, and the precession was found to have the same phase in both layers. These unexpected results indicate that the CoFe and NiFe layers are strongly exchange coupled and rotate entirely together. An ac spin current could not be observed in this sample due to the exchange coupling. We suspect two possible origins for the coupling. Either the NiO layer contains oxygen deficiencies and metallic Ni components mediate the coupling, or else pinholes within the NiO layer allow the ferromagnetic layers to directly couple to each other.

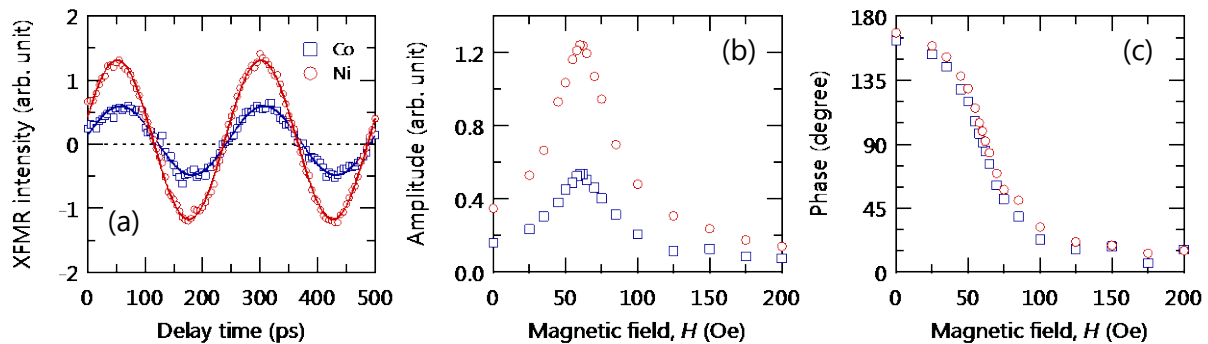
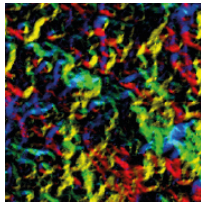


Figure 1: (a) XFMR delay scans with a static magnetic field H of 60 Oe, (b) fitted amplitudes, and (c) fitted phases for Co (blue squares) and Ni (red circles) L_3 edges. The sine curves in (a) are fits to the experimental data. 4-GHz microwaves were supplied through the coplanar waveguide (CPW) with a variable delay relative to the x-ray pulses, and generated an in-plane rf magnetic field orthogonal to the CPW, while H was parallel to the CPW.

- [1] H. Wang et al., Phys. Rev. Lett. 113, 097202 (2014).
- [2] J. Li et al., Phys. Rev. Lett. 117, 076602 (2016).



Magnetism 2018

P:33 Influence of interfacial structure and heavy metal thickness on spin mixing conductance for the enhancement of damping

C Swindells, A Hindmarch, A Gallant and D Atkinson

Durham University, UK

Understanding the role of the interface is crucial to developing spintronic and high frequency devices. The ability to inject spins into another layer by propagating spin angular momentum across an interface, a process referred to as spin pumping, is often quantified by the spin mixing conductance [1]. Heavy metals, such as Pt, are well known for their ability to enhance damping [2], with a marked increase achievable via enhanced spin mixing conductance in certain conditions [3]. The difference in properties such as the induced moment within Pt layers depending on the interface complicates matters further [4].

Here we present results on the effect of increasing ultrathin heavy metal capping and underlayers on the effective spin mixing conductance, for both amorphous and crystalline ferromagnetic films. Samples were grown using magnetron sputtering and measured using in-plane Vector Network Analyser (VNA) FMR. This method has the advantage of removing the need for either assuming a constant g-factor, or fitting a Kittel curve with strongly coupled parameters. For amorphous FM materials, the spin mixing conductance increases with increasing NM thickness, whereas for crystalline materials it is highly dependant on both the crystal structure and the interface considered.

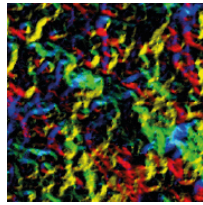
- [1] S Azzawi et al J. Phys. D: Appl. Phys. 50 473001 (2017).
- [2] S.Azzawi et al. *Physical Review B* 93(5): 054402. (2016).
- [3] M. Tokaç, *Physical Review Letters* 115(5): 056601. (2015).
- [4] R. Rowan-Robinson *Scientific Reports* 7,: 16835 (2017).

P:34 Ferromagnetic resonant modes of synthetic antiferromagnetic structures

H J Waring, I J Vera-Marun and T Thomson

The University of Manchester, UK

Antiferromagnetic spintronics has generated much interest as an emerging research field, with a particular emphasis of exploring its potential for high frequency devices extending towards the THz band [1]. Antiferromagnets typically display much faster spin dynamics compared with their ferromagnetic counterparts due to their higher anisotropy and the resonant modes available [2]. This is currently a topic which is attracting significant research activity due to the ever increasing technological demands for enhanced operational speeds of RF and microwave devices [3]. In this work, we investigate the FMR signals of synthetic antiferromagnets (SAFs), where two ferromagnetic layers are separated by an ultrathin ($\sim 0.8\text{nm}$) non-magnetic spacer layer, here ruthenium, as shown in Figure 1(a). In such a stack, the magnetic properties can be tailored through the RKKY interaction, with the presence of ferromagnetic or antiferromagnetic coupling dependent on the thickness of the spacer layer. Initial work has concentrated on the fabrication of SAFs incorporating CoFeB as the ferromagnetic components due to its proven ability to form a SAF [3]. The SAFs have been fabricated using magnetron sputtering and characterized using procedures including XRR to measure layer thickness, Vector Vibrating Sample Magnetometry (VSM) to verify basic antiferromagnetic coupling and a Vector Network Analyzer – Ferromagnetic Resonance (VNA-FMR) setup which allows key dynamic properties to be explored. Figure 1(b) shows initial results obtained for a CoFeB(8nm)/Ru(0.7nm)/CoFeB(8nm) sample. FMR and XRR results on a spacer layer thickness series of samples will be presented at the conference.



Magnetism 2018

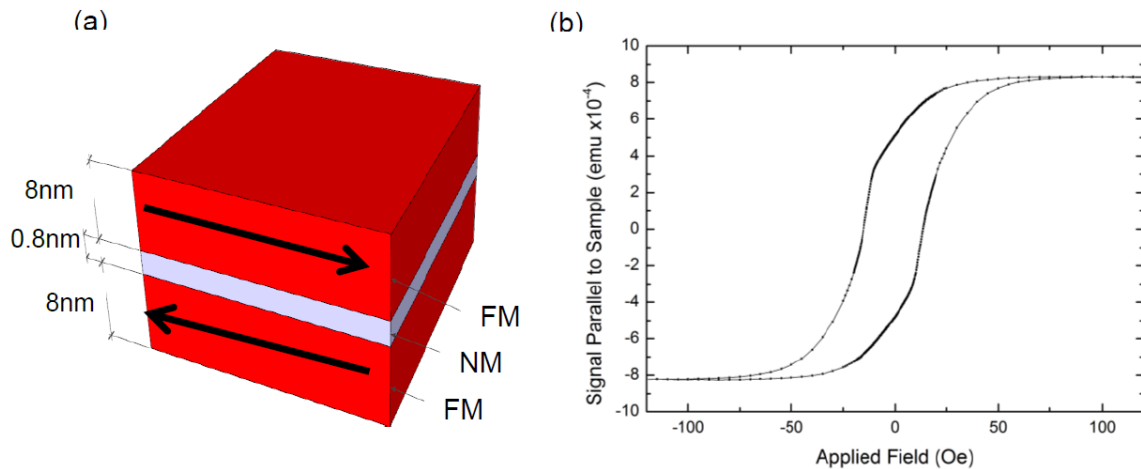


Figure 1: (a) A synthetic antiferromagnet comprised of FM (Ferromagnetic)/NM (Non-Magnetic)/FM stack. The non-magnetic layer is typically ruthenium. The arrows represent the magnetisation direction in each ferromagnetic layer when antiferromagnetic interlayer coupling is present. (b) Vector VSM hysteresis loop of a CoFeB(8nm)/Ru(0.7nm)/CoFeB(8nm) structure.

- [1] J. Walowski et al. *J. Appl. Phys.* 120, 140901, 2016.
- [2] H. V. Gomonay et al. *Low Temp. Phys.* 40, 17, 2014.
- [3] S. Li et al. *Adv. Funct. Mater.* 26, 21, 2016.
- [4] S. Li et al. *Adv. Funct. Mater.* 26, 21, 2016.

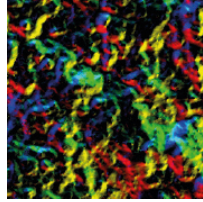
P:35 Theory of linear spin wave emission from a Bloch domain wall

N J Whitehead¹, S A R Horsley¹, T G Philbin¹, A N Kuchko² and V V Kruglyak¹

¹University of Exeter, UK, ²Institute of Magnetism, Ukraine

The generation of small wavelength spin waves for future magnonic technologies will require nanometre-sized spin wave sources. Recent work has shown that pinned domain walls can generate spin waves when excited by a microwave external field¹⁻⁴ or spin-polarised current⁵, even with wavelengths down to tens of nanometres. These results would benefit from a quantitative, theoretical explanation of the underpinning physics.

We use analytical theory to demonstrate and explain the emission of exchange spin waves from a Bloch domain wall driven by a uniform microwave magnetic field directed perpendicular to the plane of the wall⁶. Crucially, we find that the spin wave emission (Fig. 1) is the result of a linear process, meaning that the spin wave frequency matches that of the excitation field. Furthermore, we explore the peculiar characteristics of the Pöschl-Teller potential well, which naturally represents the graded magnonic index due to the Bloch domain wall in the Schrödinger-like linearized Landau-Lifshitz equation. This potential is known to allow 100% transmission of incident waves at any frequency, for certain parameters of the potential. We find that the domain wall is naturally sized not only to exhibit this property, but also to maximize its spin wave emission.



Magnetism 2018

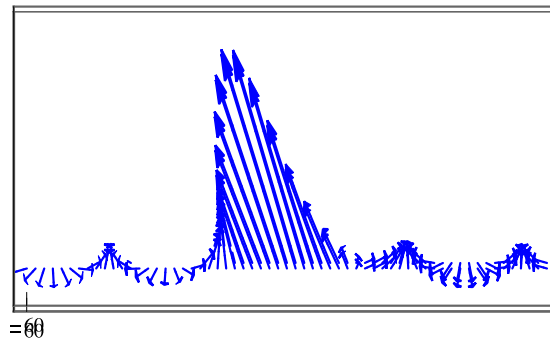


Figure 1. Projection onto the x-y plane of the magnetization vectors for the Bloch domain wall is shown for phase = 0 and (inset) phase = π .

- [1] S. J. Hermsdoerfer, H. Schultheiss, C. Rausch, S. Schäfer, B. Leven, S.-K. Kim, and B. Hillebrands, *Appl. Phys. Lett.* 94, 223510 (2009).
- [2] P. E. Roy, T. Trypiniotis, and C. H. W. Barnes, *Phys. Rev. B* 82, 134411 (2010).
- [3] B. Mozooni and J. McCord, *Appl. Phys. Lett.* 107, 042402 (2015).
- [4] V. Sluka, M. Weigand, A. Kakay, A. Erbe, V. Tyberkevych, A. Slavin, A. Deac, J. Lindner, J. Fassbender, J. Raabe, and S. Wintz, in *2015 IEEE Magnetics Conference (INTERMAG)* (2015).
- [5] B. Van de Wiele, S. J. Hämäläinen, P. Baláz, F. Montoncello, and S. van Dijken, *Sci. Rep.* 6, 21330 (2016).
- [6] N. J. Whitehead, S. A. R. Horsley, T. G. Philbin, A. N. Kuchko, and V. V. Kruglyak, *Phys. Rev. B.* 96, 064415 (2017).

P:36 Magnonic studies of ferromagnetic nanostructures

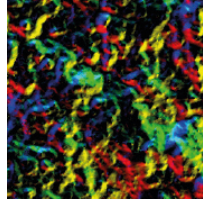
G Venkat^{1,2} and A Prabhakar¹

¹Indian Institute of Technology Madras, India, ²Loughborough University, UK

Magnetization dynamics is a widely studied research area, with interest from both a fundamental and applied point of view. For example, there are possibilities of microwave nanoscale devices such as couplers, multiplexers and processors is a great motivation for such studies. In this context, we study spin waves (SWs) in a variety of structures.

The ferromagnetic waveguide and study of the corresponding SW dispersion is a standard problem which can be used to compare different micromagnetic packages [1]. We will present a comprehensive study of SW dispersion profiles and corresponding dynamics for different structures and boundary conditions. This will demonstrate the use of micromagnetic simulations in these cases, as well as Brillouin light scattering to study SW dynamics, alongside magnetometry and magnetic domain imaging.

We will show that the introduction of a parabolic absorbing boundary condition can be used to improve models of SW dispersions [2]. This will be followed by a study of the SW dynamics in rings, where we will show that the SW coupling efficiency between structure ends can be enhanced by changing bias field configurations. We also consider a ring shaped defect in an antidot magnonic crystal of permalloy and show that SWs get preferentially guided through the defect [3]. As the modes allowed through the defect lie in the band gap of the magnonic crystal, this suggests that a filtering action was obtained. Finally we will show analysis of static and dynamic magnetization in ferrite films [4].



Magnetism 2018

Figure 1 : (a) A schematic of a spin wave. (b) A magnonic waveguide and the fundamental SW mode in it. (c) Backward volume dispersion of SWs and (d) excitation of the fundamental backward volume SW mode. (e) SW guiding in a ring defect in a magnetic crystal, (f) shows the in-plane hysteresis curve and (g) shows domain images of a ferrite film.

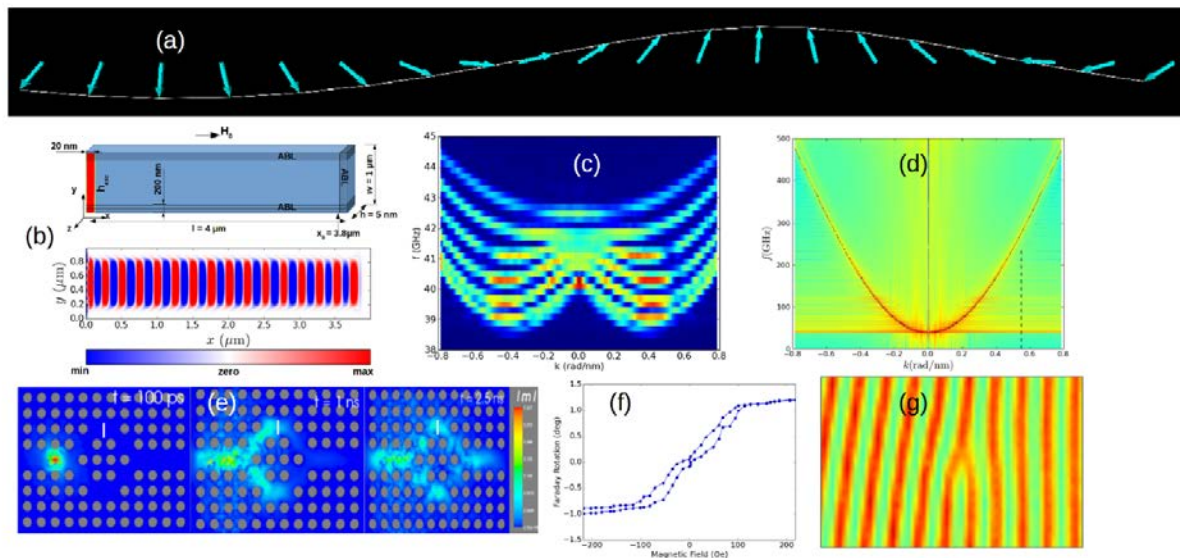


Figure 1 : (a) A schematic of a spin wave. (b) A magnonic waveguide and the fundamental SW mode in it. (c) Backward volume dispersion of SWs and (d) excitation of the fundamental backward volume SW mode. (e) SW guiding in a ring defect in a magnetic crystal, (f) shows the in-plane hysteresis curve and (g) shows domain images of a ferrite film.

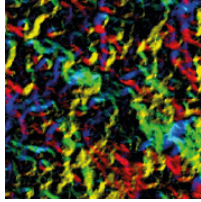
- [1] G. Venkat et. al., IEEE Trans. Magn., vol. 49, pp. 524-529, 2013.
- [2] G. Venkat et. al., Journal of Magnetism and Magnetic Materials, 2017.
- [3] G. Venkat et. al., IEEE Trans. Magn., vol. 50, pp.1-4, 2014.
- [4] M. Malathi et. al., Journal of Magnetism and Magnetic Materials, 2017.

P:37 Strain manipulation of the magnetoresistance in nickel and permalloy thin films

M S Al-Qayoudhi, D P Pattnaik, K W Edmonds, and A W Rushforth

University of Nottingham, UK

The manipulation of magnetisation in ferromagnetic films plays a very important role in the development of novel spintronics devices especially for information storage and logical operations. The ability to control the magnetisation of material using an electric field can facilitate the development of new devices with lower power consumption and efficient processing. A way to perform this, is by means of the inverse magnetostrictive effect in hybrid multiferroic structures, where a voltage-induced strain modifies the magnetic anisotropy energy [1]. The main aim of this study is to investigate the effect of strain on spin-valve structures containing Ni and NiFe thin films. In order to study the strain effect on the spin valve structure, three samples were grown in addition to the spin-valve samples to serve as controls for the separate study of each layer's effect. We have investigated the role of voltage induced in-plane uniaxial strain on the



Magnetism 2018

magnetisation reversal processes of such hybrid structures of permalloy and nickel thin films bonded onto a piezoelectric transducer. Preliminary results show that the magnetostrictive properties of the nickel and permalloy were different than expected, as the strain affected the permalloy rather than the nickel [2]. For the permalloy sample (4nm), magnetotransport measurements reveal that the strain dependent magnetic anisotropy energy is manipulated by the in-plane strain and is evident by the unique transverse and longitudinal resistance features for different values of voltage induced strain as shown in Fig. (1) and (2). The strain induces a change in the net magnetic anisotropy. By contrast, results for the nickel sample (5nm) show near-zero magnetostriction. For ultra-thin films, the properties are different than they are for bulk because of the surface effect at a small scale [3].

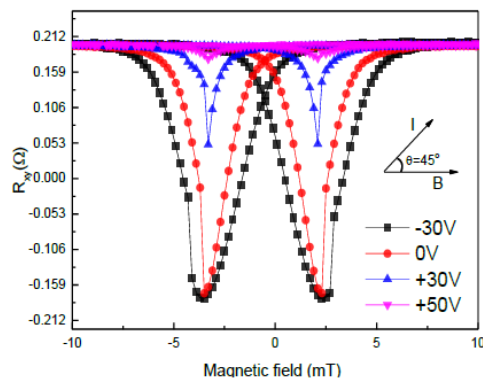


Fig (1). Transverse resistance R_{xy} for the (4nm) Permalloy film for field along $\theta = 45^\circ$, as a function of voltage applied to the transducer.

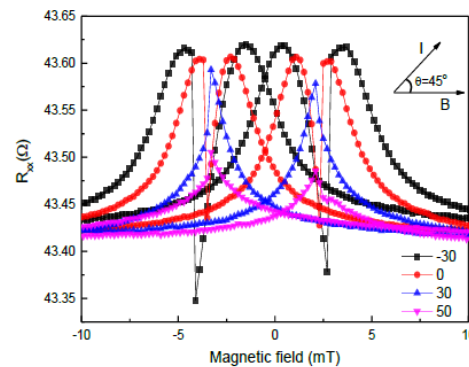


Fig (2). Longitudinal resistance R_{xx} for the (4nm) Permalloy film for field along $\theta = 45^\circ$, as a function of voltage applied to the transducer.

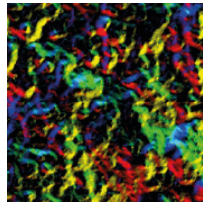
- [1] Na Lei, Thibaut Devolder, Guillaume Agnus, Pascal Aubert, Laurent Daniel, Joo-Von Kim, Weisheng Zhao, Theodossis Trypiniotis, Russell P. Cowburn, Claude Chappert, Dane Ravelosona, and Philippe Lecoeur. Strain-controlled magnetic domain wall propagation in hybrid piezoelectric/ferromagnetic structures. *Nat Commun*, 4:1378, 2013.
- [2] E. Klokholm and J. A. Aboaf, "The saturation magnetostriction of permalloy films," *Journal of Applied Physics*, vol. 52, p. 2474, 1981.
- [3] Y. K. Kim, and T. J. Silva. Magnetostriction characteristics of ultrathin permalloy films. *Appl. Phys. Lett.* 68, 2885, 1996.

P:38 Time resolved imaging of coupled nano-contact spin transfer vortex oscillators

E O Burgos Parra¹, P S Keatley¹, S R Sani², J Åkerman³ and R J Hicken¹

¹University of Exeter, UK, ²KTH-Royal Institute of Technology, Sweden, ³University of Gothenburg, Sweden

In this work pairs of STVOs with NCs of 100 nm diameter and center-to-center separation ranging from 200 nm to 1100 nm have been studied, with a combination of electrical measurements and time-resolved scanning Kerr microscopy (TRSKM) being used to explore the microwave emission and associated magnetization dynamics as a function of NC separation. Electrical measurements were richly featured, often exhibiting multiple modes and their harmonics as in shown in Figure 1.a. The Kerr images acquired for the NC pair with 200 nm separation reveal significant differences in the spatial character of the magnetization dynamics when compared to those observed previously for a pair with 900 nm separation, for which the dynamic interaction is expected to be weaker. For a separation of 900 nm, localized regions of magnetization dynamics were observed close to each NC (Fig. 1.c and 1.e, yellow arrows), each region



Magnetism 2018

having similar spatial character to that found within single NC devices, suggesting that a separate vortex had formed at each NC.[3] However, for a pair of NCs with 200 nm separation (Fig. 1.b and 1.d, blue arrow), a single region of lower amplitude dynamics was observed to span the region occupied by the NCs. At the same time, large amplitude dynamics were also observed some microns from the NCs. We speculate that these dynamics are due to the oscillation of anti-vortices (AV) that were pushed away from the NCs, pinned by stray DC electromagnetic fields from the device contact pads, and then excited by the stray RF Oersted field. An improved understanding of the interaction of pairs of NC-STVOs obtained from time-resolved imaging of their magnetization dynamics is crucial for the realization of networks of phase-locked STVOs that share common magnetic layers.

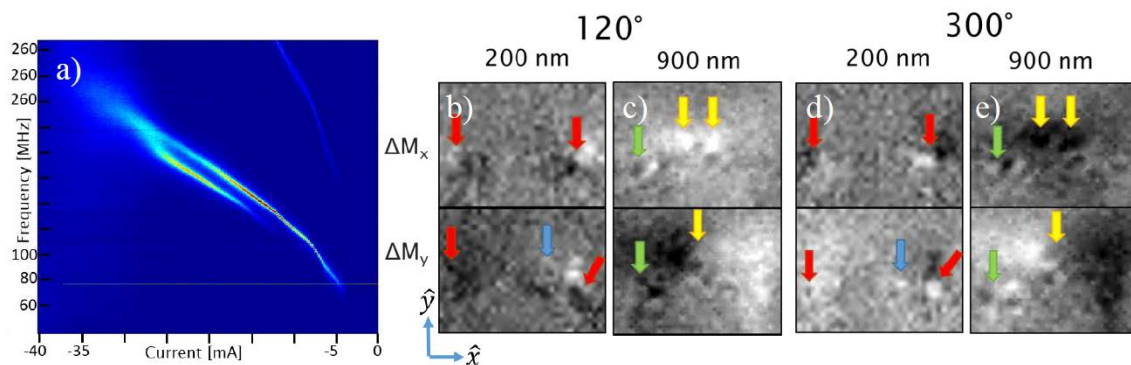


Figure 1: a) Transport measurements at zero external field for a STVO with a pair of NC of 100 nm diameter and separated by 200 nm where is possible to observe two gyration modes of magnetic vortices produce in the film. Time Resolved Scanning Kerr Microscopy (TRSKM) was used to image the dynamic magnetization within two devices with NC separation of 200 nm (b) and (d) and 900 nm (c) and (e). Blue and yellow are dynamics associated to vortex motion while red and green arrows are associated to antivortices motion.

- [1] M. R. Pufall *et al.*, Phys. Rev. B, 75, 1 (2007).
- [2] Q. Mistral *et al.* Phys. Rev. Lett. 100, 257201 (2008)
- [3] P. S. Keatley *et al.* Phys. Rev. Lett. 94, 060402(R) (2016).

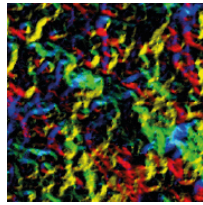
P:39 In-Situ PNR of the spin Seebeck effect

A J Caruana^{1,2}, C D W Cox², C J Kinane¹, T R Charlton^{1,3}, M D Cropper² and K Morrison²

¹STFC Rutherford Appleton Laboratory, UK, ²Loughborough University, UK, ³Oak Ridge National Lab, USA

The spin Seebeck effect (SSE) has attracted a large amount of interest due to its potential use in energy harvesting. When a thermal gradient is applied to a magnetised ferromagnet (FM) it can induce a spin current, JS [1]. By placing a heavy metal (NM) in contact with a FM material, JS can be converted to a charge current, JC, via the inverse spin Hall Effect (ISHE). The SSE is measured by detecting the induced voltage from the ISHE – i.e. an indirect measurement of the SSE.

Polarised neutron reflectometry (PNR) measures the nuclear and magnetic scattering lengths of thin layers as a function of depth [2], ultimately yielding information about the depth dependent magnetisation of the sample [3]. By combining PNR with a specially designed cell that applies a thermal gradient to the sample *in-situ* ($\Delta T \neq 0$), it is hoped that the change in magnetisation profile for the $\Delta T = 0$ case compared to the $\Delta T \neq 0$ case may be observed – providing a direct measurement of the SSE.



Magnetism 2018

We will present results detailing the development of the thermal cell sample environment and methodology. This will include provisional in-situ SSE-PNR measurements for a variety of NM/FM bi-layer and multilayer SSE devices (including Pt/FeOx bi-layer devices previously investigated here [4]), which show subtle differences between the $\Delta T=0$ and $\Delta T \neq 0$ cases. Finally, we will discuss the potential experimental and physical interpretations of these results.

- [1] K. Uchida *et al*, *J. Phys. Condens. Matter*, 26, 343202 (2014)
- [2] J.F. Ankner, G.P. Felcher, *Journal of Magnetism and Magnetic Materials*, 200, 741-754 (1999)
- [3] S. J. Blundell and J. A. C. Bland, *PRB*, 46, 3391 (1992)
- [4] A. Caruana *et al.*, *PSS: RRL*, 10, 623-617 (2016)

P:40 Dynamic modelling of spin accumulation

L Elliot, R Chantrell and R Evans

University of York, UK

The burgeoning field of spintronics offers exciting possibilities for new technologies, having already found great success in GMR read heads. In exploring these possibilities, the development of theoretical models capable of accurately describing spin effects become paramount.

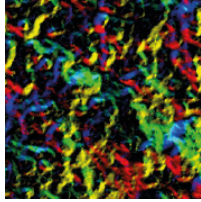
One such area of interest is that of spin transport, the manner by which spin propagates through a system. The constituent phenomena of spin accumulation, whereby spin buildup is observed at the interfaces between ferromagnetic and paramagnetic materials, is the focus of this work.

Spin accumulation is posited as a potential mechanism for the control of magnetic ordering by means of the spin transfer torque effect. This would have significant implications for the development of ultrafast high-density information storage technologies.

Early work is presented detailing current progress on the development of a dynamic model of spin accumulation to be used in computational simulations, representing an advancement on previous work on the equilibrium case.

Success would pave the way to complete spintronic device simulation, with implications for cost and development speed of new technologies.

- [1] Zhang, S., Levy, P. M., & Fert, A. (2002). Mechanisms of spin-polarized current-driven magnetization switching. *Physical Review Letters*, 88(23), 236601. <http://dx.doi.org/10.1103/physrevlett.88.236601>
- [2] Chureemart, P., D'Amico, I., & Chantrell, R. W. (2015). Model of spin accumulation and spin torque in spatially varying magnetisation structures: limitations of the micromagnetic approach. *Journal of Physics: Condensed Matter*, 27(14), 146004. <http://dx.doi.org/10.1088/0953-8984/27/14/146004>.



Magnetism 2018

P:41 Manipulating the spin-dependent transport – thin films and β -Tungsten

M Gradhand¹, M Uryszek¹ and D Stewart²

¹University of Bristol, UK, ²Western Digital Company, USA

The spin Hall effect can be exploited to switch the spin orientation of magnetic materials and might be key in future low-power magnetoresistive random access memory (MRAM) devices. In order to achieve that the goal is to maximize the spin Hall angle, defined as the ratio between the induced transverse spin Hall conductivity and the longitudinal electrical conductivity. Various methods have been proposed, impurity doping, thin films and highly resistive materials such as β -W. For ultra-thin films values as high as 0.8 [1] have been predicted but more relevant for applications are the very large spin Hall angles (0.30) in high resistive materials already observed experimentally [2].

Despite this significant progress in manipulating the spin Hall angle there is still a considerable lack in the understanding of the effects in realistic systems. There is a fundamental problem in treating the spin accumulation in thin films theoretically which is key in the description of realistic devices. In addition, the first principles description of highly resistive and often disordered materials is numerically highly demanding and only a few attempts have been made.

Here, we present theoretical work on both aspects treating the spin accumulation in thin films, induced by impurities, as well as the intrinsic spin Hall effect in β -W within a density functional theory Green's function (KKR) method. [3, 4] While the large spin Hall angle in β -W is calculated and confirmed by fully relativistic band structure calculations the spin accumulation in thin films show surprisingly complex and non-intuitive behaviour. All results are supported by the analysis of the relativistic band structure highlighting the significance of spin-orbit induced avoided band crossings. For β -W, we predict spin Hall angles ranging from 0.1 (bulk) to 0.18 (film) in contrast to the low spin Hall angles for α -W ranging from 0.008 (bulk) to 0.021 (film), in agreement with experiment [1].

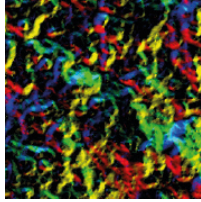
- [1] C. Herschbach et al. *Phys. Rev. B* 90, 180406(R) (2014)
- [2] C. H. Pai et al, *Appl. Phys. Lett.* 101, 122404 (2012)
- [3] M. Gradhand et al., *Phys. Rev. B* 80, 224413 (2009)
- [4] M. Gradhand et al., *Phys. Rev. B* 84, 075113 (2011).

P:42 Simulation study of ballistic spin-MOSFET devices with ferromagnetic channels based on Heusler and oxide compounds

P Graziosi¹ and N Neophytou²

¹CNR – ISMN, Italy, ²University of Warwick, UK

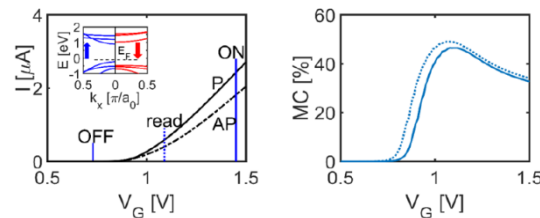
Newly emerged materials from the family of Heuslers and complex oxides exhibit finite bandgaps and ferromagnetic behaviour with Curie temperatures much higher than even room temperature. In this work, using the semiclassical top-of-the-barrier FET model, we explore the operation of a spin-MOSFET that utilizes such ferromagnetic semiconductors as channel materials, in addition to ferromagnetic source/drain contacts. Such a device could retain the spin polarization of injected electrons in the channel, the loss of which limits the operation of traditional spin transistors with non-ferromagnetic channels. We examine the operation of three material systems that are currently considered some of the most prominent known ferromagnetic semiconductors, three Heusler-type alloys (Mn₂CoAl, CrVZrAl, CoVZrAl) and one from the oxide family (NiFe₂O₄). We describe their bandstructures by using data from DFT calculations. We investigate under which conditions high spin polarization and significant $I_{\text{ON}}/I_{\text{OFF}}$ ratio, two essential requirements for the



Magnetism 2018

spin- MOSFET operation, are both achieved. We show that these particular Heusler channels, in their bulk form, do not have adequate bandgap to provide high I_{ON}/I_{OFF} ratios, and have small magnetoconductance compared to state-of-the-art devices. However, with confinement into ultra- narrow sizes down to a few nanometers, and by engineering their spin dependent contact resistances, they could prove promising channel materials for the realization of spin-MOSFET transistor devices that offer combined logic and memory functionalities. Although the main compounds of interest are Mn_2CoAl , $CrVZrAl$, $CoVZrAl$, and $NiFe_2O_4$ alone, we expect that the insight we provide is relevant to other classes of such materials as well. [1]

The following figure shows the simulation for the case of $CrVZrAl$ thin layer channel (band structure in the inset) spin MOSFET. Left: drain current versus gate voltage characteristics at $V_D = 0.75$ V. The vertical solid lines show V_G^{off} and V_G^{on} for which high I_{on}/I_{off} ratio (10^4) is achieved for a bias window $V_G = V_D = 0.75$ V for both orientations. The vertical dotted line represents the 'read' gate bias V_G for memory operation. Right: magnetoconductance (MC) percentage as a function of V_G for $V_D = 0.75$ V. The dotted line represents the MC when taking into account non-parabolicity effects in the $CrVZrAl$ bandstructure.



[1] P. Graziosi and N. Neophytou, J. Appl. Phys. accepted.

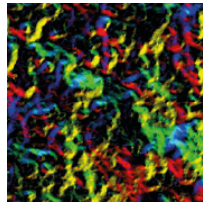
P:43 Exploration of new $L1_0$ -ordered materials for their spintronic applications

D Huskisson, P Thompson and T Thomson

The University of Manchester, UK

Ferromagnetic materials for use in spintronics devices such as spin torque oscillators (STO's) must have a large magnetic anisotropy energy, low magnetic damping coefficient and an appropriate magnetisation [1]. $L1_0$ -ordered FePt, CoPt and FePd have the desired high anisotropy and can be orientated in the perpendicular direction [1-3]. However, due to the heavy metal elements of Pt and Pd their damping factor is much larger than required for practical STO's. Mn-based alloys such as $L1_0$ -MnAl [1-3] and $L1_0$ -MnGa [4-6] are heavy metal free and show a large magnetic anisotropy energy and small damping [1-3]. A combination of Low damping and moderate magnetisation produces a low critical switching density useful for devices based on MTJ such as spin torque transfer magnetic random-access memory (STT-MRAM) and STO's [1].

The nature of spintronics devices, which relies on spin engineering at the interfaces dictate that only thin film materials can be used. In this work, we report some initial findings on the potential of MnAl as a thin film material for spintronic applications. However, ferromagnetic thin films of MnAl are metastable during deposition and this complicates the fabrication process. Sample deposition conditions are therefore key in determining the magnetic properties of thin films [1-3]. Vibrating Sample Magnetometer (VSM) measurements performed on a thin film structure of MgO(substrate)/MnAl(50nm), using co-sputtering from Mn and Al elemental targets, show varying saturation values for different deposition parameters:



Magnetism 2018

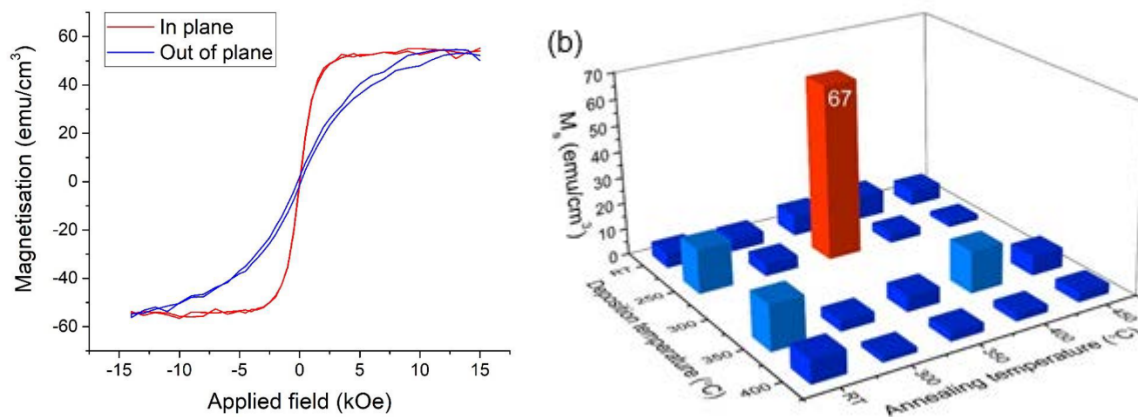


Figure 1: (a) Room temperature hysteresis loop measured using a VSM. (b) Magnetisation data exploring the deposition parameter space.

An example of the correlation between deposition/annealing temperatures and the magnetic properties of the MnAl thin films is shown in figure 1(b). These measurements to optimise the deposition and annealing processes allow thin films to be varied with the goal of creating very thin films with saturation magnetisation close to the literature values of 550 emu/cm³ [1-3]. Due to the complex fabrication only limited results have been reported to date [1-3]. The aim of this research is to more thoroughly explore the fabrication parameter space of MnAl thin films. For example, through various seed layers and additional elements to the MnAl layer to help the deposition process and encourage L1₀ phase growth increasing the samples magnetic properties.

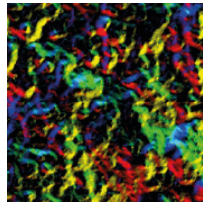
- [1] Saruyama, H et al. Japanese Journal of Applied Physics, 52(6R), p.063003. (2013)
- [2] Watanabe K et al. Japanese Journal of Applied Physics, 56(8), pp.0802B1. (2017)
- [3] Huang, E. and Kryder. IEEE Transactions on Magnetics, 51(11), pp.1-4. (2015)
- [4] F. Wu et al. Applied Physics Letter 94 122503. (2009)
- [5] S. Mizukami et al. Physics Review Letter 106 117201. (2011)
- [6] J. H. Park et al. Japanese Journal of Applied Physics, 107 09A731. (2010).

P:44 Finite size effects in antiferromagnetic materials

S Jenkins, R W Chantrell and R F L Evans

University of York, UK

Antiferromagnetic spintronics is a newly emerging field which has renewed interest in antiferromagnetic (AFM) materials. This is because they are resistant to perturbation from magnetic fields, they display ultra fast dynamics and interesting magnetotransport effects. The Néel temperature is the anti-ferromagnetic equivalent of the Curie temperature and sets the thermal threshold for data retention in a device. Most spintronics applications are for ultrathin films and therefore the finite size dependence of the Néel temperature is important for device operation. For the technologically relevant AFM γIrMn_3 , the bulk Néel temperature is around 750K, but it has been proposed that it is strongly thickness dependant[1]. Here we have developed atomistic spin models of two technologically important antiferromagnets γIrMn_3 and Mn_2Au , considering localised atomic spin moments coupled with Heisenberg exchange[2]. The temperature dependent properties of the system is simulated using a metropolis Monte Carlo algorithm. Our model successfully reproduces the magnetic ground state spin configurations and bulk Néel temperatures of γIrMn_3 and Mn_2Au . We have performed a systematic study of the thickness dependence of the Néel temperature, shown in Fig. 1. The finite size effect is small for this material except for the smallest film thicknesses, where a catastrophic drop



Magnetism 2018

in the Néel temperature is seen. We have found that this is due to the existence of point defects at the surface which leads to large fluctuations of surface spins. We will also present results on the effects of interface mixing and comparative results for $L1_2$ ordered IrMn thin films.

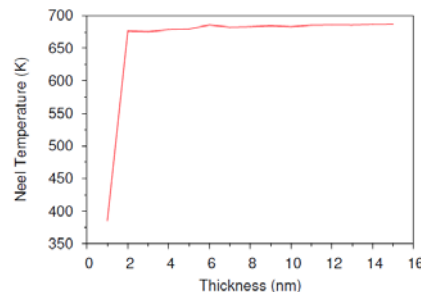


Figure. 1: Thickness dependance of the Néel temperature for γ - IrMn₃

- [1] L. Frangou, S. Oyarzun, S. Auffret, L. Vila, S. Gambarelli, and V. Baltz. Enhanced spin pumping efficiency in anti-ferromagnetic irmn thin films around the magnetic phase transition. *Phys. Rev. Lett.*, 116:077203, Feb 2016. doi: 10.1103/PhysRevLett.116.077203. URL <https://link.aps.org/doi/10.1103/PhysRevLett.116.077203>.
- [2] Evans R F L, Fan W J, Chureemart P, Ostler T A, Ellis M O A, and Chantrell R W. Atomistic spin model simulations of magnetic nanomaterials. *Journal of Physics:Condensed Matter*, 26, 2014.

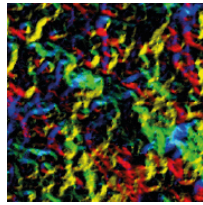
P:45 Magneto-optical detection of spin accumulation under the influence of mechanical rotation

J-y Kim¹, Y Baba², B A Murphy¹, B Ng³, Y Yao³, K Nagao² and A Hirohata¹

¹University of York, UK, ²Nagaoka University of Technology, Japan, ³City University of Hong Kong, Hong Kong

Generation of spin-polarised carriers in non-magnetic materials holds the key to realise highly efficient spintronic devices. To date, spin currents have been generated predominantly by spin injection from a ferromagnet, application of electro-magnetic fields, Zeeman splitting and thermal gradients [1, 2]. Recently, it has been shown that large spin-orbit coupling can induce spin-polarised currents in rotating noble metals such as tungsten and platinum [3].

In this study, we have developed a highly sensitive magneto-optical set-up to measure a mechanically-induced spin current in a paramagnetic foil [4]. The schematic of the set-up can be seen in Fig. 1(a). Samples were mounted on NdFeB magnets fixed on a carbon-fibre plate which rotated at frequencies up to 210 Hz. Fig. 1(b) shows representative MOKE signals from a Pt foil on a 5 kOe magnet, where the inset plots gradients of the MOKE signal against rotation frequency on different magnets. Signs of higher order dependencies at fields stronger than 4 kOe suggest spin accumulation due to mechanically-generated spin currents. The magnitude of the effect is expected to increase with a larger rotational diameter and a higher angular velocity. Our experiment offers a noble method to investigate mechanical generation of spin-polarised currents via optical detection of spin accumulation.



Magnetism 2018

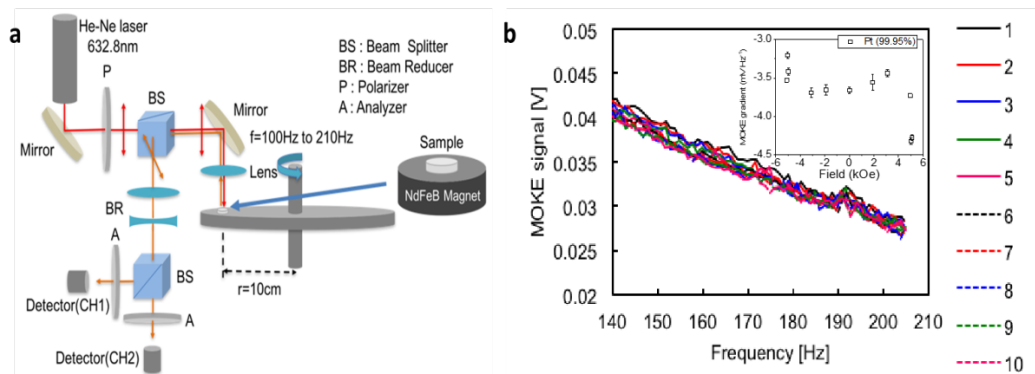


Figure 1 (a) Magneto-optical Kerr effect measurement set-up and (b) representative MOKE signals of a Pt foil on a 5 kOe magnet. (Inset) MOKE signal gradients against rotation frequency with different magnet strengths.

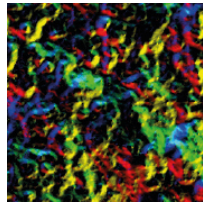
- [1] Maekawa, S., Valenzuela, S. O., Saitoh, E., & Kimura, T. (Eds.), Spin Current, page 48-68 (Oxford University Press, Oxford, 2012).
- [2] Hirohata, A. & Takanashi, K., *Journal of Physics D: Applied Physics*, 47, 193001 (2014).
- [3] Matsuo, M., Ieda, J., Saitoh, E. & Maekawa, S., *Physical Review Letters* 106, 076601 (2011).
- [4] Hirohata, A., Baba Y., Murphy B. A., Ng B., Yao Y., Nagao K. & Kim J.-y., *Scientific Reports* 8, 1974 (2018).

P:46 Proximity induced magnetization in Co₂FeAl ultrathin films: effects of the annealing temperature and the heavy metal material

A Mora-Hernández¹, B Nicholson¹, O-O Inyang¹, A T Hindmarch¹, L Bouchenoire² and C J Kinane³

¹Durham University, UK, ²XMaS, European Synchrotron Radiation Facility, France, ³Rutherford Appleton Laboratory, UK

Proximity Induced Magnetization (PIM) is important for spintronics as it may determine the interface transparency to spin-currents [1] and influence interfacial Dzyaloshinskii-Moriya interactions [2]. We have studied PIM in Pt and Ir layers adjacent to Co₂FeAl (CFA) ultrathin films. Two different sample structures, Pt/CFA/MgO (PIM-Pt) and Ir/CFA/MgO (PIM-Ir), are investigated; each with a duplicate to which an anneal process has been made. The depth-resolved magnetism has been measured using Polarised Neutron Reflectivity (PNR). PIM-Pt samples were ferromagnetic in both as-deposited (figure 1) and annealed cases, but the annealed PIM-Ir sample showed no magnetism at room temperature [3]. It appears that Ir is diffusing into the ferromagnetic CFA layer during the thermal process, removing the CFA magnetization [4]. The presence of PIM in these materials is confirmed using x-ray resonant magnetic reflectivity (XRMR). Very strong PIM is found for PIM-Pt (figure 2), PIM-Ir and PIM-Pt annealed, but no PIM is induced in Ir for the PIM-



Magnetism 2018

Ir annealed sample due to the absence of magnetism in the CFA layer at room temperature.

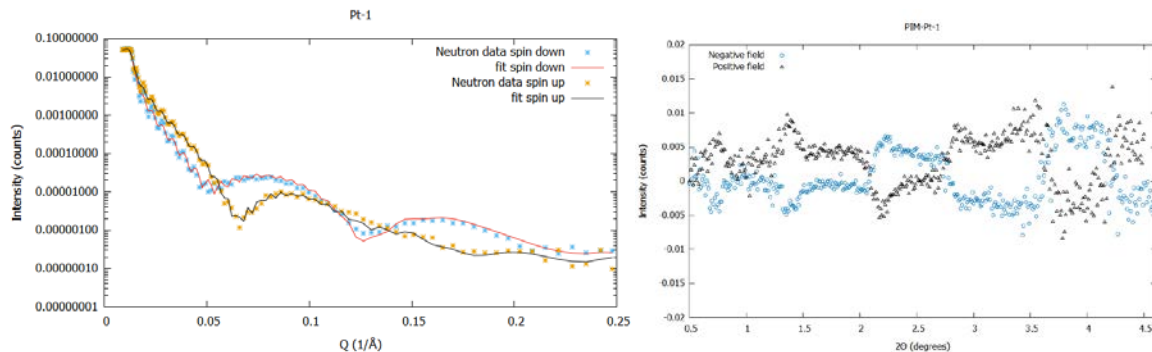


Figure 1. PNR for as-deposited PIM-Pt. Figure 2. XRMR asymmetry (magnetic signal) for as-deposited PIM-Pt

- [1] Nature Physics volume 11, pages 496–502 (2015)
- [2] Scientific Reports volume 7, Article number: 16835 (2017)
- [3] arXiv:1711.07776 [cond-mat.mtrl-sci]
- [4] AIP ADVANCES 7, 115022 (2017)
- [5] Scientific REPORTS | 7: 16835 | DOI:10.1038/s41598-017-17137-z.

P:47 Towards a standard spin seebeck measurement

K Morrison¹, C D W Cox¹, T Rose¹ and A J Caruana^{1,2}

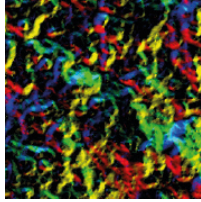
¹Loughborough University, UK, ²STFC Rutherford Appleton Laboratory, UK

It was recently demonstrated that a thermal gradient applied across a magnetic material can result in the generation of a spin polarised current: the spin Seebeck effect (SSE) [1]. This is observed indirectly by placing a heavy metal such as Pt in direct contact with the magnetic material such that a voltage, V_{ISHE} , is generated by the inverse spin Hall effect. One application of this effect is waste heat harvesting technologies (thermoelectrics)[2].

For conventional thermoelectrics, the figure of merit, zT , has proven especially useful as a single parameter to assess the efficiency of potential materials. For example, it allows engineers to separately assess thermal expansion matching and efficiency of operation when choosing materials for the p- and n- type pillars of a typical Peltier cell. So far, however, there is no such single measurement for spin Seebeck based thermoelectrics.

Measurements of the SSE are typically conducted as a function of magnetic field, B , and temperature difference, ΔT , across the device, as shown in Figure 1a. For thin films this results in a substrate dependant contribution to the SSE due to a trade-off between the heat flow, q , and the temperature differences across the active material (ΔT_2) and the substrate itself (ΔT_3) [3].

Overall, there are a myriad of variables that affect the magnitude of the observed voltage in a spin Seebeck measurement. This includes, but is not limited to: the thickness of the magnetic material; the thickness of the Pt detection layer; the contact separation; the thermal conductivities of the layers; the spin diffusion length, spin Hall angle and spin mixing conductance; and the roughness of the interface. If we are to start comparing spin Seebeck measurements we need to find a standard measurement (and normalisation) procedure.



Magnetism 2018

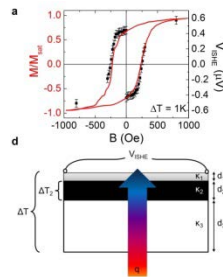


Figure 1: (a) Example spin Seebeck measurement for 79nm Fe_3O_4 : 2.5nm Pt, and (b) schematic showing the measurement geometry for a thin film spin Seebeck device where layer 1 = Pt, layer 2 = Fe_3O_4 and layer 3 = the substrate.

Here we will present results from measurement of bulk and thin film spin Seebeck effect, where we demonstrate the importance of the heat flow for normalisation of SSE measurements. Finally, we will discuss the surprising result that the voltage, V_{ISHE} , is scaled not just by the contact separation and device thickness, but the area (of the device) as well.

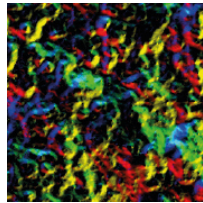
- [1] G.E.W. Bauer *et al.*, Nat. Mater. 11, 391 (2012)
- [2] K. Uchida *et al.*, Appl. Phys. Exp. 5, 093001 (2012)
- [3] A.J. Caruana *et al.*, Phys. Status Solidi RRL 10, 613-617 (2016).

P:48 Investigating the role of Ga-substitution in $Fe_{1-x}Ga_x$ (Galfenol) thin films

S Roy, D P Pattnaik, K W Edmonds and A W Rushforth

University of Nottingham, UK

Magnetostrictive thin films are of interest for a range of applications, including the development of magnetisation based information storage devices. A promising candidate is Galfenol which is an alloy of Fe and Ga, and has been demonstrated[1] to have a very high magnetostriction coefficient. Magnetostriction in bulk Galfenol has been widely studied, but only recently the study of epitaxial grown thin films have come to light. The first measurement of magnetostriction in epitaxial thin films was reported recently by Parkes *et.al*[2] who found that epitaxial thin films of $Fe_{81}Ga_{19}$ show magnetostriction values as large as the bulk material. We have investigated the role of Ga substitution on the magnetic anisotropy and the magnetisation reversal of sputter grown thin films of $Fe_{1-x}Ga_x$ ($x=70$ to 93) grown on GaAs substrates. Longitudinal Magneto-optical Kerr Effect (MOKE) measurements (Figs. 1 and 2) reveal that the anisotropy evolves from cubic to isotropic as the Ga concentration increases.



Magnetism 2018

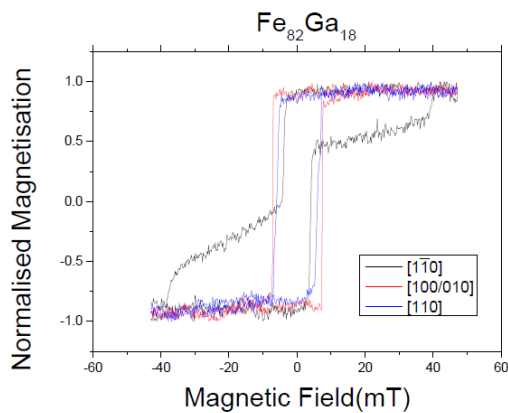


Fig. 1: Longitudinal MOKE at low Ga concentration.

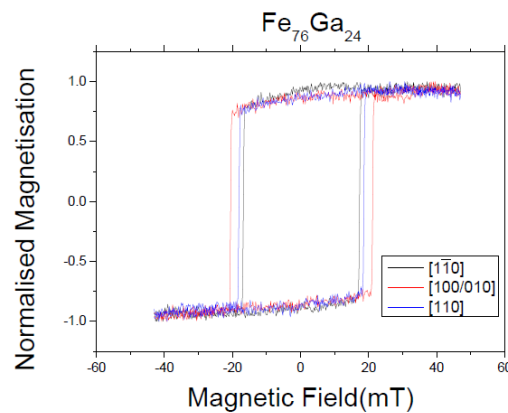


Fig. 2: Longitudinal MOKE at high Ga concentration.

- [1] Wu Ruqian, "Origin of Large Magnetostriction in FeGa Alloys." *Journal of Applied Physics*, 91, 7358 (2002).
- [2] D.E. Parkes, et al., "Magnetostrictive Thin Films for Microwave Spintronics." *Scientific Reports*, 3, 10.1038, 2013.

P:49 Theory of power combining of spin-torque nanooscillators

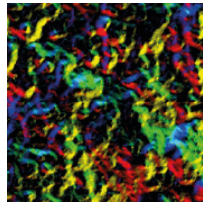
A R Safin, N N Udalov and M V Kapranov

National Research University "MPEI", Moscow, Russia

Synchronization between mutually coupled nonlinear oscillators is a very important and universal concept in many branches of physics, biology, chemistry, economics, and other sciences. Networks of oscillators have been studied for many years, due to their wide applicability and potentiality, such as laser arrays, Josephson junctions, neural networking, spintronic nanooscillators and artificial intelligence (AI) design, etc. The authors predominantly study the single-frequency (or single-mode) regime, when synchronization between oscillators in the network occurs only on one frequency. Also, it is assumed that the majority of oscillators are identical or nearly identical, and weakly coupled. However, there are many systems in different scientific branches, which are able to work on two (double-mode) or many (multi-mode) frequencies. Such a situation can be observed in modern neuro-inspired computing and AI-design, where neuronal network activity is observed across different frequency ranges.

In real networks as there are as many frequencies (we will call modes) as the number of oscillators. When more than two oscillators are mutually coupled the finding of each mode structure and determination of their (or group of them) stability become the main problem to be clarified. When the dissipation parameter is small enough, one can use the linear normal mode formalism to analyze the dynamics of the network of oscillators [9]. If this condition is not satisfied, then one can use the nonlinear normal mode formalism, which is much harder than the linear one. In general, the majority of the networks have the small dissipation parameter; therefore, it is possible for these systems to use the linear normal mode formalism.

The purpose of this paper is to analyze the structure of linear normal mode and their stability in different type of networks of nonlinear microwave oscillators, from simple to complex cases. We investigate how does network topology influence modes stability for the microwave oscillators. We show the impact of degeneration and synchronization of oscillation modes to the problem of optimal bio-inspired network



Magnetism 2018

design and microwave synthesizers. We find that hierarchical networks are characterized by a smaller number of stable nontrivial modes than partially hierarchical or randomly organized networks. Our analysis gives rise to an approach to specify topological transformations of networks that can enhance synchronization.

In this work we investigate that network topology influences very strong to the modes stability for the nonlinear limit-cycles oscillators. We find that hierarchical networks are characterized by a smaller number of stable nontrivial modes than partially hierarchical or randomly organized networks. Our analysis gives rise to an approach to specify topological transformations of networks that can enhance synchronization. In particular, for the task of power summation and mutually phase locking, it is better to use the hierarchically organized network, where the number of degenerate modes is high. From the other hand for the task of multimode communication it is better to use randomly distributed networks, because the number of degenerate modes is low.

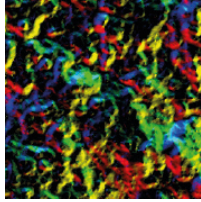
This work is supported by a Russian President grant for young scientists (project No MK-7026.2016.8).

P:50 Current-induced domain-wall motion in pinned magnetic wires

M Samiepour¹, J Y Kim¹, I Polenciuc¹, T Hayward², D A Allwood², G Vallejo-Fernandez¹, K O'Grady¹ and A Hirohata¹

¹University of York, UK, ²University of Sheffield, UK

In racetrack memory [1] digital data is stored in a series of magnetic domain walls (DWs) in ferromagnetic nanowires. The racetrack memory operates on the base that the DWs can be moved along the nanowires by passing a current through the wire. When a current is applied to a ferromagnetic nanowire, it becomes spin-polarised. The interaction between angular momentum of spin-polarised electrons and the DW, induces a torque on the magnetic moments in the DW and move the DW. Therefore, the racetrack memory is a solid state device without moving parts and can operate faster than hard disk drives (HDDs). In our previous work, we have fabricated a simple pinning scheme for the DWs in straight wires using exchange bias. We have patterned IrMn antiferromagnetic (AF) wires with different widths perpendicularly above and below the CoFe ferromagnetic (F) wires. The AF wires induce exchange bias at AF/F crossing points which act as pinning sites. In the racetrack memory having uniform domain wall pin is essential to control the motion of DWs along the nanowires [3]. Prior to the fabrication of our devices, a vibrating sample magnetometer (VSM, ADE, Model10) was used to characterise an unpatterned continuous film to estimate the pinning strength. The magnetisation curves for the unpatterned films exhibits a loop shift of $H_{ex}=46$ Oe which is induced by the exchange bias at the CoFe (10nm) / IrMn (5nm) interface [2]. Focused Magneto-Optical Kerr Effect (MOKE) was used to measure local magnetic properties of the FM wires in different devices with four AF wire widths of 1, 1.5, 2, 2.5 μm . The unset racetrack devices show a very small degree of pinning as expected. For the bottom-biased devices, pinning fields increase only slightly with increasing AF wire width. For the top-biased devices, the pinning is larger than that for the bottom-biased structure. These previous results prove that such a structure is ideal for producing DW pins with controlled strength. Following this study we designed a L-shaped magnetic wire with a round corner with a diameter of 650 μm , in which one end of the wire is connected to a diamond shaped pad (1.5 μm square) to inject DW and the other end is a sharp arrow to prevent the nucleation of DW. The SEM image of device is shown in Figure 1. We observed that exchange bias gives rise to the domain wall pin therefore we used IrMn bars to pin the DW in our new devices. In this study we fabricated a variety of devices with different AF widths between 100 nm and 500 nm deposited on the 500 nm width F layer. We will report details of current-induced domain wall displacement measured in these devices.



Magnetism 2018

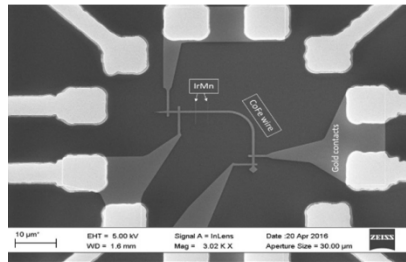


Figure 1: SEM image of actual device. The L-shaped CoFe wire contains the injector diamond shaped pad and the sharp arrow at the end. The two IrMn bars are 100 nm and 200 nm wide. The electrical current are applied to the wire by the gold contacts.

- [1] S. S. P. Parkin, M. Hayashi, and L. Thomas, Science 320 (2008) 190.
- [2] I. Polenciuc, A. J. Vick, D. A. Allowood, T. J. Hayward, G. Vallejo-Fernandez, K. O'Grady, and A. Hirohata, Applied Physics Letters 105 (2014) 162406.
- [3] M. Hayashi, L. Thomas, R. Moriya, C. Rettner, and S. S. P. Parkin, Science 320 (2008) 209.

P:51 Current biased splitting in the Peltier signal observed using lateral spin valves

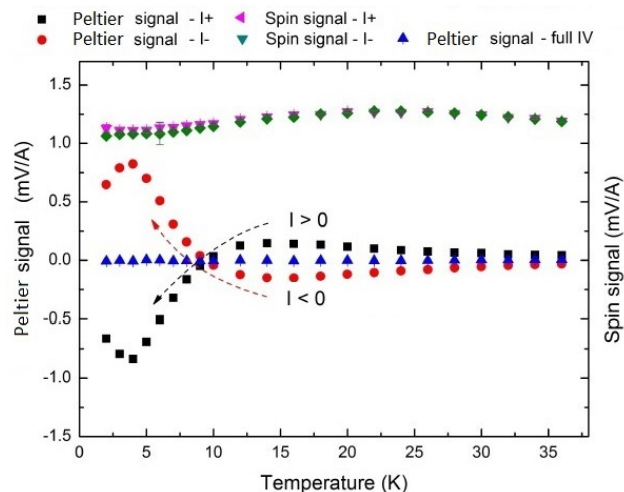
G K Stefanou¹, K A Moran¹, J T Batley³, M Ali¹, M C Rosamond², G Burnell¹ and B J Hickey¹

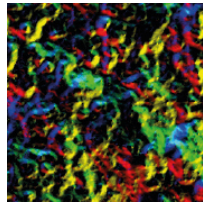
¹University of Leeds, UK, ²University of Minnesota, USA

Along with the pure spin current that can be generated using a lateral spin valve, thermal effects arise as well[1,2]. Although they started attracting more attention, there are fundamental properties of those that have not been fully understood.

The Peltier effect is responsible for a thermal offset present in the spin current voltage as a function of temperature of a lateral spin valve[3]. Since the Peltier effect is linear in the current direction, we find a surprising current dependence in the Peltier signal that persists up to 270 K (see fig.1). The phenomenon is independent of the magnetic field used to switch the injector and detector electrodes.

We study this new effect as a function of ferromagnetic separation, temperature and material combination to find the origin of this unusual effect.





Magnetism 2018

Figure 1: Spin and Peltier signal measured using a Py/Ag/Py lateral spin valve. The spin signal remains unaffected for the different current directions, while the Peltier signal splits into two different branches.

- [1] F. Casanova et al, PRB 79, 184415 (2009).
- [2] S. Kasai et al, APL 104, 162410 (2014).
- [3] F. L. Bakker et al, PRL 105, 136601, (2010).

P:52 XMCD studies of heavy-metal/ferromagnet heterostructures

L Stuffers¹, H Ohldag², K Morrison¹ and N Banerjee¹

¹Loughborough University, UK, ²Stanford Synchrotron Radiation Laboratory, USA

Heavy normal metal(HNM)/Ferromagnet(FM) heterostructures exhibit tuneable perpendicular magnetic anisotropy and Rashba spin-orbit coupling due to structural inversion asymmetry. Recently, a fundamental connection was discovered between triplet superconductivity and spin-orbit coupling using these structures [1], which shows spin-orbit coupling can be used to control triplet superconductivity [2]. In view of the importance of HNM/FM structures in spintronics and superconducting spintronics, it is essential to understand the origin of spin-orbit coupling in these structures.

Here, we use X-ray Magnetic Circular Dichroism (XMCD) to measure spin and orbital moments of HNM/FM/HNM tri-layers and to measure the orbital moment anisotropy as a function of the FM layer thickness and nature of the HNM.

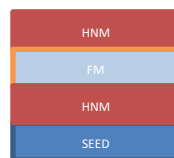


Figure 2- Heterostructures grown by sputtering analysed.

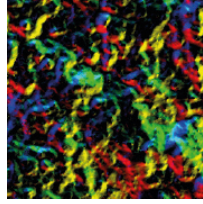
- [1] Banerjee, N. *et al.*, arXiv:1709.03504 (2017)
- [2] S.H.Jacobsen, J.A.Ouassou, and J.Linder, Phys. Rev. B. 92, 024510 (2015).

P:53 Paramagnetic spin hall magnetoresistance

A L Westerman, M Ali and B J Hickey

University of Leeds, UK

Bilayers of a magnetic insulator and a metal with high spin-orbit coupling have previously been shown to exhibit spin Hall magnetoresistance (SHMR), where the resistance of the metal is altered depending on the relative orientation of the spin polarisation axis and the magnetisation of the insulator [1,2]. We report a new form of SHMR in an ultrathin Pt film with localised Fe impurities at the interface with an Al₂O₃ substrate. A cosine squared dependence of the resistivity on the angle in the transverse-perpendicular (yz) plane develops due to the paramagnetic spin Hall magnetoresistance (PSHMR), not previously reported. Its magnitude is comparable to the SHMR in YIG/Pt bilayers [3] with a strong dependence on both temperature and concentration. An anisotropic magnetoresistance is observed in the longitudinal-perpendicular (xz) plane only below 100 K, as observed previously in YIG/metal bilayers [4, 5]. The PSHMR is shown to be present in measurements of the SHMR in YIG/Pt bilayers; various interface preparation



Magnetism 2018

methods lead to a field-dependence of the SHMR. This additional contribution is found to share the PSHMR temperature dependence and to be strongly dependent upon the interface preparation method. Hence measurements of the SHMR are susceptible to an additional contribution from the PSHMR which is dependent upon the magnitude of the applied field in a paramagnetic manner.

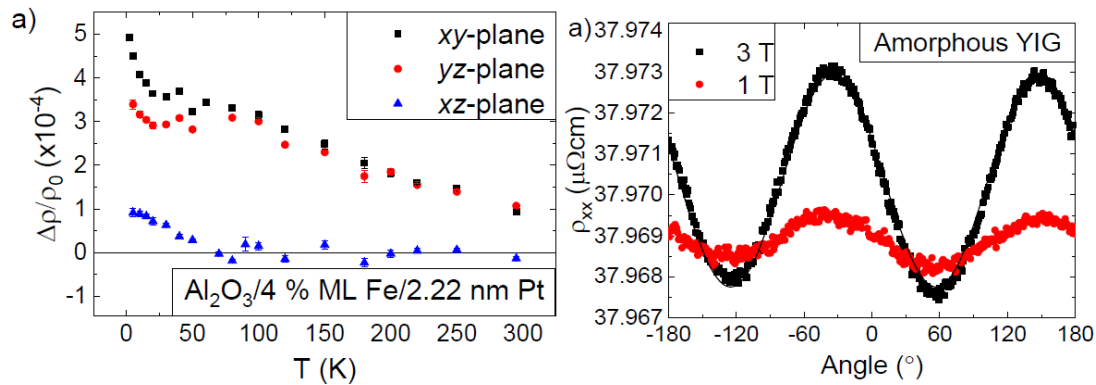


Fig. 1: The angle dependent magnetoresistance in 2.22 nm Pt with a) 4 % of a monolayer (ML) of Fe beneath on an Al₂O₃ substrate as a function of temperature at an applied field of 3 T and b) as a function of angle in the yz plane and applied field for 2.22 nm Pt on GGG/36 nm amorphous YIG at 100 K. The PSHMR

- [1] PRL 110, 206601 (2013).
- [2] PRB 87, 144411 (2013).
- [3] PRB 89, 220404 (2014).
- [4] PRL 113, 037203 (2014).
- [5] PRB 94, 174405 (2016).

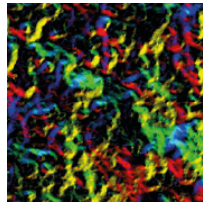
P:54 Multilayers for skyrmion-based devices

Y Zang, T Thomson and C Moutafis

The University of Manchester, UK

The current magnetic recording technology such as perpendicular magnetic recording (PMR), was proposed in 1970s and firstly introduced into the market in 2006 [1]. PMR offers a better signal to noise ratio (SNR) compared to the last generation data storage technology and also improves storage density and thermal stability. However, PMR is close to reaching its limits opening an opportunity for alternative technologies to be explored. One promising next generation data storage technologies recently proposed is the use of the magnetic skyrmion in devices with enhanced functionality. In skyrmion-based devices, skyrmions are used as information carriers. There are two types of skyrmions, Bloch-type and Néel-type, as shown in Figure 1 [2]. The size of the skyrmions is small and the information density can be extremely high. Magnetic skyrmions are swirling spin texture with particle-like properties. The swirling spin texture leads to a topologically protected field [2,3]. Skyrmions can be created in a non-centrosymmetric magnet with broken symmetry and the Dzyaloshinskii-Moriya interactions (DMI) [4].

At present, there are still many challenges in the material systems and device structures in order to exploit the huge potential for skyrmions [3,5]. The most widely used skyrmion systems are B20 material (MnSi), monolayers (Fe) or bilayers (Fe/Pd) of ferromagnetic materials, inversion-symmetry-broken multilayers (Pt/Co/Ta) [3,6]. By engineering asymmetric multilayers, sub-100 nm confined skyrmions were observed at room temperature due to the additive interfacial chiral interactions [6]. At the same time, another group



Magnetism 2018

found asymmetric multilayers can host skyrmions at room temperature without any external fields [7]. According to their simulation, the size of skyrmions can reach 10 nm by adjusting relevant parameters. In this contribution, our initial studies aimed at addressing some of the challenges in the tailoring of multilayers for hosting skyrmions will be presented.

a) Bloch-type skyrmion b) Néel -type skyrmion

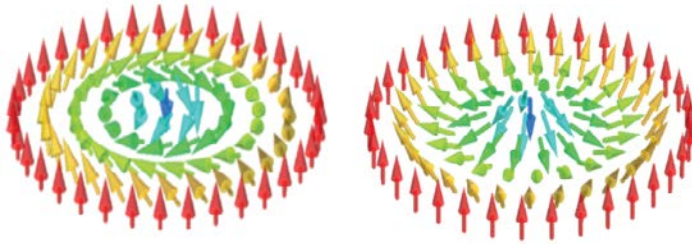


Figure 1. Bloch-type and Néel-type skyrmion. In the Bloch-type and Néel-type skyrmions, spin points at up direction at the edge, points at down direction at the core and rotates from the core to the edge. Figure was taken from [3].

- [1] Piramanayagam, S. and Chong, T. (2012).
- [2] Fert, A. et.al. Nature Reviews Materials, 2(7), p.17031 (2017).
- [3] Nakajima, T. et.al. Science Advances, 3(6), p.e1602562 (2017).
- [4] Seki, S and Mochizuki, M. (2016).
- [5] Kang, W. et.al. Proceedings of the IEEE, 104(10), pp.2040-2061(2016).
- [6] Moreau-Luchaire, C. et al. Nature Nanotechnology, 11(5), 444-448. (2016).
- [7] Boulle, O. et al. Nature Nanotechnology, 11(5), 449-454. (2016).

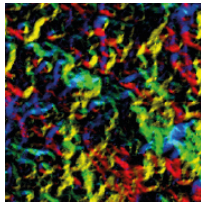
P:55 Muon measurements of magnetism in the frustrated spin-chain compound $\text{Sr}_3\text{NiIrO}_6$

J A T Barker¹, J Sannigrahi² and D T Adroja²

¹Paul Scherrer Institut, Switzerland, ²STFC Rutherford Appleton Laboratory, UK

The Ising-like spin-chain material $\text{Sr}_3\text{NiIrO}_6$ is a member of a family of oxides that have attracted much attention, as they exhibit a wide variety of unconventional magnetic properties. The structure consists of alternating IrO_6 distorted octahedra and NiO_6 trigonal prisms arranged in chains along the c -axis, with Sr spacers dispersed between the chains. A complicated magnetic structure arises as a result of the interplay between low-dimensionality, magnetic frustration, and magneto-crystalline anisotropy.

We have performed muon-spin spectroscopy measurements on a polycrystalline sample of $\text{Sr}_3\text{NiIrO}_6$, as a complement to neutron measurements of this material [1]. By analyzing the internal fields experienced by implanted muons (see Fig. 1), we show that this system appears to have two distinct regions in the magnetic phase diagram: a frozen regime below about 40 K, and a highly dynamic region between 40 and 70 K. We compare our results to those from the neutron study, and attempt to find a description of this system that satisfies all experimental observations to date.



Magnetism 2018

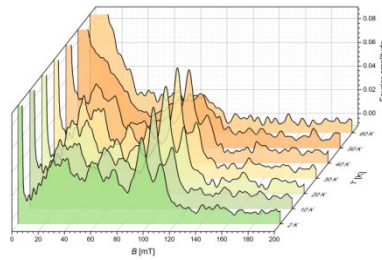


Figure 3: Waterfall plot of the internal field distribution experienced by muons in $\text{Sr}_3\text{NiIrO}_6$.

[1] Lefrançois, E., Chapon *et. al.*, Phys. Rev. B 90, 014408 (2014).

P:56 Towards control of uniaxial anisotropy in $S=1$ magnetic systems

S P M Curley¹, R C Williams¹, P A Goddard¹, W J Blackmore¹ and J L Manson²

¹University of Warwick, UK, ²Eastern Washington University, USA

Tuning uniaxial anisotropy D within $S=1$ materials can allow access to exotic ground states, such as the Haldane gapped state in quasi-one-dimensional systems [1-2]. We have studied several low-dimensional systems based upon $S=1$ Ni^{2+} ions, connected via molecular bridging ligands, to establish if the magnitude and sign of D can be chemically controlled from the point of synthesis. Currently we are investigating two compounds which contain NiF_2 octahedral coordination environments; $[\text{NiF}_2(3,5\text{-lut})_4]\cdot\text{H}_2\text{O}$ and $\text{Ni}(\text{HF}_2)_2(3,5\text{-lut})_4$ (where 3,5-lut = 3,5-lutidine, chemical formula $\text{C}_7\text{H}_9\text{N}$). Comparison to prior work on materials sharing this environment [3] should move towards a better understanding, and thus control, of the anisotropies within these materials.

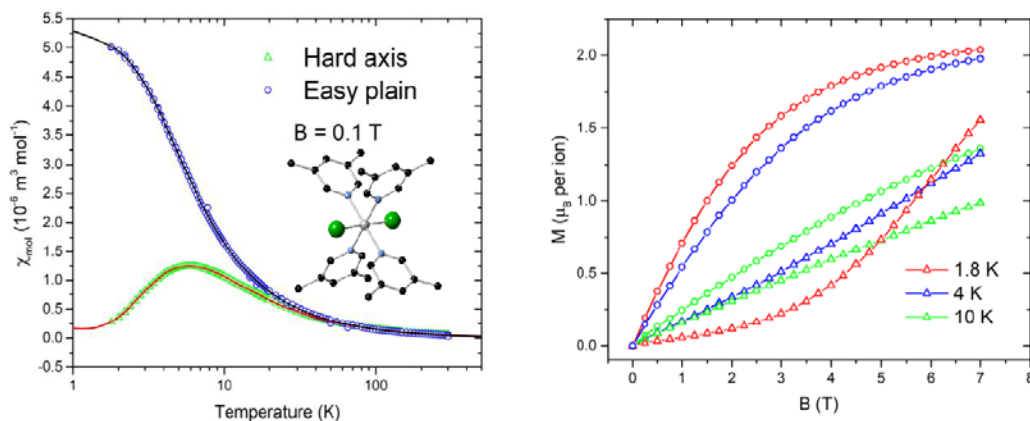
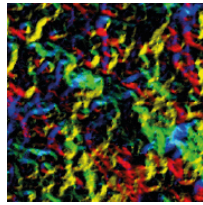


Figure 1: SQUID magnetometry data for $[\text{NiF}_2(3,5\text{-lut})_4]\cdot\text{H}_2\text{O}$ with hard (easy) axis orientation denoted by triangles (circles) a) Susceptibility plot where solid lines denote a fitting function used to extract D . Inset is local Ni environment with hydrogens and water molecules omitted. b) Magnetisation curves at fixed temperatures.

- [1] M. Enderle, M. Kenzelmann and W.H. Buyers. arXiv:1711.03862v1, (2017)
- [2] K. Wierschem and P. Sengupta. Mod.Phys.Rev.Let.B, 28:1430017, (2014)
- [3] J. Brambleby, P. A. Goddard, J. Singleton, M. Jaime, T. Lancaster, L. Huang, J. Wosnitza, C. V. Topping, K. E. Carreiro, H. E. Tran, Z. E. Manson, and J. L. Manson. Phys. Rev. B, 95:024404, (2017).



Magnetism 2018

P:57 Intermediate magnetic phase of charge-stripe ordered $\text{La}_2\text{NiO}_{4.11}$ and the trigger for static magnetic ordering

P G Freeman¹, M Skoulatos², R A Mole³ and D Prabhakaran⁴

¹University of Central Lancashire, UK, ²Technical University of Munich, Germany, ³Bragg Institute, Australia, ⁴Oxford University, UK

Two decades after the discovery of charge-stripe order in a La-based cuprate, the roll of charge-stripes in cuprate high temperature superconductors remains unresolved [1]. La-based cuprates are poor cuprate superconductors with superconductivity only observed below 40 K. The lower superconducting transition temperature of La-based cuprates is matched by only having a partial gapping of the magnetic excitation spectrum caused by superconductivity[2]. This allows the magnetic excitations of La-based to be studied to lower energies than in other cuprate materials[2], with these excitations often compared to the magnetism of charge-stripe ordered $\text{La}_{2-x}\text{Sr}_x\text{NiO}_{4+\delta}$ [1,3].

Advances in understanding the cuprates have been made by observing universal behaviour in several series of materials, such as the hourglass shaped magnetic excitation spectrum [4]. Recent findings include two striking observations at base temperatures in La based cuprates, a low energy kink in the magnetic excitation spectrum [5], and an offset between the centring of low energy magnetic excitations and the position of magnetic Bragg peaks[6]. A combined neutron diffraction, inelastic neutron scattering and μSR study of charge-stripe ordered $\text{La}_2\text{NiO}_{4.11}$, shows similar effects as in the La-based cuprates [5,6]. In $\text{La}_2\text{NiO}_{4.11}$ the offset between the low energy magnetic excitations and the position of magnetic Bragg peaks puts a stricter limit on the origin of this effect. Whilst the temperature evolution of the magnetism identifies an intermediate magnetic phase, and how static magnetic order is triggered in $\text{La}_{2-x}\text{Sr}_x\text{NiO}_{4+\delta}$.

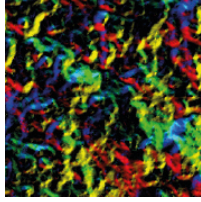
- [1] J. M. Tranquada et. al. Nature 375, 561 (1995).
- [2] M. Kofu, S.-H. Lee, M. Fujita, H.-J. Kang, H. Eisaki, and K. Yamada, Phys. Rev. Lett. 102, 047001 (2009).
- [3] Yoshizawa et. al., Phys. Rev. B 61, R854 (2000).
- [4] S. M. Hayden et al., Nature 429, 531 (2004); J. M. Tranquada, et al., Nature 429, 534 (2004).
- [5] Zhijun Xu, et. al, Phys. Rev. Lett. 113, 177002 (2014).
- [6] H. Jacobsen, et. al., Phys. Rev. Lett. 120, 037003 (2018).

P:58 Magnetic properties of $\text{Sr}_{3-x}\text{Y}(\text{Fe}_{1.25}\text{Ni}_{0.75})\text{O}_{7-\delta}$: a combined experimental and theoretical investigation

S Keshavarz¹, S Kontos¹, D Wardecki^{2,3,4}, Y O Kvashnin¹, M Pereiro¹, S K Panda¹, B Sanyal¹, O Eriksson^{1,5}, J Grins², G Svensson², K Gunnarsson¹ and P Svedlindh¹

¹Uppsala University, Sweden, ²Stockholm University, Sweden, ³University of Warsaw, Poland, ⁴Chalmers University of Technology, Sweden, ⁵Örebro University, Sweden

We present a comprehensive study of the magnetic properties of $\text{Sr}_{3-x}\text{Y}(\text{Fe}_{1.25}\text{Ni}_{0.75})\text{O}_{7-\delta}$ ($0 \leq x \leq 0.75$). Experimentally, the magnetic properties are investigated using superconducting quantum interference device (SQUID) magnetometry and neutron powder diffraction (NPD). This is complemented by the theoretical study based on density functional theory as well as the Heisenberg exchange parameters. Experimental results show an increase in the Néel temperature (T_N) with the increase of Y concentrations and O occupancy. The NPD data reveals all samples are antiferromagnetically ordered at low temperatures, which has been confirmed by our theoretical simulations for the selected samples. Our first-principles



Magnetism 2018

calculations suggest that the 3D magnetic order is stabilized due to finite inter-layer exchange couplings. The latter give rise to a finite inter-layer spin correlations which disappear above the T_N .

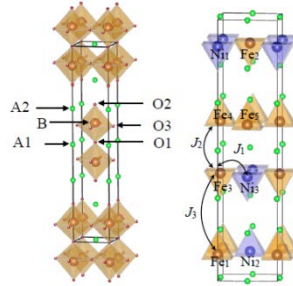


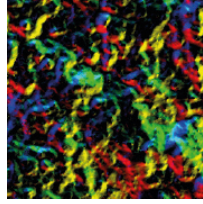
Figure 1. crystal structure of the ideal A3B2O7 RP structure: A1 and A2 are the alkaline/rare earth elements and the octahedra are surrounding the transition metal elements. Right) the simulated structure.

The converged electronic structure of the system in LDA+ U has been used to extract the exchange parameters. This is done through mapping the magnetic excitations onto the Heisenberg Hamiltonian.

$$\hat{H} = -\frac{1}{2} \sum_{i \neq j} J_{ij} \vec{S}_i \vec{S}_j, \quad (1)$$

where J_{ij} is the exchange parameter between two spins, located at sites i and j . The exchange parameters were computed using a formalism initially suggested in Ref. [1] and adapted for the current bases set in Ref. [2].

The magnetic properties of $\text{Sr}_{3-x}\text{Y}_x(\text{Fe}_{1.25}\text{Ni}_{0.75})\text{O}_{7-\delta}$ ($0 \leq x \leq 0.75$) and $0 < \delta < 1$) as obtained from SQUID magnetometry and NPD have been presented. The results are in good agreement with the *ab initio* calculations based on DFT+ U that provide magnetic moments and Heisenberg exchange parameters. Both the calculated magnetic moments as well as the ordering temperature are in acceptable agreement with observations. All the studied samples are antiferromagnetically ordered at low temperatures showing an increase in the ordering temperature with Y concentration. Due to no visible asymmetry in the magnetic Bragg profiles, the NPD results strongly indicate 3D magnetic ordering. As opposed to many other RP systems reporting 3D magnetic ordering stabilized by magnetic dipole-dipole interaction, the observed 3D AFM ordering in the samples studied here is attributed to the inter-layer exchange coupling that our theoretical calculations show is not negligible. As a result of the finite interlayer exchange interaction, we observe significant spin-spin correlations among magnetic moments in different crystallographic layers, at temperatures reaching the ordering temperature. The intralayer spin-spin correlation is found to be finite, even at temperatures larger than the ordering temperature.



Magnetism 2018

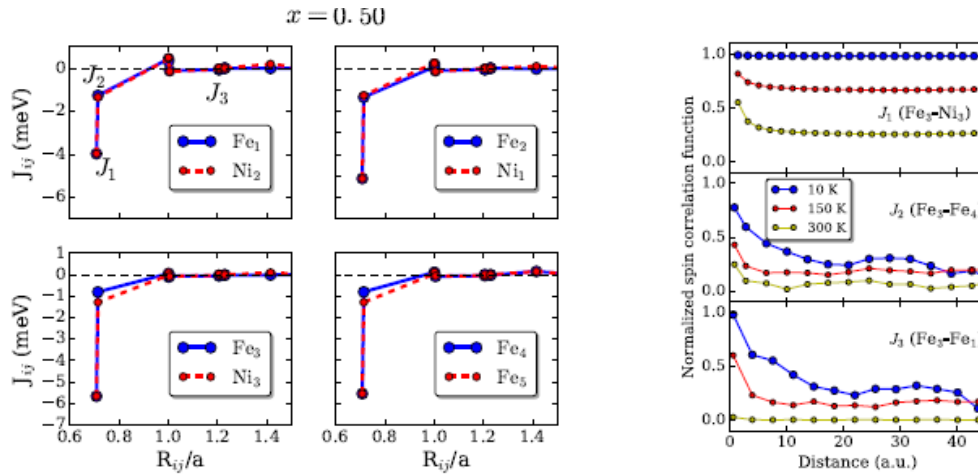


Figure 2. exchange parameters between an atom shown in the legend and all its magnetic neighbours as a function of distance for $x = 0.50$. Right) spin correlation function as function of distance in atomic unit (a.u.) for the case of interactions between Fe3 and its neighbours

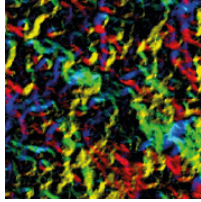
- [1] A. I. Liechtenstein, M. I. Katsnelson, V. P. Antropov, and V. A. Gubanov, Journal of Magnetism and Magnetic Materials 67, 65 (1987).
- [2] Y. O. Kvashnin, O. Granas, I. Di Marco, M. I. Katsnelson, A. I. Liechtenstein, and O. Eriksson, Phys. Rev. B 91, 125133 (2015).

P:59 Theory of L -edge spectroscopy of strongly correlated systems

J Lüder^{1,2}, J Schött¹, B Brena¹, M W Haverkort³, P Thunström¹, O Eriksson¹, B Sanyal¹, I Di Marco¹ and Y O Kvashnin¹

¹Uppsala University, Sweden, ²National University of Singapore, Singapore, ³Heidelberg University, Germany, ⁴Örebro University, Sweden

X-ray absorption spectroscopy measured at the L -edge of transition metals (TMs) is a powerful element-selective tool providing direct information about the correlation effects in the $3d$ states. The theoretical modeling of the $2p \rightarrow 3d$ excitation processes remains to be challenging for contemporary *ab initio* electronic structure techniques, due to strong core-hole and multiplet effects influencing the spectra. In this work we present results obtained by combining the density-functional theory with multiplet ligand field theory. With this approach, a single-impurity Anderson model (SIAM) is constructed, with almost all parameters obtained from first principles, and then solved to obtain the spectra. In our implementation we adopt the language of the dynamical mean-field theory and utilize the local density of states and the hybridization function, projected onto TM $3d$ states, in order to construct the SIAM. The developed computational scheme is applied to calculate the L -edge spectra for several TM monoxides. A very good agreement between the theory and experiment is found for all studied systems. The effect of core-hole relaxation, hybridization discretization, possible extensions of the method as well as its limitations are discussed.



Magnetism 2018

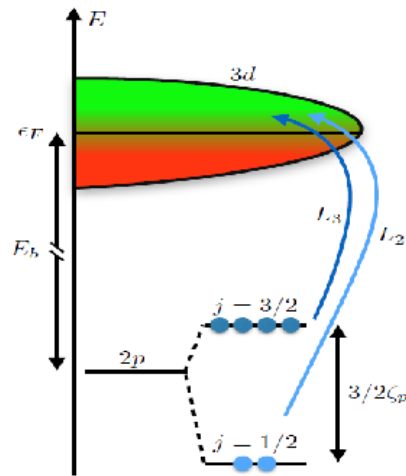


Figure 1: Schematic picture of the $L_{2,3}$ -edge XA process. An electron is excited from the TM-2p core states to the TM-3d valence states. Note that the energy scale is schematic. In the presently investigated compounds the binding energy E_b of the 2p state is of the order of 700 eV, the spin-orbit splitting $\frac{3}{2}\zeta_p$ of the 2p level is of the order of 10 eV and the width of the unoccupied part of the 3d valence band is a few eV.

P:60 Local field distribution and orbital ordering in a multiferroic perovskite metal-organic framework

Z Yang, A Phillips, and A Drew

Queen Mary University of London, UK

The magnetic ordering in the multiferroic metal-organic frameworks, copper guanidinium formate ($(\text{CNH}_2)_3\text{Cu}(\text{HCOO})_3$, CuGF), is presented. Due to Jahn-Teller distortion (JTD) about the Cu^{2+} orbitals, CuGF exhibits quasi-1D spin correlations even above the Néel temperature (4.6 K). The local field distributions are studied by muon spin rotation (μSR), where the amplitudes at different muon sites change with the rotation angle. The angular dependence of the dipolar contributions of the frequencies follows a cosine function. On the other hand, we report using synchrotron X-ray that the JTD to the copper oxygen octahedra is suppressed under pressure, whilst a structural phase transition is likely to occur at $\sim 2.60\text{ GPa}$.

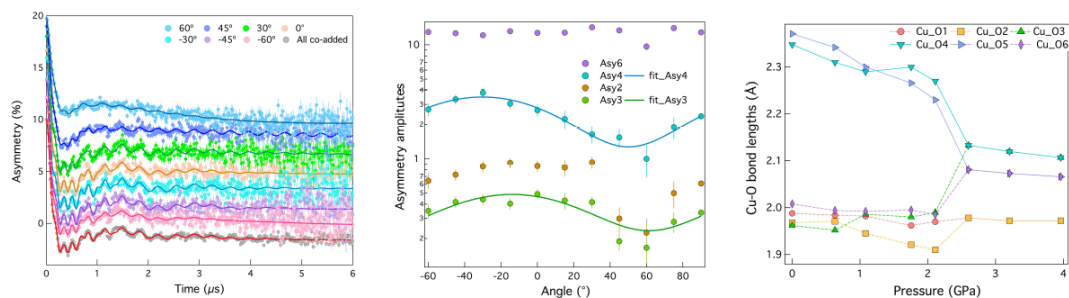
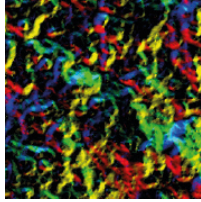


Figure. 1: (a) The total asymmetry of muon spin vs time at different rotation angles. (b) The asymmetry at different muon sites as a function of the rotation angle, and are fitted to a cosine function. (c) The Cu-O bond lengths as a function of applied pressure in Diamond anvil cell., where the distortion of the octahedra is suppressed. There is likely a phase transition at $\sim 2.60\text{ GPa}$.



Magnetism 2018

P:61 Emergent propagation modes of ferromagnetic swimmers in constrained geometries

M.T Bryan, S R Shelley, M J Parish, P G Petrov, C P Winlove, A D Gilbert and F Y Ogrin

University of Exeter, UK

Microscale magnetic swimmers have huge potential for advanced medical interventions, having the capability to transport reagents in microfluidic devices, target drugs to specific sites or perform localised micro-surgery. Motion of microswimmers is dominated by viscous drag, such that time-reversible movements cancel out and result in zero net motion. While a number of strategies have been demonstrated to produce propulsion in bulk fluids, the effects of encountering a barrier has received little attention. Given that applications require micro-robots to drive towards a surface, for example a cell membrane, it is essential to understand how geometrical features affect swimming behaviour.

Here, we model microswimmers composed of elastically-connected hard and soft ferromagnets as they interact with a surface or a planar channel under an elliptical field. Swimmers may move at twice the speed of bulk swimmers when approaching a barrier, but travel on a trajectory that bends parallel to the surface. When placed in a channel, swimming speed and direction of travel depend on the channel width and its alignment with the long-axis of the magnetic field, ψ (fig. 1). The confinement generates new modes of propagation that affect how the swimmer contacts the surface, so may influence swimmer functionality in applications.

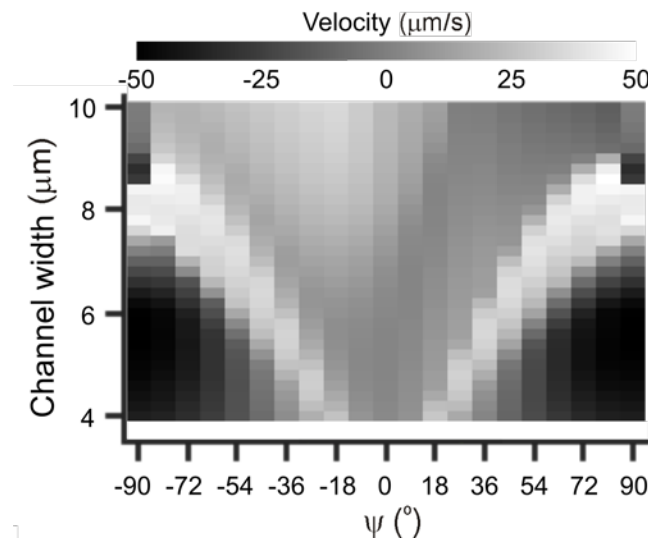
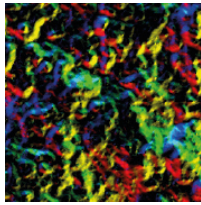


Figure 1: The dependence of the swimming velocity on the channel width and angle between the channel plane and the major axis of the elliptical field (ψ). $\psi = 0$ when the major axis is parallel to the channel.



Magnetism 2018

P:62 Demagnetising factors of rectangular prisms packed with magnetic nanoparticles

S M McCann, T Mercer, R D Cookson

University of Central Lancashire, UK

When measuring the magnetic characteristics of a material it is critical that the demagnetising effects are taken into account [1]. A numerical model has been devised that calculates the demagnetising factors of all the particles within a rectangular prism (Figure 1). The model has been used to examine the effects on the demagnetising factors caused by: (i) particle packing fraction; (ii) particle shape; (iii) particle distribution; (iv) aspect ratio of the containing rectangular prism. The average particle demagnetisation factor of the model matches (within 0.01%) with an accepted single-valued analytical theory [2], with exception of particle shape other than spheres. The demagnetising fields (at saturation) of rectangular prisms packed with magnetite spheres, typical diameters of 10 nm, have been measured using both a vibrating sample magnetometer and a transverse susceptibility apparatus and agree within uncertainty to give a value of $(54 \pm 5) \text{ kAm}^{-1}$. These measured fields are approximately 25% larger than both approaches. However, with particle agglomeration the numerical model shows an increase in the maximum particle demagnetisation factor consistent with the increased demagnetisation field observed at saturation. This gives confidence in the numerical model moving beyond the limits of the analytical model by taking into account non-uniform structures

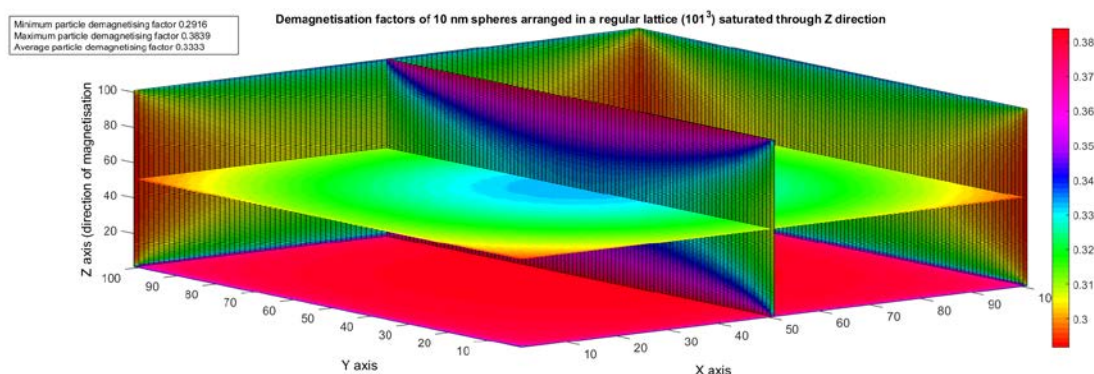
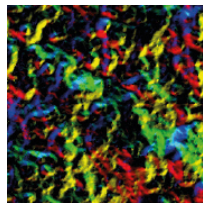


Figure 1. An example of the output of the numerical model. This shows the demagnetisation factors of regularly spaced spherical particles in a lattice of 101^3 particles for a saturating field in the z direction (packing fraction of 0.2). The particles show a spread of demagnetisation factors between 0.2916 and 0.3839 with an average value of 0.3333.

- [1] Bjork, R.; Bahl, C. R. H., "Demagnetization factor for a powder of randomly packed spherical particles", APPLIED PHYSICS LETTERS Volume: 103 Issue: 10 Article Number: 102403 Published: SEP 2 2013.
- [2] Breit, G, "Calculations of the effective permeability and dielectric constant of a powder", supplement number 46 to the communications from the Physical Laboratory at Leiden, 1922.



Magnetism 2018

P:63 The role of faceting and shape on the effective magnetic anisotropy of magnetite nanocrystals

S Poyser, R Moreno Ortega, A Meo, G Vallejo, S Majetich, V Lazarov and R F L Evans

University of York, UK

Magnetite nanoparticles are promising for magnetic hyperthermia due to their biocompatibility and heating properties. However the magnetic properties of the particles are complex due to their small size leading to significant finite size and surface effects. In their highly crystalline form the nanoparticles can form well defined facets depending on their method of preparation. Using an atomistic spin model we investigate the effects of size, elongation and faceting on the effective magnetic anisotropy of magnetite nanocrystals using the VAMPIRE code. We find that even small elongations of a few monolayers along one axis lead to a dominant uniaxial contribution to the effective anisotropy energy. In addition differently faceted crystals show different size and shape dependent behaviour leading to different contributions to the effective magnetic anisotropy as a function of the aspect ratio of the particle, as shown in Fig. 1. Finally we determine the effective higher order anisotropy energy surface due to the competing shape and cubic magnetocrystalline anisotropy contributions. We conclude that surface anisotropy is not a requirement for enhanced magnetic anisotropy in nanoparticle systems with even a small amount of shape anisotropy.

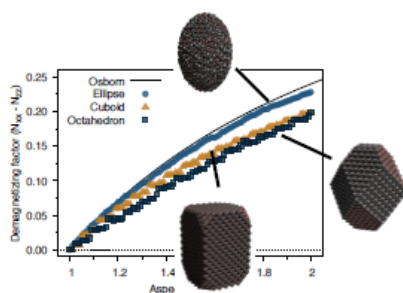


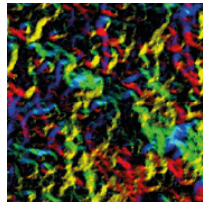
Figure 1 Calculated magnetic energy barrier as a function of aspect ratio for different particle facetings. The discontinuous nature of the jumps is due to monolayer additions of spins. A visualisation of different surface faceted nanocrystals is shown inset.

P:64 Multiwavelength magneto-optical characterization of magnetic nanoparticles for magnetic hyperthermia

R Soucaille¹, M E Sharifabad², N D Telling² and R J Hicken¹

¹University of Exeter, UK, ²Keele University, UK

Magnetic nanoparticles (MNP) have received great attention due to their potential for use in magnetic hyperthermia (MH). In the MH technique, MNPs can kill cancer cells due to localized heating that occurs when they are exposed to a high-frequency (typically 100's kHz) AC magnetic field. To optimize the heating capabilities of the MNPs, we need to first understand their dynamic response to a magnetic field, in terms of both the dependence of the area of the hysteresis loop upon the frequency of the magnetic field, and their agglomeration may influence this. The magneto-optical Faraday effect is an efficient tool with which to probe the magnetic and optical properties of MNPs through a wide range of frequencies in the visible spectrum. As a first step it is necessary to characterize the magneto-optical properties that have a strong dependence on wavelength [Figure 1]. We can then look for the role of agglomeration by observing how the transmitted light depends upon the time for which the magnetic field is applied [1]. By considering these effects and



Magnetism 2018

selecting the optimum measurement wavelength, the magnetic susceptibility of the MNP can be explored and the losses induced by an AC magnetic field may be quantified.

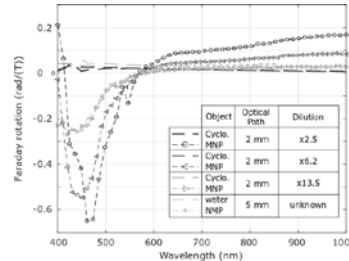


Figure 1: Dependence of the Faraday rotation of magnetite nanoparticles (MNPs) versus wavelength for different MNP concentrations. The MNPs were suspended in either water or cyclohexane with the dilution factor stated within the legend. Each pair of curves shows separately the contribution of the linear background (non-ferromagnetic) and ferromagnetic part

- [1] Jingyu Jin, Dongxing Song, Jiafeng Geng, Dengwei Jing, *Journal of Magnetism and Magnetic Materials* 447 (2018) 124–133

P:65 Dynamic simulation of a two-dimensional skyrmion lattice

Y Li¹, L Pierobon², M Charilaou², C Moutafis¹, J F Löffler² and J Miles¹

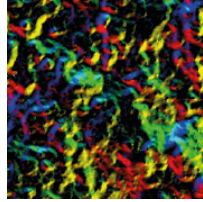
¹The University of Manchester, UK, ²ETH Zurich, Switzerland

Skyrmions (Fig. 1a, 1b), are unique magnetic structures in magnetic recording materials that can be generated through the competition between short-range and long-range interactions. By virtue of their topologically protected stability and well-behaved scalability, skyrmions have been proposed as promising candidates for the next generation non-volatile magnetic storage devices [1]. A fundamental system for studying these topological objects are two-dimensional high-density skyrmion lattices (SKL), whose existence have been proved theoretically and experimentally. Simulations of SKL have indicated high stability as required for data storage, but have assumed defect-free materials. In practical systems materials will have defects that are likely to affect the stability of magnetic structures. It is therefore important to investigate the impact of defects on SKL stability.

We employ numerical dynamic simulations of skyrmions using the GPU-accelerated software Mumax3 [2] to study SKL in the presence of defects. In our simulation, in increasing applied magnetic fields defects induce a lattice melting process which is a second-order phase transition, rather than the first-order transition seen in perfect SKL (Fig. 1) [3]. As a result, the simulations predict that magnetic defects will significantly reduce the stability of SKL systems.

The behaviour of a SKL is determined by the combined interaction of external field and internal magnetic environment, and the contribution of defects plays a crucial role for the whole process. Due to the short-range interaction, the local existence of defects will result in a non-uniform equilibrium state for skyrmions, and their different reactions for the location- dependent defect field will accelerate the “melting” process, causing the system collapse prematurely.

Defects exist in most materials and cannot be completely prevented during nanofabrication so the influence of their distribution and the physical mechanisms that they induce need to be comprehensively studied. By means of the statistics of topological charge and other methods of characterisation, the behaviour of skyrmions in the presence of defects and the transition process can be quantified and analysed, which will provide invaluable information on the importance of different defect characteristics.



Magnetism 2018

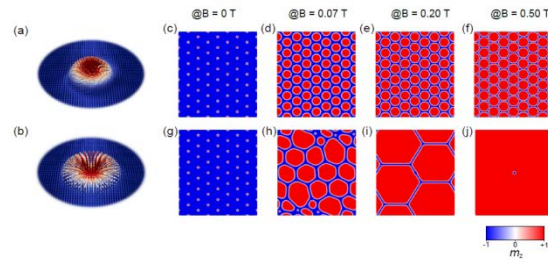


Figure 1. (a) and (b): the schematics of Bloch Skyrmion and Neel Skyrmion, respectively. (c – f): simulation results for an SKL in a perfect material under sweeping magnetic field, the magnitude of the field is labeled above each image. (g – j): simulation results for an SKL in a defective material with the same applied fields. The defect is located in the centre of configuration.

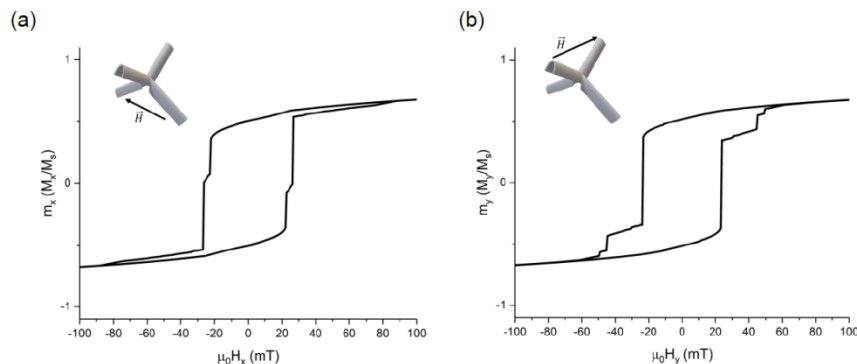
- [1] Fert A, Cros V and Sampaio J 2013 *Nat. Nanotechnol.* 8 152–156
- [2] Vansteenkiste A, Leliaert J, Dvornik M, Helsen M, Garcia-Sanchez F and Van Waeyenberge B 2014 *AIP Adv.* 4 107133
- [3] Bauer A, Garst M and Pfleiderer C 2013 *Phys. Rev. Lett.* 110 177207.

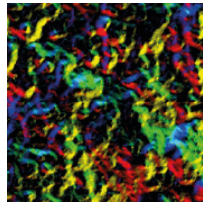
P:66 Magnetic nanowires of curved cross-section: A Micro-magnetic study

A van den Berg, M Hunt, A May and S Ladak

Cardiff University, UK

Three-dimensional nanostructuring of magnetic materials offers a new means to control micro-magnetic textures by harnessing standard geometry dependent magnetic energies as well as those provided by more subtle curvature-driven terms. Precise control of the 3D geometry within magnetic nanowires allows access to a vast range of exotic physics including ultrafast domain wall motion that deviates from a Walker limit, topologically protected domain walls [1] and magnetochiral effects [2]. In this work, we investigate micro-magnetic switching of magnetic nanowires with curved cross-section. Such nanowires have recently been realised using a combination of two-photon lithography and line-of-sight deposition [3]. In this study, finite element simulations were performed upon single magnetic nanowires, bipod structures and tetrapod structures. The switching of tetrapod structures was found to be complex, with a number of abrupt transitions and plateaus indicative of domain wall pinning. These hysteresis loops will be discussed in terms of the micro-magnetic structure of underlying single wires and bipods. Finally, the extent to which these systems can be used as domain wall conduits will be explored.





Magnetism 2018

Figure 1: Hysteresis loops for Ni₈₁Fe₁₉ tetrapod structure with field applied as indicated within inset.

- [1] S. Da Col, S. Jamet, N. Rougemaille, A. Locatelli, T. O. Montes, B. Santos Burgos, R. Afid, M. Darques, L. Cagnon, J. C. Toussaint and O. Fruchart, "Observation of Bloch- point domain walls in cylindrical magnetic nanowires," *Phys Rev B*, vol. 89, 2014.
- [2] O. M. Volkov, D. D. Sheka, Y. Gaididei, V. P. Kravchuk, U. K. Rössler, J. Fassbender and D. Makarov, "Mesoscale Dzyaloshinskii-Moriya interaction: geometrical tailoring of the magnetochirality," *Scientific Reports*, vol. 8, 2018.
- [3] A. May, M. Hunt, A. van den Berg, A. Hejazi and S. Ladak, *in preparation*, 2018.

P:67 Implementing superconductivity into a green's function (KKR) method to explore the interactions between superconductivity and magnetism

T G Saunderson, G Csire, J F Annette and M Gradhand

University of Bristol, UK

There is a plethora of problems regarding our understanding of the interaction between superconductivity and magnetism. One example is recent theoretical work on Sr₂RuO₄ [1] which is predicted to have cooper pairs with an intrinsic orbital magnetic moment. The focus of this work is on spin-dependent transport phenomena induced or influenced by the superconducting state as exemplified by the spin Hall effect [2]. Of crucial importance in the understanding of transport effects is the correct consideration of impurities and interfaces. In order to fully include all these aspects into the description of the electronic and magnetic properties of superconducting materials, we are implementing the Bogoliubov-de Gennes equation into a Green's function (KKR) density functional theory method [3]. By using a Green's function method, it is possible to model problems containing impurities and interfaces without the need of supercells. This will provide insight into the coupling between superconductivity and magnetism influenced by impurities and ultimately spin-orbit coupling. Here we are going to present first steps in the implementation and discuss the challenges and advancement made so far.

- [1] J. Robbins *et al*, Phys. Rev. B. 96, 144503 (2017) [2] T. Wakamura *et al*, Nat. Mater. 14(7), 675 (2015) [3] G. Csire *et al*, Phys. Rev. B, 91(16), 1-11 (2015).

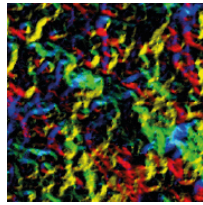
P:68 First principles study of magnetisation of ZnO/Co and ZnCoO/Co systems

F M Gerriu, A M Fox and G Gehring

University of Sheffield, UK

ZnO doped with transition metals is one of II-VI semiconductors that attracted much attention in the past decades since Dietl prediction of high Curie temperature by mean-field theory [1]. More- over, since the first experimental observation of room-temperature in Co-doped ZnO films by Ueda *et al* [2], much experimental and theoretical investigations of the source of the observed ferromagnetism (FM) have been performed. Experimentally, when ZnO films are doped with Co, most of the Co substitutes Zn sites, however, a fraction of that amount forms metallic clusters under specific preparation conditions such as low oxygen pressure and when using different types of target precursors for films grown by PLD [3]. Although there are many recent experimental reports of Co nanoparticles in ZnO and many experimental and theoretical studies of Co-doped ZnO, there is no theoretical modelling for Co nanoparticles in ZnO.

In this work, we present first principles study of Co nanoparticles in ZnO. The model is constructed from a number of Co monolayers on two ZnO unit cells. The magnetisation at both inter- faces of ZnO/Co system is



Magnetism 2018

investigated. The effect of the presence of substituted Co^{2+} is studied by calculating the density of the states and exchange energies for the system with and without doped Co atoms. Furthermore, the effect of Al-doping in ZnCoO on the magnetisation and the magnetic exchange between Co nanoparticles is examined in details.

- [1] Tomasz Dietl, H Ohno, F Matsukura, J Cibert, and e D Ferrand. Zener model description of ferromagnetism in zinc-blende magnetic semiconductors. *science*, 287(5455):1019–1022, 2000.
- [2] Kenji Ueda, Hitoshi Tabata, and Tomoji Kawai. Magnetic and electric properties of transition- metal-doped zno films. *Applied Physics Letters*, 79(7):988–990, 2001.
- [3] Minju Ying, Harry J Blythe, Wala Dizayee, Steve M Heald, Fatma M Gerriu, A Mark Fox, and Gillian A Gehring. Advantageous use of metallic cobalt in the target for pulsed laser deposition of cobalt-doped zno films. *Applied Physics Letters*, 109(7):072403, 2016.

P:69 Magnetic Hyperthermia: Easy axis alignment of magnetic nanoparticles driven by Brownian rotation.

S E Rannala, S Ruta and R Chantrell

University of York, UK

The application of magnetic hyperthermia as a cancer therapy has shown great promise. The current project looks to investigate the effect of Brownian rotation on the heat produced via magnetic hyperthermia. To do this a novel model has been developed which accounts for the coupling of the particle to the surrounding fluid and also the coupling of the magnetisation to the internal degrees of freedom, thus accounting for both Néel and Brownian rotation mechanisms (figure 1). The model has shown the presence of easy axis alignment during magnetic hyperthermia. This alignment will have an impact on the heat generated via magnetic hyperthermia, due to its effects on the squareness of the hysteresis profiles obtained during the process. Currently easy alignment has been observed both perpendicular to the applied field and also towards the applied field, for certain system configurations. We aim to identify the causing factors driving the type of easy axis alignment occurring within the system. The end goal is the ability to predict the easy axis alignment behaviour based on initial system conditions, which may then enable magnetic hyperthermia systems to be tailored to take advantage of the alignment to improve heat generation.

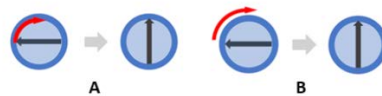
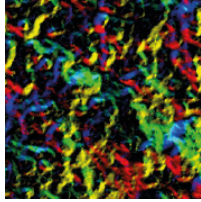


Figure 1: Diagram A shows Néel relaxation. In this process the particle remains static whilst the magnetisation rotates. Diagram B shows Brownian motion, here the particle rotates causing the magnetisation to rotate also.



Magnetism 2018

P:70 3D FDTD-LLG modelling of magnetisation dynamics in thin film ferromagnetic structures

F Y Ogrin

University of Exeter, UK

There is a growing need in high frequency tuneable microwave materials for applications in the areas of microwave electronics, transformation optics, photonics. Due to their intrinsic RF phenomena, such as FMR, ferromagnetic thin films have always been of great interest and led to a great amount of experimental research very often supported by numerical simulations. While purely magnetostatic solvers, such as OOMMF or Mumax, have always been the standard benchmark tools and usually provide a precise description of the magnetisation processes in thin-film ferromagnetic structures, these systems are however limited in applications where full electromagnetic solutions are required, especially when the material properties are extremely non-uniform (e.g. dielectric/metal interfaces). In such cases one needs to consider a modelling approach where a full solution of Maxwell equations is needed alongside the materialistic equations, such as e.g. Landau-Lifshits-Gilbert (LLG) providing the relation between the magnetisation and the magnetic field. Here we propose such a model which uses 3D finite-difference-time-domain (FDTD) approach together with LLG to find the exact solutions for magnetisation dynamics in thin film ferromagnetic structures. As a benchmark testing we demonstrate application of such model for different classical phenomena such as Faraday effect, and then explore the dynamic characteristics of thin films in magnetostatic applications. In particular we consider propagation of magnetostatic/spin waves in metallised magneto-dielectric thin films and magnetic structures and demonstrate their dispersion characteristics. The results are compared with the standard analytical solutions and the simulations by using Mumax³. We also discuss the advantages of the model and its limitations for using in realistic prototype materials.

[1] M. M. Aziz, Progress In Electromagnetics Research B 15, (2009) 1-29

[2] M. Kostylev et al. J. Appl. Phys. 113 (2013) 043927.

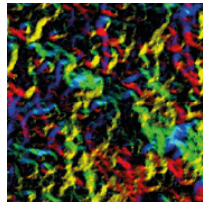
P:71 Mode analysis of the tree-like bio-inspired networks of vortex-based spintronic nanooscillators

O S Katkova, A R Safin, N N Udalov and M V Kapranov

National Research University "MPEI", Russia

The discovery problem of many mutually interacted objects in complex networks is very important in theoretical and practical aspects. Recent years have witnessed much scientific progress in synchronization area of nonlinear oscillators in non-high dimensional networks (so called small-world networks). At the same time, various problems in the modern fundamental physics and techniques are very difficult to describe by small-world prototypes and, as a result, it is needed very serious numerical calculations of large networks. In the last decade the network theory have received a very strong attention, because of its applications for solving many practical problems.

A fundamental contribution to the mathematical aspects of collective synchronization was given by Kuramoto. He proposed a model to describe the behavior of coupled nonlinear phase-oscillators. Usually, the pay a special attention to the identical or small nonidentity. However, for the large network of oscillators, this classical problem is more complicated and interesting. The corresponding equations for the small variable amplitudes could be more difficult than classical van der Pole equations (nonisochronous, phase delay and strongly nonidentical regenerative components). Therefore, we will describe more general approach, which is very useful for the networks in the nonlinear wave theory. We will call this approach as quasi-Hamiltonian formalism.



Magnetism 2018

We will focus our attention on the nonlinear oscillators, which could be describe by quasi-Hamiltonian formalism, with ultrametric geometrical topology (tree-like bio-inspired networks). We demonstrate the fractal structure of the normal modes spectrum, which have a fractal structure. After spectrum calculation we shift to the truncated equations for slowly varying amplitudes and phases in the normal coordinates using generalized quasi-Hamiltonian approach.

We construct adjacency matrices of different type of m-adic tree-like bio-inspired networks, where m is the number of branches from one node, and calculate the normal modes. We demonstrate the fractal structure of the normal modes spectrum, which looks like devils staircase fractal. After spectrum calculation we shift to the truncated equations for slowly varying amplitudes and phases in the normal coordinates using generalized quasi-Hamiltonian approach. Finally, the stability analysis of the normal modes is presented.

This work is supported by a Russian President grant for young scientists (project No MK-7026.2016.8).

P:72 FP-LAPW calculations : Electronic and magnetic properties of Pr₂Fe₁₇ intermetallic compound

K Bakkari¹, E K Hlil², R Fersi¹ and N T Mliki¹

¹Université de Tunis El Manar, Tunisia, ²Université Grenoble Alpes, France

Intermetallics based on rare-earth and metal transition elements are extensively studied in order to synthesize new materials or to improve their magnetic properties. However, the theoretical investigations still quite limited.

In this work, we focus on electronic and magnetic properties of the Pr₂Fe₁₇ compound. This is investigated by means of the Full Potential Linear Augmented Plane Wave (FP-LAPW) computational method. In the framework of GGA+U approximation, DFT calculations are carried out in order to estimate the self consistently total energy, the local and total magnetic moments as well. Th₂Zn₁₇ type crystal structure is selected for this compound. The main results indicate that a large total magnetic moment is found to be equal to $35.1 \mu_B / f.u$. This magnetic moment value is in accordance with the previously experimental study [1], reporting a momentum of $35.2 \mu_B / f.u$. Such high ferromagnetic state is discussed in terms of strong spin polarization observed in the total DOS. Finally, all computed magnetic quantities would be also discussed in the light of the efficiency in technological applications.

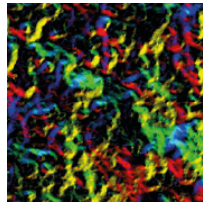
[1] O. Isnard, S.Miraglia, M.Guillot, D. Fruchart Journal of Applied Physics 75, 5988 (1994).

P:73 3D-Printing polymer-based permanent magnets

R Domingo-Roca, J C Jackson and J F C Windmill

University of Strathclyde, UK

Manufacturing processes used to develop permanent magnets are time-consuming and demand very specific machinery to apply exceptionally high pressures, temperatures, and magnetic fields. Furthermore, these manufacturing processes generate by-products and hazardous waste, making the whole process environmentally-detrimental. On the other hand, the magnets produced using such approaches have the advantage of exhibiting extremely large magnetic fields. In this work we address this problem using 3D-printing technology to develop polymer-based permanent magnets, a much simpler technique that allows production in a more time-efficient and environmentally- friendly manner. This permits the development of different types of magnets by simply modifying specific parameters of both the matrix and the filler. Here we report the results of work to 3D-print magnetic materials on the micro-scale and their full magnetic



Magnetism 2018

characterization. 3D-printing materials with different magnetic properties at this scale, could allow their use in a wide range of applications in biomedicine, biotechnology, medical science, and information storage among many others. The M - H hysteresis loops, the curves of the change of magnetic moment and the surface plots of the magnetic field intensity and orientation of the 3D-printed samples before and after magnetic poling are shown in Figures 1 and 2, respectively.

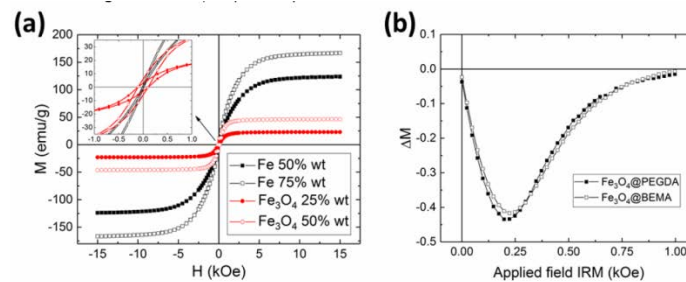


Figure 1: (a) The M - H hysteresis loop plots of the 3D-printable composites. The top-left corner graph shows the low-field regime in close-up. (b) The change of magnetic moment of the synthesized magnetic composites.

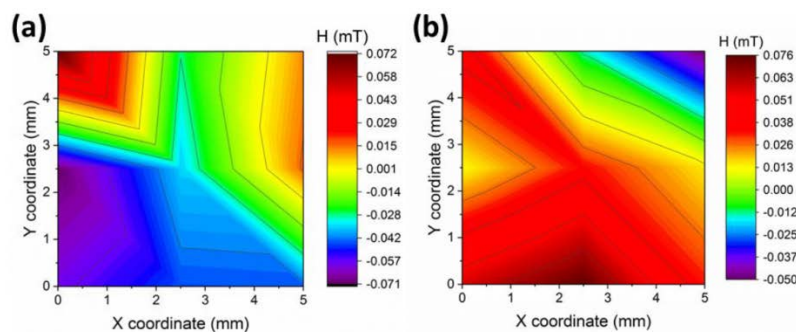


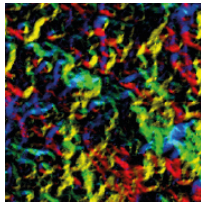
Figure 2: (a) and (b) show the surface plot of the orientation and intensity of the magnetic field displayed by one of the 3D-printed samples before and after magnetic poling, respectively.

P:74 The structural and magnetic properties of $\text{GdCo}_5 - \text{Ni}_x$

A Tedstone, C E Patrick, R S Edwards, M R Lees, G Balakrishnan, S Kumar, E Mendive Tapia, G Marchant and J B Staunton

University of Warwick, UK

We have investigated the substitutional doping of nickel onto the cobalt sublattice of GdCo_5 to gain insight into the important SmCo_5 type permanent magnet and how its magnetic properties are affected by changes in sublattice magnetisation. We have formed polycrystalline samples of $\text{GdCo}_5 - \text{Ni}_x$ by arc melting for $x = 0 - 5$ in steps of 0.5. Microstructural characterisation was carried out by powder x-ray diffraction and optical and SEM imaging of metallographic slides which revealed lamellae of $\text{Gd}_2(\text{Co}, \text{Ni})_7$ for compositions $x < 2.5$ in low enough concentration to be unobserved in the x-ray patterns. We also carried out magnetisation measurements. The total magnetisation is fully compensated at absolute zero at a composition of $\sim x = 1$. The compensation temperature increases with increasing nickel content until $x = 3$; for higher x compensation is no longer observed. A peak in coercivity and a minimum in magnetisation occur at $\sim x = 1$ at 10 K which may be understood via the Stoner-Wolfarth model. We have performed calculations based on



Magnetism 2018

density functional theory within the disordered local moment picture and found good agreement with experimental measurements.

P:75 Atomistic calculations of magnetic properties of $\text{Sm}_{(1-x)}\text{Zr}_x\text{Fe}_{12}$

S C Westmoreland¹, R F L Evans¹, G Hrkac², T Schrefl³, G T Zimanyi⁴, M Winklhofer⁵, N Sakuma⁶, M Yano⁶, A Kato⁶, T Shoji⁶, A Manabe⁶, M Ito⁶ and R W Chantrell¹

¹University of York, UK, ²University of Exeter, UK, ³Danube University Krems, Austria, ⁴University of California, USA ⁵Carl von Ossietzky University of Oldenburg, Germany, ⁶Toyota Motor Corporation, Japan

We have investigated the effect of Zr substitution in SmFe_{12} (Sm,ZrFe_{12}), a promising candidate for permanent magnet applications due to its high anisotropy and remanent magnetisation. It has been reported [1, 2] that substitution of the rare-earth sites in RFe_{12} compounds with Zr improves both phase and thermal stability. Zr is non-magnetic, thus the improvement in thermal stability upon substitution can be attributed to the fact that the Zr atomic radius is $\sim 89\%$ that of a Sm atom [3], causing a shrinking of the crystal lattice, leading to an increase in the effective exchange energy between atomic sites and the atomistic coordination number. Using data from Sakurada *et al.* (1992) [4] on the effect of Zr substitution on lattice parameters, we have used the VAMPIRE software package [5] to calculate the temperature dependent magnetisation of $\text{Sm}_{(1-x)}\text{Zr}_x\text{Fe}_{12}$. The results (Fig. 1) show that there is an increase in the TC as the amount of Zr is increased up to $x = 0.5$, however the TC drops as the Zr concentration is increased further to $x = 0.75$. Similar behaviour has been seen in experimental studies. The behaviour is a result of two competing factors: first the reduction in lattice size and consequent increase in coordination number, and second the reduction in total number of interactions as Sm is replaced by the non-magnetic Zr, acting to reduce the TC.

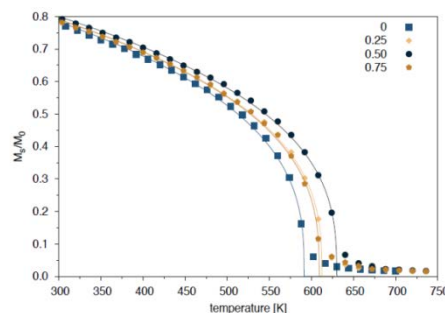
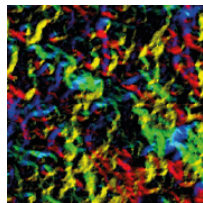


Figure 1. Calculated magnetisation vs temperature curves for $\text{Sm}_{(1-x)}\text{Zr}_x\text{Fe}_{12}$ for varying values of x . The data show that up to $x = 0.5$, there is an increase in the TC while increasing the Zr content further to $x = 0.75$ results in a decrease in TC.

This work is based on results obtained from the future pioneering program "Development of magnetic material technology for high-efficiency motors" commissioned by the New Energy and Industrial Technology Development Organization (NEDO).

- [1] Gabay, A. M., Cabassi, R., Fabbri, S., Albertini, F. & Hadjipanayis, G. C. Structure and permanent magnet properties of $\text{Zr}_{1-x}\text{R}_x\text{Fe}_{10}\text{Si}_2$ alloys with $\text{R} = \text{Y, La, Ce, Pr}$ and Sm . *J. Alloys Compd.* 683, 271–275 (2016).
- [2] Suzuki, S. *et al.* A new magnet material with ThMn_{12} structure: $(\text{Nd}_{1-x}\text{Zr}_x)(\text{Fe}_{1-y}\text{Co}_y)_{11}+\text{zTi}_{1-z}\text{N}_a$ ($\alpha=0.6-1.3$). *J. Magn. Magn. Mater.* 401, 259–268 (2016).



Magnetism 2018

- [3] Slater, J. C. Atomic Radii in Crystals. *J. Acoust. Soc. Am.* 36, 2346 (2005).
- [4] Sakurada, S., Tsutai, A. & Sahashi, M. A study on the formation of ThMn_{12} and NaZn_{13} structures in $\text{RFe}_{10}\text{Si}_2$. *J. Alloys Compd.* 187, 67–71 (1992).
- [5] Evans, R. F. L. *et al.* Atomistic spin model simulations of magnetic nanomaterials. *J. Phys. Condens. Matter* 26, 103202 (2014).

P:76 Magnetic exchange disorder in low-dimensional quantum magnets

W J A Blackmore¹, P A Goddard¹, T Lancaster², M J Pearce¹, C P Landee³, M M Turnbull³, J Singleton⁴, S Birnbaum⁴, R C Williams^{1,2} and F Xiao⁵

¹University of Warwick, UK, ²Durham University, UK, ³Clark University, USA, ⁴NHML Los Alamos, USA,

⁵University of Bern, Switzerland

Despite much theoretical work [1,2] the effect of random exchange strengths in two-dimensional (2D) antiferromagnets is still not fully understood [3]. This project aims to rectify this by investigating the quasi-2D coordination polymer $(\text{QuinH})_2\text{Cu}(\text{Cl}_x\text{Br}_{1-x})_4 \cdot 2\text{H}_2\text{O}$. The exchange pathway is through Cu-halide-Cu bonds [4], and by randomising the proportion of Cl and Br atoms in the unit cell, magnetic exchange disorder can be introduced into the system. We use pulsed-field magnetisation to determine the saturation field (H_c), a measure of the size of short-range correlations [5], and muon-spin relaxation measurements to determine the onset of long-range order (T_N) for different values of x . Whilst short range correlations are reasonably robust to small changes of x , long-range order appears to be lost rather more quickly (Fig. 1). The data is consistent with a quantum disordered phase emerging above $x = 0.4$.

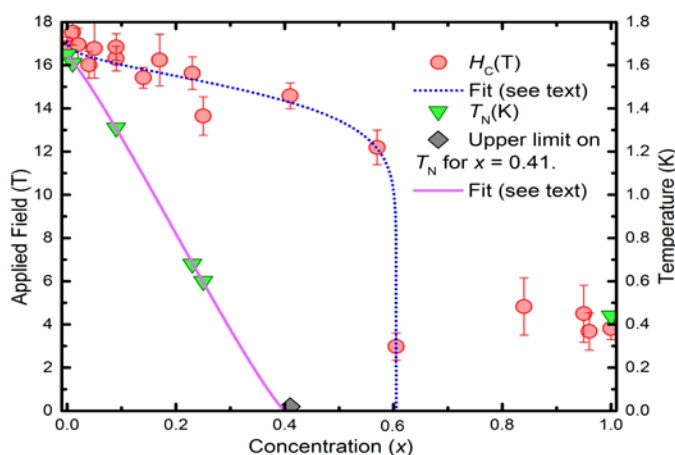
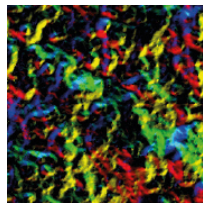


Figure 1: Phase diagram of $(\text{QuinH})_2\text{Cu}(\text{Cl}_x\text{Br}_{1-x})_4 \cdot 2\text{H}_2\text{O}$, showing how H_c and T_N varies with x . Both data sets were fitted to the phenomenological function $y = A[1 - (x/x_c)^\beta]^\alpha$ below $x = 0.6$.

- [1] N. Laorencie *et al.*, Phys. Rev. B 73, 060403 (R) (2006).
- [2] R. Yu *et al.*, Phys. Rev. B 73, 064406 (2006).
- [3] A.M. Tsvelik, Quantum Field Theory in Condensed Matter Physics (CUP) (2007).
- [4] R. Butcher, *et al.*, Inorg. Chem. 49, 427 (2010).
- [5] Goddard, P. A., *et al.*, Phys. Rev. Lett., 108, 077208 (2012).



Magnetism 2018

P:77 Scanning probe microscopy at magnetic fields up to 34 T

L Rossi, J Gerritsen, L Nelemans, A Khajetoorians and B Bryant

Radboud University, The Netherlands

Up to now, low temperature Scanning Probe Microscopy (SPM) has been limited to a magnetic field strength of 18 T, as the majority of designs have been based on superconductor magnets. For some experimental applications – for example the study of fractal spectra in graphene superlattices, the room temperature quantum Hall effect and some metamagnetic transitions – higher fields are required. Static fields of more than 30 T can be generated in dedicated high-field facilities by water-cooled, resistive Bitter magnets or hybrid resistive-superconducting magnets. However, implementing SPM in a Bitter magnet is a major challenge, due to the high level of vibrational noise produced by the turbulent cooling water, in addition to the strong space constraints resulting from the small magnet bore.

We present a novel cryogenic Scanning Tunnelling Microscope (STM) designed to operate inside a water-cooled Bitter magnet, which can reach a magnetic field of 38 T. The performance of the STM is demonstrated through Landau level tunnelling spectroscopy of graphite, at 4.2 K in magnetic fields up to 34 T¹.

Additionally we show the design of a highly compact Atomic Force Microscope (AFM) for operation at cryogenic temperatures in an extremely high magnetic field. We present preliminary imaging data on the frustrated spinel CdCr₂O₄ at up to 30 T.

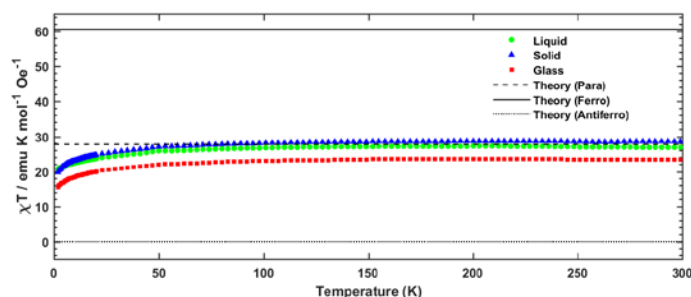
- [1] Tao, W. *et al.* A low-temperature scanning tunneling microscope capable of microscopy and spectroscopy in a Bitter magnet at up to 34 T. *Rev. Sci. Instrum.* 88, 93706 (2017).

P:78 Magnetic properties of Bis-Lanthanoates

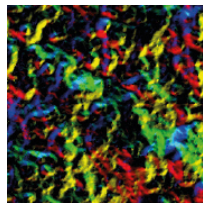
K Esien, E McCourt, P Nockemann and S Felton

Queen's University Belfast, UK

Magnetic ionic liquids (MILs) are a class of ionic liquid incorporating one or more magnetic atoms into the anion or cation of the ionic liquid, endowing the ionic liquid with magnetic properties alongside the existing properties of ionic liquids. MILs have applications in *e.g.* fluid-fluid separations, electrochemistry, and polymer chemistry.



In this study three different types of bis-lanthanoates, that exist in different phases, have been synthesised and characterised (Ln = lanthanide): 1) imidazolium lanthanide acetate – [C4Mim]2[Ln2(OAc)8] – forms a crystalline solid at room temperature, 2) phosphonium lanthanide acetate – [P666 14]2[Ln2(OAc)8] – is in a solid glassy state, and 3) phosphonium lanthanide octanoate – [P666 14]2[Ln2(Oct)8] – is an ionic liquid. X-ray diffraction of the crystalline solid 1) confirm that the Ln(III) ions form dimers, bridged by carboxyl groups, but cannot yield information about samples 2) and 3) since these lack long-range order.



Magnetism 2018

SQUID magnetometry studies show that all three samples have effective magnetic moments consistent with non-interacting Ln(III) ions at room temperature, but deviate from this behaviour in the same way below 50 K, see figure. The implications of this for the structure of the glass and ionic liquid will be discussed, as well as the nature of the magnetic interaction in all three samples.

P:79 Ferromagnetic swimmers: Fabrication, controlled swimming, and applications

J K Hamilton¹, M T Bryan¹, A D Gilbert¹, T O Myers² and F Y Ogrin¹

¹University of Exeter, UK, ²Platform Kinetics, UK

Microscopic swimming devices hold promise for radically new applications in lab-on-a-chip and microfluidic technology, diagnostics and drug delivery etc. We propose a new class of autonomous ferromagnetic swimming devices, actuated and controlled solely by an oscillating magnetic field. Experimentally, we investigate macro-scaled ferromagnetic swimming devices of different designs.

One device of interest is based on a pair of interacting ferromagnetic particles of different size and different anisotropic properties joined by an elastic link and actuated by an external time-dependent magnetic field. The net motion is generated through a combination of dipolar interparticle gradient forces, time-dependent torque and hydrodynamic coupling.

We investigate the dynamic performance of a prototype (3.6 mm) of the ferromagnetic swimmer in fluids of different viscosity as a function of the external field parameters and demonstrate stable propulsion over a wide range of Reynolds numbers. Manipulation of the external magnetic field resulted in robust control over the speed and direction of propulsion.

We also demonstrate that our ferromagnetic swimmer working as a macroscopic prototype of a microfluidic pump. By physically tethering the swimmer, instead of swimming, the swimmer generates a directional flow of liquid around itself.

- [1] F. Y. Ogrin, P. G. Petrov, C. P. Winlove, Phys. Rev. Lett. 2008, 100, 218102.
- [2] A. D. Gilbert, F. Y. Ogrin, P. G. Petrov, C. P. Winlove, Q. J. Mech. Appl. Math. 2011, 64, 239.
- [3] J. K. Hamilton, P. G. Petrov, C. P. Winlove, A. D. Gilbert, M. T. Bryan, F. Y. Ogrin, Sci. Rep. 2017, 7, 44142
- [4] J. K. Hamilton, A. D. Gilbert, M. T. Bryan, F. Y. Ogrin, T. O. Myers, Sci. Rep. 2018, 8, 933

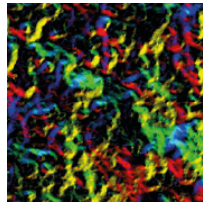
P:80 Dynamics of the flux line lattice in high purity niobium studied with stroboscopic neutron scattering

C B Larsen¹, E Tekin¹, A Sokolowski², U Keiderling², R Toft-Petersen³ and M Laver¹

¹University of Birmingham, UK, ²Helmholtz-Zentrum Berlin, Germany, ³Technical University of Denmark, Denmark

High purity niobium is a conventional type-II superconductor, that nonetheless displays a feature-rich phase diagram with several flux line lattice (FLL) structural transitions. Time- resolved stroboscopic small-angle neutron scattering provides an opportunity to study both the structure of the FLL as well as dynamic features[1].

By applying an AC field perpendicular to the static field, we have been able to observe how the vortices are pulled away from their equilibrium positions and how they subsequently relax back into them. An example of our experimental data is shown in Fig. 1, where the field-dependence of the structure of the FLL is apparent. From the data we have extracted the elastic constants of the FLL, which have been compared to predictions



Magnetism 2018

from Ginzburg-Landau theory[2]. Our study has especially been focused of the behaviour of the elastic constants close to the structural transitions in order to explore softening of the FLL.

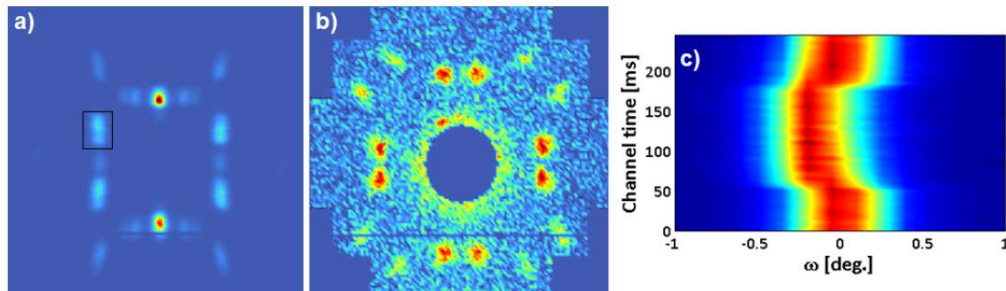


Figure 1: a) and b): 2D scattering images obtained at base temperature with a static field of 200 mT and 340 mT, respectively. Both images are summed over a full rocking curve scan. As the static field is increased, the FLL transitions from a scalene phase to a square phase. c) Time-resolved rocking curve of the flux line spot high-lighted with a black box in plot a).

- [1] S. Muhlbauer *et al*, Phys. Rev. B 83, 184502 (2011)
- [2] E. H. Brandt, Rep. Prog. Phys. 58, 1465 (1995).

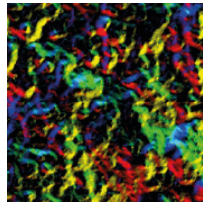
P:81 Probing proximity induced triplet states with point contact Andreev spectroscopy

A Moskalenko¹, K A Yates¹, L F Cohen¹, A Di-Bernardo², A Srivastava² and J Robinson²

¹Imperial College London, UK, ²University of Cambridge, UK

The interface between a disordered ferromagnet (F) and a superconductor (S) has been extensively researched owing to the discovery of the long-ranged spin triplet proximity effect (LRSTPE). In this effect the singlet Cooper pairs from the superconductor are converted via a process of spin mixing and spin rotation into a spin-polarized triplet state that can be sustained for large distances through a ferromagnetic layer [1]. However, direct observation of these states has remained elusive. We use point contact Andreev spectroscopy to interrogate thin films of Au deposited onto Ho/Nb layers. This method has the advantage of directly measuring the transport current through a contact. We explore the influence of the thickness of the Au layer and the Ho layer in the generation of the LRSTPE as well as the effect of microwaves on the Andreev spectra.

- [1] Matthias Eschrig, Spin-polarized supercurrents for spintronics: a review of current progress, Reports on Progress in Physics, Volume 78, Number 10q



Magnetism 2018

P:82 Propagating spiral spin waves in magnetic nanostructures

D Osuna Ruiz, A P Hibbins and F Y Ogrin

University of Exeter, UK

Spin waves in confined structures have widely been a subject of interest in the field of computing and magnetic memories. In nanostructures, spin waves can be excited in the GHz regime, but this is not always a desirable phenomenon since it could cause interferences while reading or writing stored data in simple structures such as circular disks. Therefore, understanding the sources, propagation and dispersion characteristics of spin waves becomes a fundamental topic for improving future technological applications.

In a relaxed single vortex state, widely used for bit storage, spin waves with circular or spiral wave fronts can usually be excited depending on the orientation of an alternating magnetic field [1]. In our work we study differences between thin and thick disks. We found that, depending on thickness, propagating spiral spin waves are more efficiently excited from different regions of the disk: Edge and core vicinity. We give a simple explanation for the origin of spiral spin waves in thick samples through Landau-Lifshitz equation of motion [2]. We also show their dispersion relations, which allows to easily identify their frequency range of work. Spiral spin waves can offer a new variety of interesting applications in contrast to circular spin waves.

- [1] S. Davies, V. D. Poimanov and V. V. Kruglyak, Mapping the magnonic landscape in patterned magnetic structures, Phys. Rev. B 96, 094430 (2017).
- [2] L. D. Landau and E. M. Lifshitz, Theory of the dispersion magnetic permeability in ferromagnetic bodies, Phys. Z. Sowietunion 8, 153 (1953).

P:83 Remote magnetic monitoring of expansion of intermediate level waste canisters

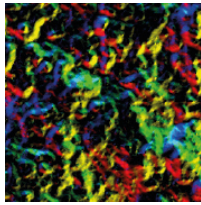
P Y C Pan¹, C Corkhill¹, G Bolton² and T Hayward¹

¹University of Sheffield, UK, ²National Nuclear Laboratory (NNL), UK

The Giant Magnetoimpedance (GMI) effect is a phenomenon where, at MHz-to-GHz frequencies, the electrical impedance of soft ferromagnetic materials can change by several hundred percent when subjected to an applied magnetic field [1]. The large magnitude of this effect makes GMI ideal for creating a range of magnetic field sensors, while its stress sensitivity offers possibilities of sensors for structural health monitoring [2]. Here, we will discuss progress towards the development of a GMI sensor addressing the challenges associated with monitoring (in real time) localised swelling of nuclear waste storage canisters.

Nuclear waste, in the UK, is generated from a “closed” operation fuel cycle. There are three levels of waste produced; High Level Waste (HLW), Intermediate Level Waste (ILW) and Low Level Waste (LLW). ILW wastes contain a moderate concentration of radioactive nuclides that remain from the fission reactions. These types of waste are securely stored in engineered stores on nuclear licensed sites until it can be safely disposed of in a Geological Disposal Facility (GDF). Due to the timescales associated with developing a GDF storage, periods of many decades are likely. Over these timescales, these waste packages evolve due to a number of evolutionary processes. A fraction of the waste packages are likely to expand due to the expansive corrosion of reactive metal within the waste [3]. It is important that the expansion is monitored to determine the stability of the waste packages during the period of interim storage to ensure they meet the acceptance criteria of the GDF.

Currently, visual inspections are used to monitor this phenomena, but there are approximately 44,000 existing ILW canisters [4]. Therefore, this technique is labour intensive and made difficult by the radiological



Magnetism 2018

hazardous environment. In this project we aim to develop an alternative, remote monitoring technique to detect the swelling by using ferromagnetic sensors that uses GMI.

The project will focus on developing a ribbon/wire of a strain-sensitive ferromagnetic material that can be used to identify localised expansion of in ILW packages by monitoring its GMI. We believe that once such a device is applied to the canisters, GMI measurements could be performed remotely, at a safe location, to allow users to distinguish the intensity of expansion in individual waste packages. Here, we present initial experimental results from an experimental system constructed for measuring GMI, and discuss our pathway to developing a sensor that is suitable for the proposed application.

- [1] M. H. Phan and H. X. Peng, "Giant magnetoimpedance materials: Fundamentals and applications," *Prog. Mater. Sci.*, vol. 53, no. 2, pp. 323–420, 2008.
- [2] C. Morón, C. Cabrera, A. Morón, A. Garcí, and M. González, "Magnetic Sensors Based on Amorphous Ferro- magnetic Materials: A Review," *Sensors*, vol. 15, pp. 28340–28366, 2015.
- [3] C. Corkhill and N. Hyatt, Nuclear Waste Management, in review. *Physics World Discovery*.
- [4] "The 2013 UK Radioactive Waste Inventory Waste Quantities from all Sources," 2014.

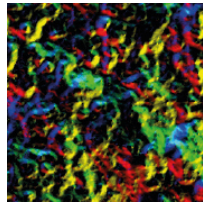
P:84 Magneto-optical imaging of dendritic flux avalanches in a superconducting MgB₂ tape

T Qureishy¹, C Laliena², E Martínez², A J Qviller³, J I Vestgård^{1,4}, T H Johansen^{1,5}, R Navarro² and P Mikheenko¹

¹University of Oslo, Norway, ²Instituto de Ciencia de Materiales de Aragón, Spain, ³nSolution AS, Norway,

⁴Norwegian Defence Research Establishment (FFI), Norway, ⁵University of Wollongong, Australia

We report first direct imaging of dendritic avalanches in a superconducting MgB₂ tape. The avalanches are caused by thermomagnetic instabilities and are known to harm the operation of superconducting devices [1]. They are often detected in magnetisation measurements. However, their lower threshold magnetic field, H_{thr} , in bulk superconductors is far above the operational range of common visualisation techniques like magneto-optical imaging (MOI) [2]. In the present work, we have imaged six different MgB₂ tapes and observed dendritic avalanches in one of them. Fig. 1 shows a superposition of three colour-coded MOI images of the sample after cooling to 3.7 K and applying magnetic fields within the operating range of the technique. The imaged abrupt flux jumps are of dendritic nature like those appearing in MgB₂ superconducting films [2]. The red, green and blue dendrites are irreproducible. They occur only once in three experiments. However, unlike thin films, the branches of few dendrites are partially reproducible, as shown by yellow, cyan and magenta colours for fragments overlapped twice. The temperature dependence of H_{thr} [3] will be discussed. When comparing with thin films, it was found that the observed H_{thr} is much lower than expected, highlighting the importance of edge defects.



Magnetism 2018

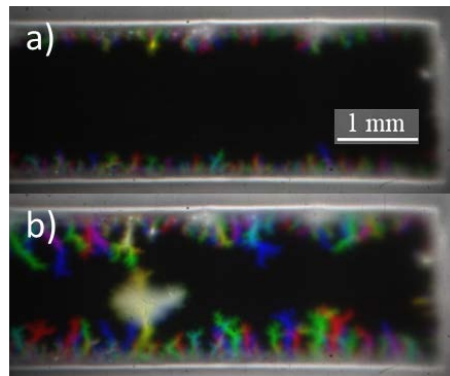


Figure 1: MOI images of an MgB_2 tape after zero-field cooling to 3.7 K and applying a magnetic field of a) 544 and b) 850 Oe. Both images are a superposition of three images obtained at the same conditions, plotted in red, green and blue. Dendrites of these colours are completely irreproducible.

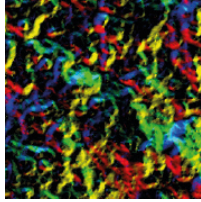
- [1] R G Mints and A L Rakhmanov, Rev. Mod. Phys. 53, 551 (1981)
- [2] T H Johansen, M Baziljevich, D V Shantsev, P E Goa, Y M Galperin, W N Kang, H J Kim, E M Choi, M-S Kim and S I Lee, Supercond. Sci. Technol. 14, 726 (2001)
- [3] T Qureishy, C Laliena, E Martínez, A J Qviller, J I Vestgård, T H Johansen, R Navarro and P Mikheenko, Supercond. Sci. Technol. 30, 125005 (2017).

P:85 Paramagnetic Meissner effect in metal-molecule hybrid systems.

M Rogers¹, F A M Mari², S Lee³, R Stewart³, T Prokscha⁴ and O Cespedes¹

¹University of Leeds, UK, ²Sultan Qaboos University, Oman, ³University of St Andrews, UK, ⁴Paul Scherrer Institute, Switzerland

The coexistence of magnetism and superconductivity observed in bulk metals and hybrid structures of conventional s-wave superconductors (SC) with ferromagnets (FM) is of relevance due to the possibility of generating spin-polarised supercurrents, enabling new opportunities for spin based electronics. The two states of matter are able to coexist due to the possibility of forming spin-triplet Cooper-pair states[1]. Fullerene C_{60} , is diamagnetic and insulating. However, its large electron affinity and low LUMO can lead to considerable charge transfer into the molecule from metallic surfaces. It has been shown that for several metal/ C_{60} interfaces, a combination of this charge transfer and orbital hybridisation can lead to emergent spin polarised interfaces and ferromagnetic ordering[2]. Here, we show that in $\text{Nb}/\text{C}_{60}/\text{Au}$ systems, cooper pair leakage leads to a proximity induced SC state in the C_{60} with a coherence length, ξ_0 , that can range from 15-100nm dependent upon growth conditions. By inserting a weakly magnetic $\text{C}_{60}/\text{Cu}/\text{C}_{60}$, we observe a massive enhancement to the measured magnetic moment by SQUID VSM below the T_c and H_C of the Nb. It is unlikely that this effect would arise due to vortex pinning as the field lies in plane to the niobium film, whose thickness is of the order of ξ_0 . Probing the local magnetic field by LE- μ SR we observe conventional diamagnetic Meissner screening in a $\text{Nb}/\text{C}_{60}/\text{Au}$ stack that extends into the Au. In a similar structure including the magnetic Cu layer in a $\text{Nb}/\text{C}_{60}/\text{Cu}/\text{C}_{60}/\text{Au}$ stack the diamagnetic screening in the niobium is slightly suppressed whereas the screening in the gold is now paramagnetic. In some hybrid SC/FM structures such effects have been attributed to the generation of odd-frequency triplet cooper pairs[3]. Our initial results demonstrate the possibility for forming unconventional cooper pairs in systems that contain no intrinsic exchange splitting and instead rely on the emergent effects that occur at molecule/metal interfaces.



Magnetism 2018

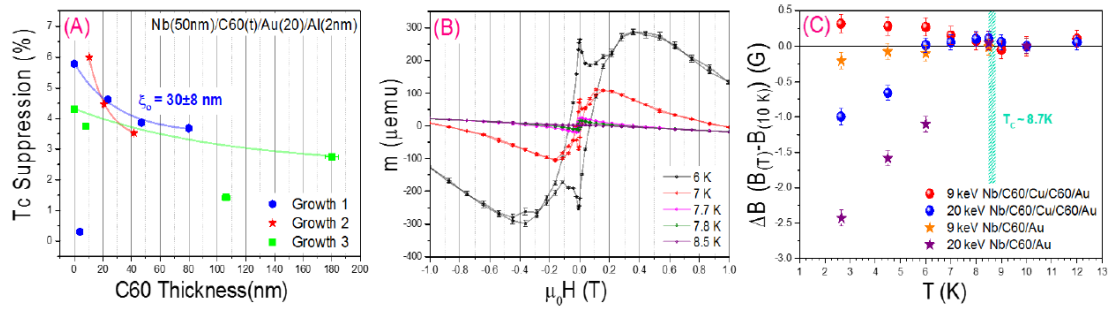


Figure 1. a. T_c suppression measured due to cooper pair leakage through the C60 into Au. B. MvH data demonstrates the reversible magnetic moment measurement which dramatically increases below T_c . c. LE- μ SR data that shows regular diamagnetic screening in Nb (20keV) but opposite screening effects in Au layers (9keV) when a magnetic Cu layer is present.

- [1] J. Linder and J. W. A. Robinson, Superconducting spintronics, Nat. Phys. 11, (2015).
- [2] Fatma Al Ma'Mari, et al. Emergent magnetism at metal-nanocarbon interfaces. PNAS. 114, (2017)
- [3] Di Bernardo A, et al. Intrinsic Paramagnetic Meissner Effect Due to s-Wave Odd-Frequency Superconductivity. Phys. Rev. X. 5, (2015).

Institute of Physics
76 Portland Place, London W1B 1NT, UK
Telephone: +44 (0)20 7470 4800
www.iop.org/conferences

Registered charity number 293851 (England & Wales) and SC040092 (Scotland)